Delano

AEDC-TR-74-75
AFATL-TR-74-113

EFFECT OF VARIOUS EXTERNAL STORES ON THE AERODYNAMIC CHARACTERISTICS OF THE F-4C AIRCRAFT

PA451

J. M. Whoric
ARO, Inc.

PROPULSION WIND TUNNEL FACILITY
ARNOLD ENGINEERING DEVELOPMENT CENTER
AIR FORCE SYSTEMS COMMAND
ARNOLD AIR FORCE STATION, TENNESSEE 37389

October 1974

Final Report for Period September 10 – October 13, 1973

Prepared for

AIR FORCE ARMAMENT LABORATORY (DLJC)
EGLIN AIR FORCE BASE, FLORIDA 32542

APPROVAL STATEMENT

This technical report has been reviewed and is approved.

Lamar R. Kissling

LAMAR R. KISSLING
Lt Colonel, USAF
Chief Air Force Test Director, PWT
Directorate of Test

Frank J. Passarello

FRANK J. PASSARELLO
Colonel, USAF
Director of Test

UNCLASSIFIED

REPORT DOCUMENTATION PAGE		READ INSTRUCTIONS BEFORE COMPLETING FORM
1. REPORT NUMBER AEDC-TR-74-75 AFATL-TR-74-113	2. GOVT ACCESSION NO.	3. RECIPIENT'S CATALOG NUMBER
4. TITLE (and Subtitle) EFFECT OF VARIOUS EXTERNAL STORES ON THE AERODYNAMIC CHARACTERISTICS OF THE F-4C AIRCRAFT		5. TYPE OF REPORT & PERIOD COVERED 6. PERFORMING ORG. REPORT NUMBER
7. AUTHOR(s) J. M. Whoric, ARO, Inc.		8. CONTRACT OR GRANT NUMBER(s)
9. PERFORMING ORGANIZATION NAME AND ADDRESS Arnold Engineering Development Center (DYFS) Arnold Air Force Station Tennessee 37389		10. PROGRAM ELEMENT, PROJECT, TASK AREA & WORK UNIT NUMBERS Program Element 62602F Project 2567
11. CONTROLLING OFFICE NAME AND ADDRESS Air Force Armament Laboratory (DLJC) Eglin Air Force Base, Florida 32542		12. REPORT DATE October 1974 13. NUMBER OF PAGES 169
14. MONITORING AGENCY NAME & ADDRESS(if different from Controlling Office)		15. SECURITY CLASS. (of this report) UNCLASSIFIED 15a. DECLASSIFICATION/DOWNGRADING SCHEDULE
16. DISTRIBUTION STATEMENT (of this Report)		
17. DISTRIBUTION STATEMENT (of the abstract entered in Block 20, if different from Report) Approved for public release; distribution unlimited.		
18. SUPPLEMENTARY NOTES Available in DDC		
19. KEY WORDS (Continue on reverse side if necessary and identify by block number) F-4C aircraft transonic flow aerodynamic characteristics longitudinal stability longitudinal control wind tunnel tests aircraft external winged stores scale model drag characteristics		
20. ABSTRACT (Continue on reverse side if necessary and identify by block number) The results obtained from wind tunnel tests, which were conducted to determine the effects of external carriage of several configurations of winged stores on the aerodynamic characteristics of the F-4C aircraft, are presented and discussed. The analysis includes evaluation of the static longitudinal stability, drag, and longitudinal control characteristics of the F-4C aircraft with winged stores. Incremental drag rise and neutral-point shift associated with some of the store loadings are compared with results obtained		

DD FORM 1 JAN 73 1473

UNCLASSIFIED

20. Abstract (Continued)

from exisiting prediction techniques and methods. Results are presented for altitudes of sea level, 10,000, 20,000, and 30,000 ft for aircraft center-of-gravity locations of 25, 33, and 36 percent of the mean aerodynamic chord over the Mach number range from 0.6 to 1.3 for gross weights applicable to the aircraft plus stores.

AFSC
Arnold AFB Tenn

PREFACE

The test program reported herein was conducted by the Arnold Engineering Development Center (AEDC), Air Force Systems Command (AFSC), at the request of the Air Force Armament Laboratory (AFATL/DLJA), AFSC, Eglin Air Force Base, Florida, under Program Element 62602F, Project 2567. The project monitor was Major Ron Van Putte. The results were obtained by ARO, Inc. (a subsidiary of Sverdrup & Parcel and Associates, Inc.), contract operator of AEDC, AFSC, Arnold Air Force Station, Tennessee. The test was conducted under ARO Project No. PA305, and data reduction and analysis of the wind tunnel data were performed under ARO Project No. PA451. Data reduction was completed on May 17, 1974, and the manuscript (ARO Control No. ARO-PWT-TR-74-50) was submitted for publication on June 21, 1974.

CONTENTS

ILLUSTRATIONS

Figure | Page

TABLE

1.0 INTRODUCTION

The F-4C was originally designed as an air defense interceptor/air superiority fighter. The primary armament consisted of four AIM-7 Sparrow III missiles carried semi-submerged at four fuselage stations. However, since its first flight, the F-4C has been modified to carry, launch, and/or deliver a wide variety of external stores or weapons as the Air Force, Navy, and Marines have adapted the aircraft as a multi-mission fighter.

Although the F-4C aircraft has proved adaptable to its role as a multi-mission fighter, the certification of the wide variety of weapons on the F-4C has posed problems in many areas of aircraft technology. Areas of particular concern have been the effect of external stores an longitudinal stability and drag.

Available prediction techniques have shown some success in determining these effects for conventional finned and unfinned stores. In Ref. 1, drag rise and neutral-point shifts determined from wind tunnel data were compared with results obtained from the prediction techniques of Refs. 2 and 3. Drag rise increments compared favorably; however, both techniques were limited to a maximum Mach number of 0.95 for drag rise increment predictions. Neutral-point predictions did not compare favorably, especially in the transonic Mach number range. Therefore, when the Air Force became interested in a number of conceptual winged stores, they decided that wind tunnel testing was the most reliable way of determining the effect of these stores on the aerodynamic characteristics of the F-4C. Such data were the object of the present wind tunnel test and analysis.

The tests were conducted in the Aerodynamic Wind Tunnel (4T) of the AEDC Propulsion Wind Tunnel Facility (PWT) utilizing 0.05-scale models of the F-4C aircraft and stores of interest. Data were obtained with these models at Mach numbers from 0.6 to 1.3 and angles of attack from -4 to 13 deg. In general, the stabilator angle was varied from 0 to -6.6 deg during these tests.

2.0 APPARATUS

2.1 TEST FACILITY

The Aerodynamic Wind Tunnel (4T) is a closed-loop, continuous-flow, variable-density tunnel in which the Mach number can be varied from 0.1 to 1.3. Also, nozzle blocks can be installed to give nominal Mach numbers of 1.6 and 2.0. At all Mach numbers, the stagnation pressure can be varied from 300 to 3700 psfa. The test section is 4 ft square and 12.5 ft long with perforated, variable-porosity (0.5- to 10-percent open) walls. It is completely enclosed in a plenum chamber from which the air can be evacuated, allowing part of the tunnel airflow to be removed through the perforated walls of the test section.

The tunnel support system for the models consists of a pitch sector, strut, and sting attachment which has a pitch angle capability of -9 to 28 deg with respect to the tunnel centerline and a roll capability of -180 to 180 deg with respect to the sting centerline.

2.2 TEST ARTICLES

The test articles were 0.05-scale models of the F-4C aircraft and associated stores and suspension equipment. The stores included the Stand-Off Missile (SOM), Extended Range Stubby HOBOS (ERSH), Trajectory Control Test Vehicle (TCTV), the Oneway Remotely Piloted Vehicle (RPV), and the Extended Range Vehicle (ERV). Models of several versions of modular weapons concepts were also used during these tests. These concepts were the Philco-Ford Modular Weapon Powered (PF Mod Wpns P) and unpowered (PF Mod Wpns UP) along with Rockwell International's Modular Weapon powered (NARC Mod Wpns Cls III) and unpowered (NARC Mod Wpns Cls II). All simulated rocket pods were solid allowing no flow through these pods.

A photograph of the F-4C configured with two ERSH stores and 370-gal fuel tanks is shown in Fig. 1. Figures 2 and 3 give the basic dimensions of the F-4C model and the characteristic dimensions of the wing panel. All stores were suspended from the inboard armament station (BL 4.075), utilizing the MAU12B/A pylon in the presence of the 370-gal fuel tank on the outboard wing station (BL 6.625). Details and dimensions of the pylon and fuel tank are given in Figs. 4 and 5. Sketches of the various stores are presented in Fig. 6. Configurations are identified in the configuration key presented in Fig. 7, which shows the store profiles to scale with respect to each other and assigns each configuration a number which will be used as a reference throughout the remainder of the report. The fin orientation of the stores as carried on the aircraft is also indicated in this figure. It should also be noted that all configurations were symmetrical except configuration 24 which had only one TCTV store which was carried on the left wing.

2.3 INSTRUMENTATION

A six-component internal strain-gage balance was used to measure the forces and moments on the F-4C model. Three base pressure measurements were made using transducers and orifice tubes which extended just inside the base of the model.

3.0 TEST DESCRIPTION

3.1 TEST PROCEDURES AND TEST CONDITIONS

Force and moment data were obtained in the conventional manner by varying the model angle of attack at a constant Mach number, Reynolds number, and stabilator angle

setting. The unit Reynolds number was held constant at a nominal value of 5.0 x 10^6 per foot. The angle of attack was varied from -4 to 13 deg.

3.2 DATA REDUCTION AND CORRECTIONS

Wind tunnel force and moment data were reduced to coefficient form in the wind axis system. Base drag was calculated using an average of the three base pressure measurements along with the base area and was used to calculate forebody coefficients. However, the base drag measured in this manner was considered negligible, and therefore, all coefficients presented are measured coefficients. Corrections for the components of model weight in the axial- and normal-force directions, normally termed static tares, were also applied to the data.

The angle of attack was corrected for sting and balance deflections caused by the aerodynamic loads. The model was tested both upright and inverted to provide the data to correct for tunnel flow angularity and model-balance misalignment. Based on these data, the angle of attack was corrected for 0.35-deg upwash at Mach number 0.6 and 0.2-deg upwash at Mach number 0.8. No other flow angle corrections were made.

3.3 PRECISION OF MEASUREMENTS

The precision of the data presented which can be attributed to inaccuracies in the balance measurements and setting tunnel conditions were determined for a confidence level of 95 percent and are presented in Table 1. The precision in setting the Mach number was ±0.002. The Mach number variation in the portion of the test section occupied by the model was no greater than ±0.005 for Mach numbers up to 0.95 and ±0.01 for Mach numbers greater than 1.0. The precision of the model angle of attack was ±0.1 deg, and the precision of the stabilator angle setting was ±0.1 deg.

4.0 TEST RESULTS, ANALYSIS, AND DISCUSSION

Included in this analysis are the trimmed aerodynamic characteristics of the F-4C aircraft for aircraft plus store gross weights representative of takeoff conditions. These characteristics were determined for altitudes of sea level, 10,000, 20,000, and 30,000 ft at cg locations of 25, 33, and 36 percent of the mean aerodynamic chord (MAC). Also included in the analysis and presented for a stabilator setting of -0.6 deg are neutral-point shifts (ΔNP) at a lift coefficient (C_L) of 0.2 and drag data at a lift coefficient of 0.3 for subsonic Mach numbers and at a C_L = 0.1 for supersonic Mach numbers. Drag numbers (DN) were also evaluated and are presented with the drag data. These data are presented so that comparisons can be made with other stores using the drag index and stability number system of Ref. 2.

The aerodynamic characteristics at trim conditions were determined from curve fits of the wind tunnel data as described in Ref. 1. The trimmed data are all presented as a function of Mach number. These data are presented for several altitudes and cg locations for the baseline configuration which is the F-4C configured with inboard MAU-12B/A pylons and outboard 370-gal fuel tanks. The data for the remaining configurations are presented and compared with the baseline configuration for several altitudes, but only with the cg location at 0.33 MAC. Trim data at Mach number 0.6 at an altitude of 30,000 ft are generally extrapolated from the wind tunnel data. As a result of this fact, data variations for these conditions are not as well behaved as the data for other conditions.

Trimmed aerodynamic characteristics are not presented for configurations 27 and 28 because sufficient data were not taken for such an analysis.

Presented in the following sections is a discussion of the aerodynamic characteristics of the baseline configuration followed by a discussion of the effects of adding external stores to this configuration. Areas which will be discussed will be longitudinal stability and handling qualities, drag characteristics, and longitudinal control. Included in these discussions will be a comparison of the wind tunnel results with the results of existing prediction techniques for drag rise and neutral-point shifts caused by the addition of external stores to the baseline configuration.

4.1 BASELINE CONFIGURATION CHARACTERISTICS

The aerodynamic characteristics of the baseline configuration (21) are presented in Figs. 8 through 14. Trim stabilator angle ($\delta_{s_{tr}}$), neutral-point location (NP), pitching-moment coefficient slope (C_{m_α}), and lift-curve slope (C_{L_α}) at trim, trim wing angle of attack, trim drag, and longitudinal control derivatives are presented in these figures as a function of Mach number. As the aircraft accelerates from Mach number 0.9 to 0.95, nose down moments and control stick movement reversal commonly known as "tuck-under" are indicated from the data in Figs. 8 and 9. This effect has been previously reported in Ref. 1. From the data in Fig. 9, one can determine the aft cg limit for takeoff as well as the changes in static margin as the aircraft accelerates through the Mach number range. In order to maintain a 1-percent MAC static margin during takeoff, these data indicate the aft cg limit to be at the 33-percent-MAC location. If the cg of the aircraft were maintained at this value as the aircraft accelerates through the transonic Mach number range, a static margin up to 10.5-percent MAC would be experienced at Mach number 0.95 at 30,000 ft. A reduction in static margin of from 3.0- to 3.5-percent MAC can be noted as the Mach number changes from 0.95 to 0.975 for all altitudes except 30,000 ft. However, since the aft cg limit of the F-4C is at 36-percent MAC, the static margin still exceeds the 1-percent MAC limit reported in Ref. 3, as the minimum acceptable stable static margin for formation flying and/or weapons delivery.

The pitching-moment coefficient slope (C_{m_α}) and the lift coefficient slope (C_{L_α}) are presented in Figs. 10 and 11, respectively. The ratio of these two parameters ($C_{m_\alpha}/C_{L_\alpha}$) determines the static margin, and hence, the neutral-point location can be calculated. These data indicate that the dominant parameter in determining the neutral-point location is the pitching-moment coefficient slope. The variation of neutral-point location with Mach number correlates with the variation of C_{m_α} with Mach number, but not with changes in C_{L_α} with Mach number. For example, as the Mach number changes from 0.9 to 0.925, C_{m_α} becomes increasingly more negative, indicating an increase in static longitudinal stability (larger static margin); whereas the lift-curve slope (C_{L_α}) shows an increase which is in the direction to decrease the static margin. Furthermore, in the Mach number range from 0.95 to 0.975, C_{m_α} decreases, i.e., tends toward a smaller static margin, while C_{L_α} decreases, which is in the direction to increase the static margin.

Figures 12, 13, and 14 show the wing angle of attack, trim drag, and longitudinal control derivatives for the baseline configuration as a function of Mach number, altitude, and cg location. These characteristics are a rather weak function of cg location. The trim wing angle of attack and trim drag show increasing values with increasing altitude, whereas the longitudinal control derivatives are relatively independent of altitude.

4.2 EFFECT OF EXTERNAL STORES ON LONGITUDINAL STABILITY AND HANDLING QUALITIES

The wind tunnel data for the baseline plus store configurations were analyzed in the same manner as the baseline configuration data. The results of that analysis pertinent to the effect of the various external store configurations on the longitudinal stability and handling qualities of the F-4C are presented in Figs. 15 through 44. The plots are comparisons of the various configurations with the baseline configuration for a cg location at 33 percent of the mean aerodynamic chord.

The comparisons presented show that the addition of external stores in all cases resulted in larger stabilator deflection requirements to keep the aircraft trimmed. Figures 15 and 30 indicate that at Mach number 0.975 as much as 2-deg additional negative deflection is required to keep the F-4C trimmed when it is carrying the SOM or the PF Mod Wpns stores than is required without stores. Again as for the baseline configuration, the increase in stability noted in the transonic Mach number range coupled with the larger required control stick movement to keep the aircraft trimmed indicates that adding external stores to the baseline configuration aggravates the tuck-under noted for the baseline configuration.

In addition to tuck-under, the change in the static margin with Mach number is another factor that affects the handling quality of the F-4C. The addition of the various external

stores to the base-line configuration had primarily two effects on the static margin changes with Mach number.

In the first place, the data in Figs. 16, 36, and 41 show that the SOM, the RPV, and the ERV stores reduced and smoothed the static margin changes with Mach number in the transonic Mach number range. Secondly, the data for the ERSH (Fig. 21), the TCTV (Fig. 26), and the PF Mod Wpns stores (Fig. 31) show that, at certain altitudes as the Mach number changes from 0.9 to 1.0, the static margin first increased sharply and then decreased abruptly to about the subsonic value.

These data imply that, when the F-4C is carrying the Stubby HOBOS stores, the TCTV store, and the Philco-Ford Mod Wpn stores, the aircraft cg location must be chosen carefully to provide the required stable static margin for weapons delivery.

At Mach numbers from 0.6 to 1.0, the addition of external stores to the baseline configuration was destablizing in all cases. Neutral-point shifts up to 4-percent MAC (Fig. 36) were experienced at Mach number 0.6 when the RPV stores were added to the baseline configuration, whereas when the other store configurations were installed, the neutral-point shift varied from 1- to 3-percent MAC in the low subsonic Mach number range. At the supersonic Mach numbers, the effect of the stores on stability is not as well defined, but in general, the data show the stores to be less destabilizing in this Mach number range. In fact, at H = 30,000 ft, the data (Figs. 16, 21, 26, 31, 36, and 41) show that the addition of external stores produces an increase in stability at Mach numbers 1.05 and 1.1 for all configurations except for configuration 24 (TCTV). These trends in stability variation with Mach number, as in the case of the baseline configuration, can be correlated with the changes in C_{m_α} that resulted from the addition of the external stores to the baseline configuration. The increase noted in trim wing angle of attack when stores were added to the baseline configuration (Figs. 19, 24, 29, 34, 39, and 44) is primarily a result of the gross weight increase due to the stores.

Presented in Fig. 45 is the neutral-point shift due to the addition of the various external stores to the baseline configuration calculated for a lift coefficient of 0.2 and stabilator setting of -0.6 deg. As stated previously, these data are presented so that the effect of the external stores on aircraft stability can be evaluated using the technique of Ref. 2. These data show a large shift in the neutral-point location due to the addition of pylon-mounted external stores in the transonic Mach number range. A destabilizing shift of up to 8-percent MAC is noted for some configurations. This forward shift generally peaks out at Mach number 0.925 and is generally followed by a sharp aft shift as the Mach number increases to 1.05. The exception to this trend is configuration 24 (TCTV). However, it should be emphasized that only one store was present on the aircraft for that configuration.

A comparison of the change in neutral-point location (ΔNP_X) at $M_\infty = 0.85$ determined from the data in Fig. 45 with the empirically determined prediction curves of Ref. 2 is shown in Fig. 46a. The data show measured forward neutral-point shifts of up to 2.5-percent MAC larger than would be predicted using the finned store prediction curve of Ref. 2.

Figures 46b, c, and d compare the neutral-point shift at trim with the neutral-point shift at trim predicted using the method of Ref. 3. This prediction technique which is a semi-empirical technique is more general than that of Ref. 2 in that it allows for predictions over the entire Mach number range from 0 to 2.0. These data show that the Ref. 3 technique under-predicts the forward shift of the neutral point due to the addition of the external stores in the subsonic Mach number range by 1- to 2-percent MAC. In the Mach number range from 0.9 to 1.0, the discrepancy between measured and predicted values generally increased. For example, a difference of about 5-percent MAC is indicated at Mach number 0.925 for configuration 30. For Mach number 1.0 and above, the trends are not well defined.

These comparisons show similar results to that reported in Ref. 1 where the largest discrepancies between predicted and measured values of neutral-point shifts were in the transonic Mach number range.

4.3 EFFECT OF EXTERNAL STORES ON DRAG CHARACTERISTICS

The effect of the addition of various external stores on the trim drag characteristics of the baseline configuration is presented in Figs. 47 through 52. In these figures, the data are presented as a function of Mach number and altitude for a cg location of 0.33 MAC. These data show that at a given altitude, the addition of external stores to the baseline configuration increases the trim drag by approximately a constant increment. Larger incremental increases in trim drag are generally noted supersonically than are noted subsonically. Configuration 22 (SOM stores) exhibits the highest trim drag, whereas configuration 23 (Stubby HOBOS) exhibits the lowest trim drag (Figs. 47 and 48).

Figure 53 presents the drag data evaluated at lift coefficients of 0.3 for subsonic Mach numbers and 0.1 for supersonic Mach numbers for a stabilator setting of -0.6 deg. By using these data, as outlined in Ref. 2, the drag number for the various stores was evaluated and is shown on these plots. This number is currently used by operational units to assess the performance of the F-4C when loaded with stores. A comparison of the drag number shows that the SOM store contributes the largest increment of drag to the baseline configuration, while the ERSH store contributes the least amount of drag. This is consistent with the results of the trim drag presentation discussed previously.

Comparisons of measured and predicted values of trim drag are presented in Fig. 54 for configurations 23, 24, and 30. By using the method of Ref. 3, these data show that higher values of drag would have been predicted than were measured with the difference being approximately a constant value for all Mach numbers. Lower values of drag are predicted than measured using the method of Ref. 2 over the Mach number range from 0.6 to 0.9. However, for Mach numbers from 0.9 to 0.95, agreement between measured and predicted drag values is good except for configuration 30 for which higher values of drag would be predicted than were measured. Overall, both prediction methods do remarkably well in predicting the drag of these three configurations.

4.4 EFFECT OF EXTERNAL STORES ON LONGITUDINAL CONTROL

Longitudinal control derivatives, $C_{m_{\delta_s}}$ (elevator power) and $C_{L_{\delta_s}}$ (elevator lift effectiveness), are presented in Figs. 55 through 60 as a function of Mach number and altitude for a cg location of 0.33 MAC. The data in Fig. 55 show that there is a reduction in elevator power and elevator lift effectiveness in the Mach number range from 0.9 to 1.0 when the SOM store is installed on the baseline configuration. Over this same Mach number range, the addition of the Stubby HOBOS store and the ERV store produced a decrease in the elevator lift effectiveness without significantly affecting the elevator power (Figs. 56 and 60). The data in Fig. 57b show that the TCTV store produces an increase in the elevator lift effectiveness subsonically and supersonically, whereas a reduction is noted over most of the transonic Mach number range. In general, there appears to be ample elevator power available when the aircraft is carrying these winged stores.

5.0 SUMMARY OF RESULTS

Wind tunnel tests were conducted to determine the effects of external carriage of several configurations of winged stores on the aerodynamic characteristics of the F-4C aircraft. Results of these tests may be summarized as follows:

1. The data presented show that the tuck-under characteristics of the baseline configuration are aggravated when winged external stores are added to the configuration.

2. The addition of the Stand-Off Missile, the Oneway Remotely Piloted Vehicle, or the Extended Range Vehicle stores to the baseline configuration reduced and smoothed the fore and aft shifting of the neutral-point location that occurred in the transonic Mach number range.

3. The addition of the Extended Range Stubby HOBOS, the Tactical Control Test Vehicle, or the Philco-Ford Modular Weapons stores to the baseline

configuation resulted in larger fore and aft shifts of the neutral point. For certain altitudes as the Mach number changed from 0.9 to 1.0, the static margin first increased sharply and then decreased sharply to about the subsonic value.

4. The addition of the Stand-Off Missile stores to the baseline configuration produced the largest increase in drag coefficient, whereas the addition of the Extended Range Stubby HOBOS stores resulted in the smallest increase in drag coefficient.

5. There was some loss of elevator power and elevator lift effectiveness in the transonic Mach number range when the stores were added to the baseline configuration; however, adequate elevator power was available to keep the aircraft in trim for the conditions analyzed.

6. Incremental drag rise predictions utilizing current prediction techniques compared favorably with measured values; however, neutral-point shift predictions did not compare favorably with measured values especially in the transonic Mach number range.

REFERENCES

1. Whoric, J. M. "Effect of Various External Stores on the Static Longitudinal Stability, Longitudinal Control, and Drag Characteristics of the F-4C Airplane." AEDC-TR-73-186 (AD914456L), November 1973.

2. Weber, William B. "Effect of External Stores on the Stability, Control, and Drag Characteristics of the McDonnell Douglas F-4 Aircraft." Aircraft/Stores Compatibility Symposium Proceedings, Vol. III, Eglin AFB, 1969, pp. 28-54.

3. Dyer, R. D. and Gallagher, R. D. "Technique for Predicting External Store Aerodynamic Effects on Aircraft Performance." Vol. 1, Dayton, Ohio, 1972, pp. 115-141.

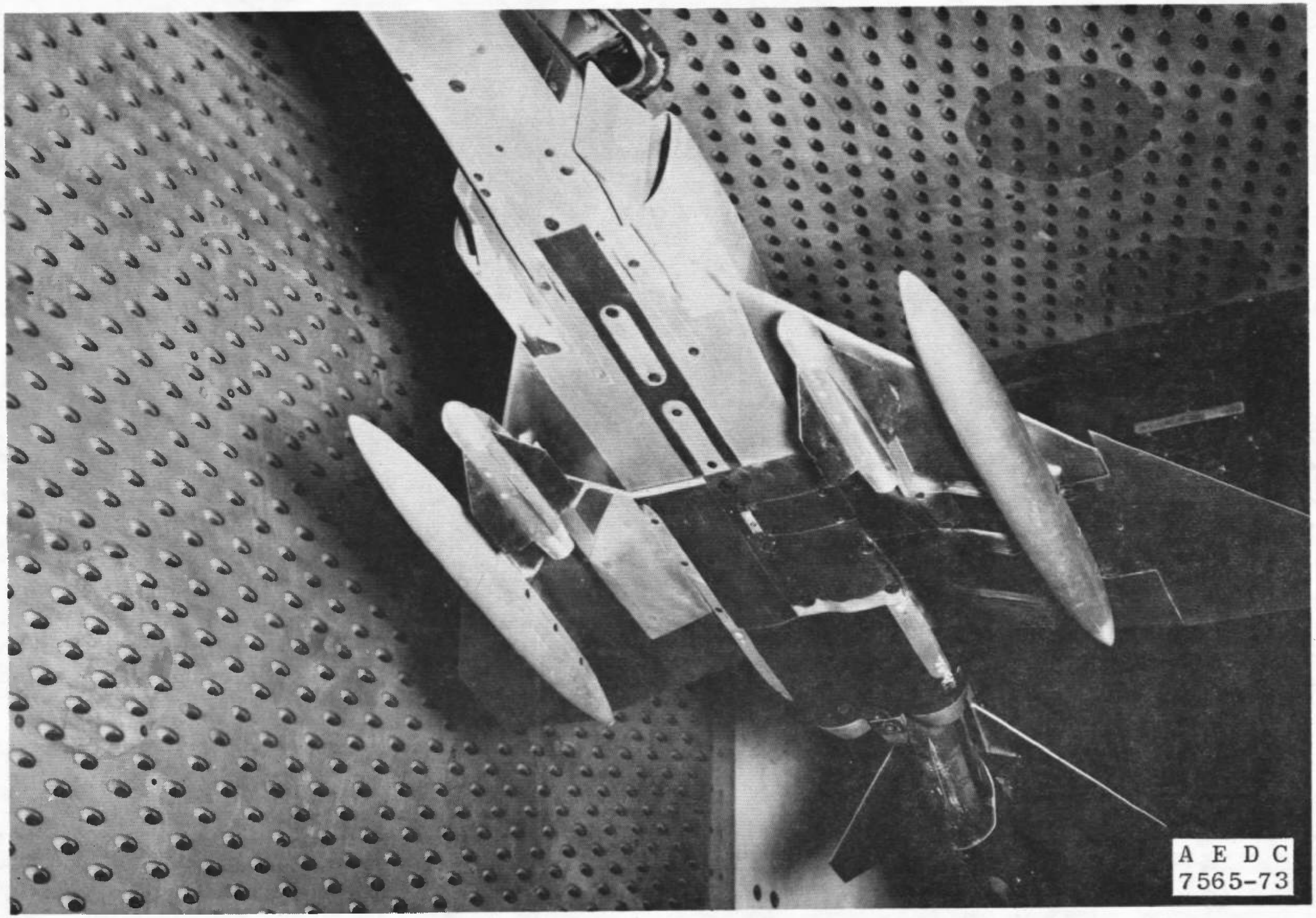

Figure 1. Wind tunnel installation of the F-4C with Stubby HOBOS stores and 370-gal tanks.

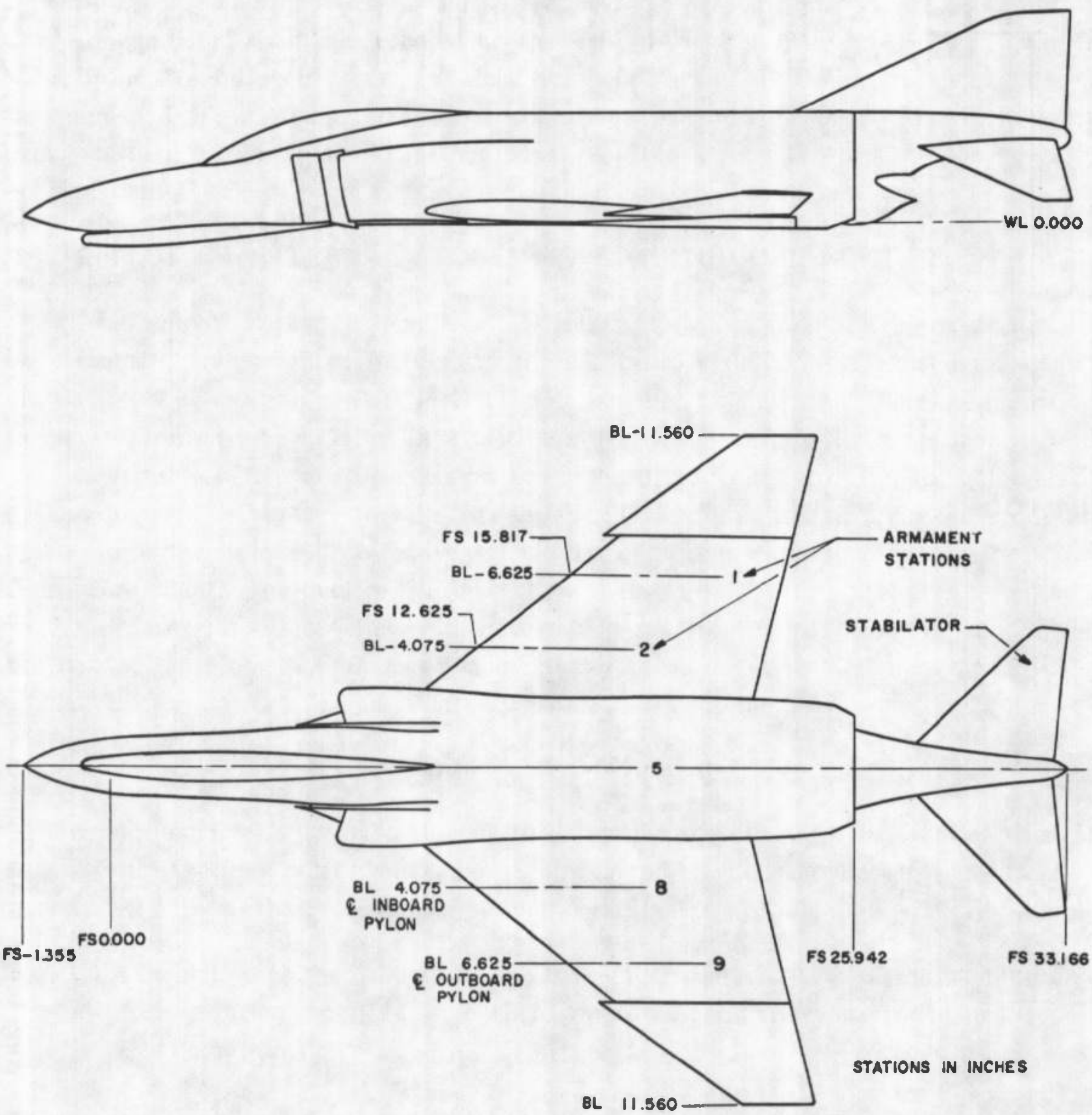

Figure 2. Sketch of 0.05-scale model of the F-4C.

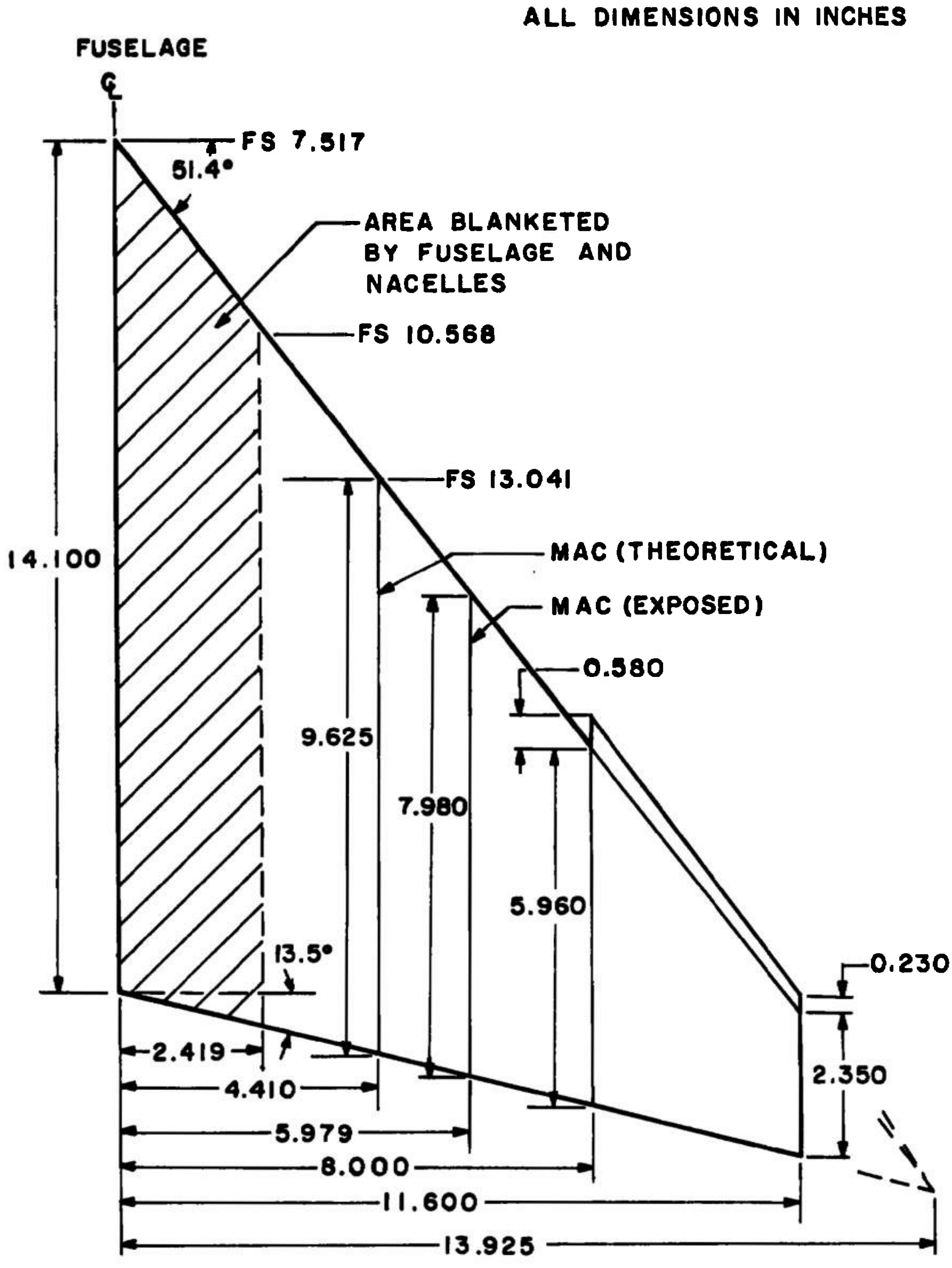

Figure 3. Sketch of F-4C wind tunnel model wing panel.

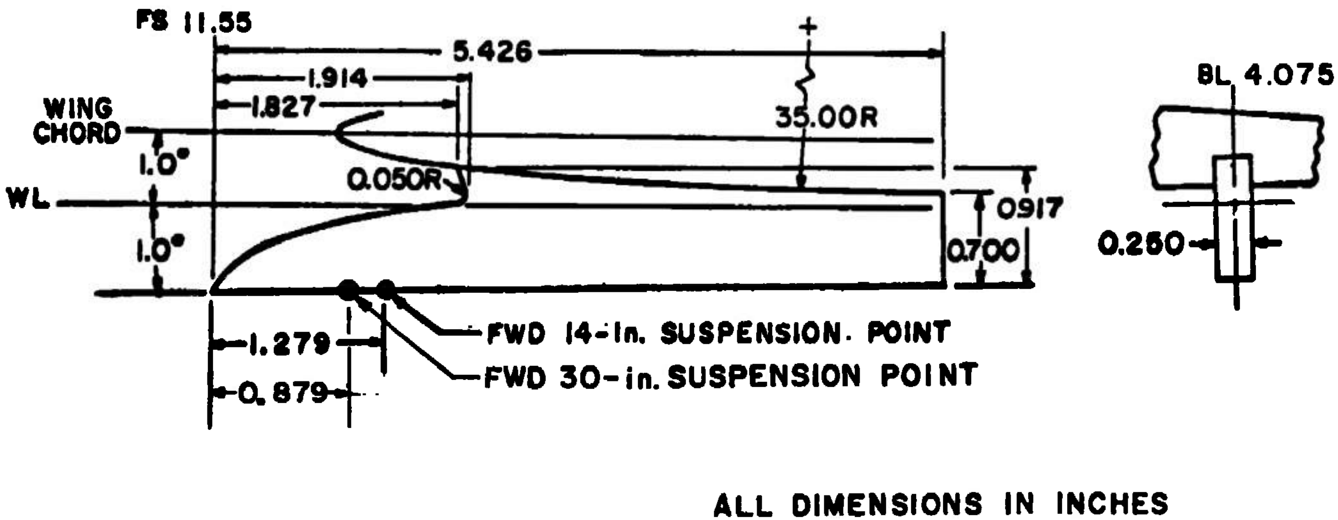

Figure 4. Details and dimensions of MAU-12B/A pylon.

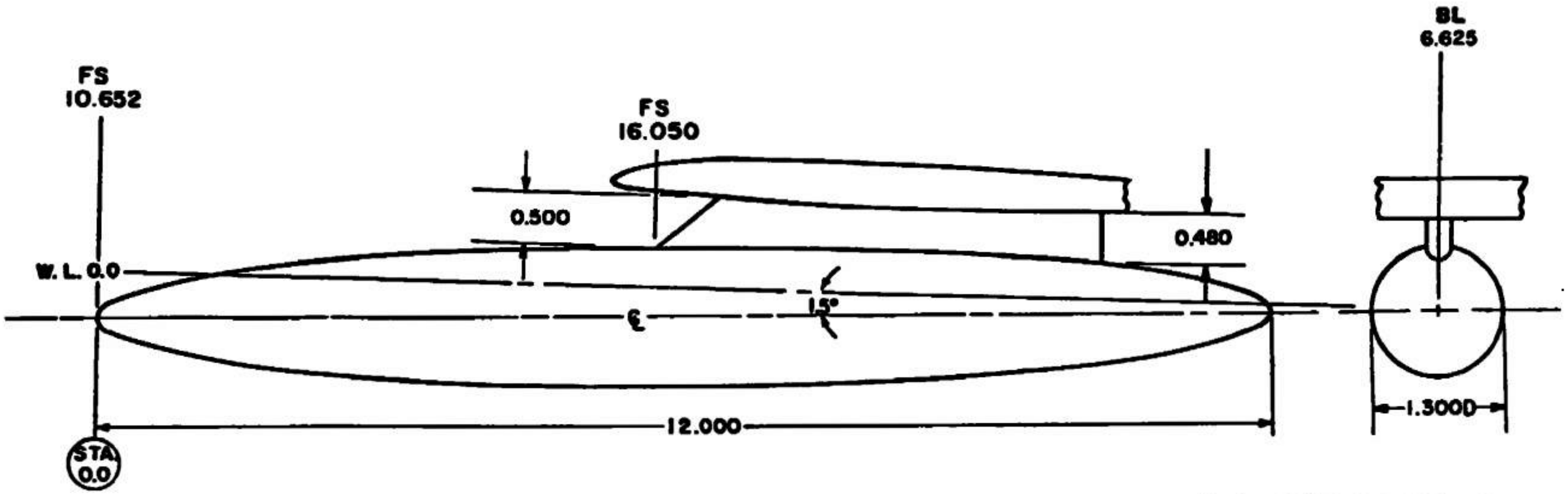

NOTE: MODEL STATIONS AND DIMENSIONS IN INCHES

BODY CONTOUR, TYPICAL BOTH ENDS

STATION	BODY DIAM	STATION	BODY DIAM
0.000	0.000	2.500	1.116
0.025	0.100	2.750	1.156
0.050	0.144	3.000	1.190
0.150	0.258	3.250	1.218
0.250	0.340	3.500	1.242
0.500	0.498	3.750	1.260
0.750	0.622	4.000	1.274
1.000	0.724	4.250	1.286
1.250	0.812	4.500	1.294
1.500	0.890	4.750	1.298
1.750	0.958	5.000	1.300
2.000	1.016	6.000	1.300
2.250	1.070		

Figure 5. F-4C, 370-gal fuel tank with suspension equipment.

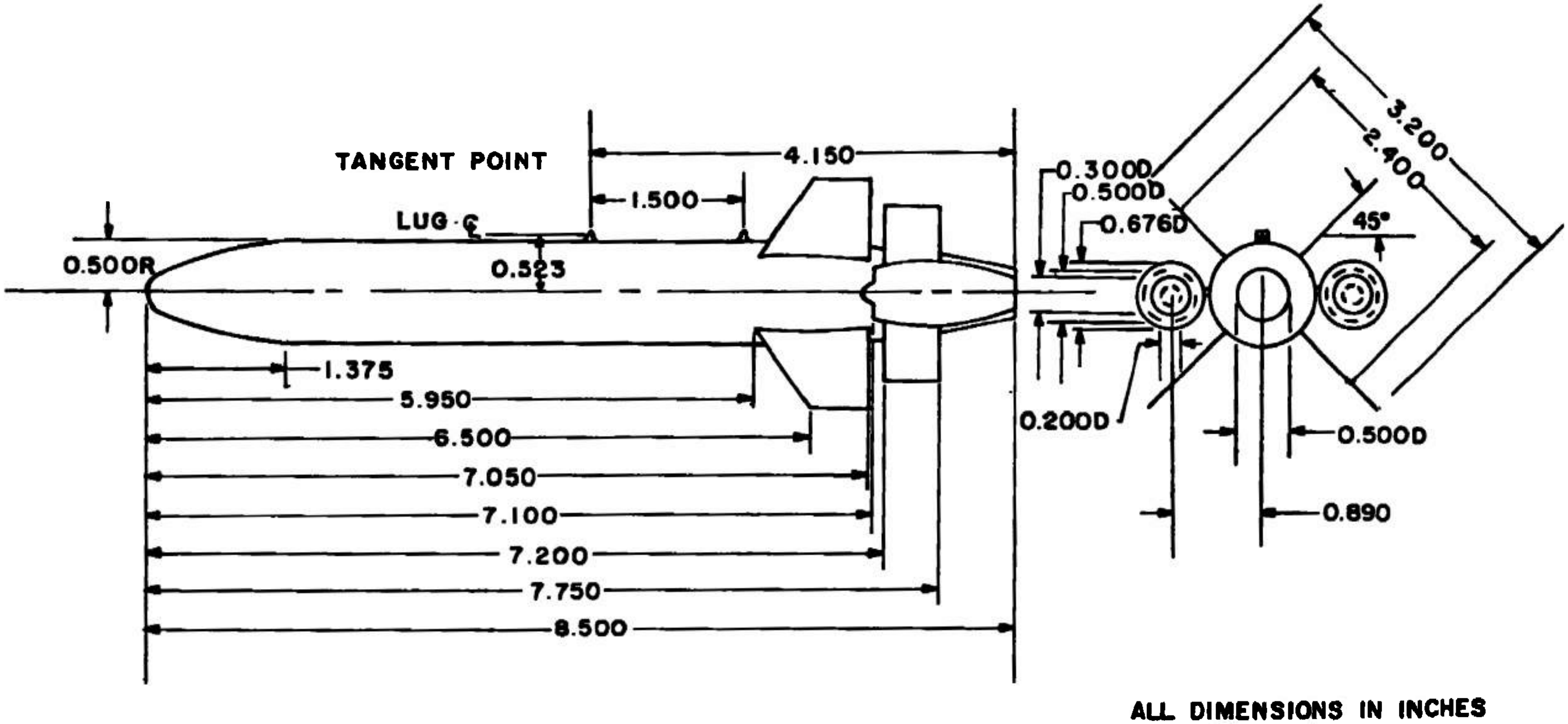

a. Stand-off missile (SOM)

Figure 6. Details and dimensions of the external stores.

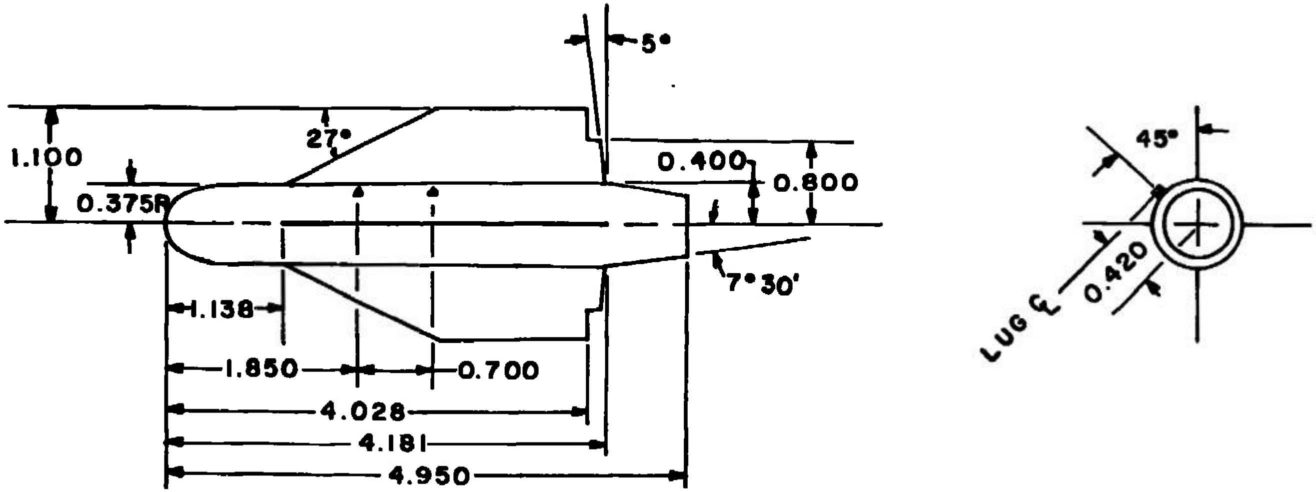

ALL DIMENSIONS IN INCHES

b. Extended Range Stubby HOBOS (ERSH)
Figure 6. Continued.

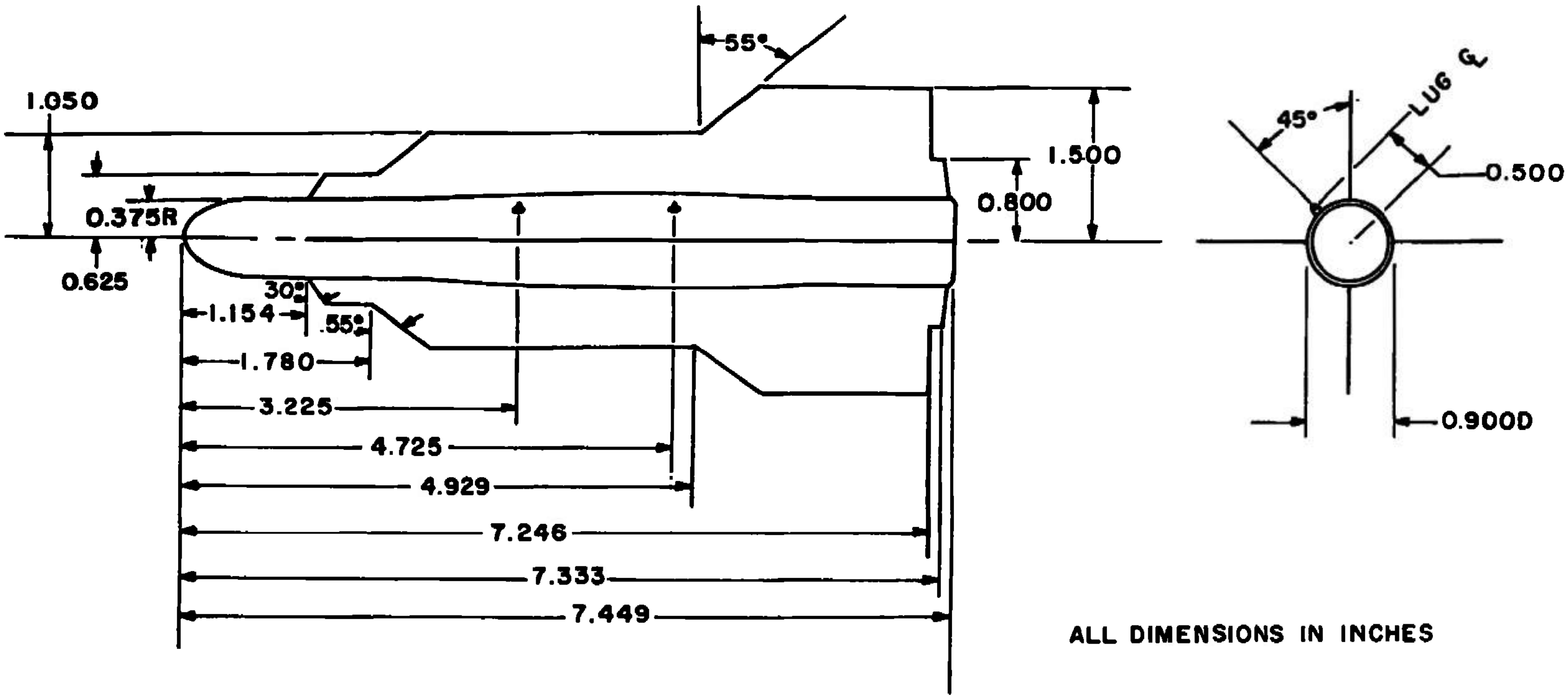

c. Tactical Control Test Vehicle (TCTV)
Figure 6. Continued.

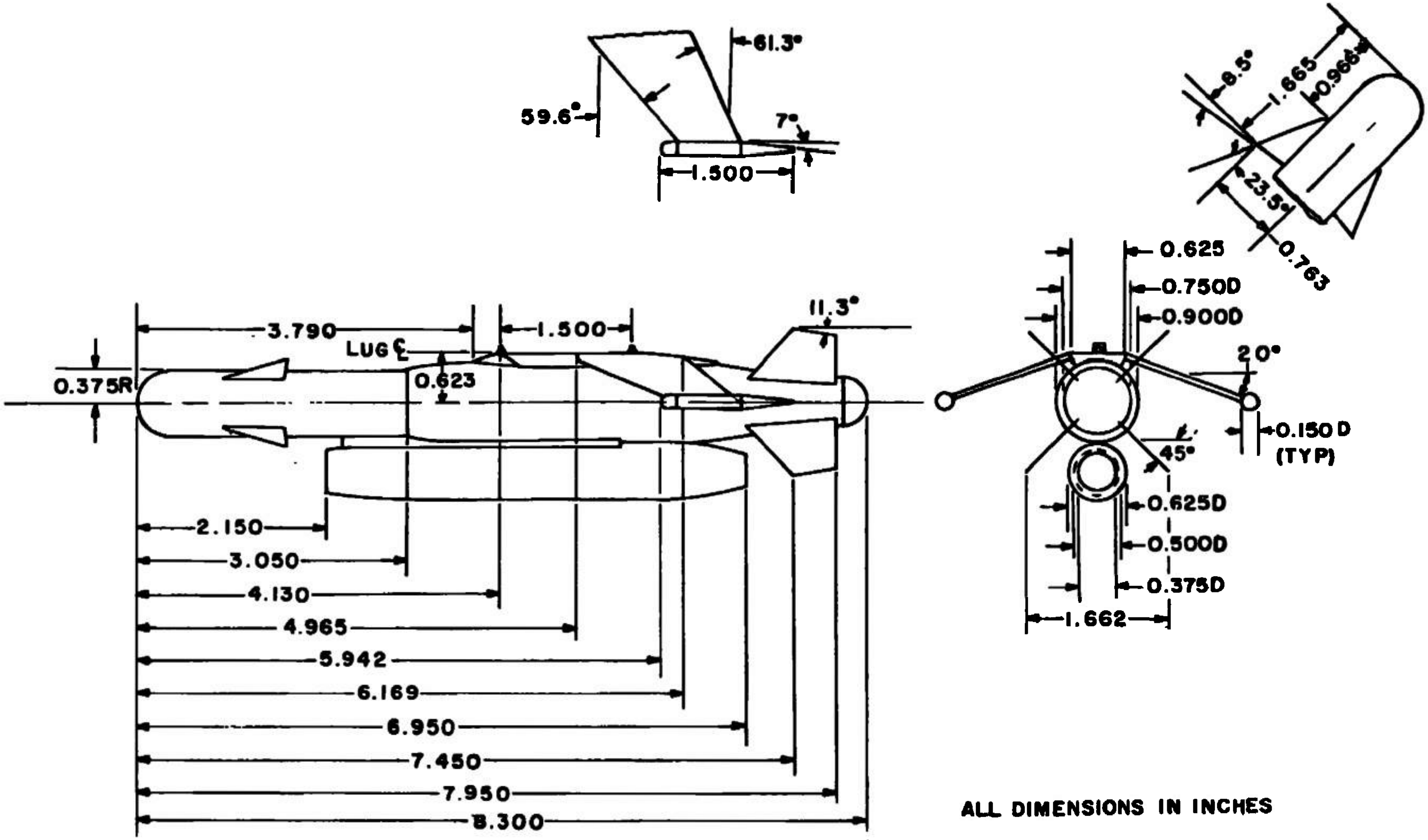

d. Philco-Ford Modular Weapons Powered

Figure 6. Continued.

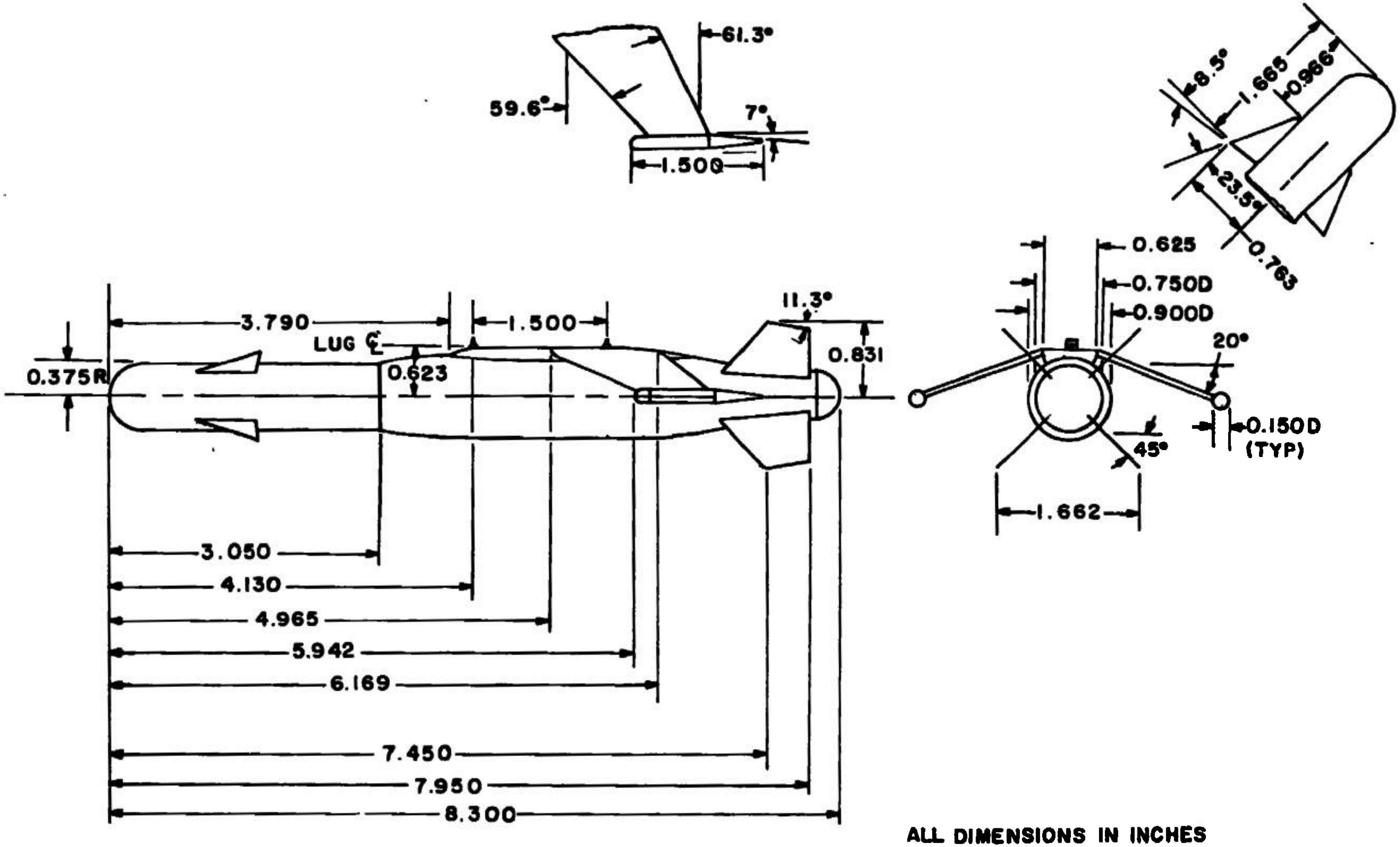

e. Philco-Ford Modular Weapons Unpowered
Figure 6. Continued.

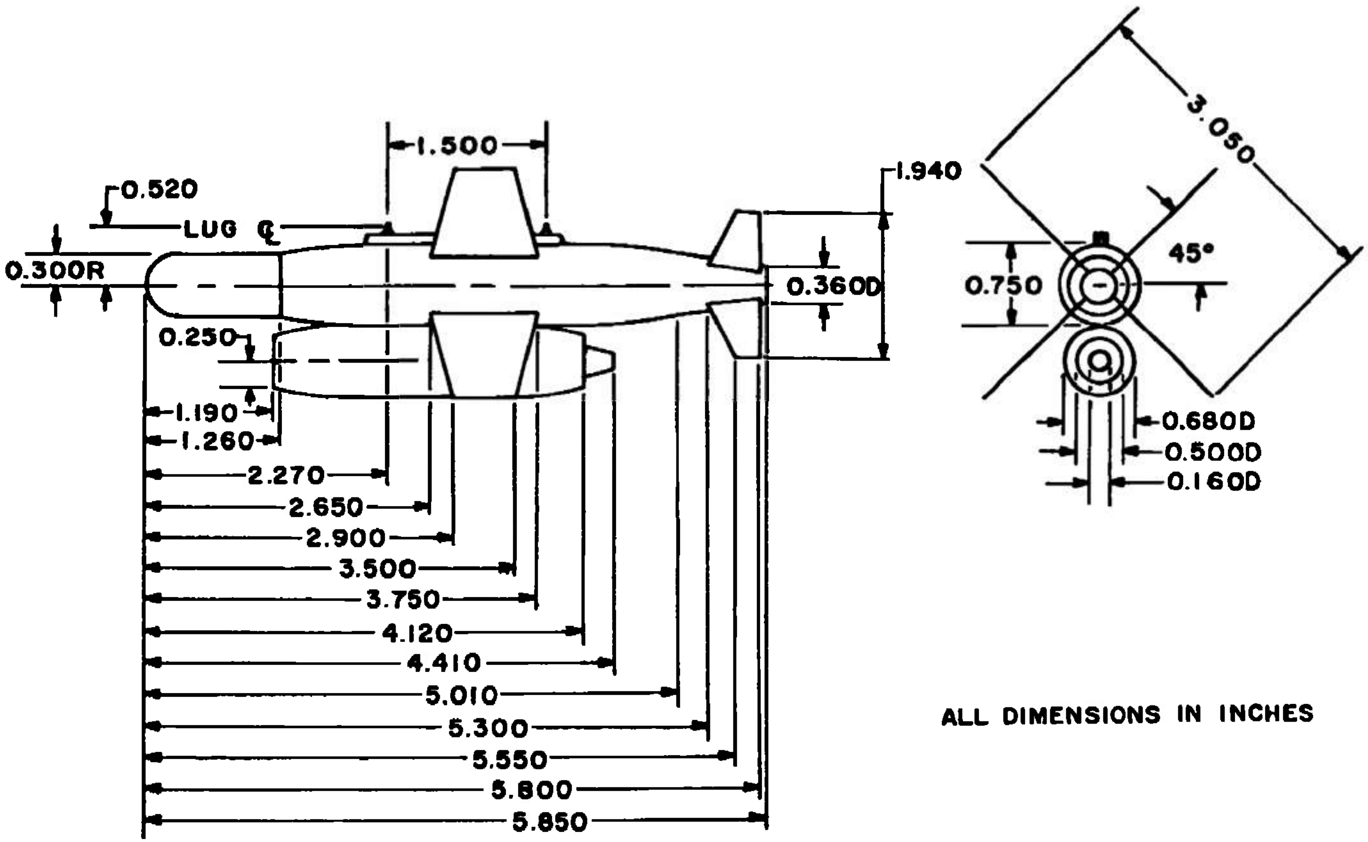

f. Rockwell International Modular Weapons Class III
Figure 6. Continued.

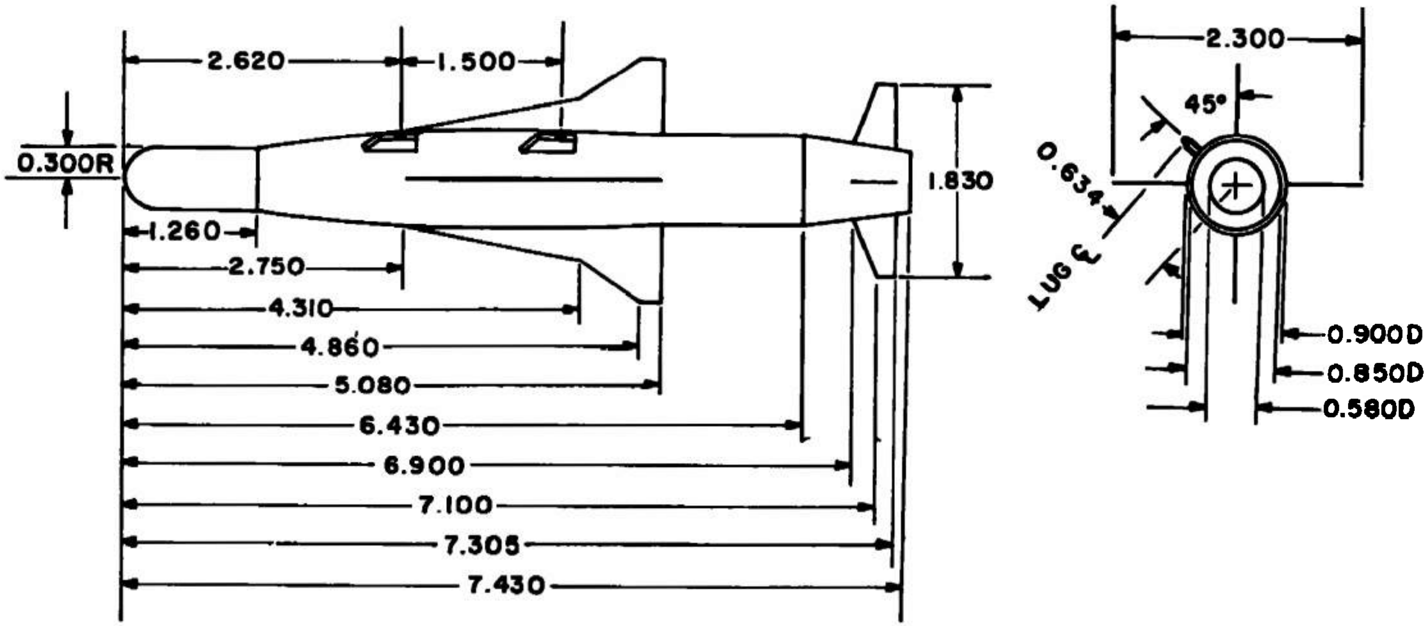

ALL DIMENSIONS IN INCHES

g. Rockwell International Modular Weapons Class II
Figure 6. Continued.

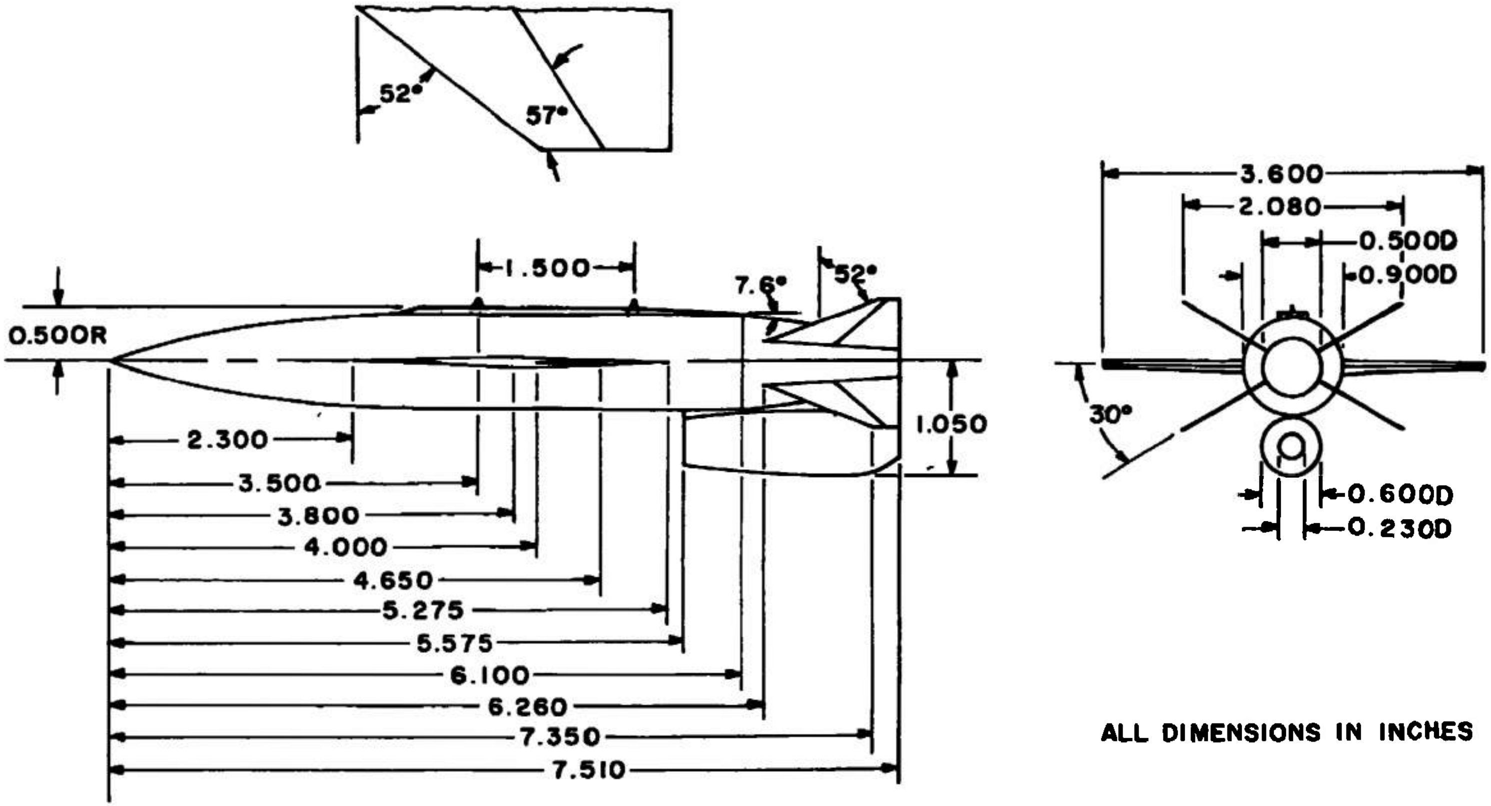

h. Oneway Remotely Piloted Vehicle (RPV)
Figure 6. Continued.

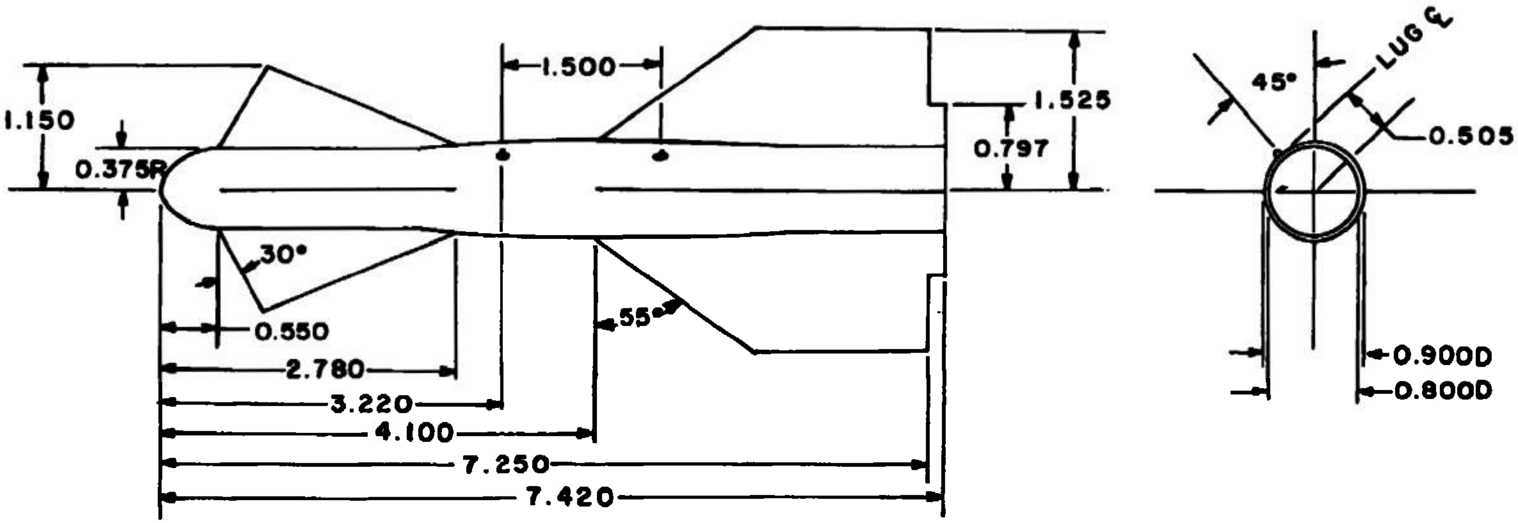

ALL DIMENSIONS IN INCHES

i. Extended Range Vehicle (ERV)
Figure 6. Concluded.

NOTE: PYLONS ARE SHOWN
ON AIRCRAFT PROFILE
ONLY TO INDICATE
ARMAMENT STATIONS

CONFIG NO	EXTERNAL ARMAMENT	ARMAMENT PROFILE	ARMAMENT STATIONS				
			1	2	5	8	9
21	370 GALLON FUEL TANK NONE			PYLON	CLEAN	PYLON	
22	370 GALLON FUEL TANK BOM	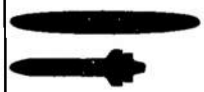			CLEAN		
23	370 GALLON FUEL TANK ERSH	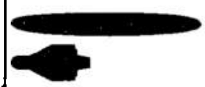			CLEAN		
24	370 GALLON FUEL TANK TCTV	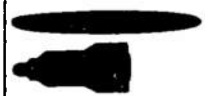			CLEAN	PYLON	
25	370 GALLON FUEL TANK PF MOD WPNS POWERED	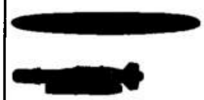			CLEAN		
26	370 GALLON FUEL TANK PF MOD WPNS UNPOWERED	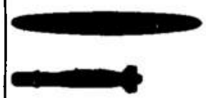			CLEAN		
27	370 GALLON FUEL TANK NARC MOD WPNS CLASS III	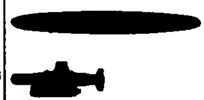			CLEAN		
28	370 GALLON FUEL TANK NARC MOD WPNS CLASS II				CLEAN		
29	370 GALLON FUEL TANK ONEWAY RPV	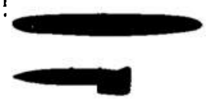			CLEAN		
30	370 GALLON FUEL TANK ERV				CLEAN		

Figure 7. F-4C configuration identification key.

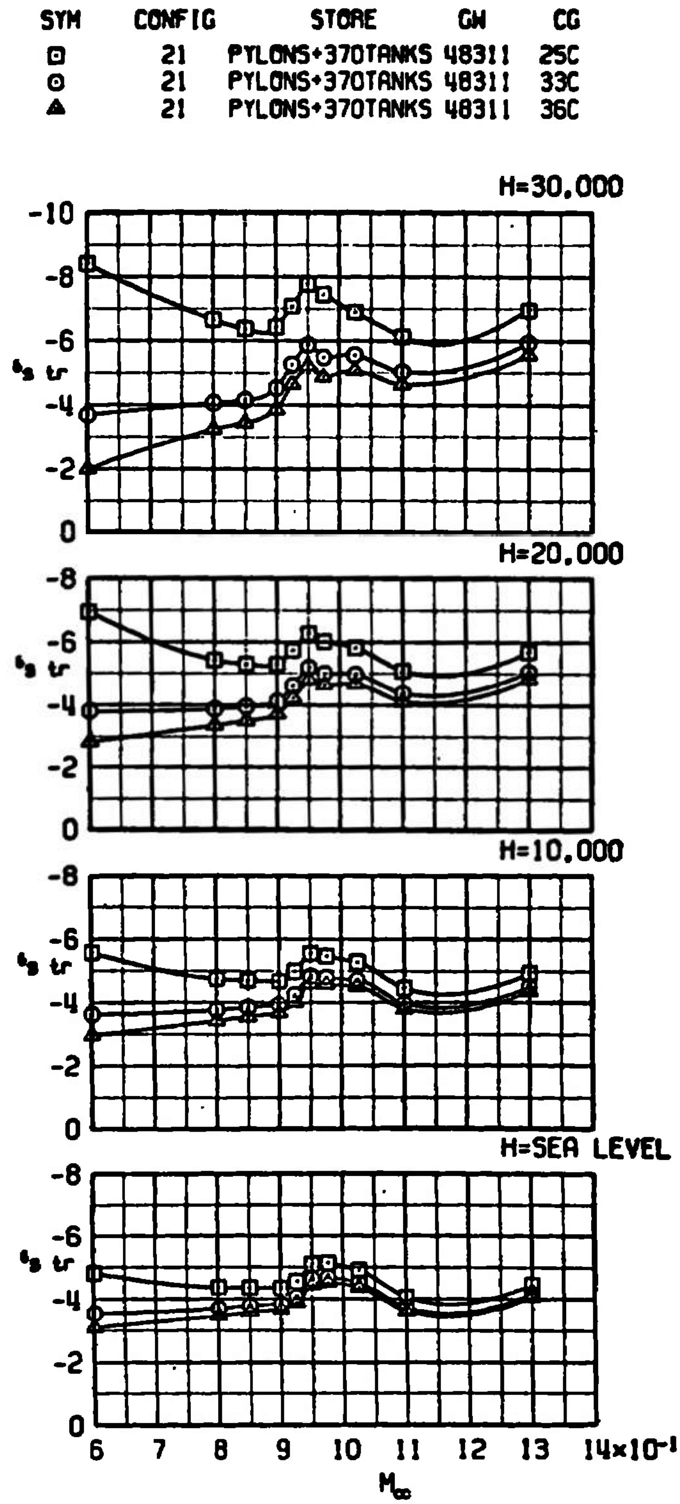

Figure 8. Trim stabilator angle as a function of Mach number, altitude, and cg location for configuration 21.

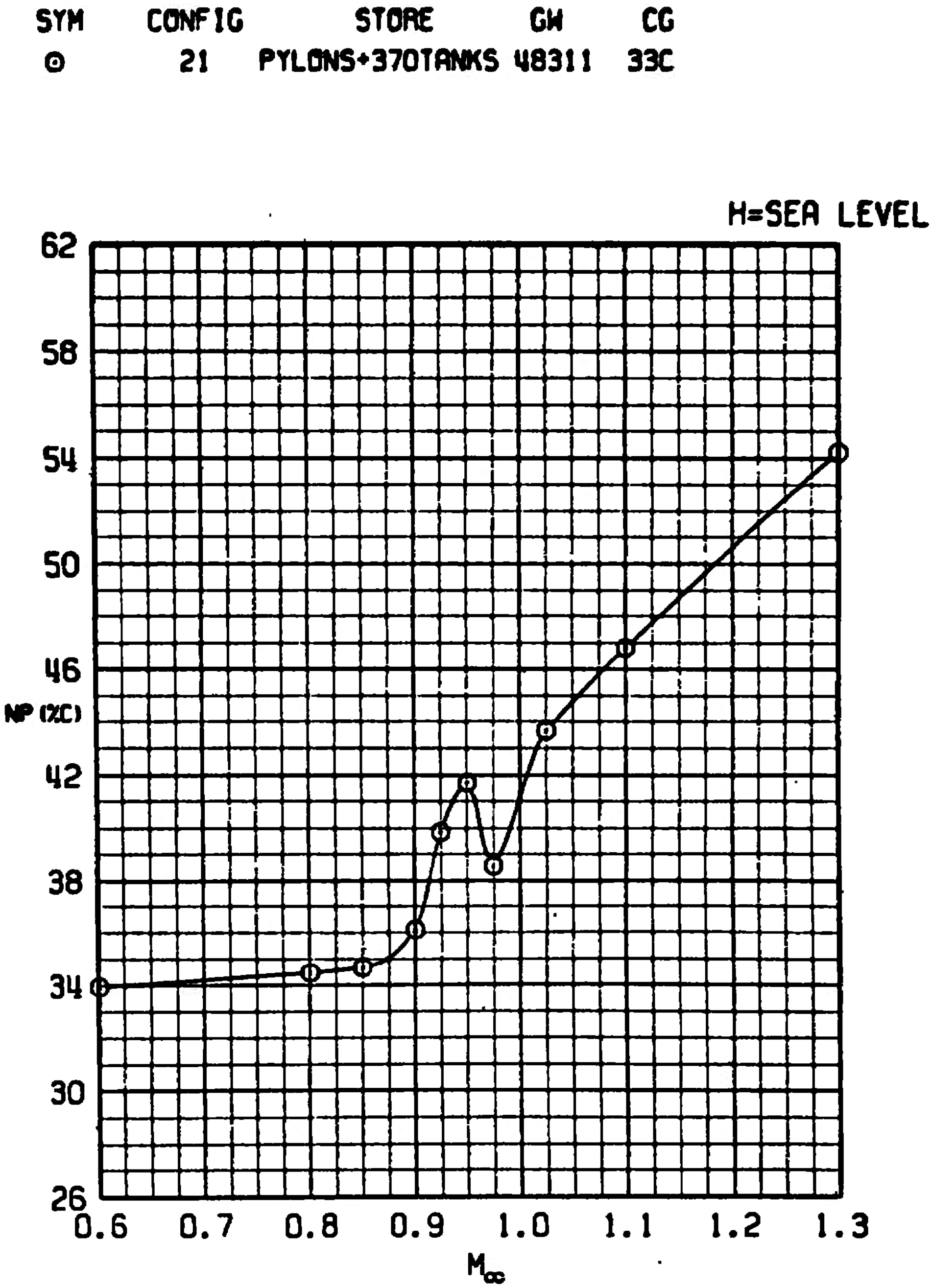

a. H = Sea level

Figure 9. Neutral-point location as a function of Mach number and altitude for configuration 21.

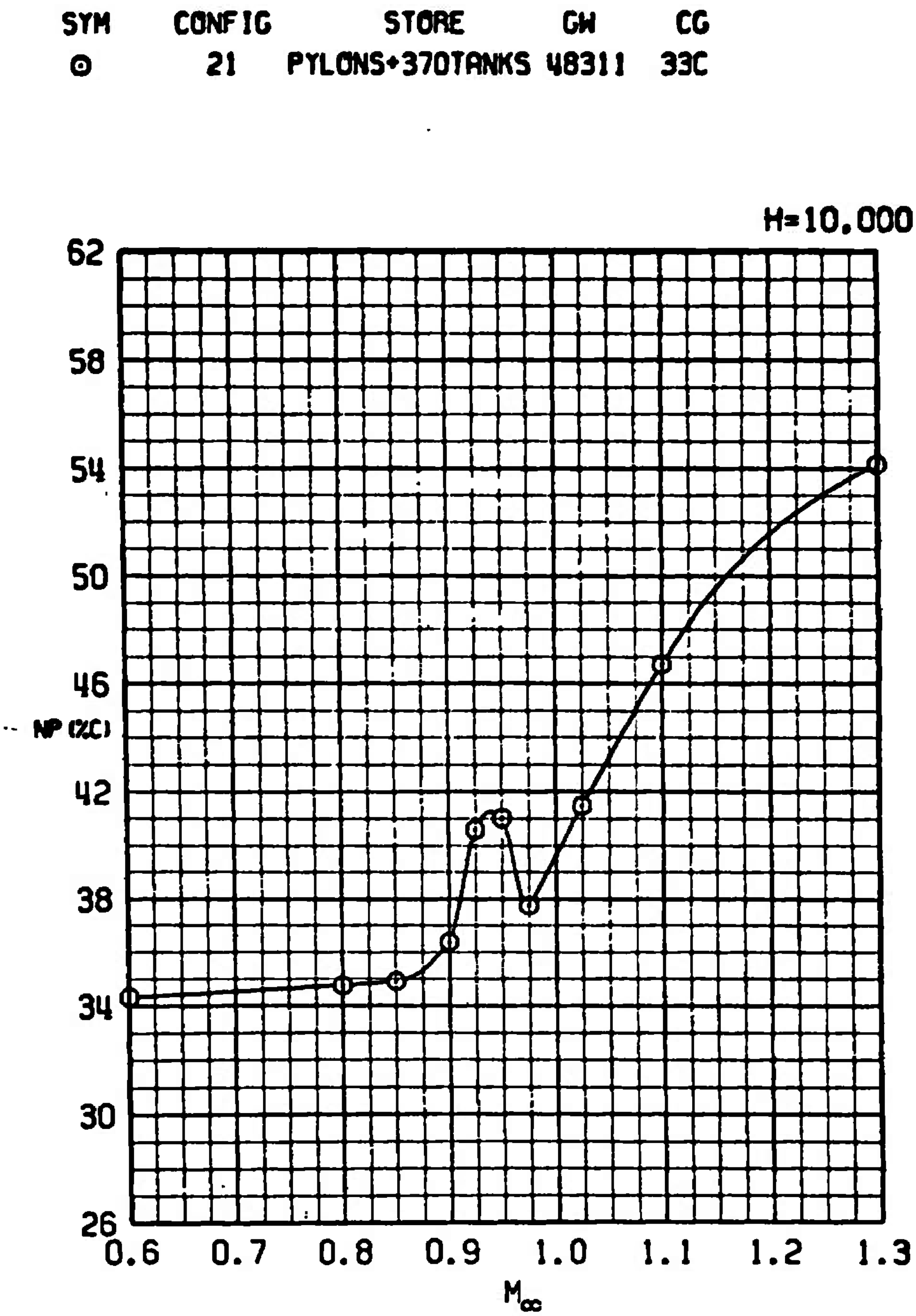

b. H = 10,000
Figure 9. Continued.

SYM	CONFIG	STORE	GW	CG
⊙	21	PYLONS+370TANKS	48311	33C

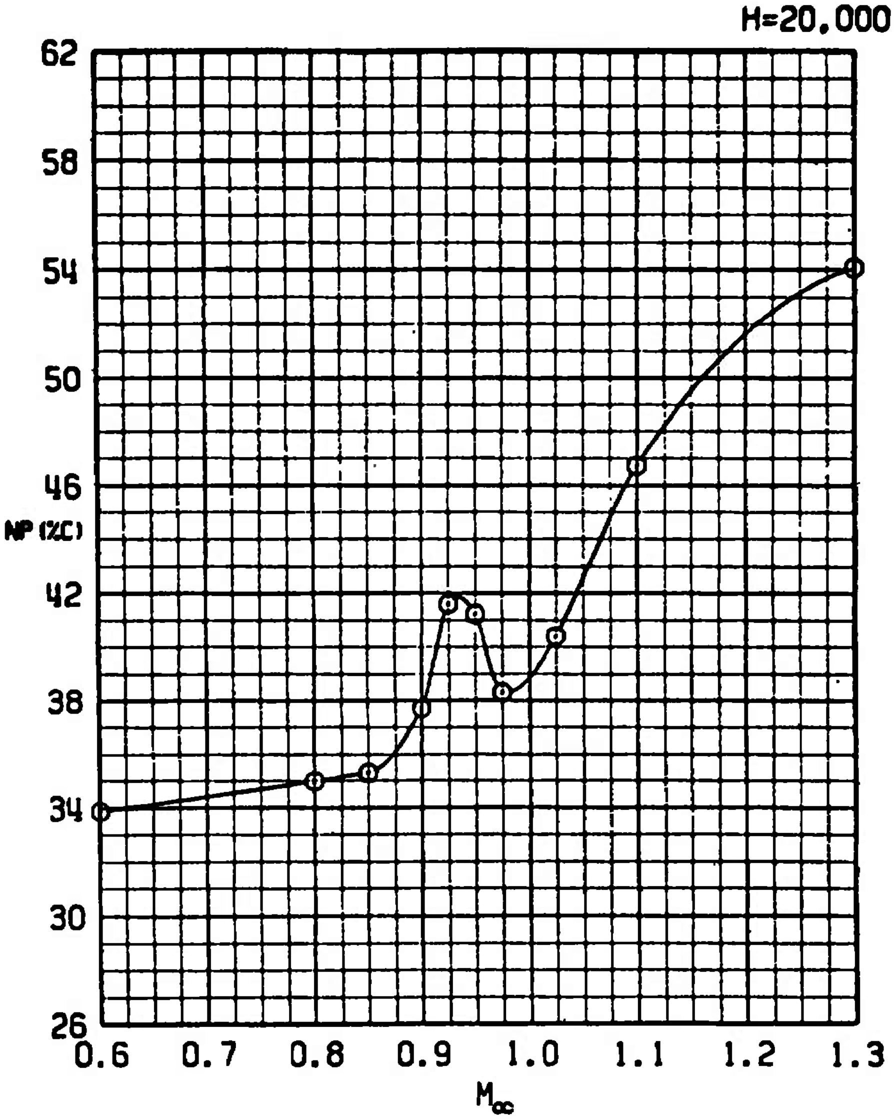

c. H = 20,000
Figure 9. Continued.

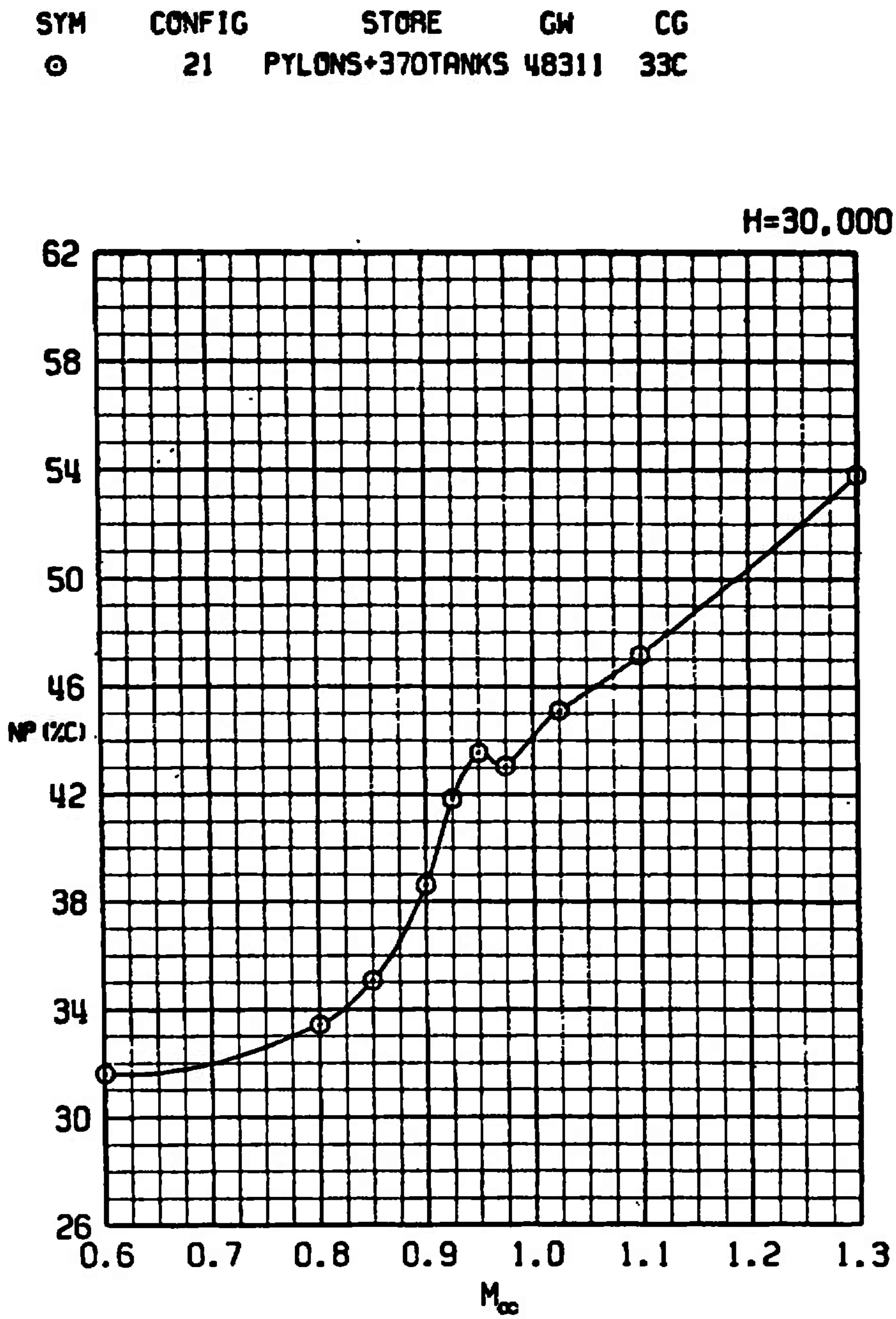

d. H = 30,000
Figure 9. Concluded.

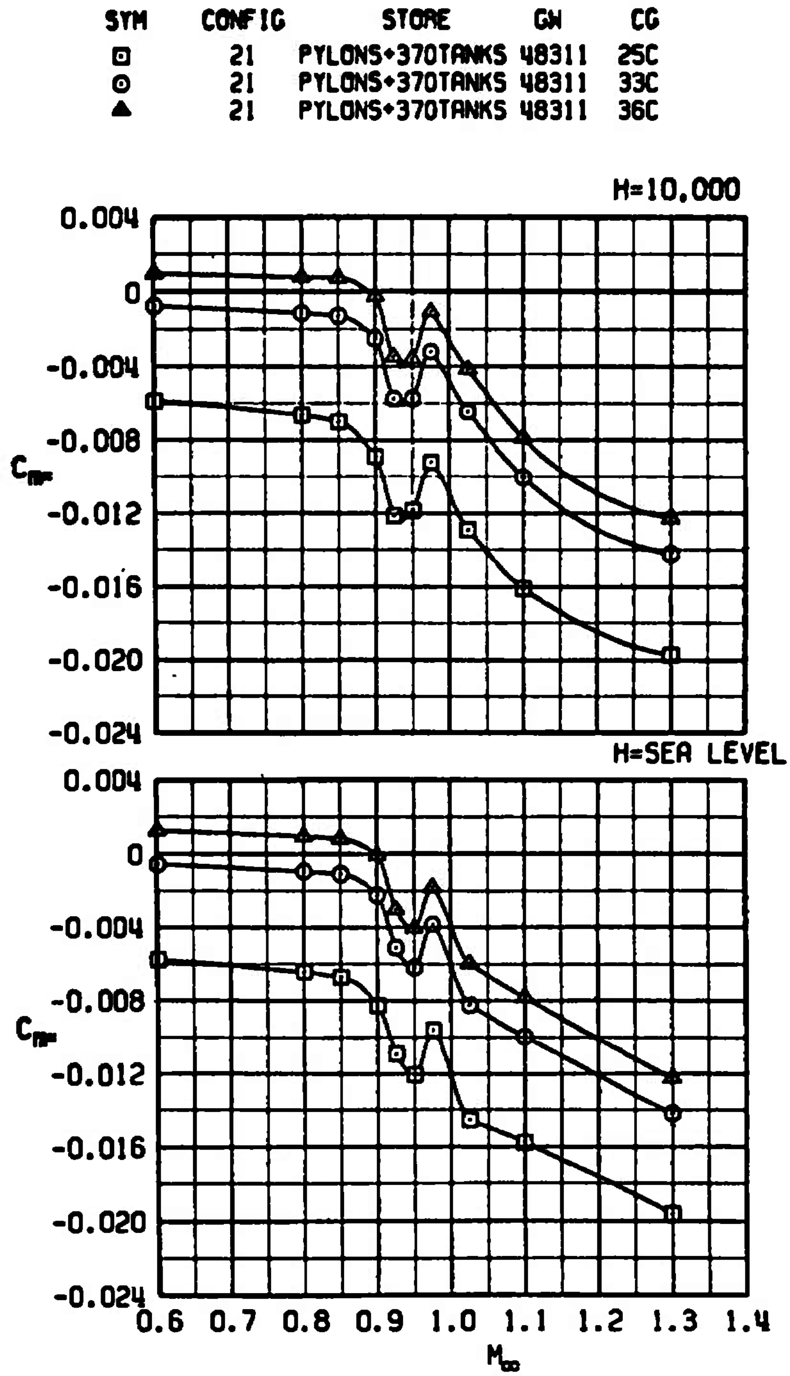

a. H = Sea level and 10,000

Figure 10. Slope of pitching-moment coefficient versus angle-of-attack curve at trim as a function of Mach number, altitude, and cg location for configuration 21.

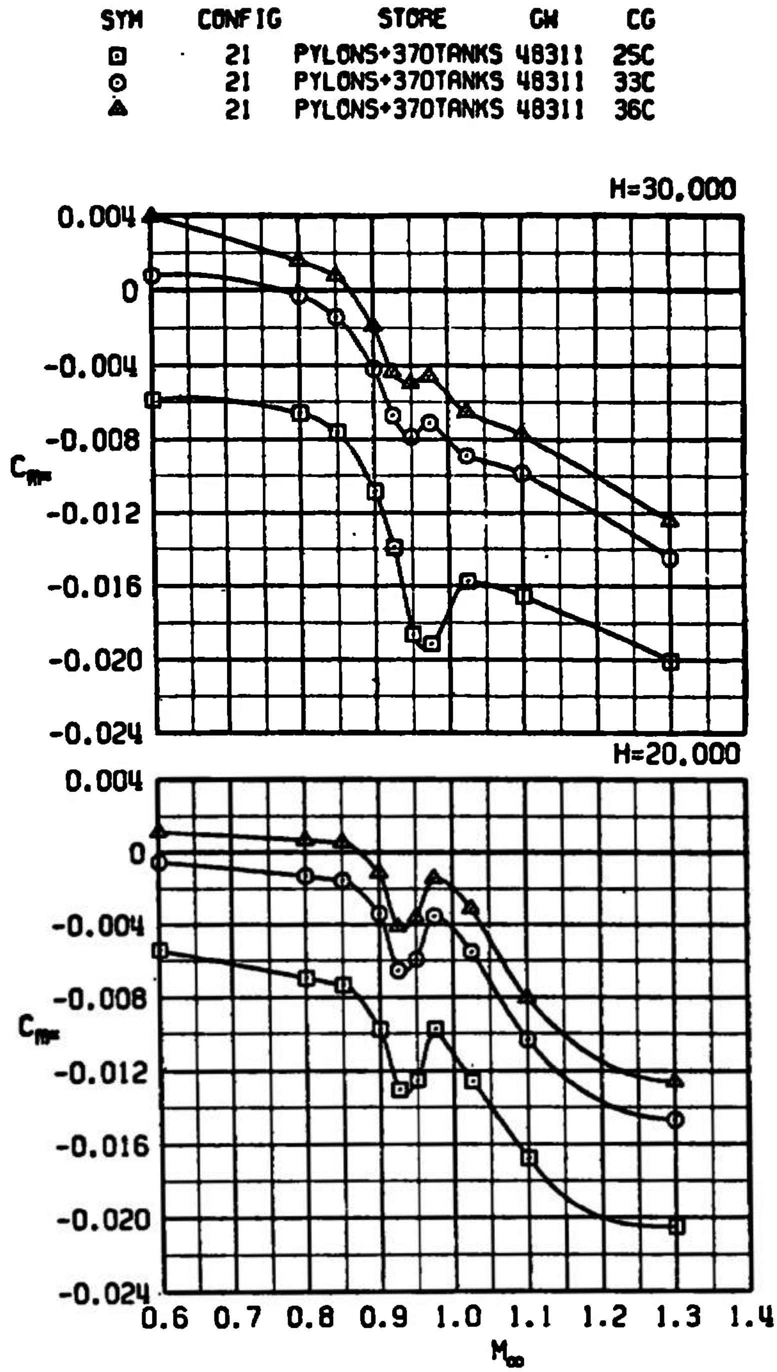

b. H = 20,000 and 30,000
Figure 10. Concluded.

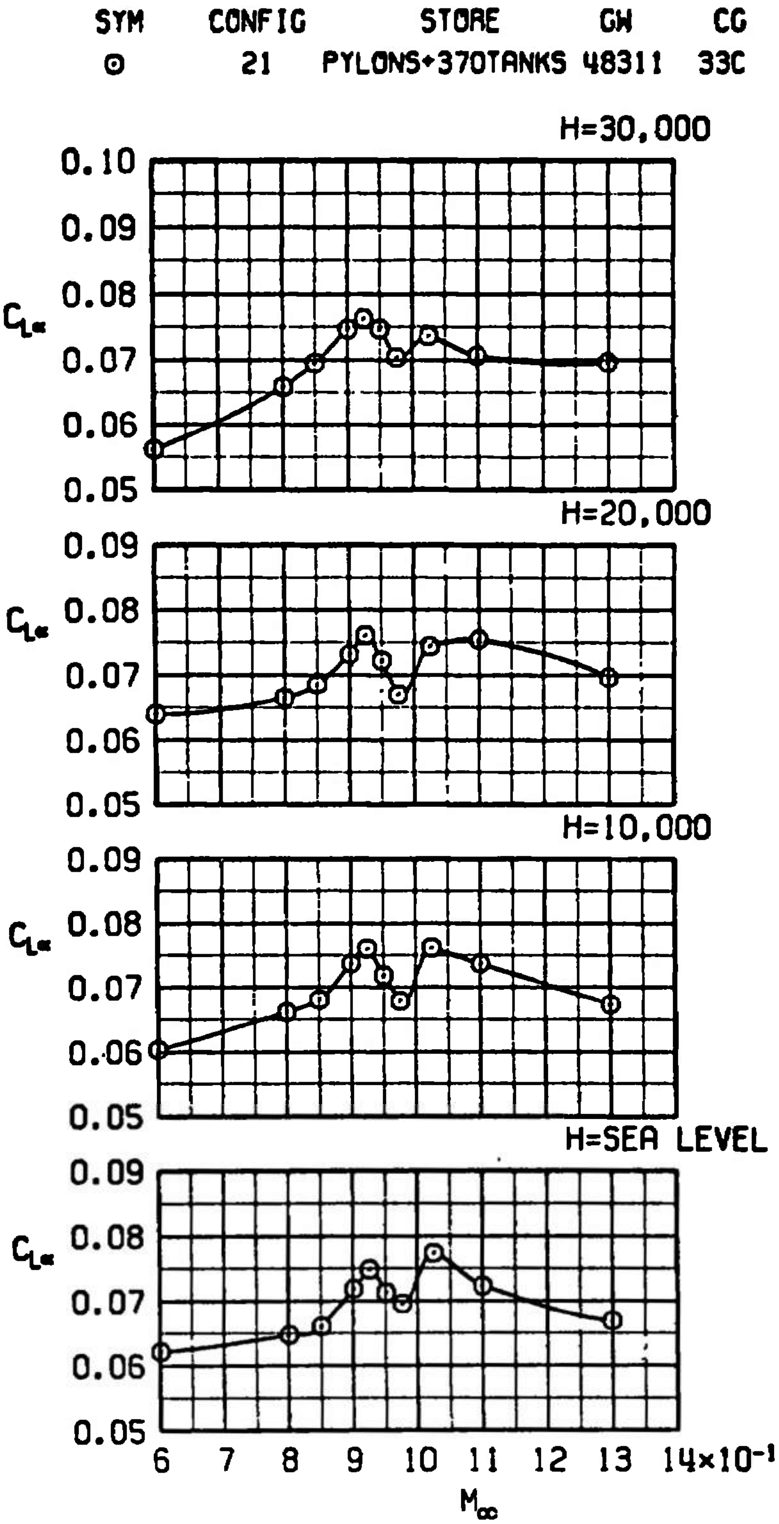

Figure 11. Lift-curve slope as a function of Mach number and altitude for configuration 21.

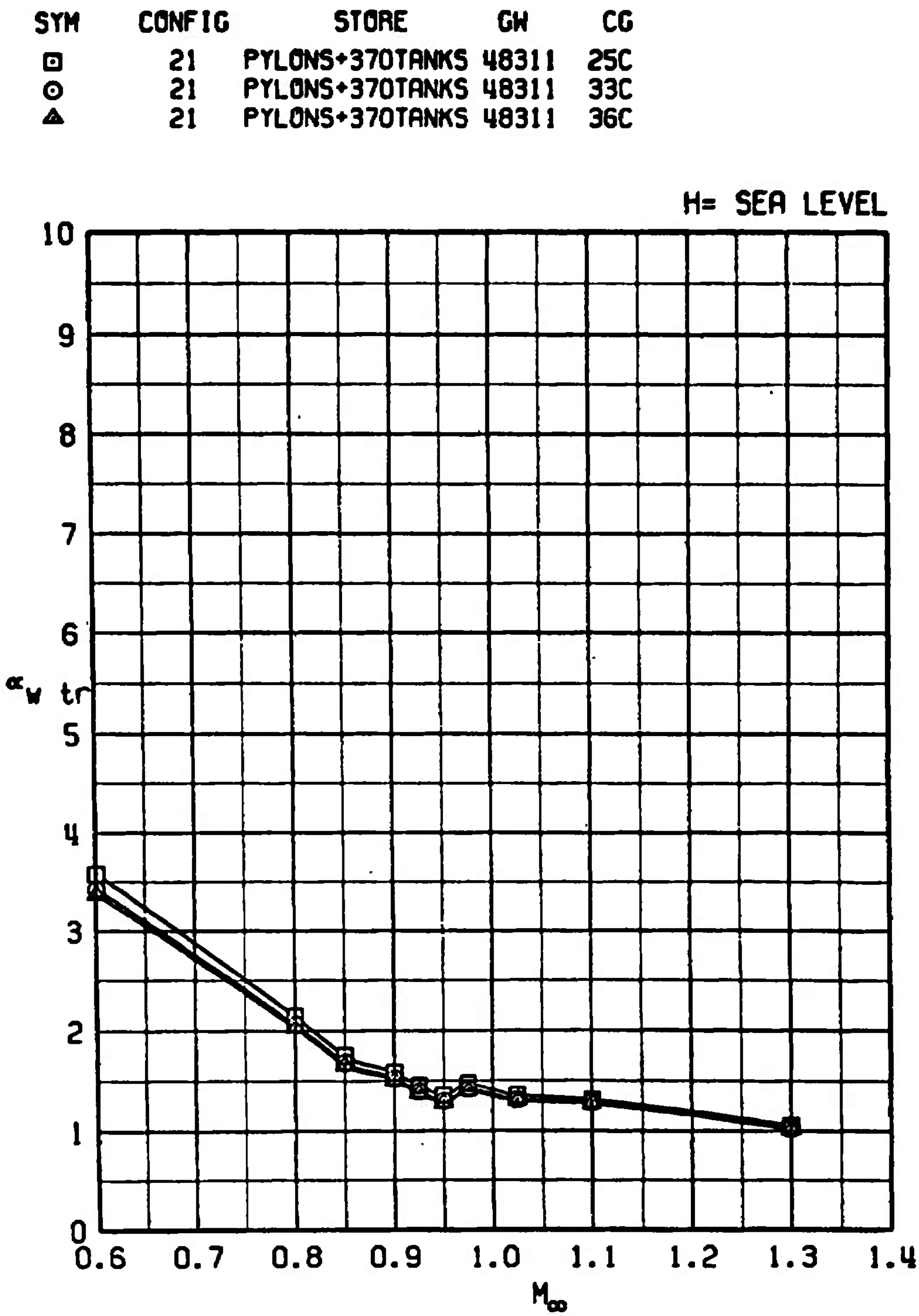

a. H = Sea level

Figure 12. Trim angle of attack as a function of Mach number, altitude, and cg location for configuration 21.

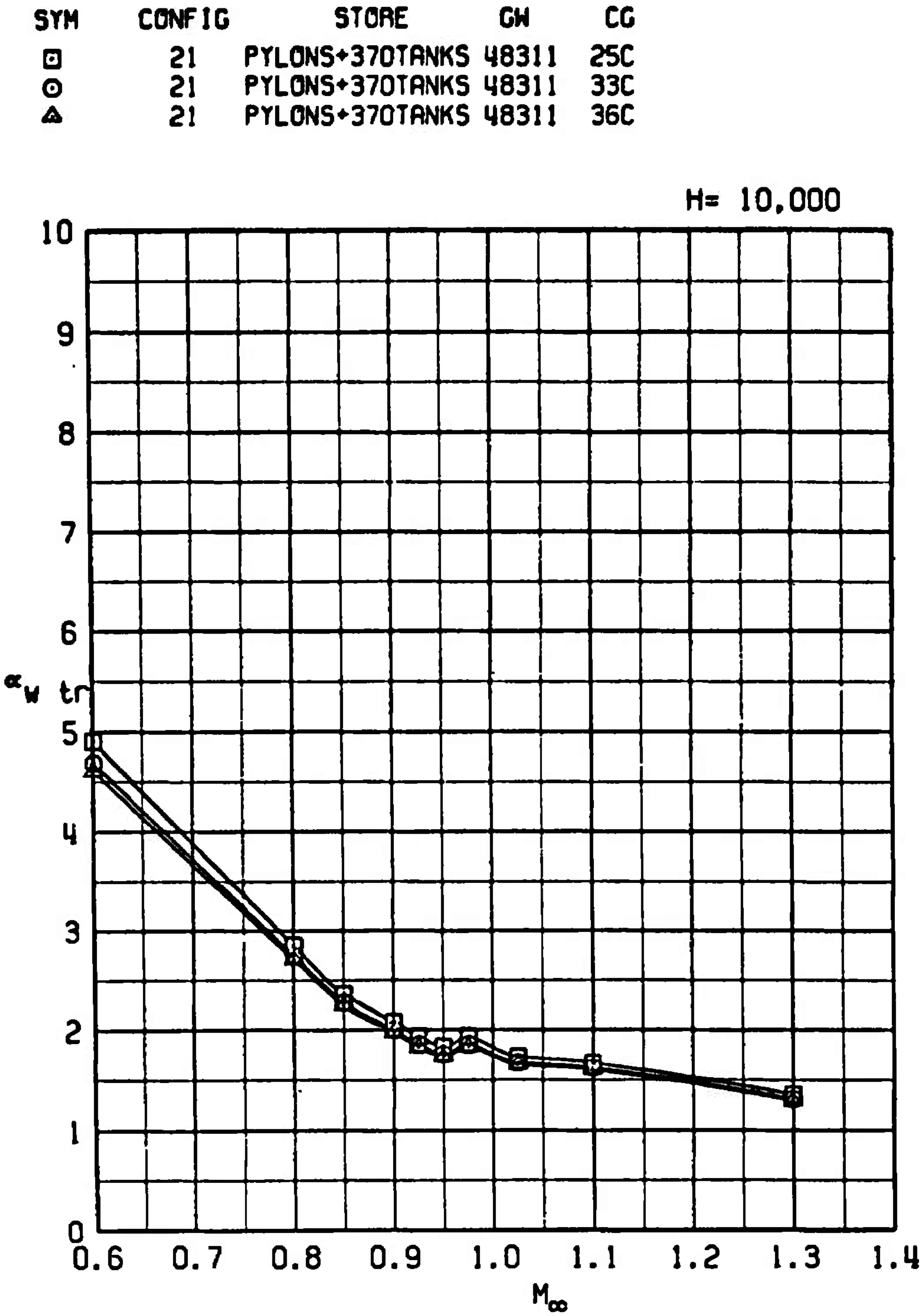

b. H = 10,000
Figure 12. Continued.

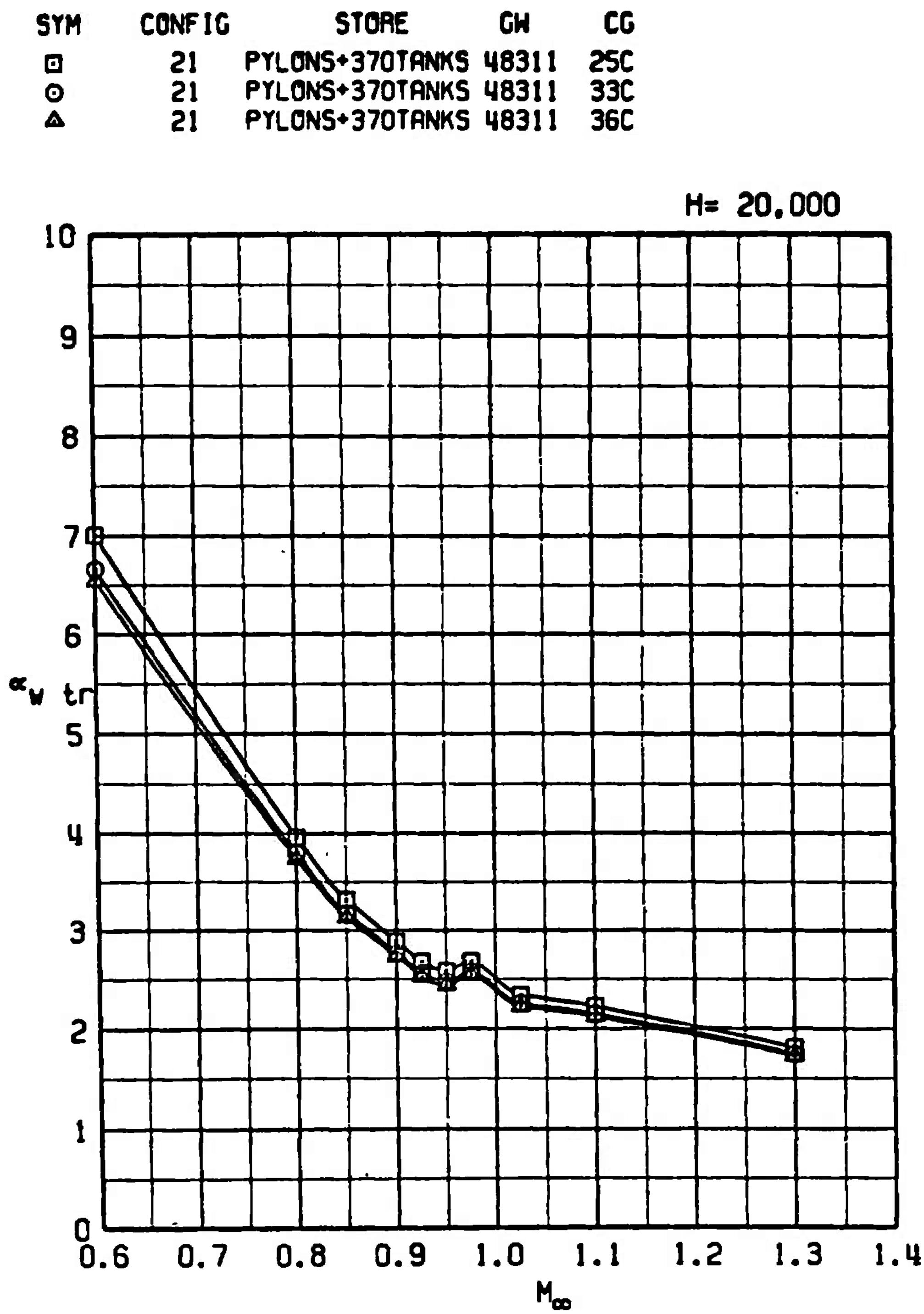

c. H = 20,000
Figure 12. Continued.

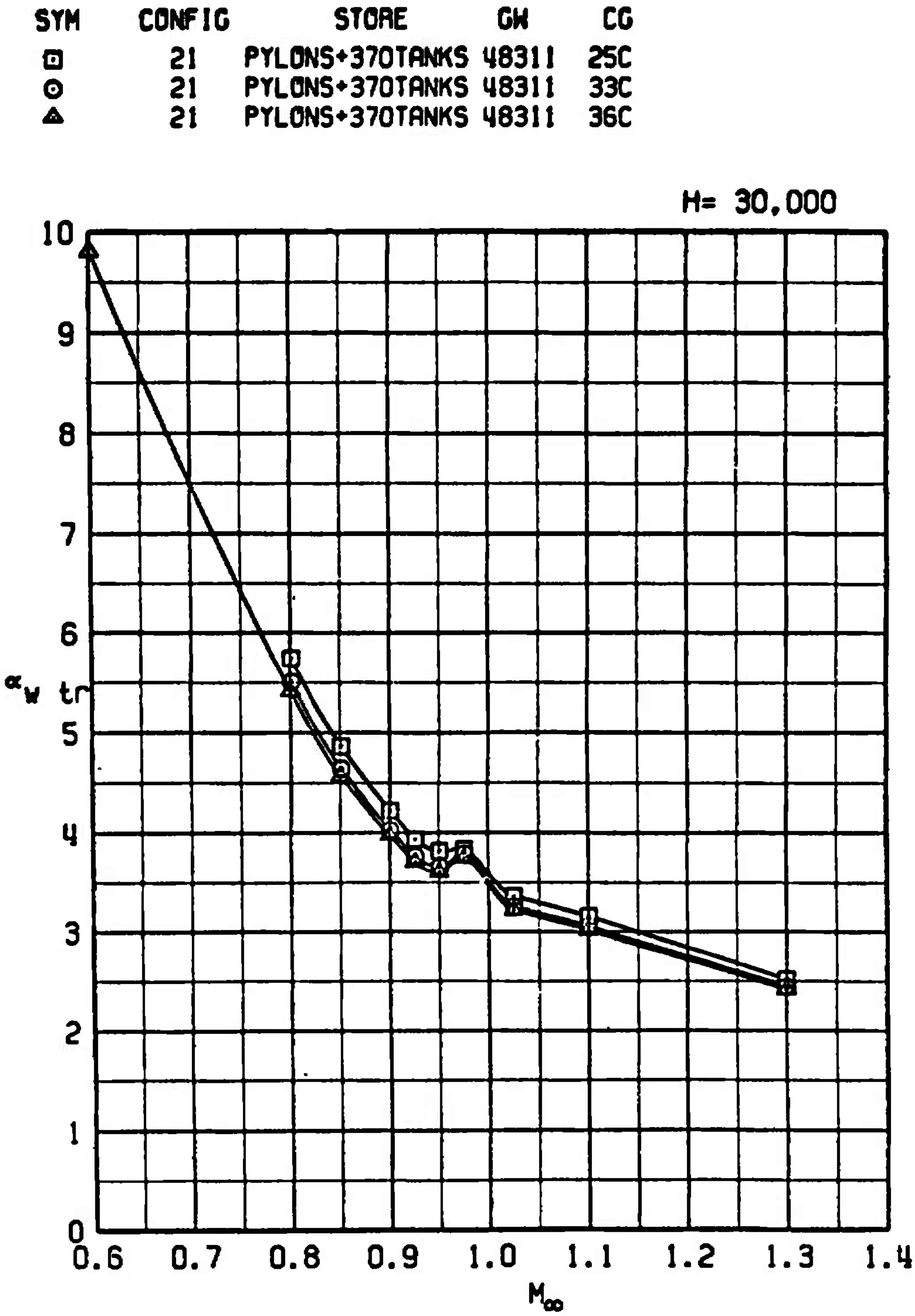

d. H = 30,000

Figure 12. Concluded.

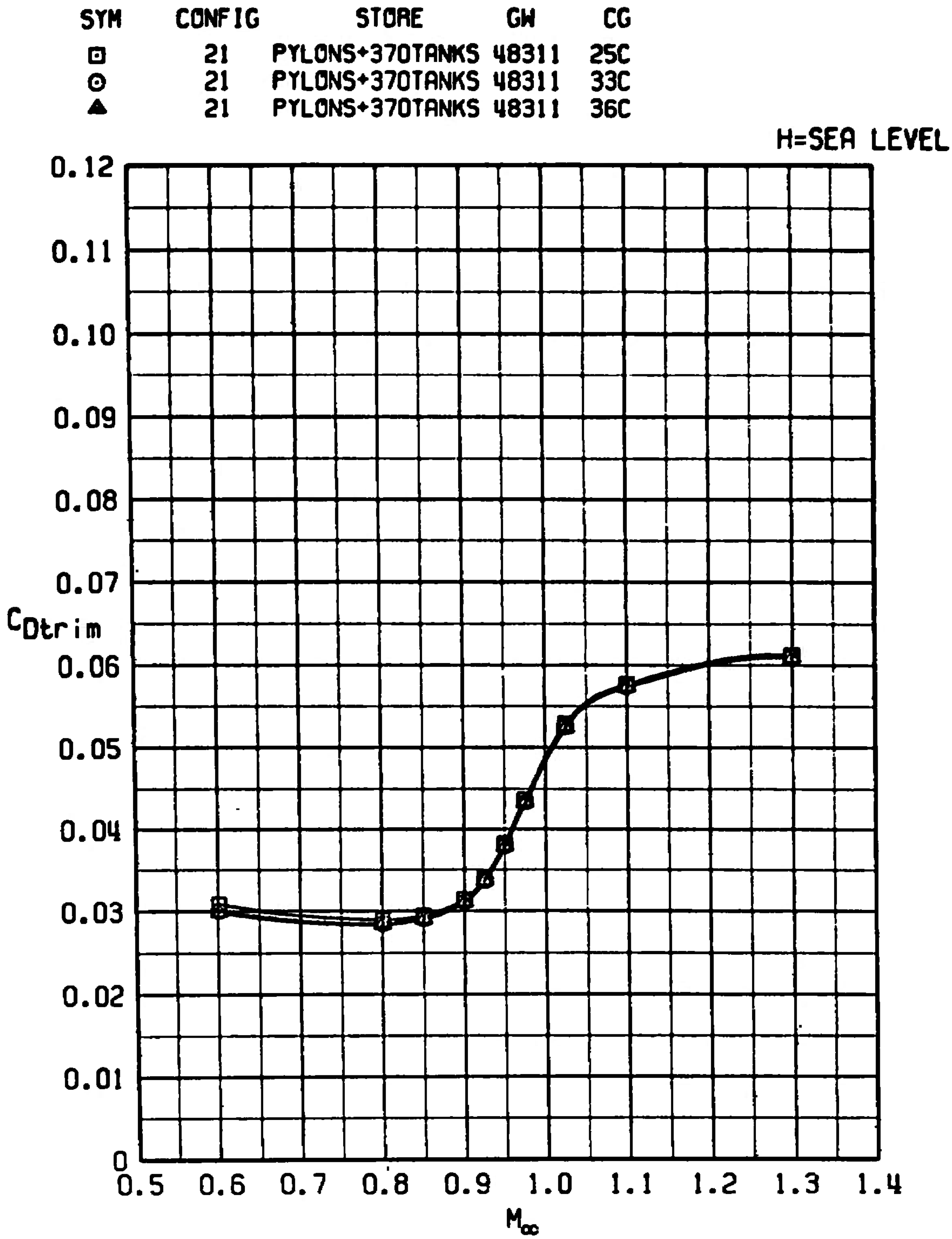

a. H = Sea level

Figure 13. Trim drag as a function of Mach number, altitude, and cg location for configuration 21.

SYM	CONFIG	STORE	GW	CG
⊡	21	PYLONS+370TANKS	48311	25C
⊙	21	PYLONS+370TANKS	48311	33C
△	21	PYLONS+370TANKS	48311	36C

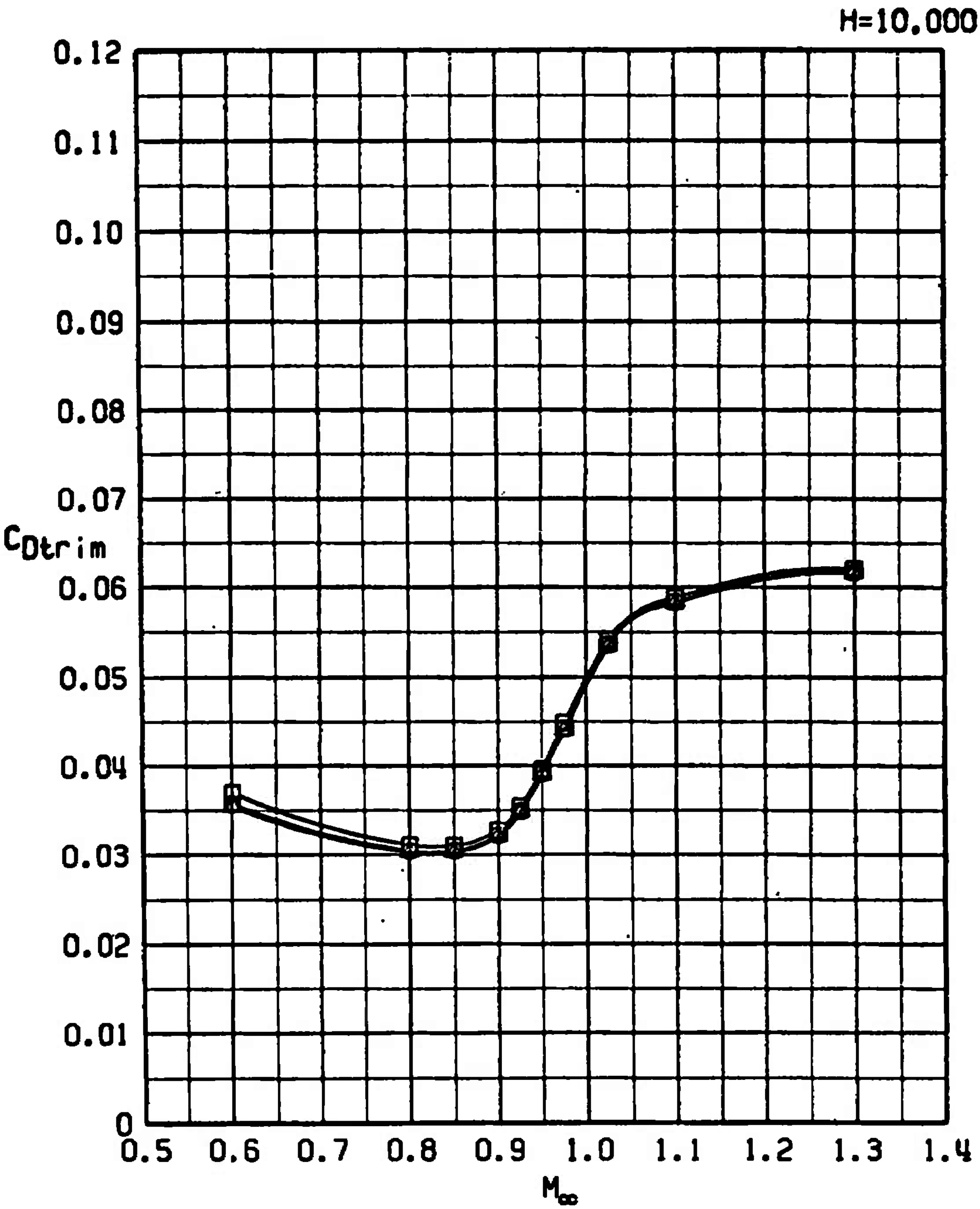

b. H = 10,000
Figure 13. Continued.

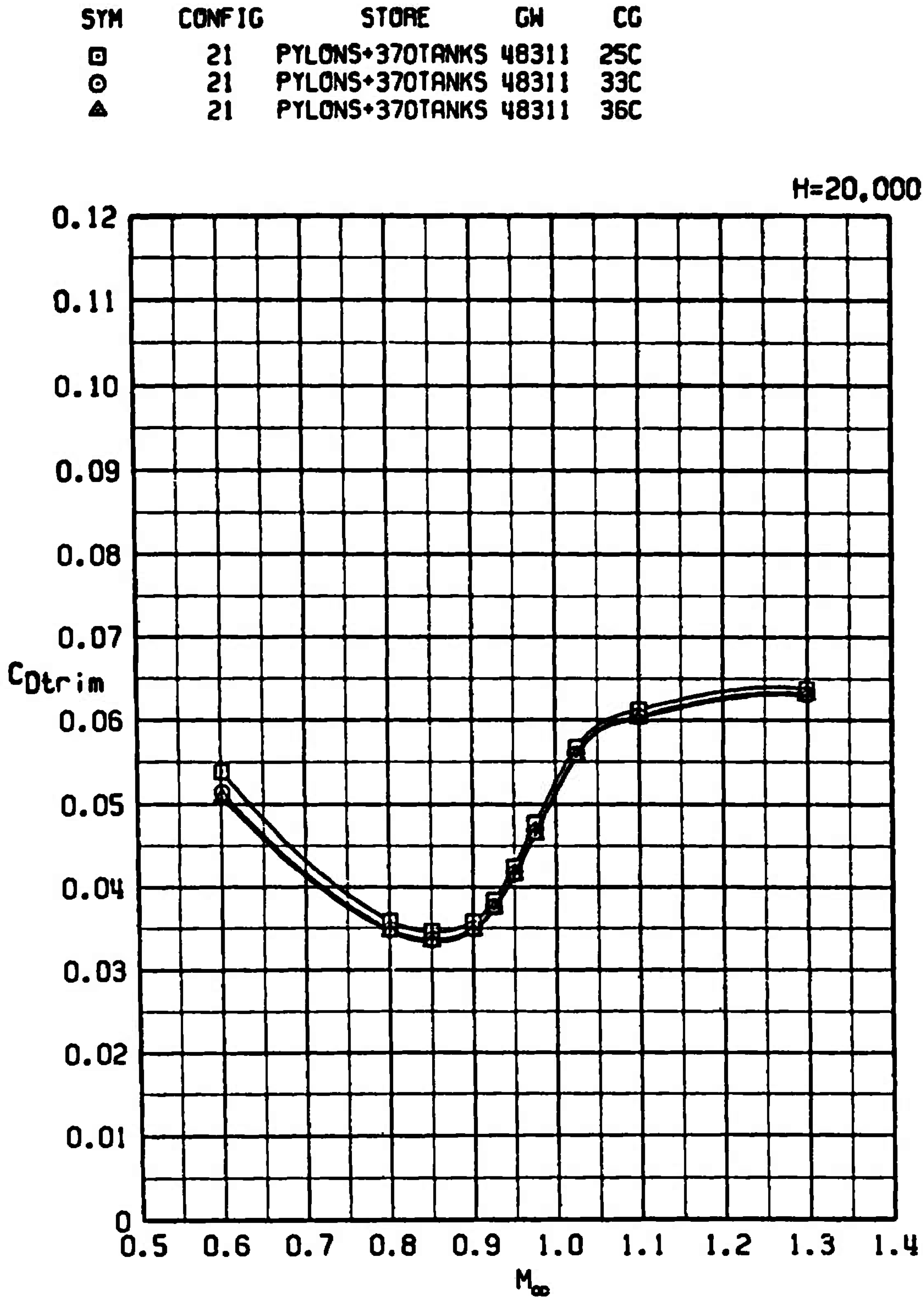

c. H = 20,000
Figure 13. Continued.

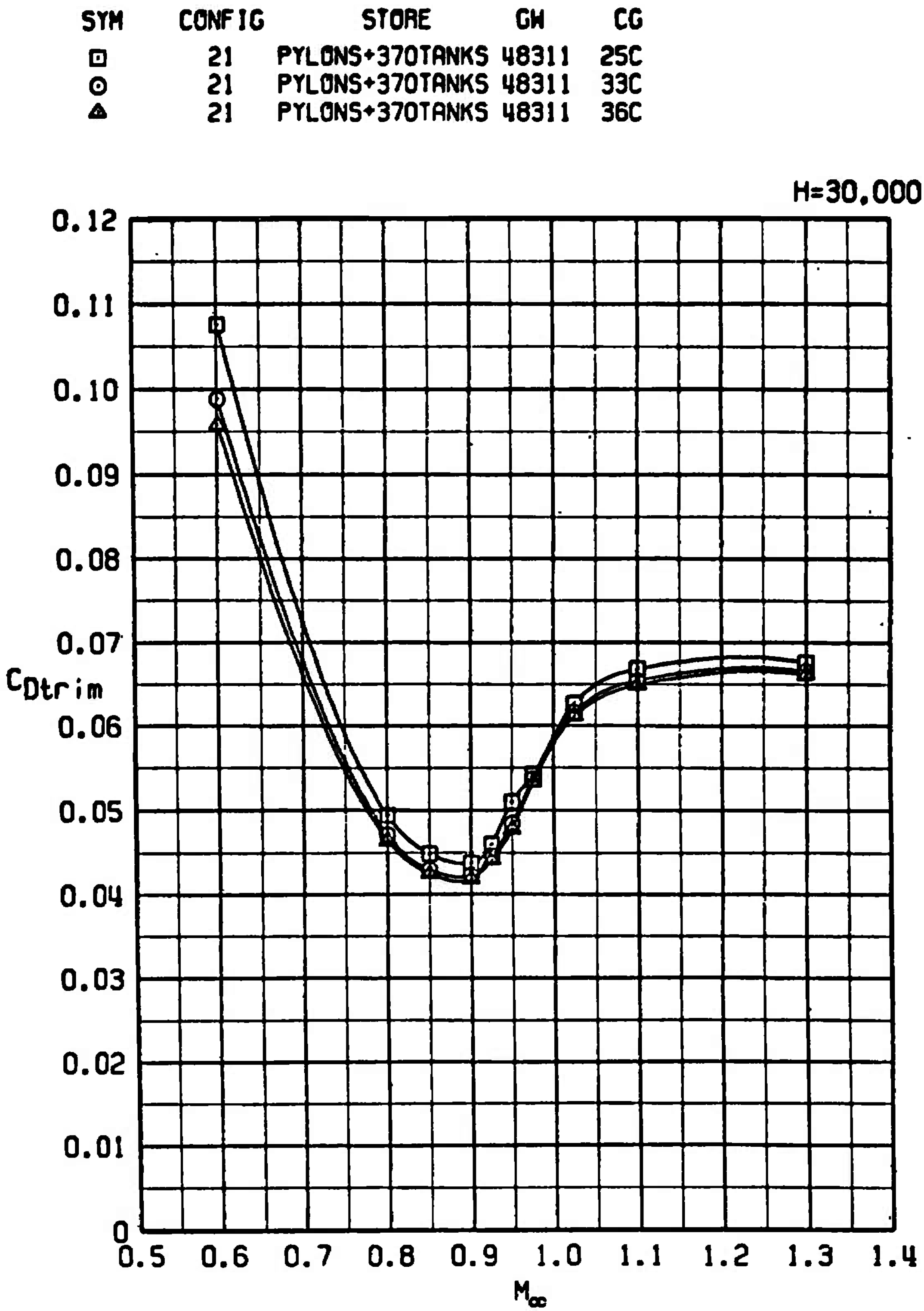

d. H = 30,000
Figure 13. Concluded.

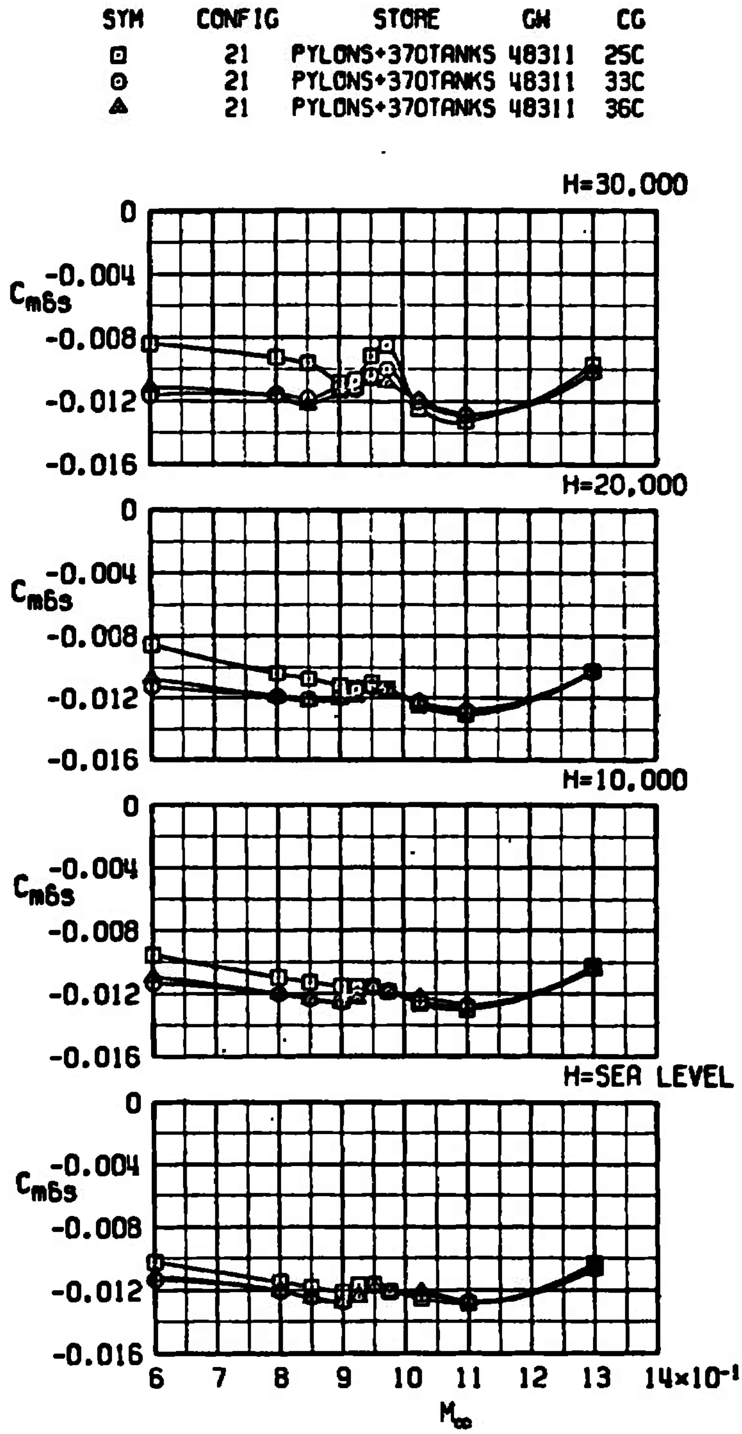

a. Stabilator power

Figure 14. Longitudinal control derivatives at trim as a function of Mach number, altitude, and cg location for configuration 21.

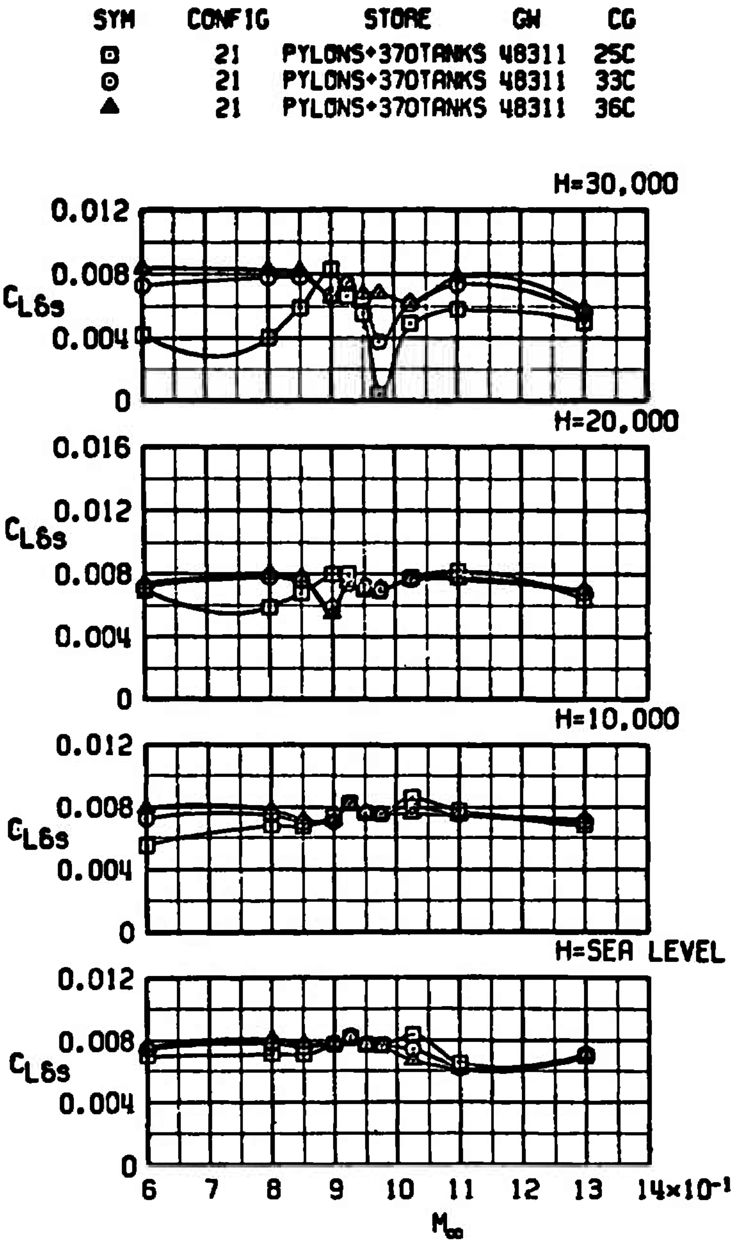

b. Stabilator lift effectiveness
Figure 14. Concluded.

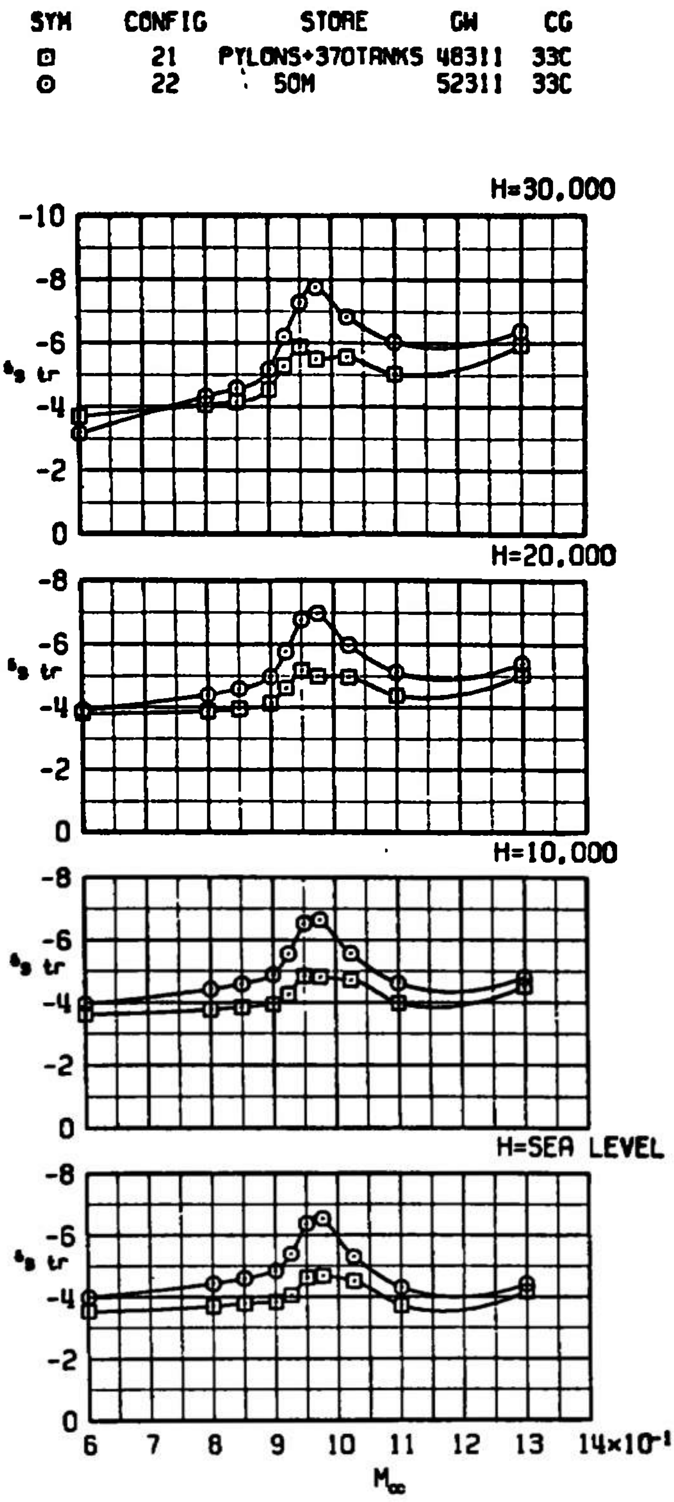

Figure 15. The effect of the SOM store on trim stabilator angle.

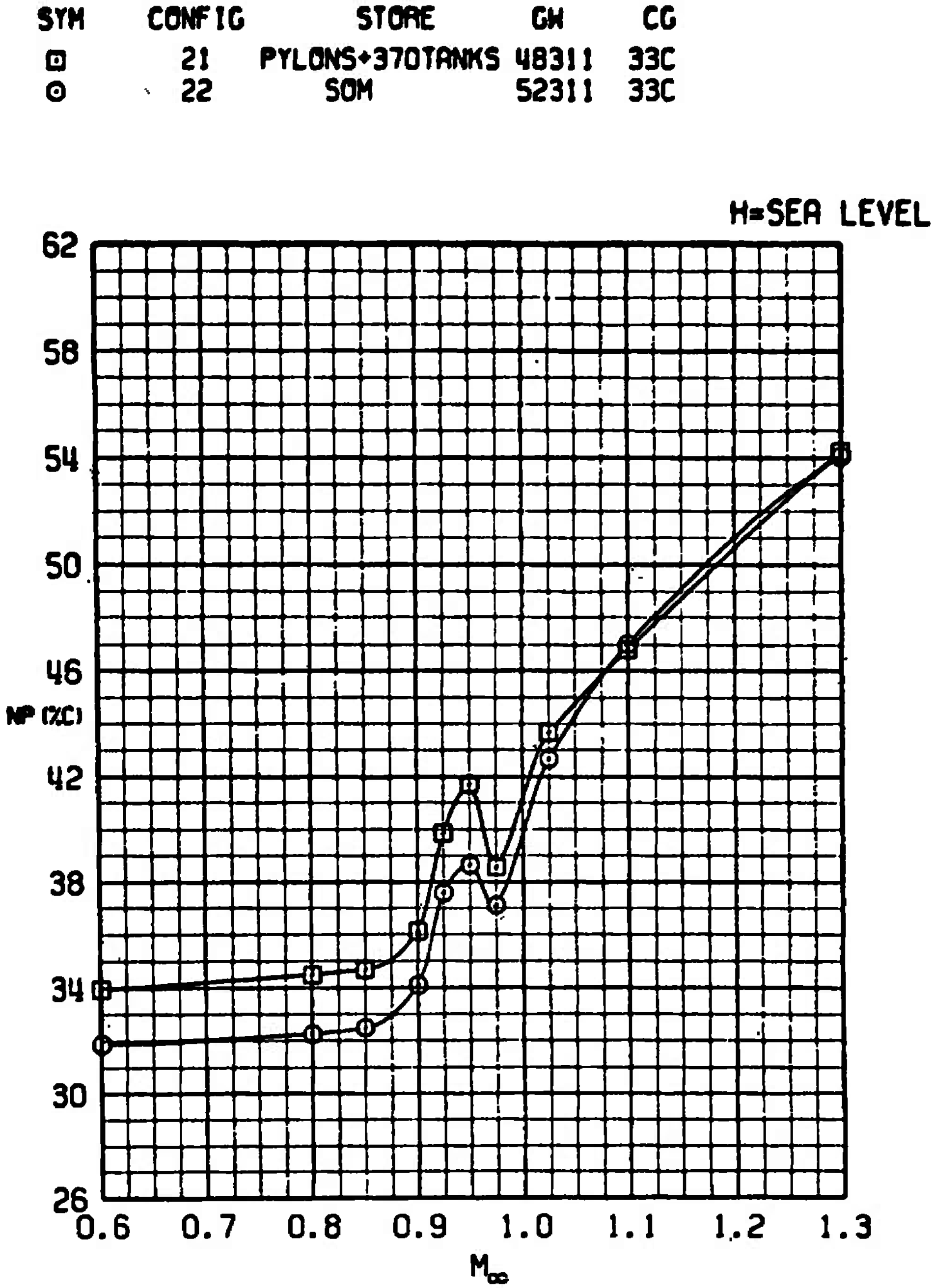

a. H = Sea level

Figure 16. The effect of the SOM store on neutral-point location.

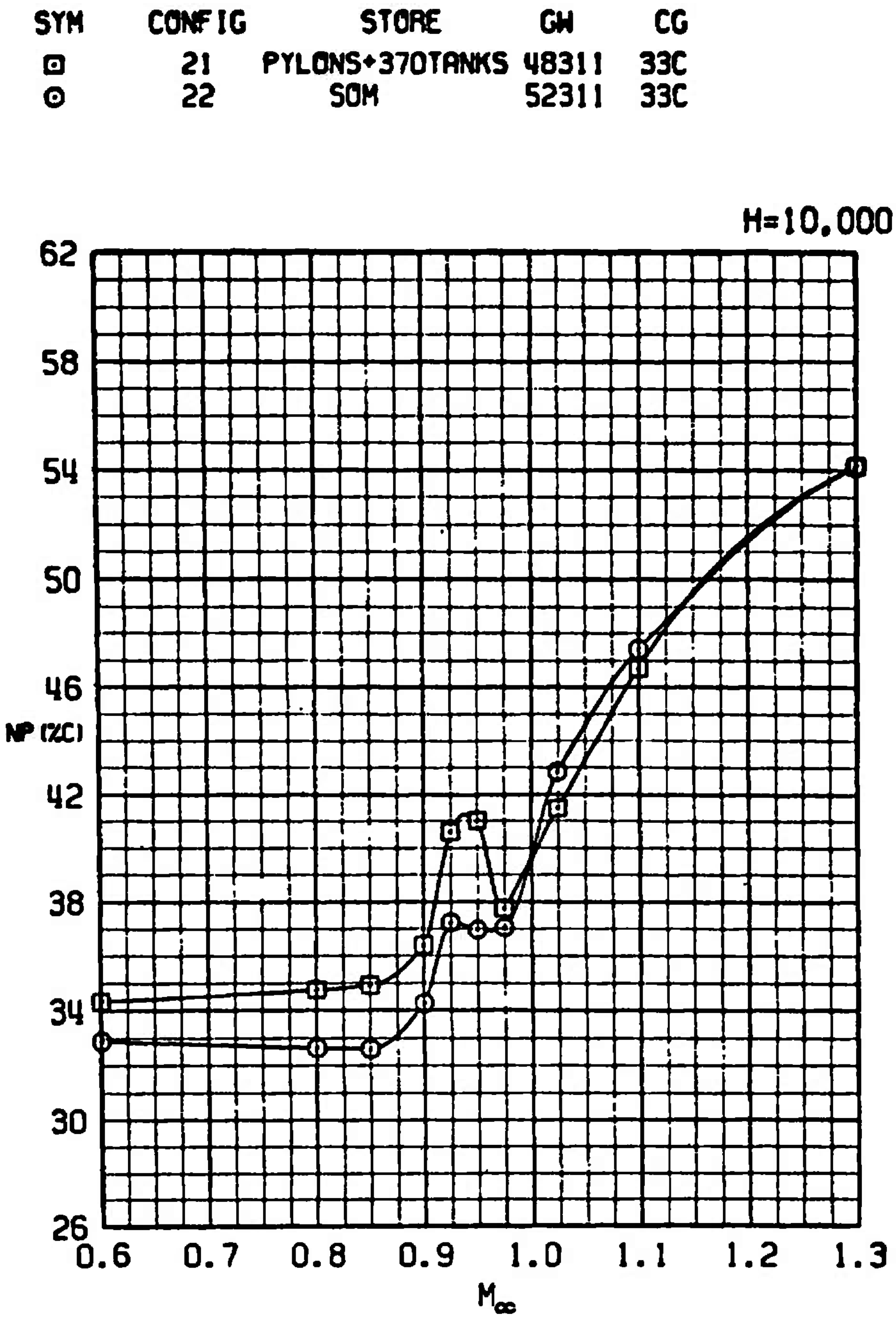

b. H = 10,000
Figure 16. Continued.

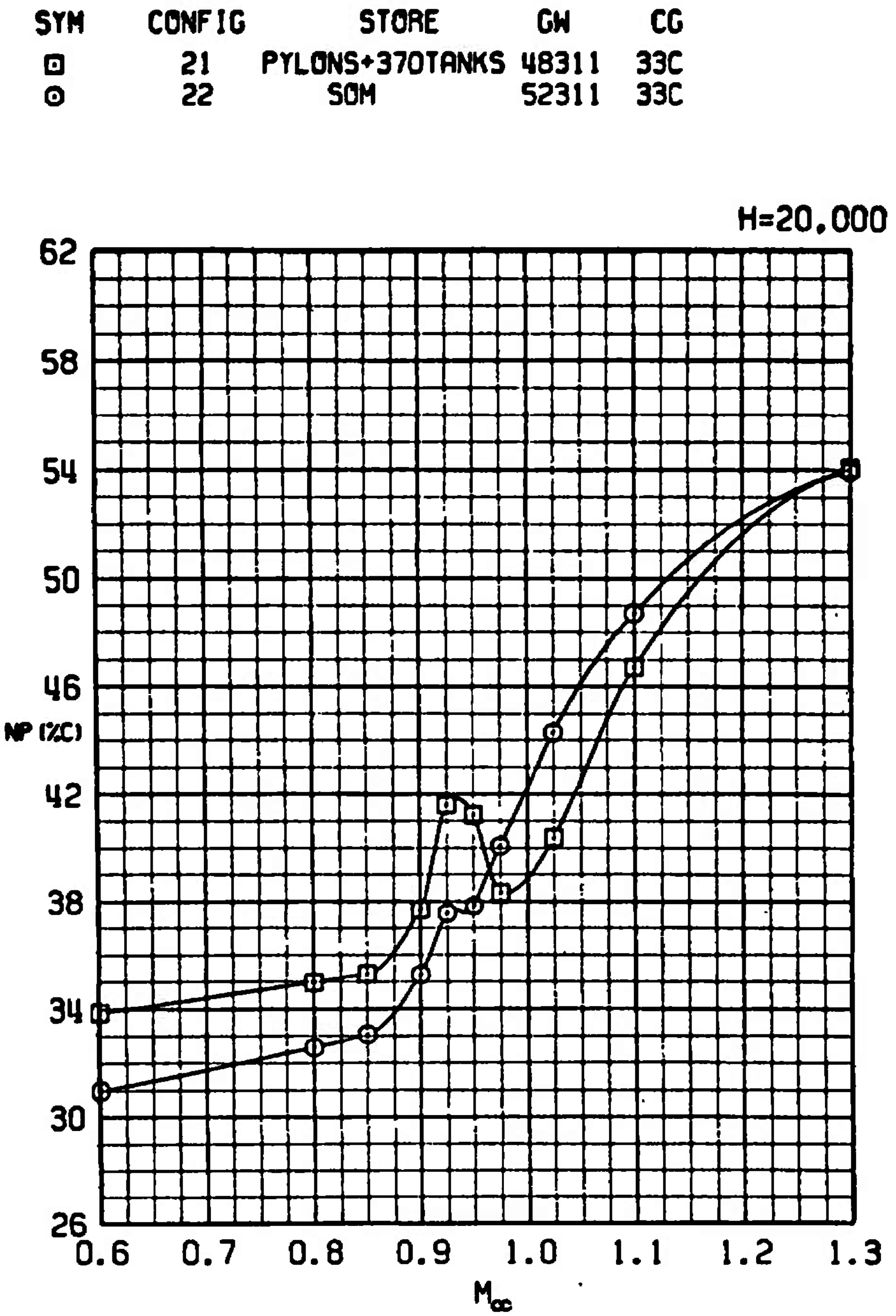

c. H = 20,000

Figure 16. Continued.

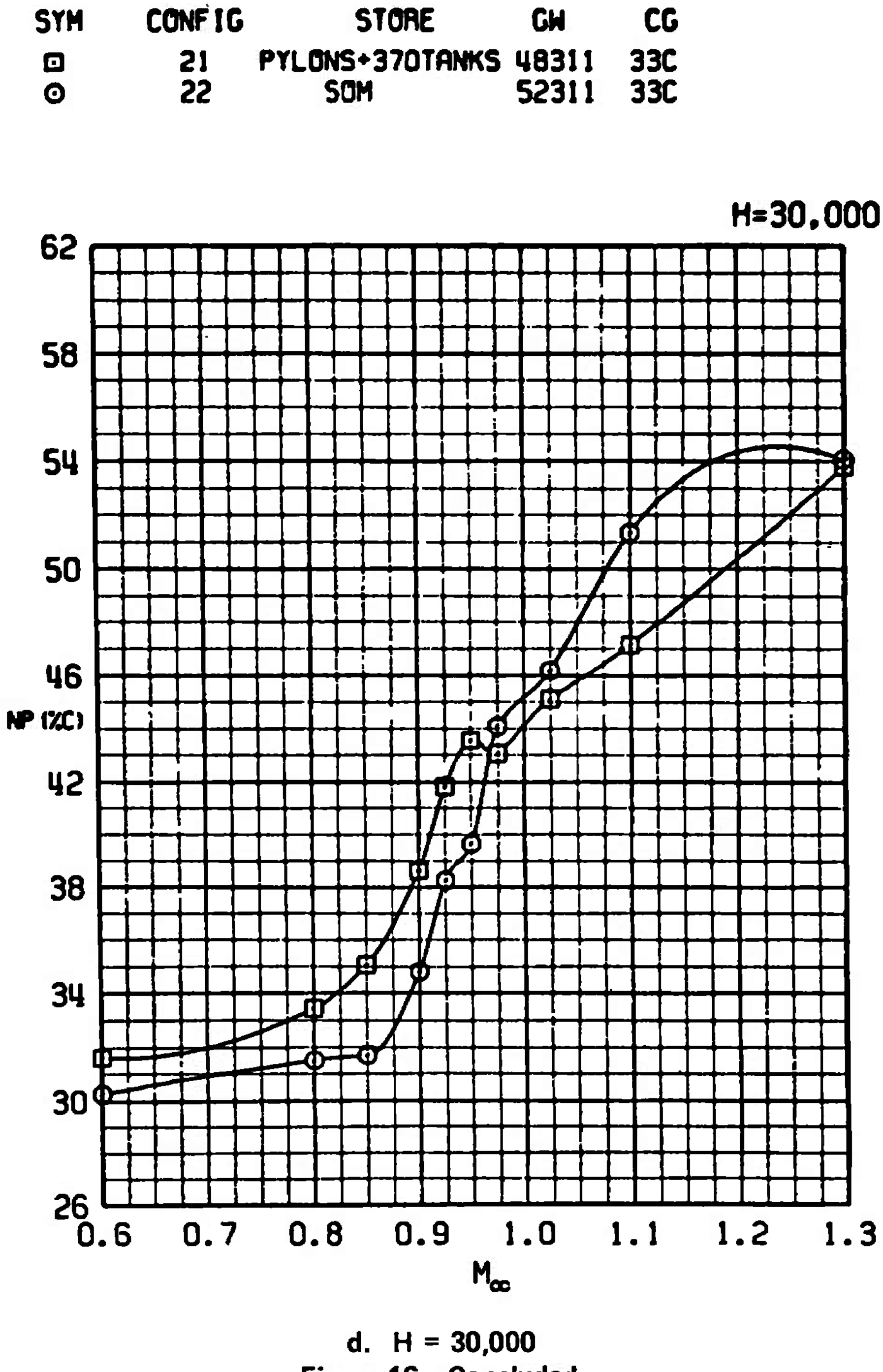

d. H = 30,000
Figure 16. Concluded.

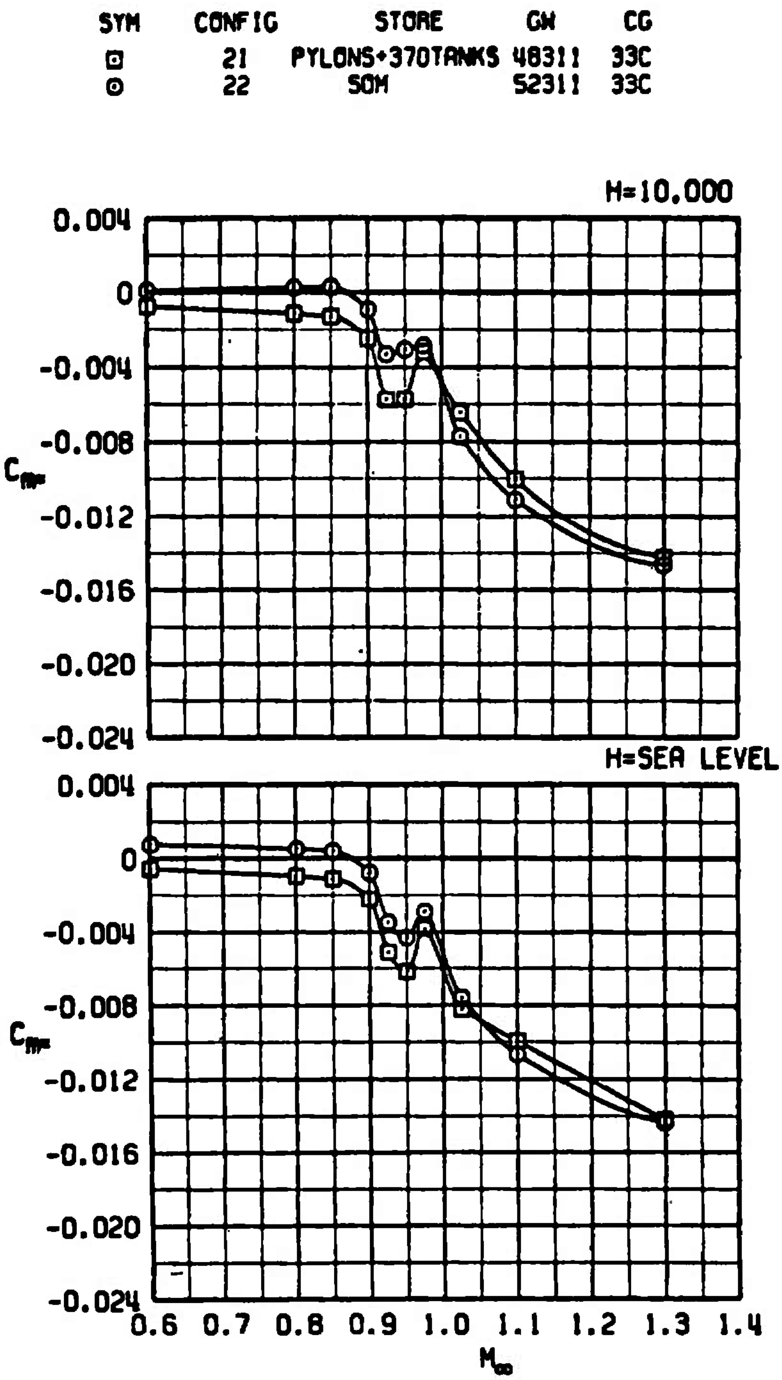

a. H = Sea level and 10,000

Figure 17. The effect of the SOM store on the slope of the pitching-moment coefficient versus angle-of-attack curve at trim.

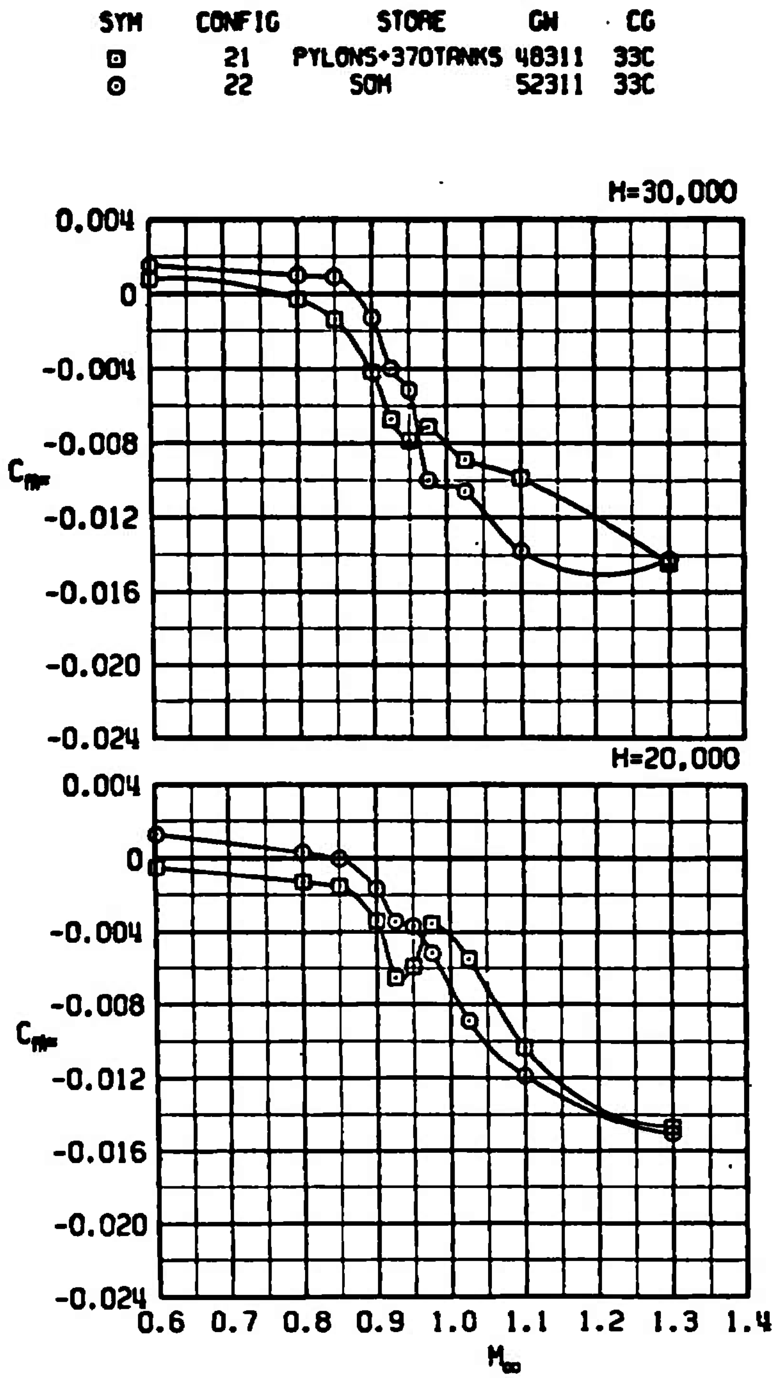

b. H = 20,000 and 30,000
Figure 17. Concluded.

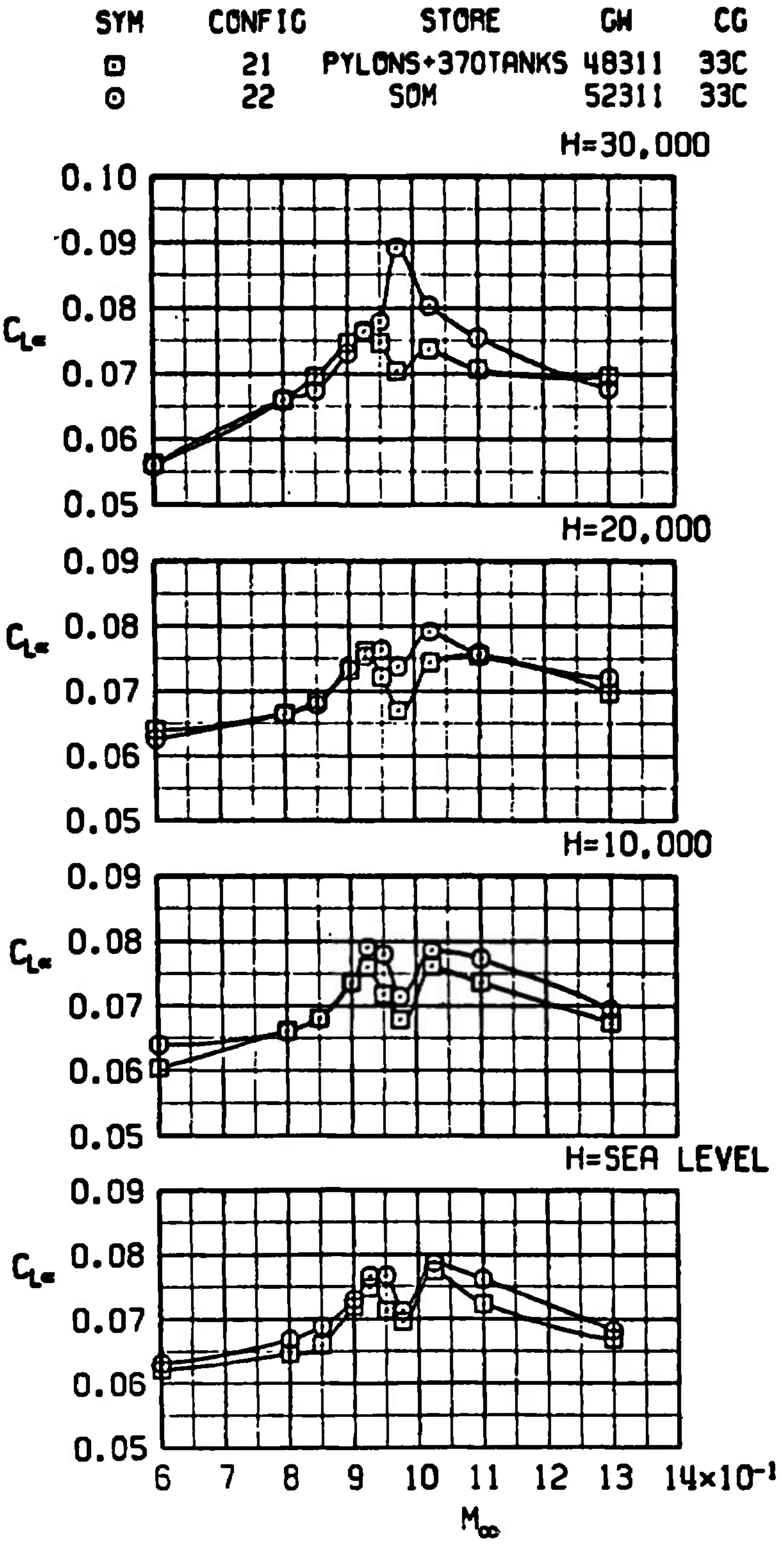

Figure 18. The effect of the SOM store on the lift-curve slope at trim.

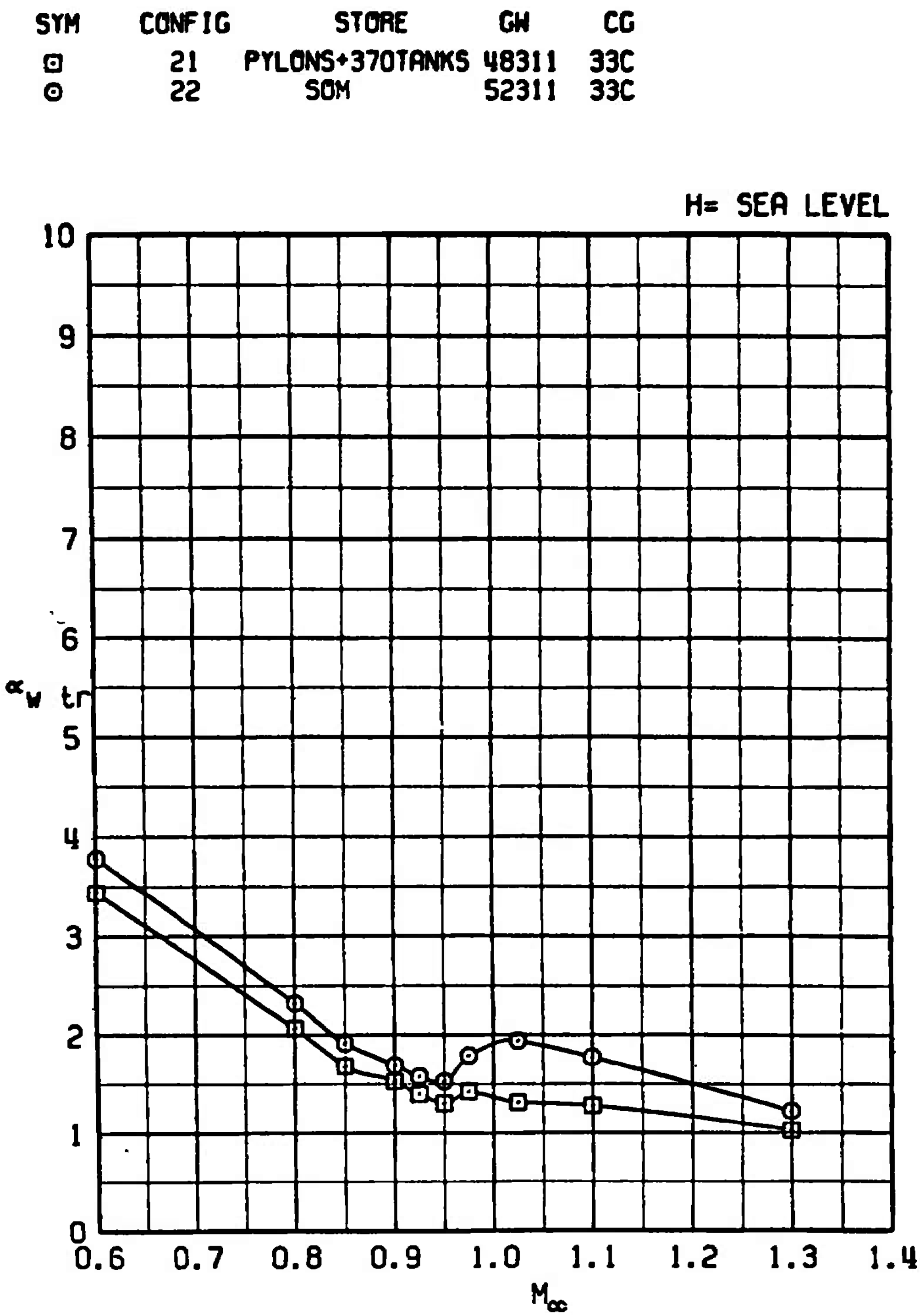

a. H = Sea level

Figure 19. The effect of the SOM store on trim wing angle of attack.

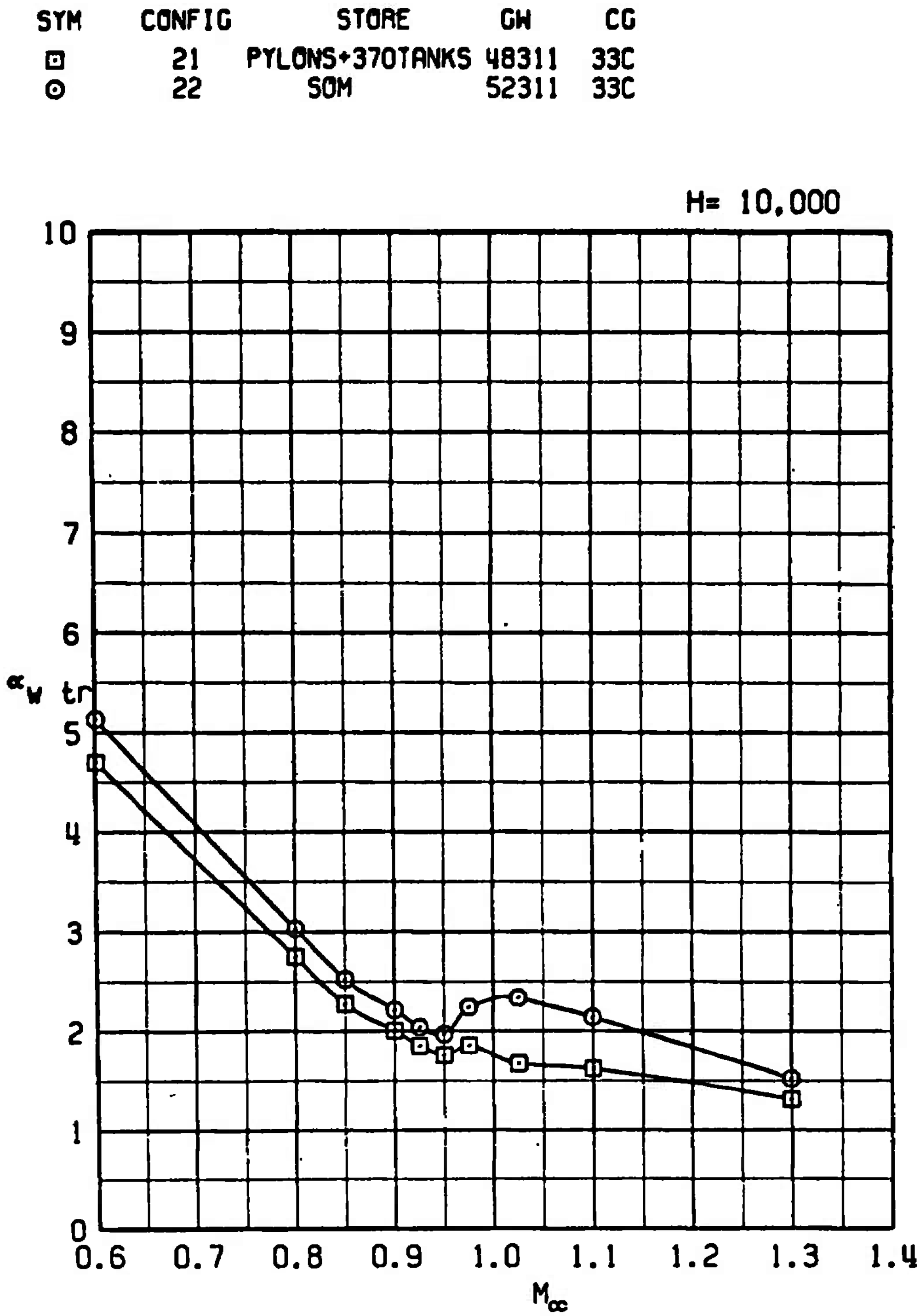

b. H = 10,000
Figure 19. Continued.

SYM	CONFIG	STORE	GW	CG
⊡	21	PYLONS+370TANKS	48311	33C
⊙	22	SOM	52311	33C

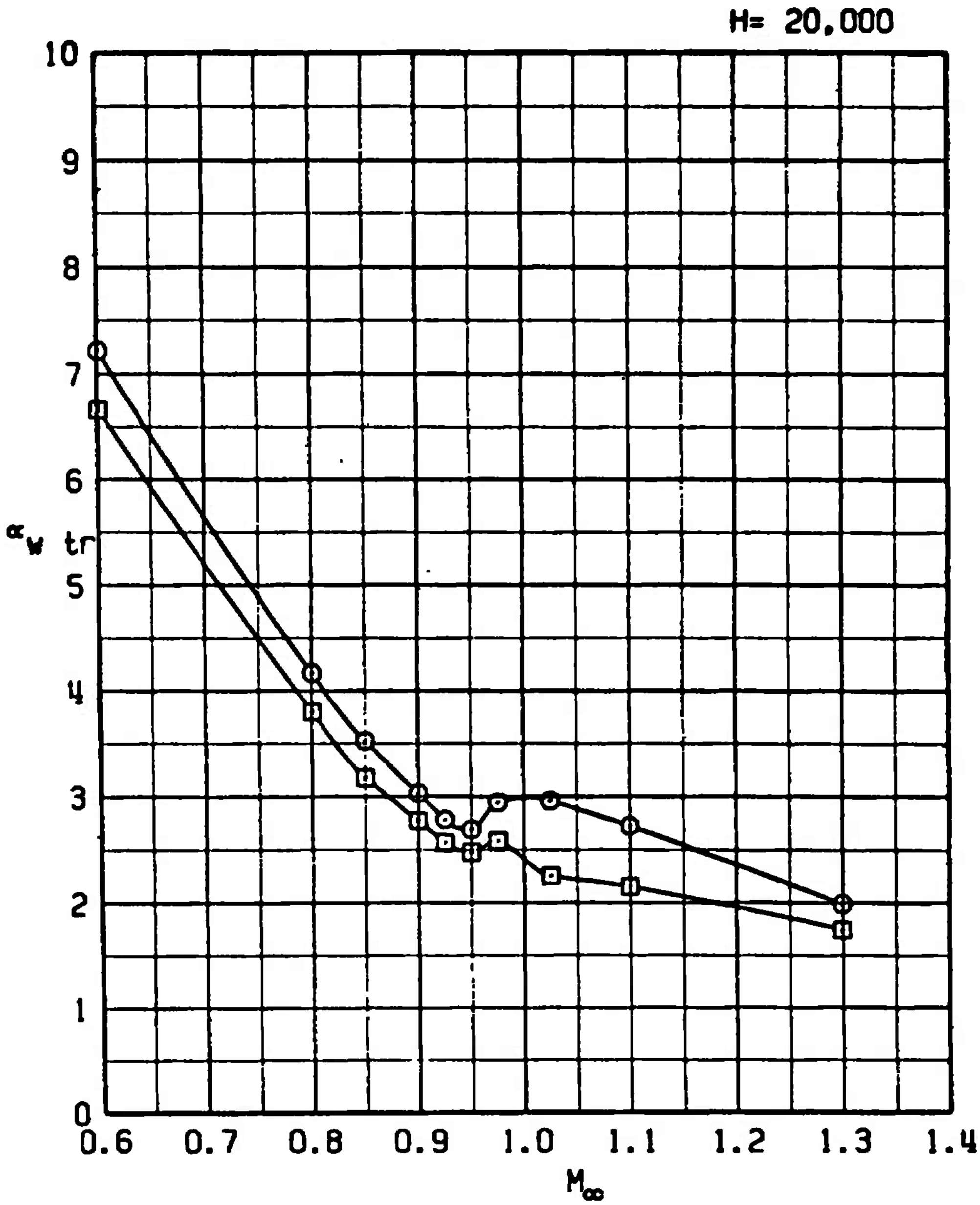

c. H = 20,000
Figure 19. Continued.

SYM	CONFIG	STORE	GW	CG
⊡	21	PYLONS+370TANKS	48311	33C
⊙	22	SOM	52311	33C

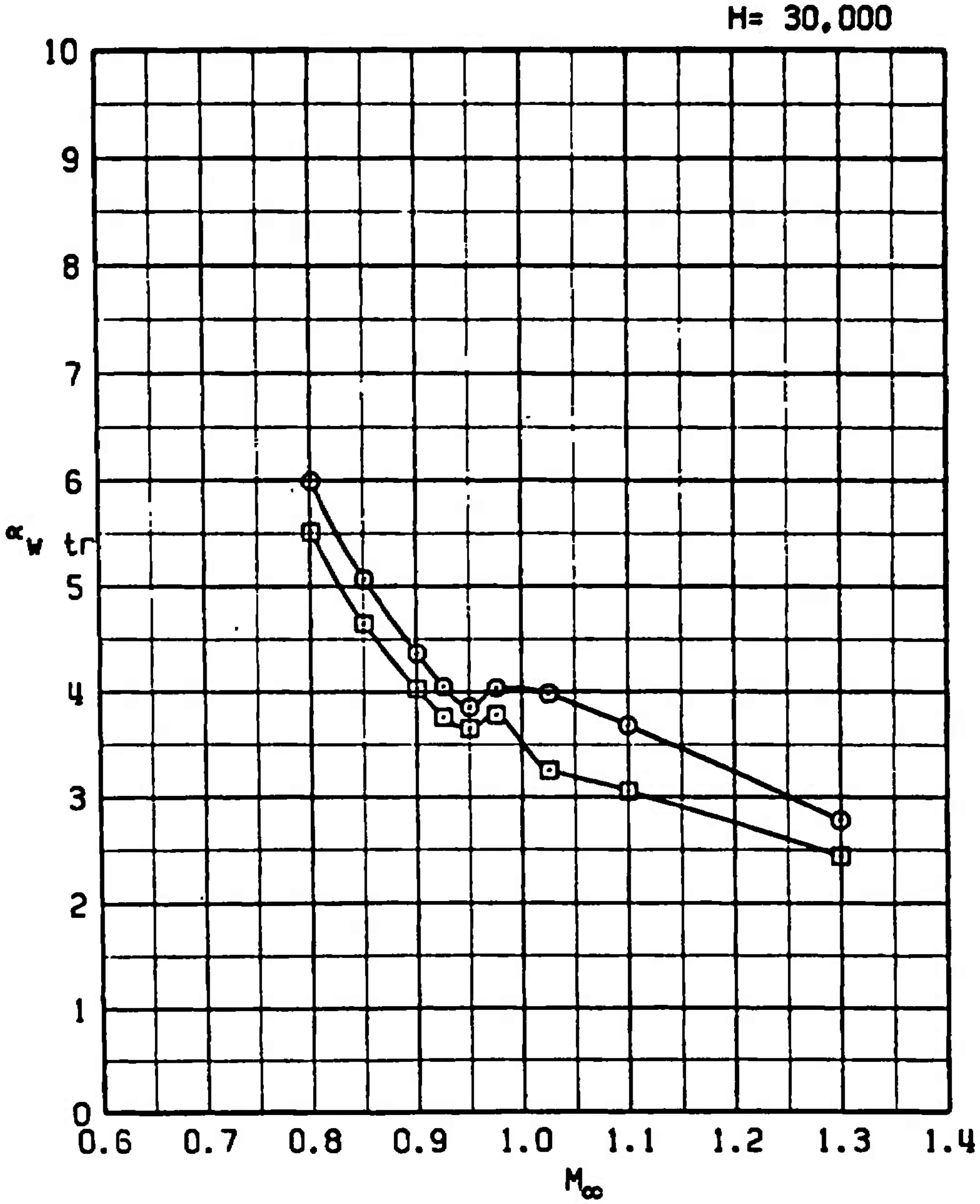

d. H = 30,000
Figure 19. Concluded.

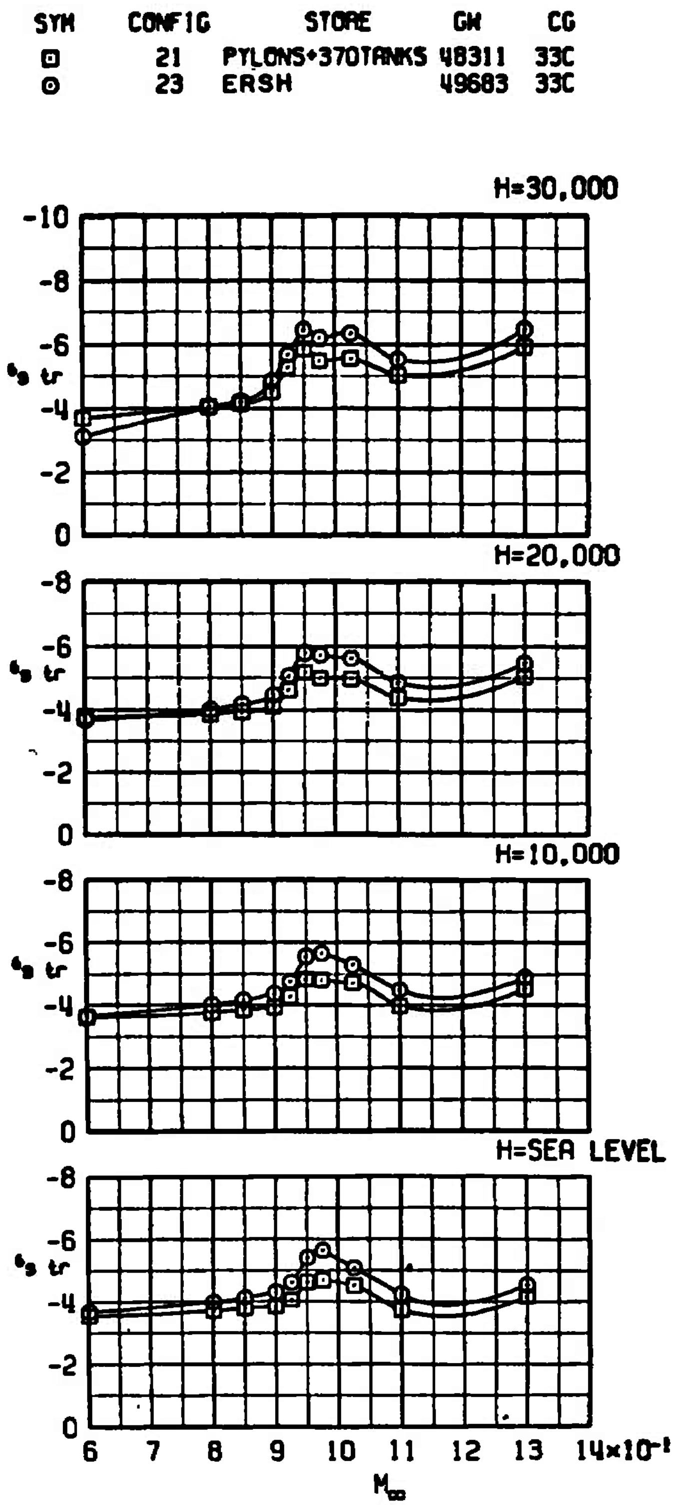

Figure 20. The effect of the Stubby HOBOS store on trim stabilator angle.

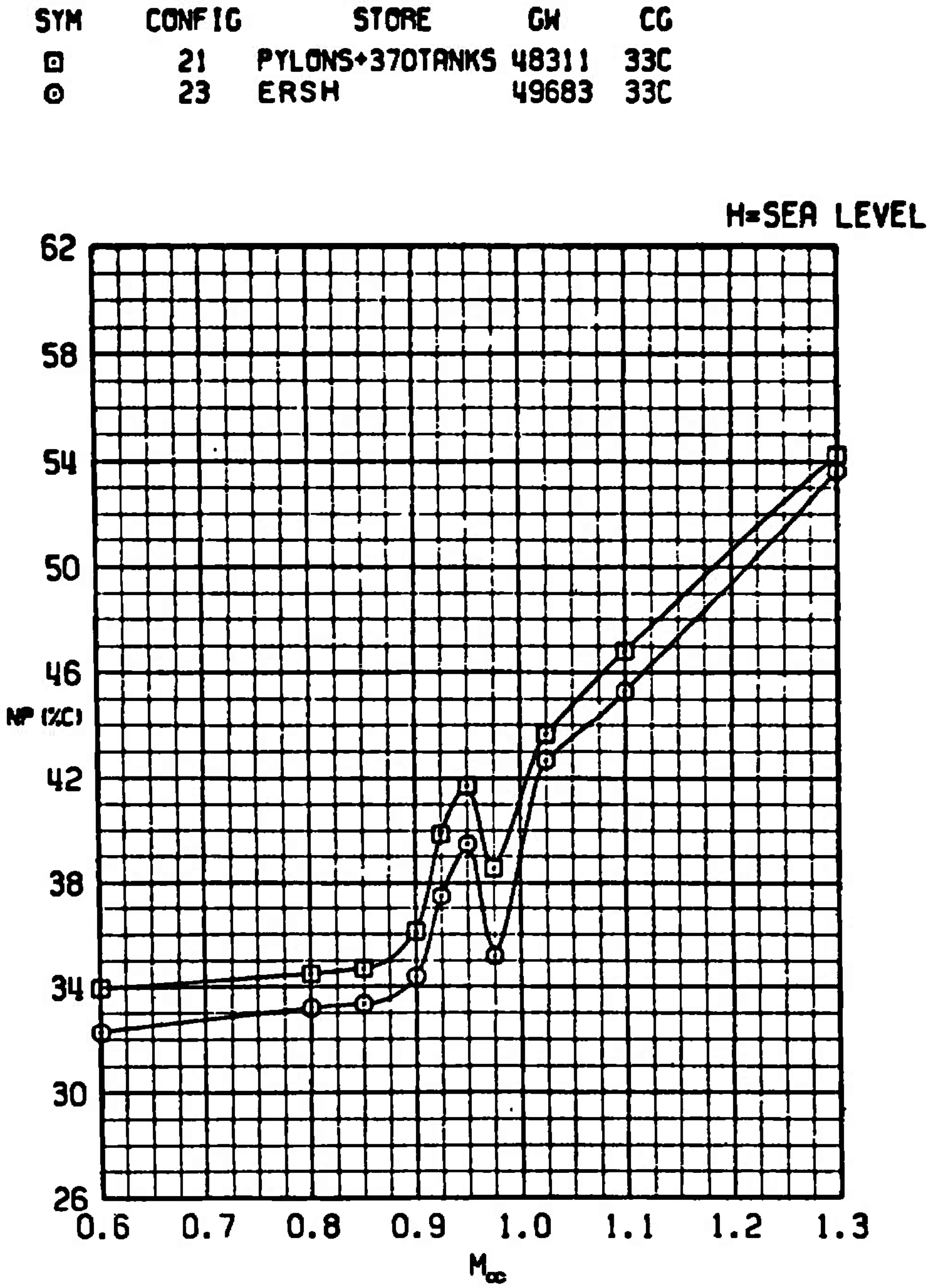

a. H = Sea level

Figure 21. The effect of the Stubby HOBOS store on neutral-point location.

SYM	CONFIG	STORE	GW	CG
⊡	21	PYLONS+370TANKS	48311	33C
⊙	23	ERSH	49683	33C

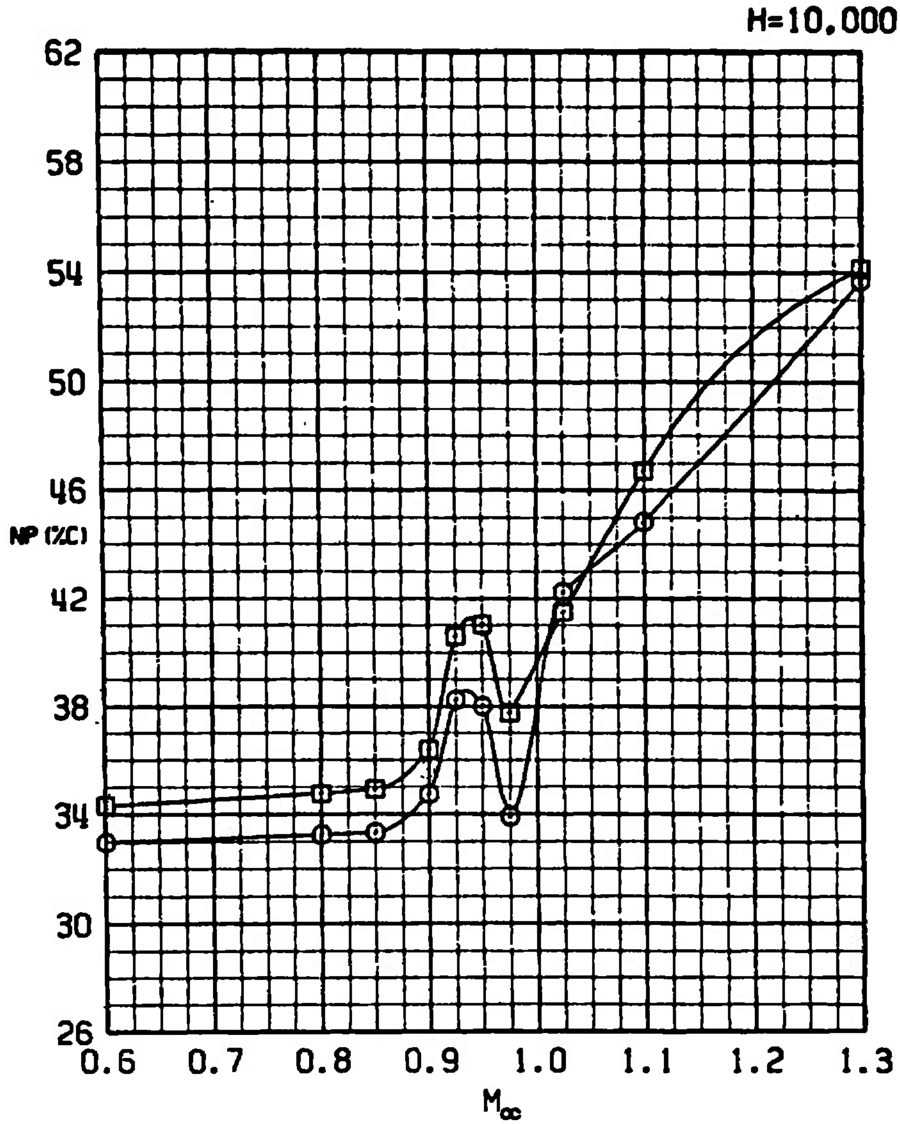

b. H = 10,000

Figure 21. Continued.

SYM	CONFIG	STORE	GW	CG
⊡	21	PYLONS+370TANKS	48311	33C
⊙	23	ERSH	49683	33C

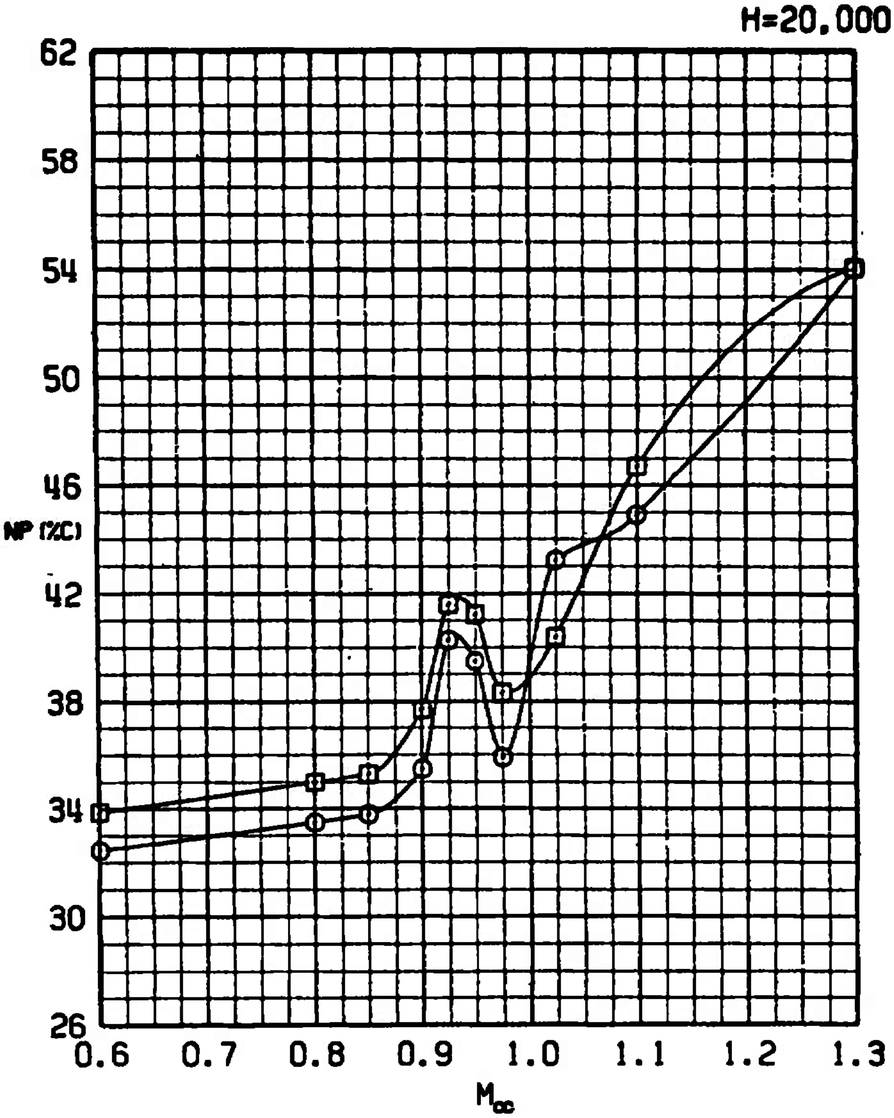

c. H = 20,000
Figure 21. Continued.

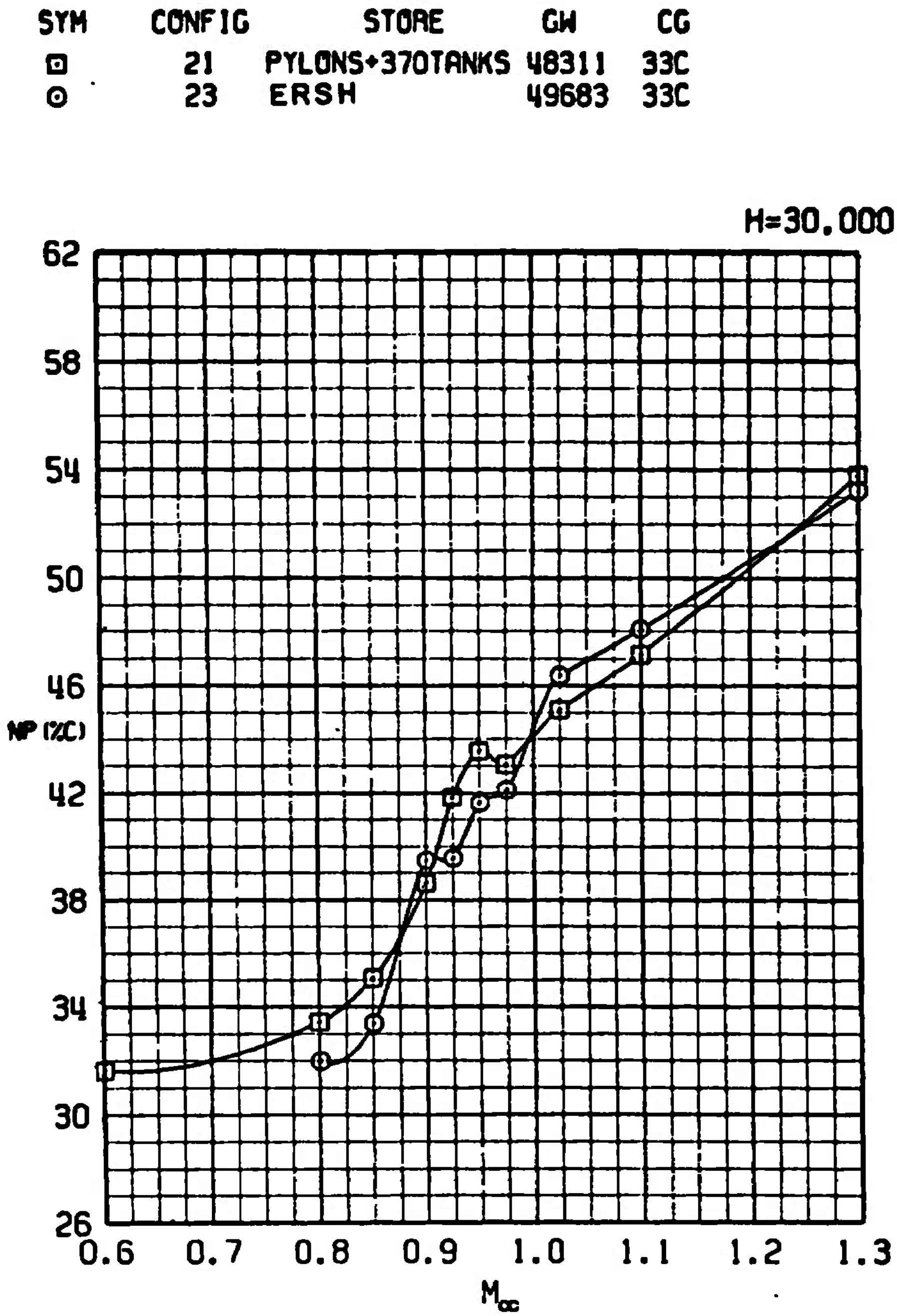

d. H = 30,000
Figure 21. Concluded.

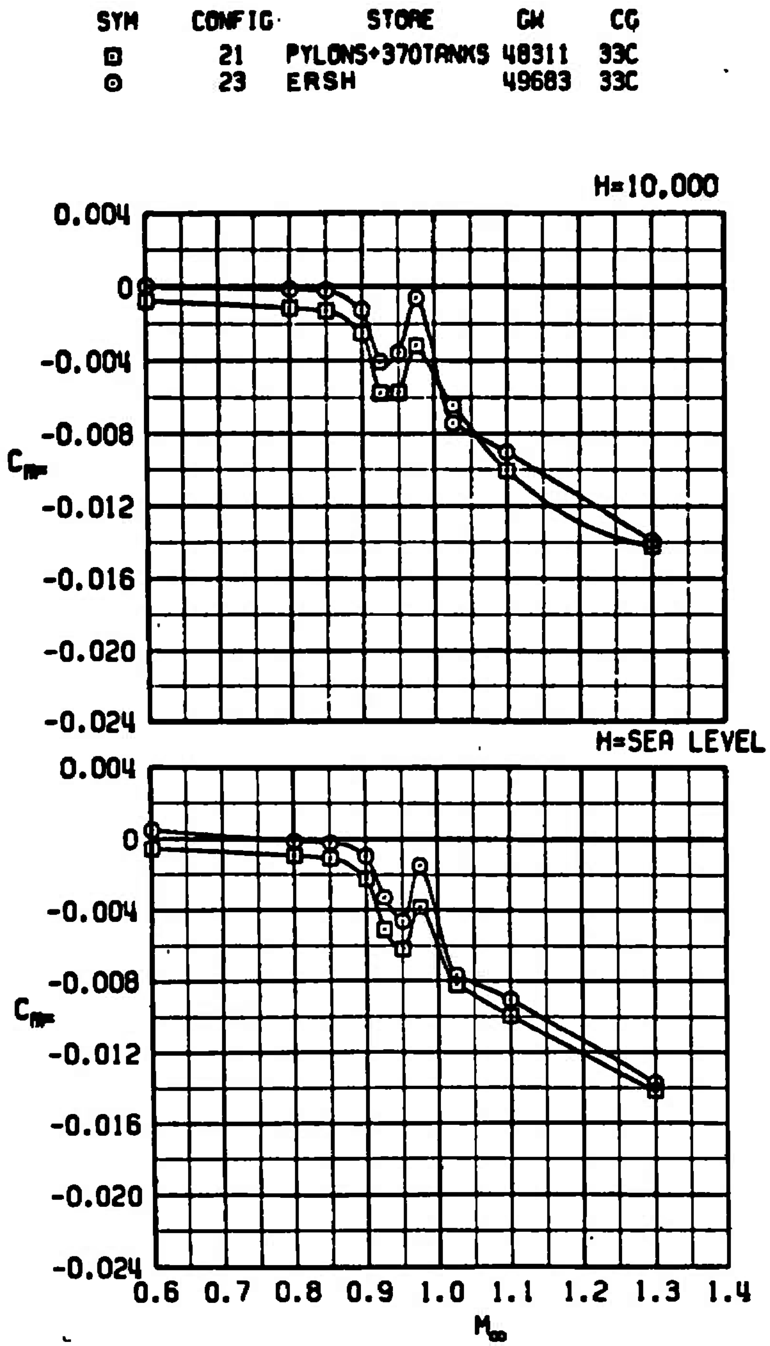

a. H = Sea level and 10,000

Figure 22. The effect of the Stubby HOBOS store on the slope of the pitching-moment coefficient versus angle-of-attack curve at trim.

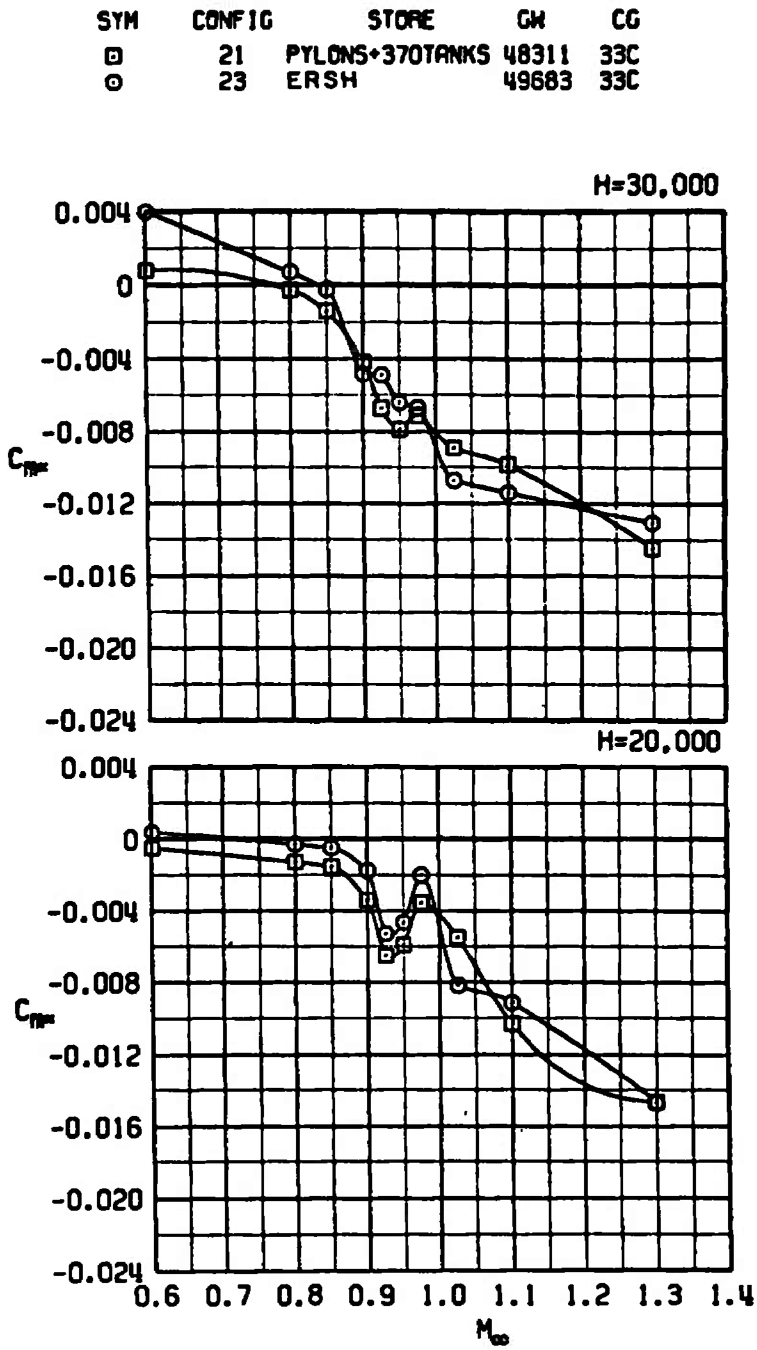

b. H = 20,000 and 30,000
Figure 22. Concluded.

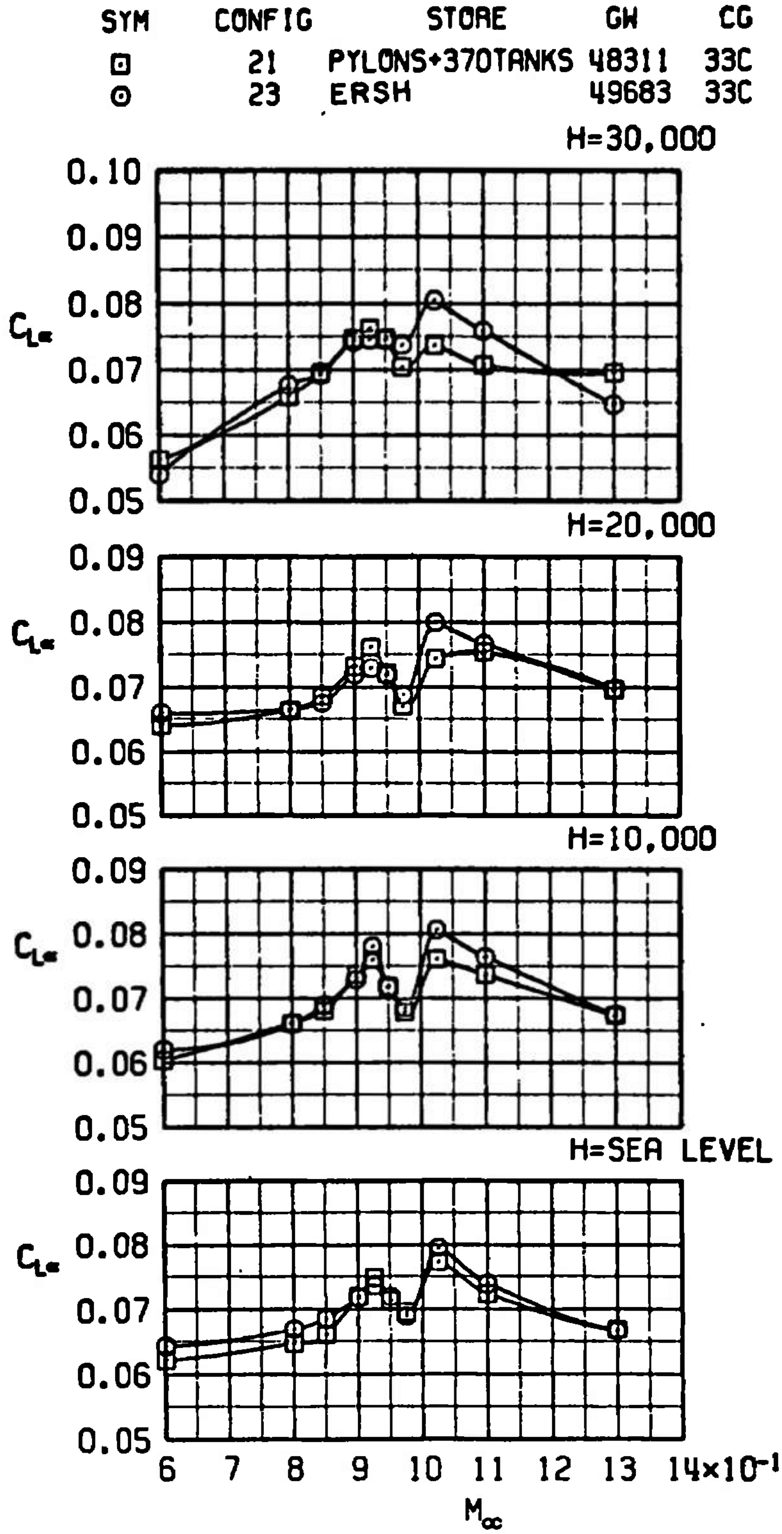

Figure 23. The effect of the Stubby HOBOS store on the lift-curve slope at trim.

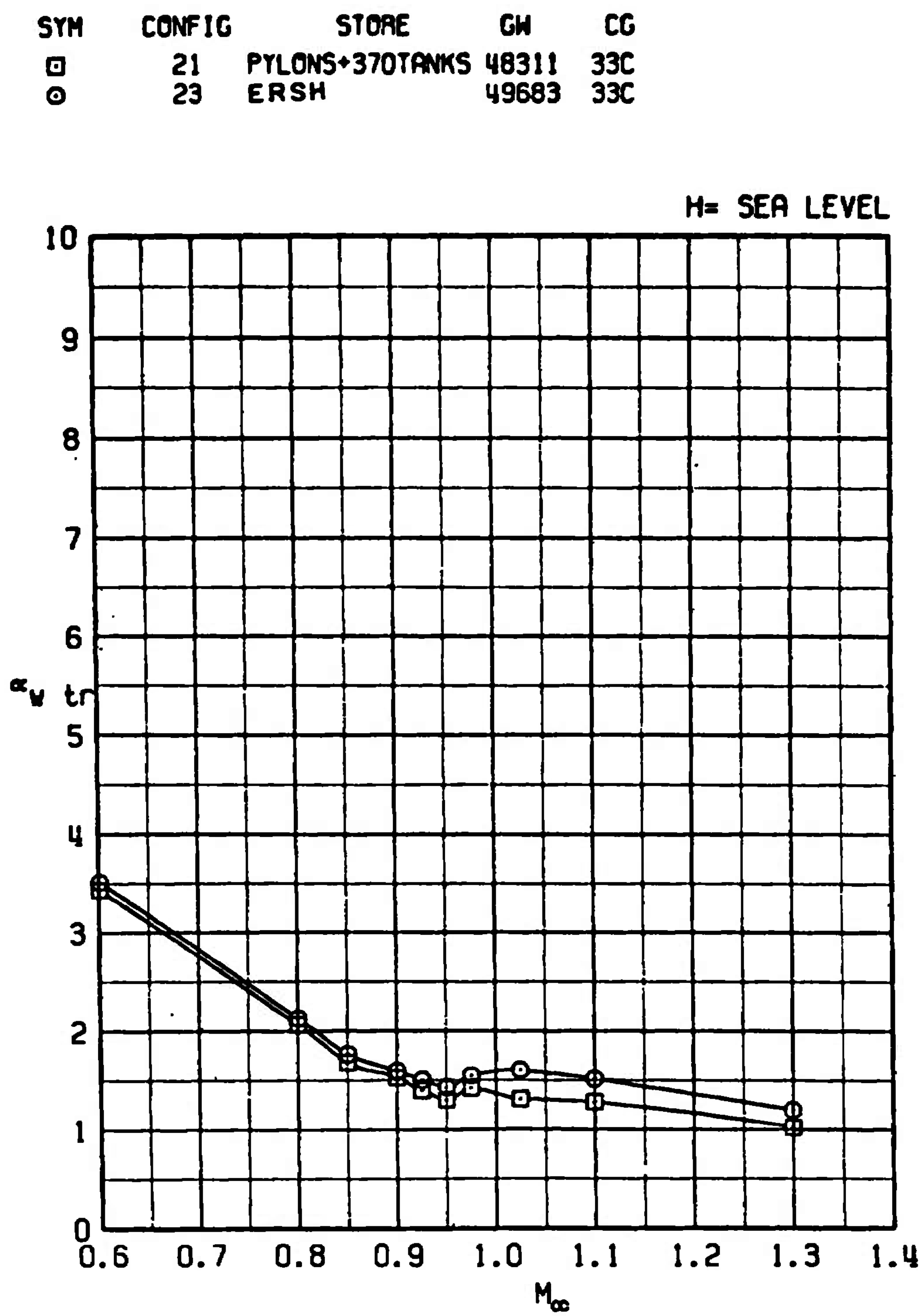

a. H = Sea level

Figure 24. The effect of the Stubby HOBOS store on trim wing angle of attack.

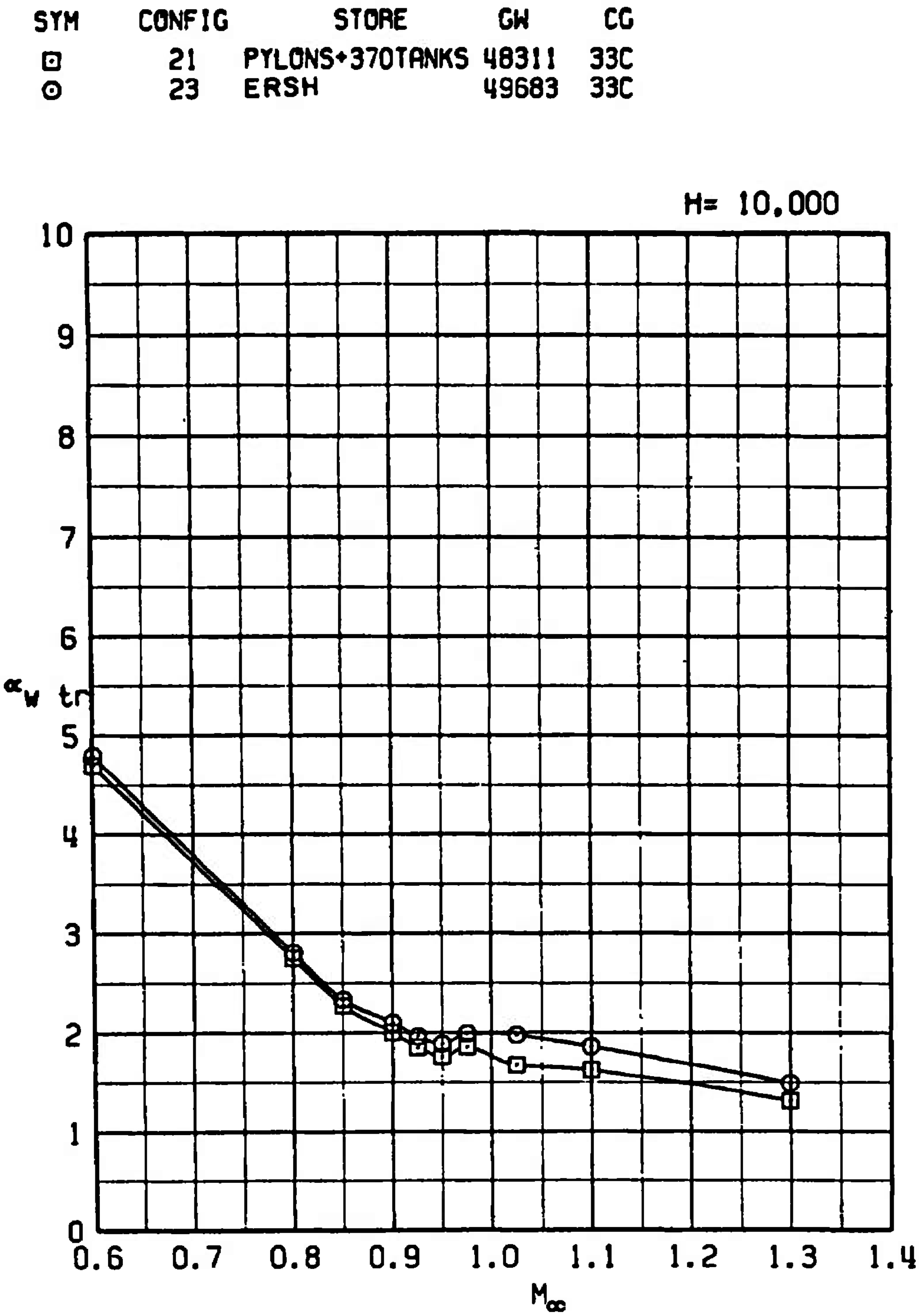

b. H = 10,000
Figure 24. Continued.

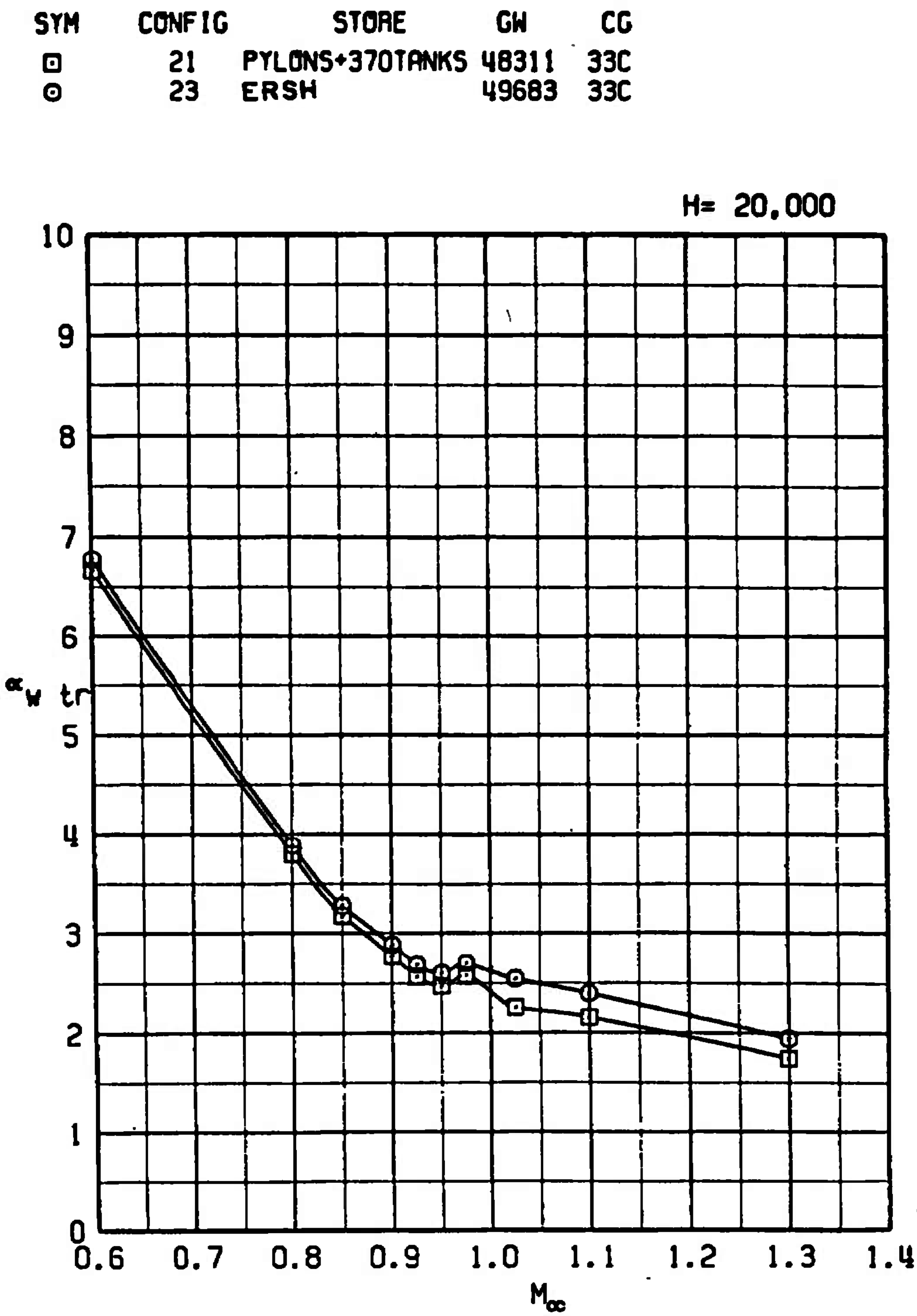

c. H = 20,000
Figure 24. Continued.

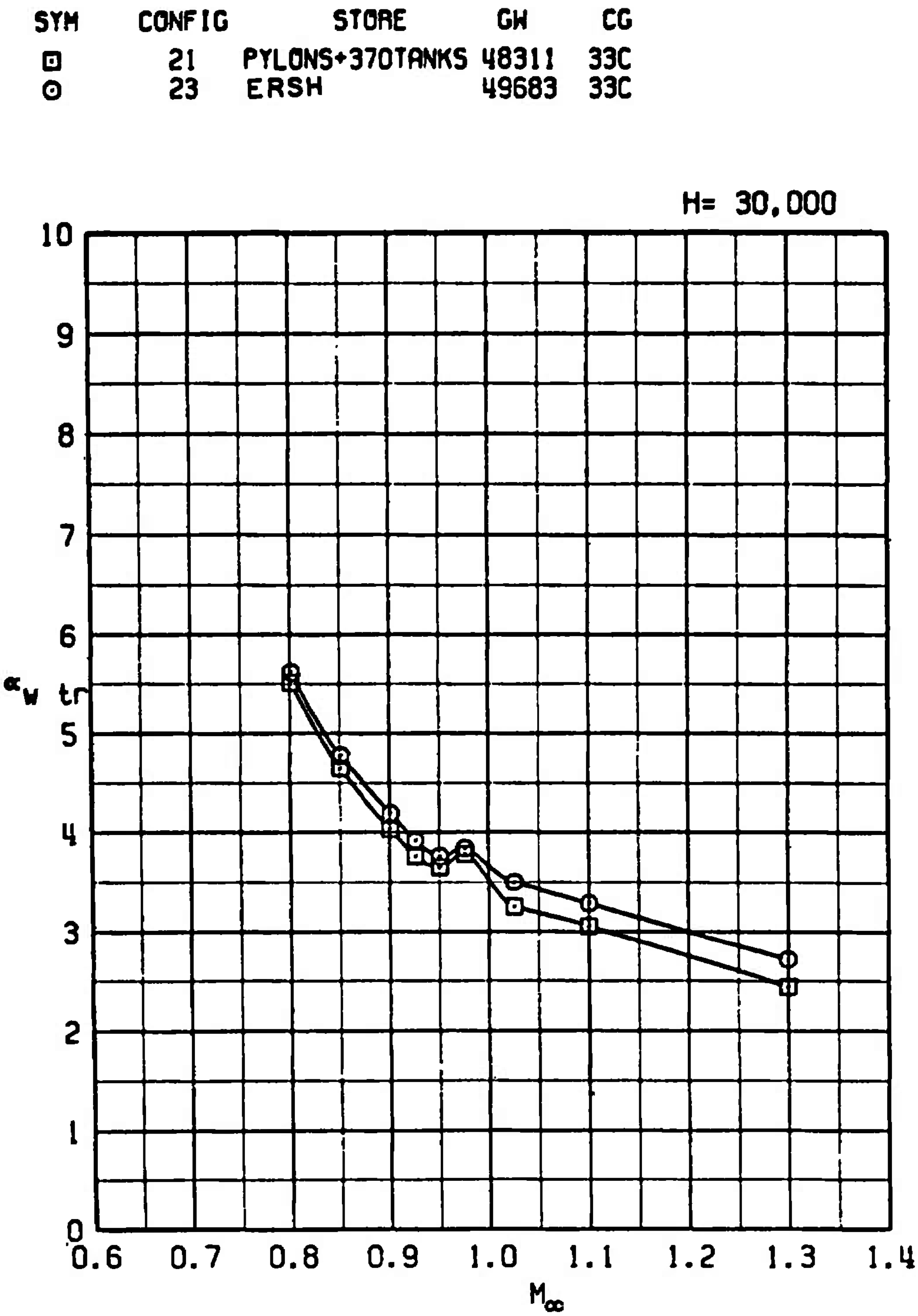

d. H = 30,000
Figure 24. Concluded.

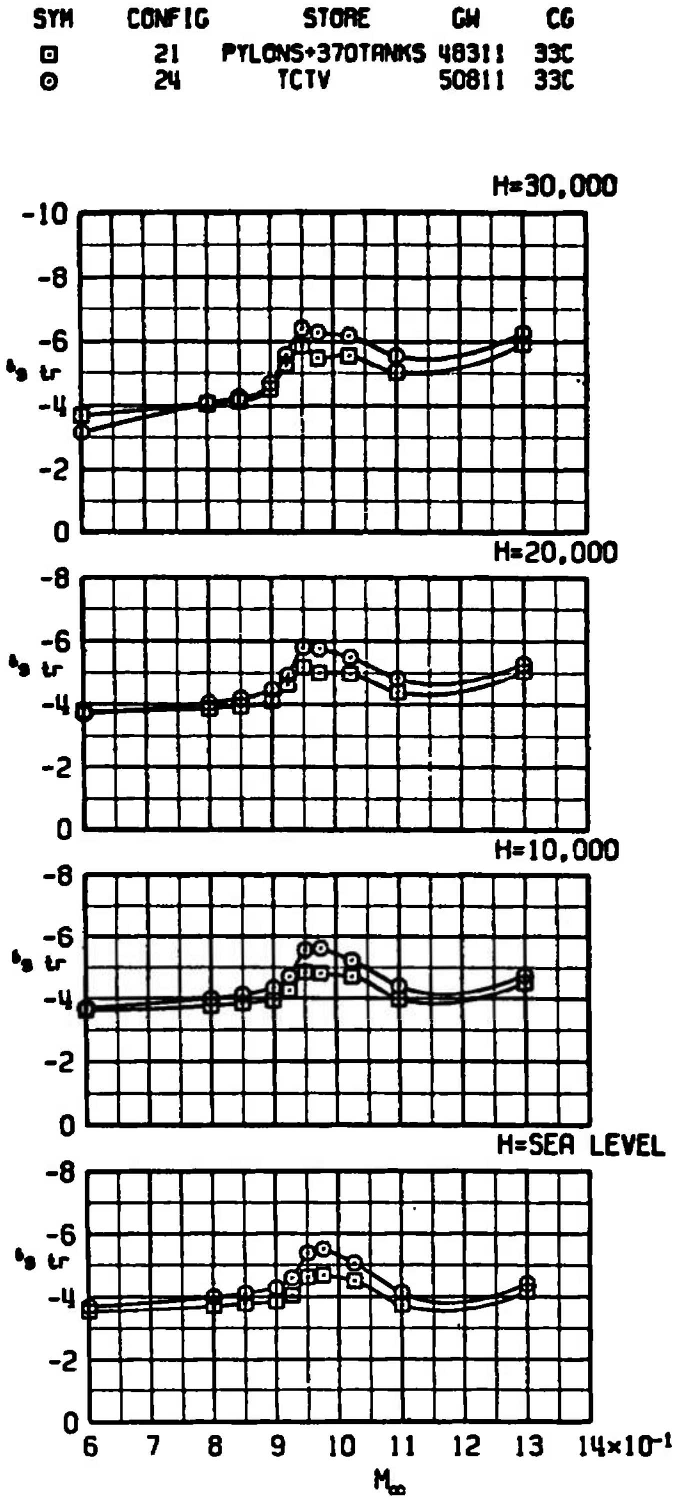

Figure 25. The effect of the TCTV store on trim stabilator angle.

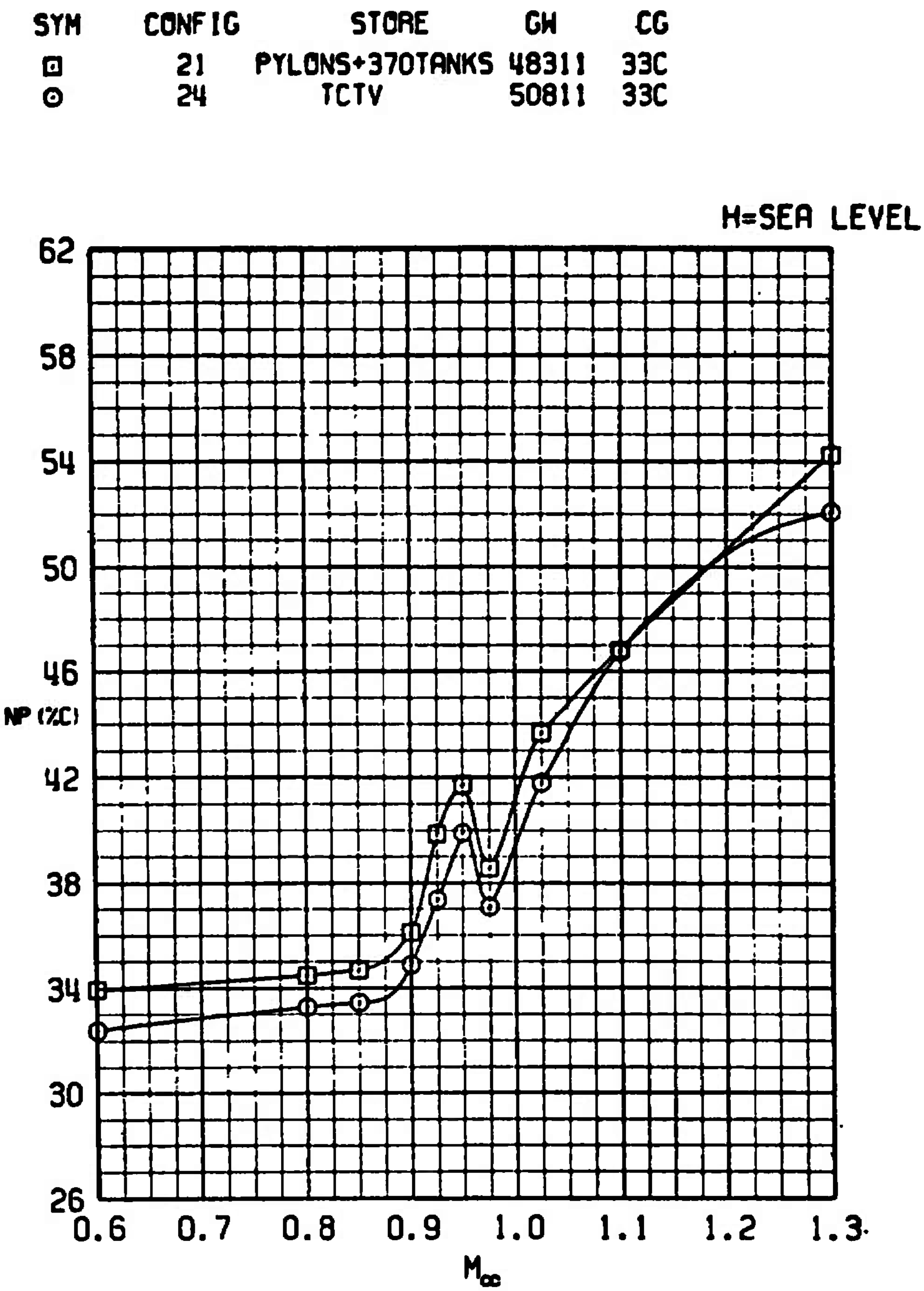

a. H = Sea level

Figure 26. The effect of the TCTV store on neutral-point location.

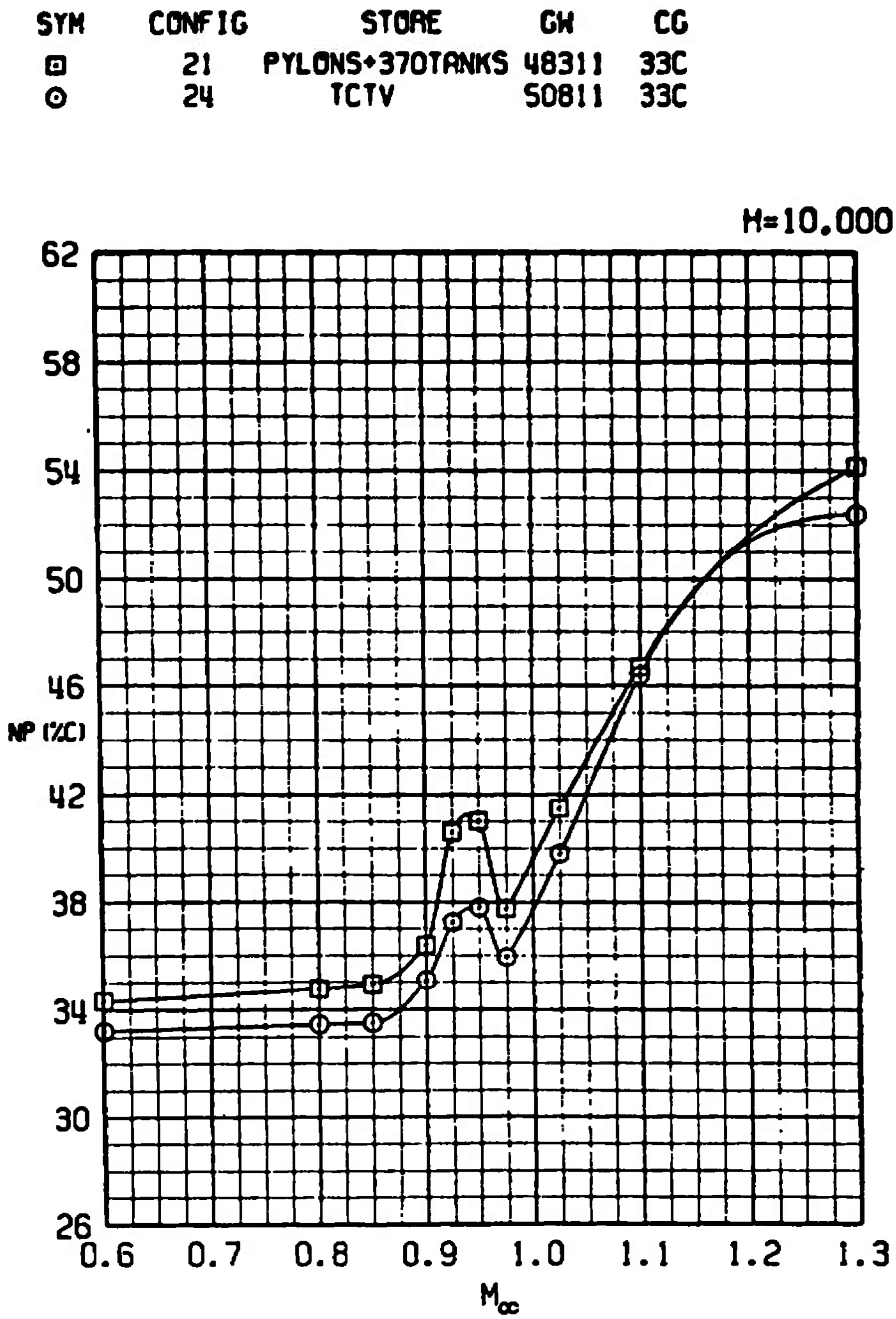

b. H = 10,000

Figure 26. Continued.

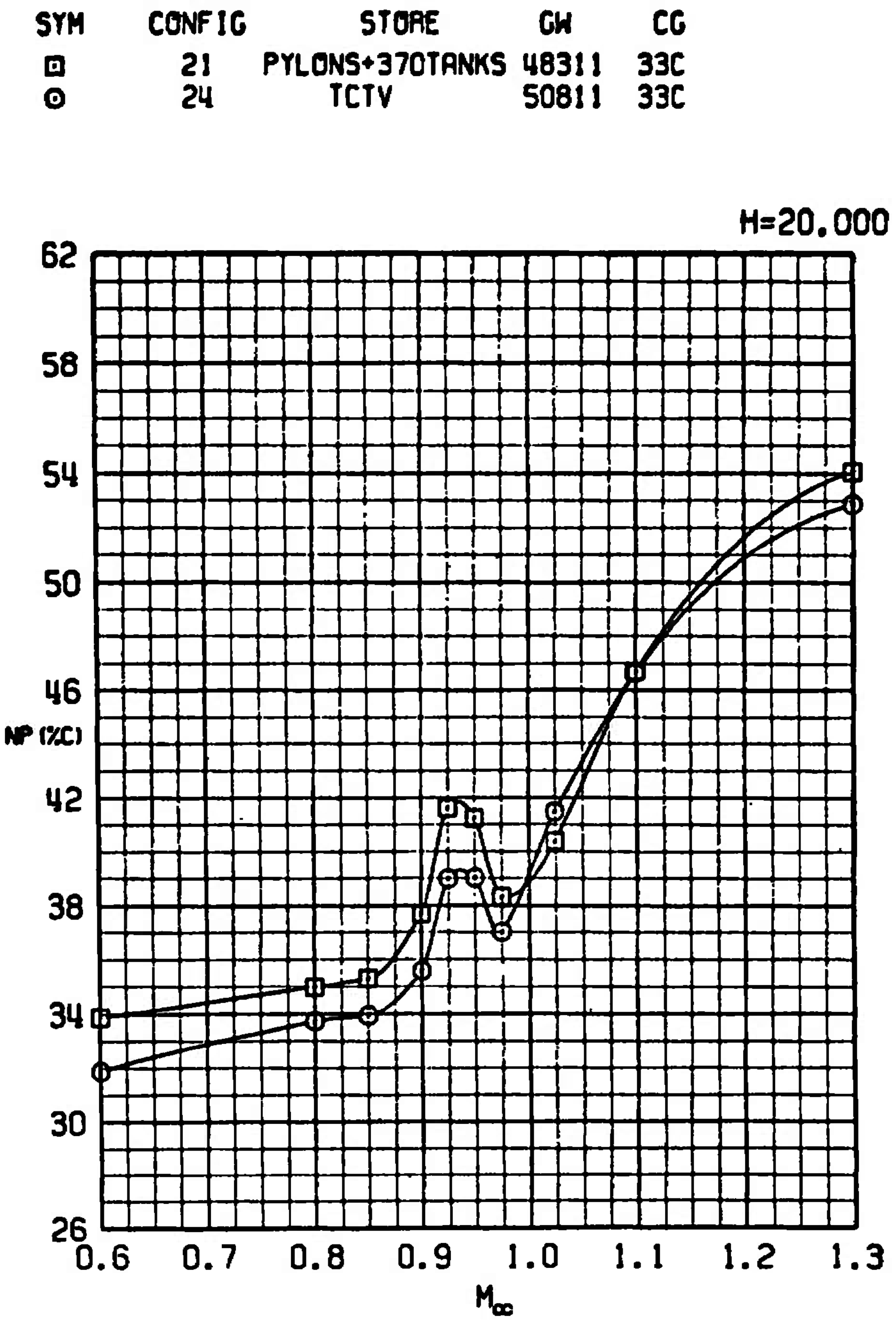

c. H = 20,000
Figure 26. Continued.

SYM	CONFIG	STORE	GW	CG
⊡	21	PYLONS+370TANKS	48311	33C
⊙	24	TCTV	50811	33C

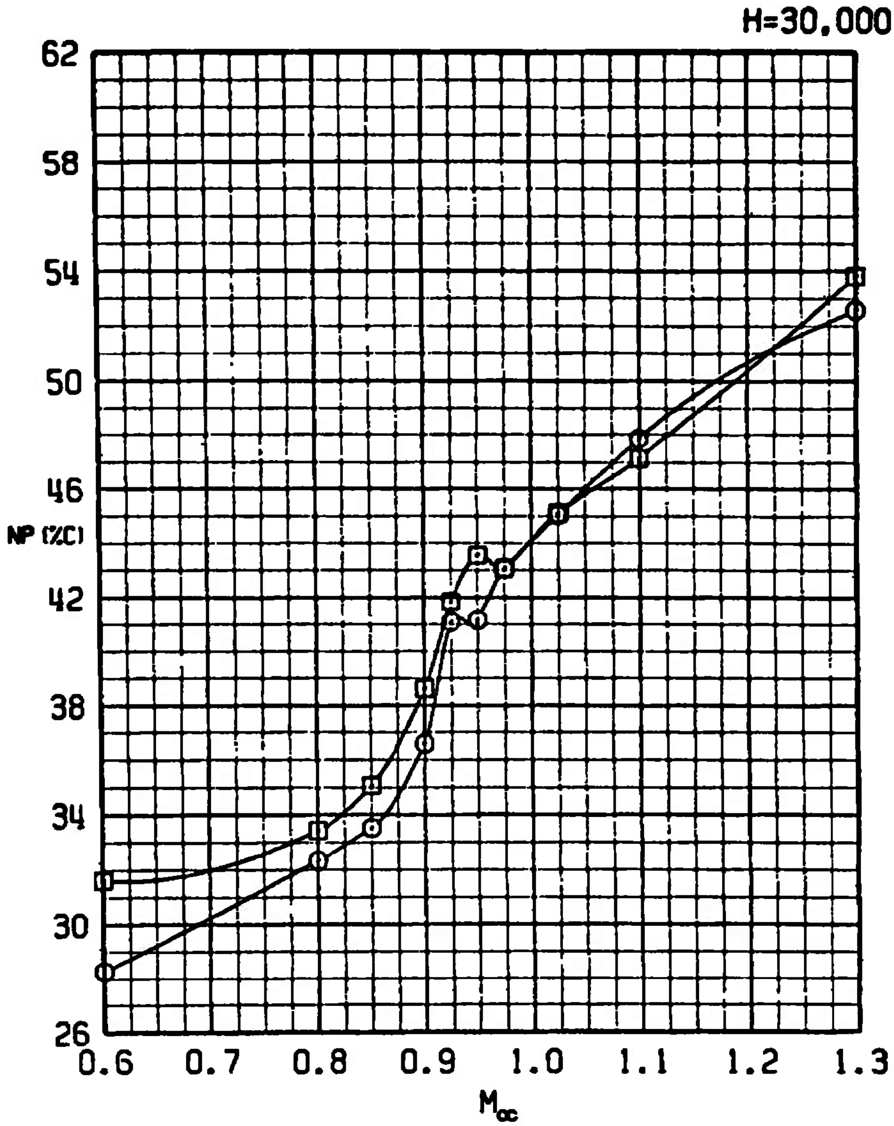

d. H = 30,000
Figure 26. Concluded.

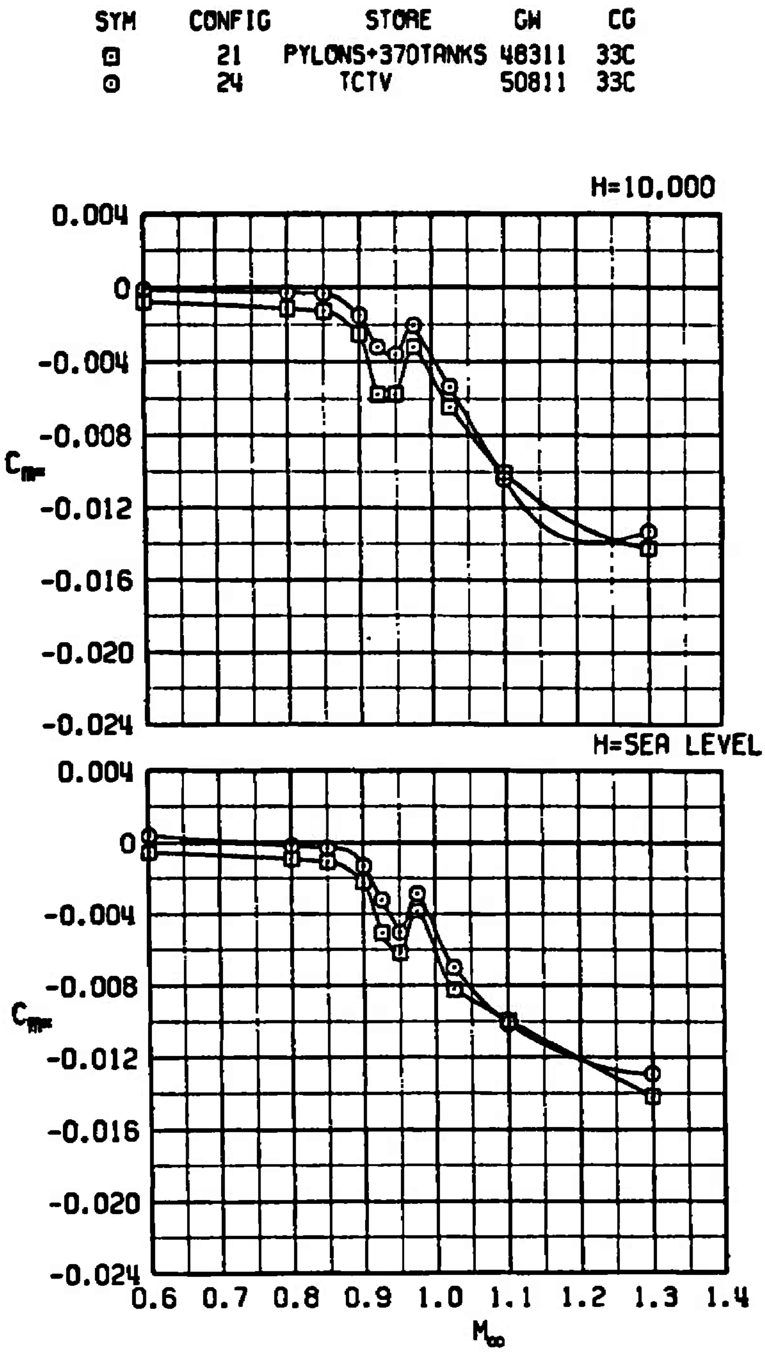

a. H = Sea level and 10,000

Figure 27. The effect of the TCTV store on the slope of the pitching-moment coefficient versus angle-of-attack curve at trim.

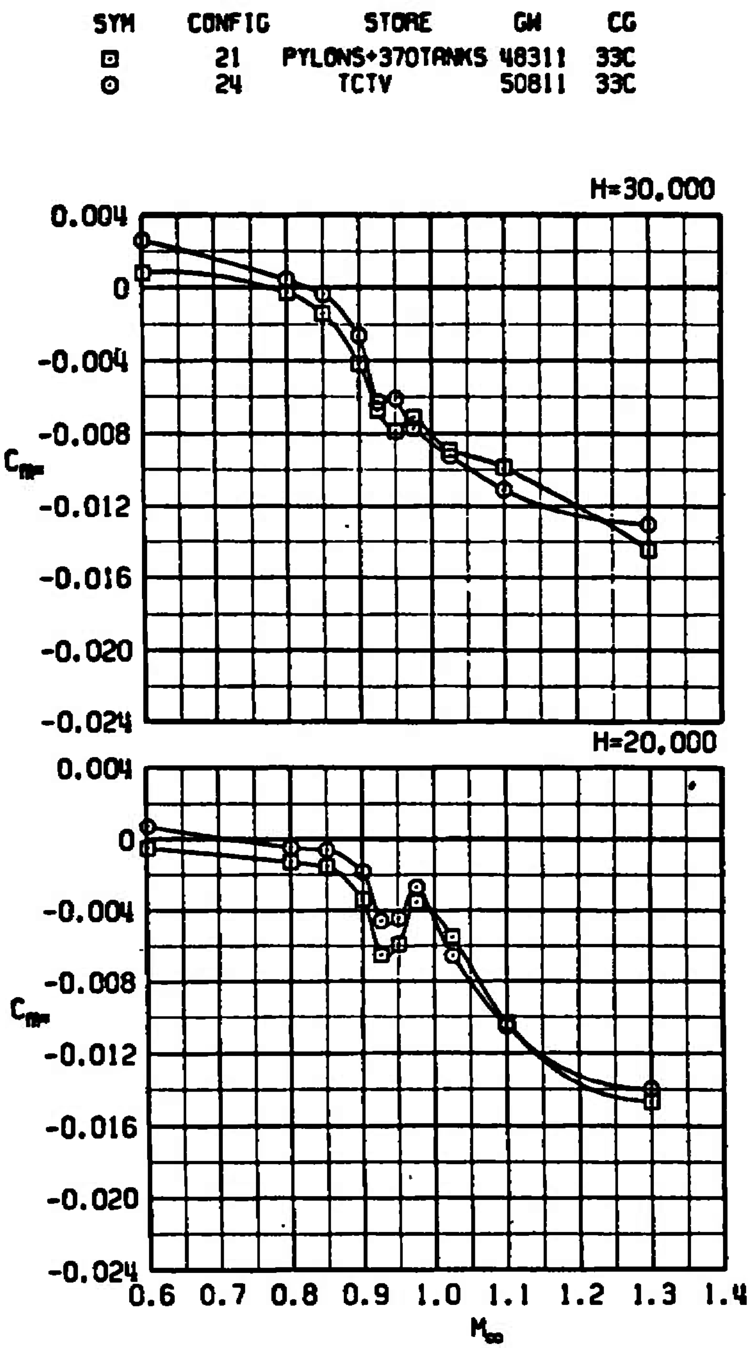

b. H = 20,000 and 30,000
Figure 27. Concluded.

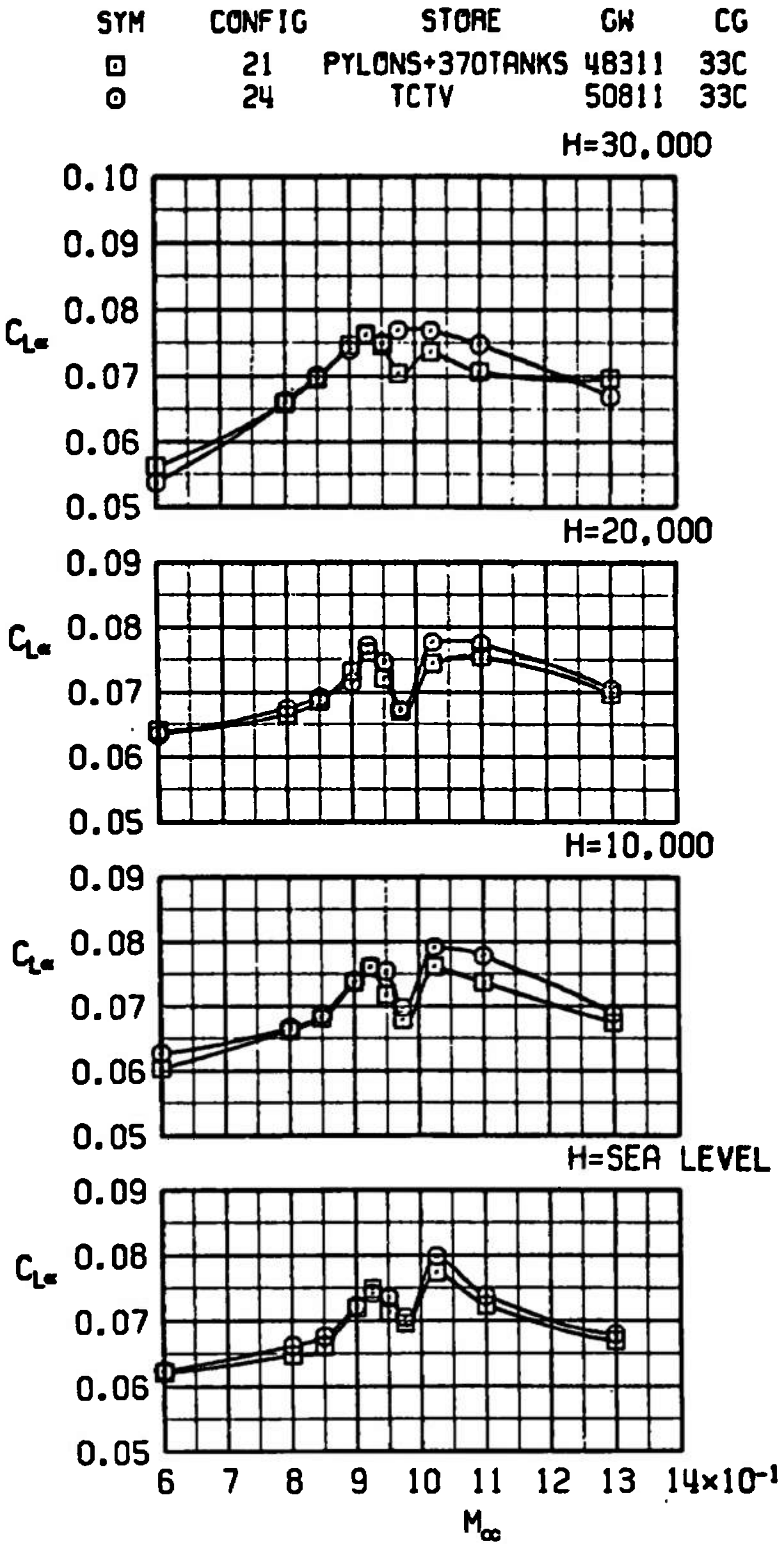

Figure 28. The effect of the TCTV store on the lift-curve slope at trim.

SYM	CONFIG	STORE	GW	CG
⊡	21	PYLONS+370TANKS	48311	33C
⊙	24	TCTV	50811	33C

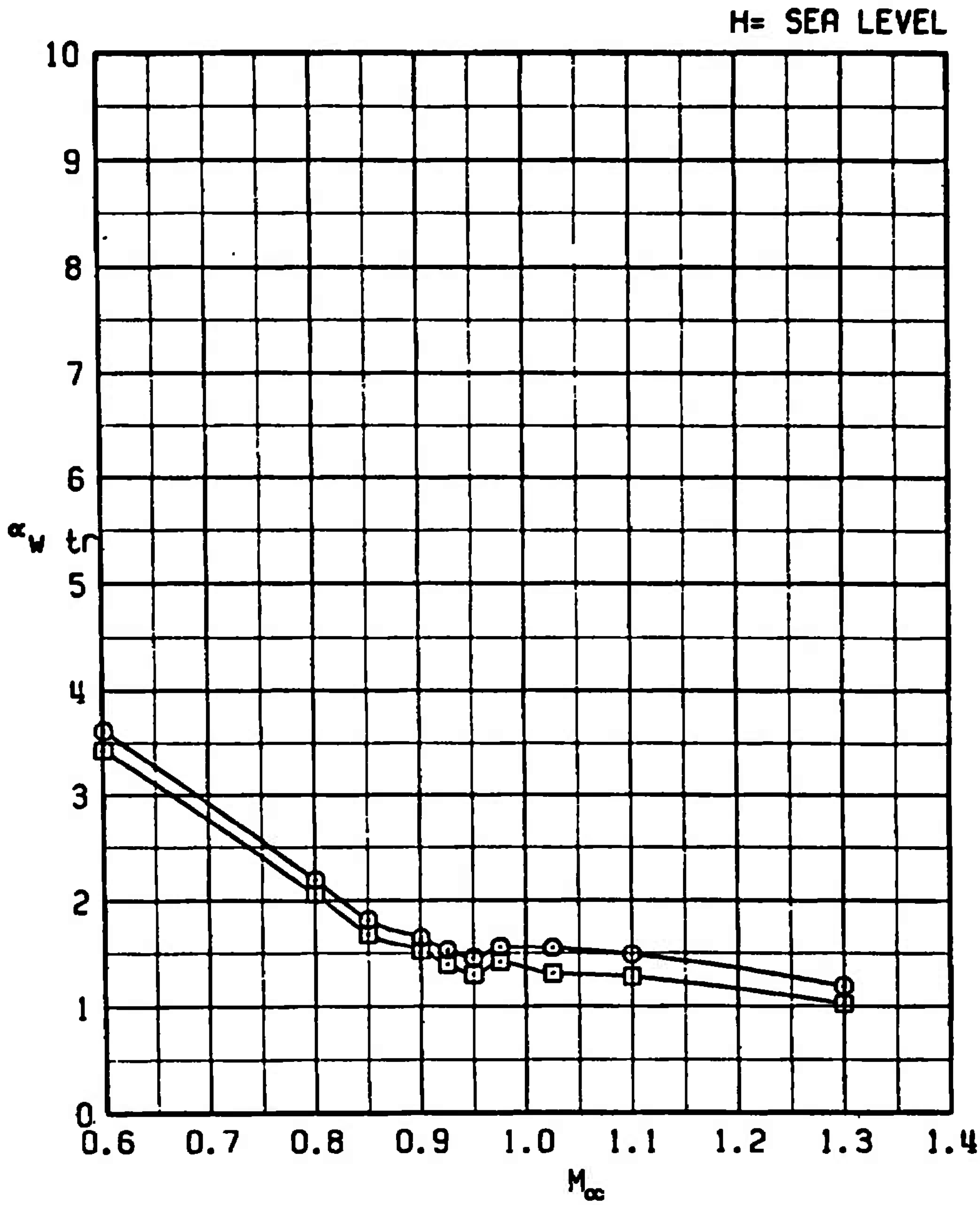

a. H = Sea level

Figure 29. The effect of the TCTV store on the trim wing angle of attack.

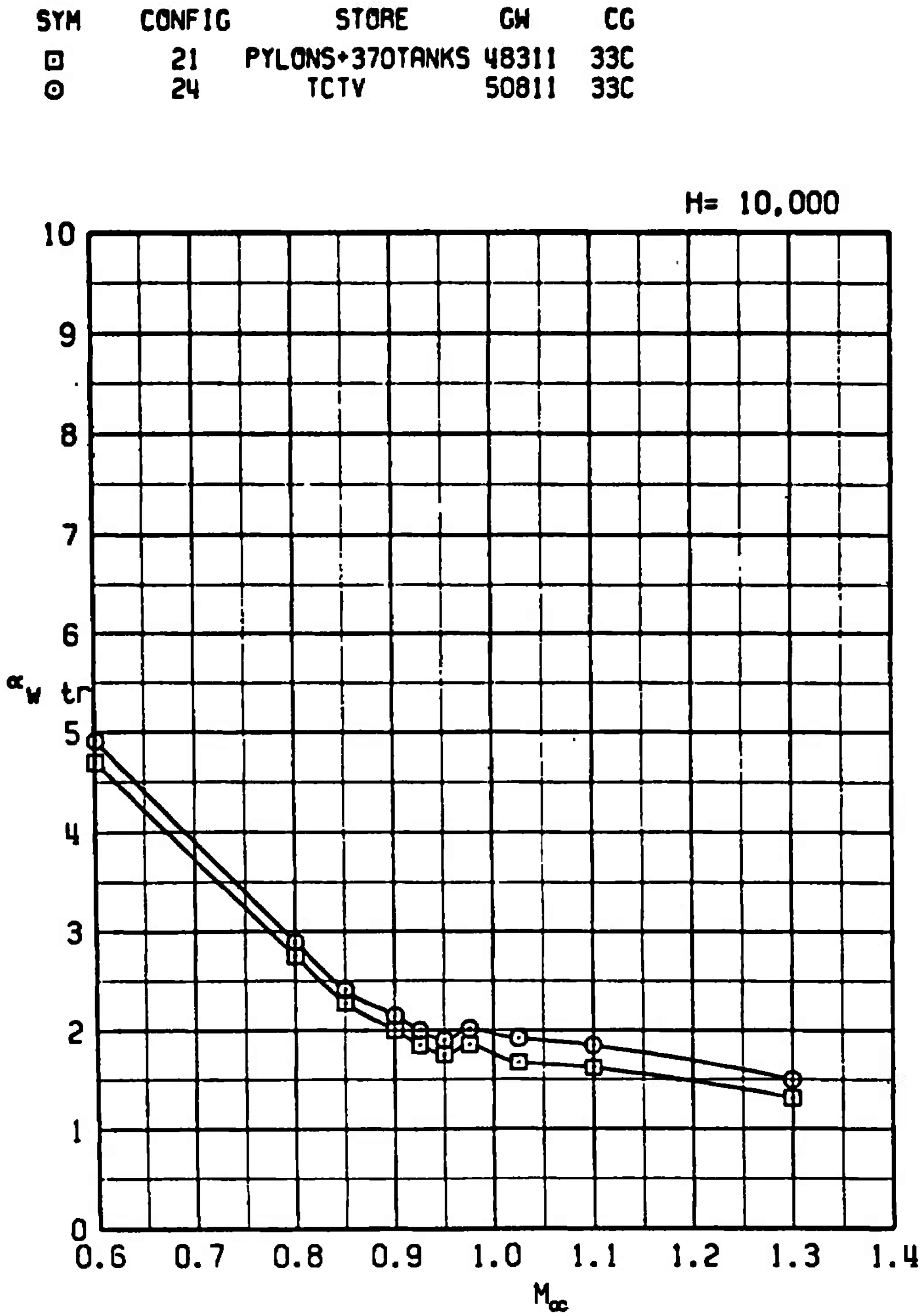

b. H = 10,000
Figure 29. Continued.

SYM	CONFIG	STORE	GW	CG
⊡	21	PYLONS+370TANKS	48311	33C
⊙	24	TCTV	50811	33C

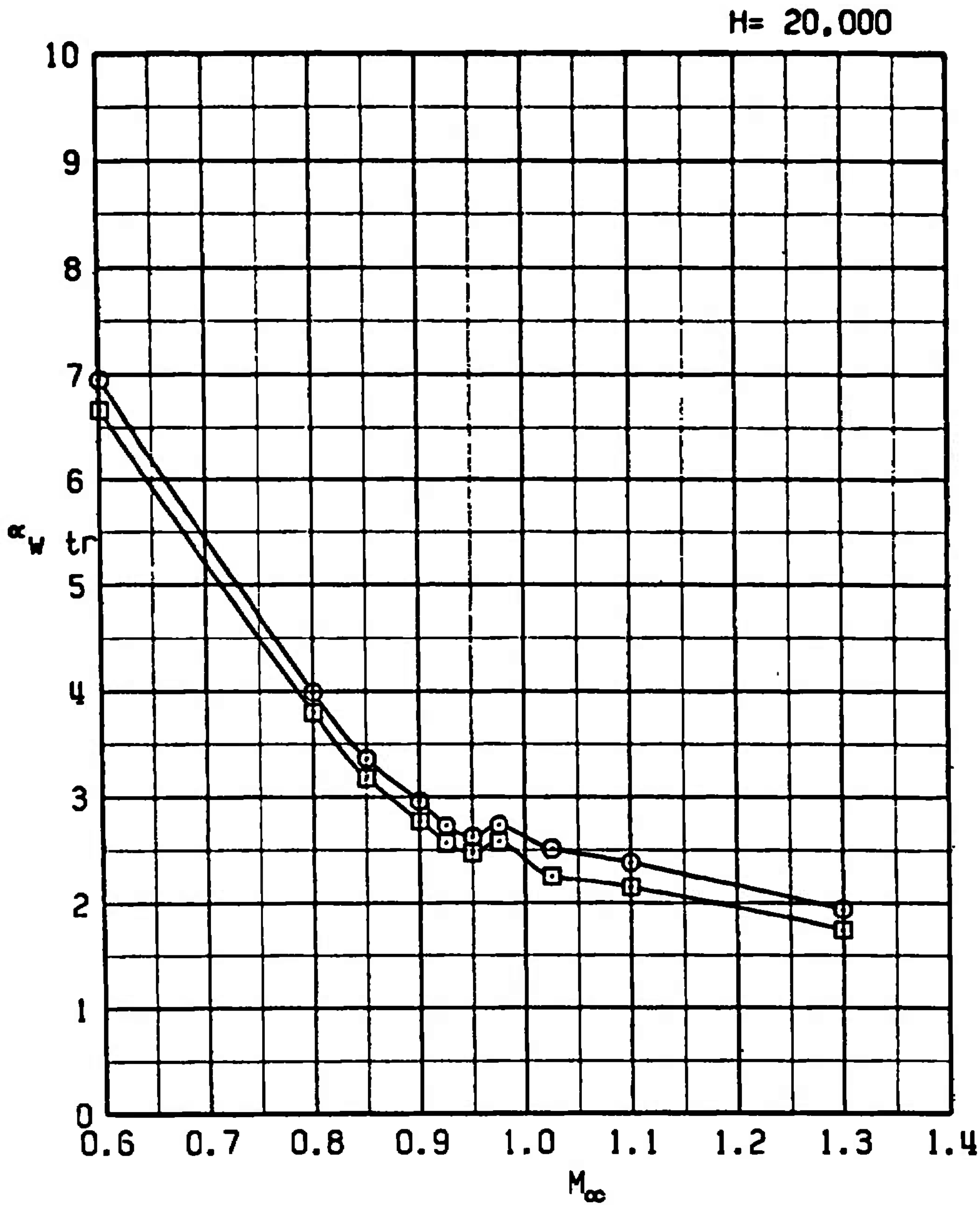

c. H = 20,000
Figure 29. Continued.

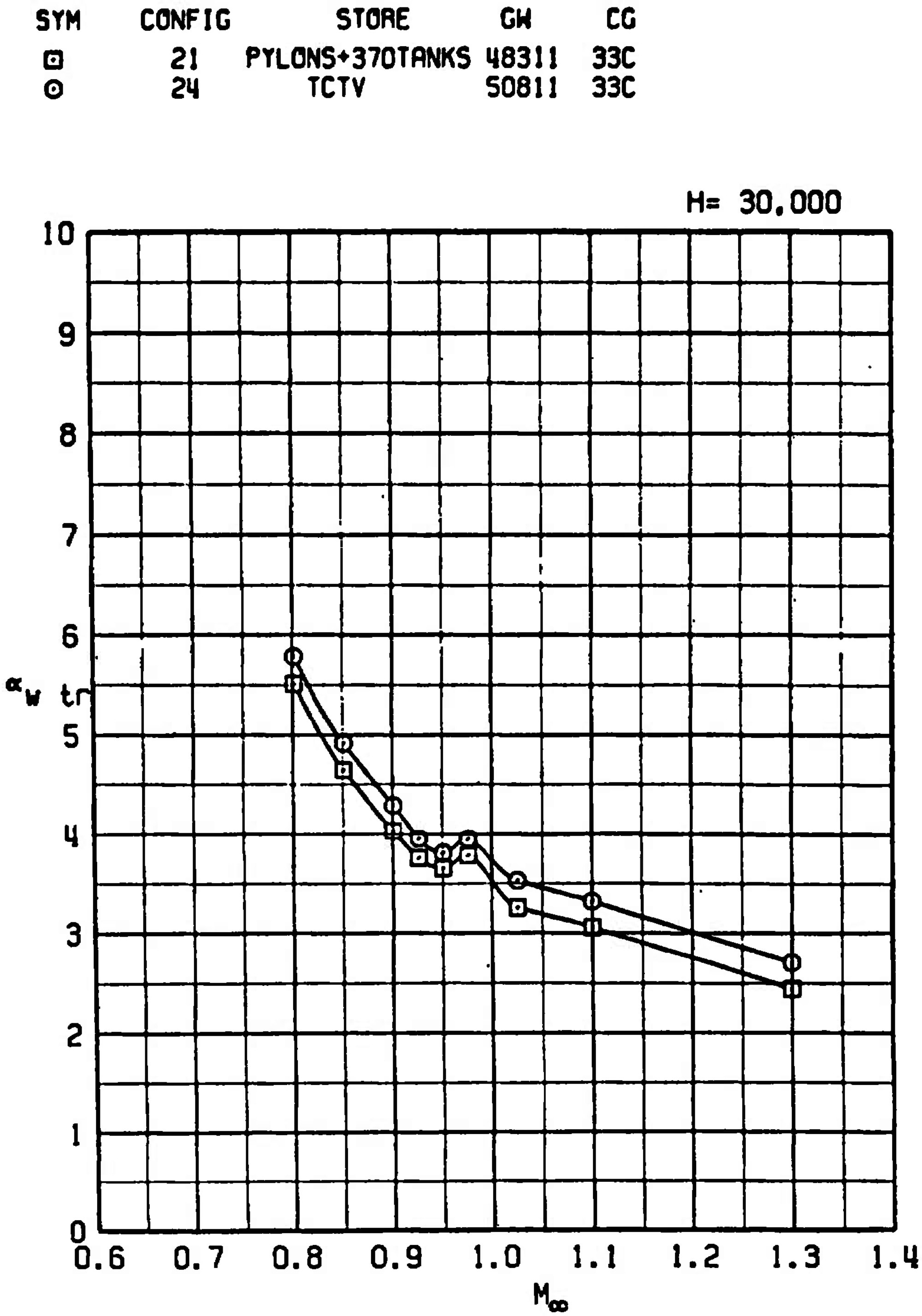

d. H = 30,000
Figure 29. Concluded.

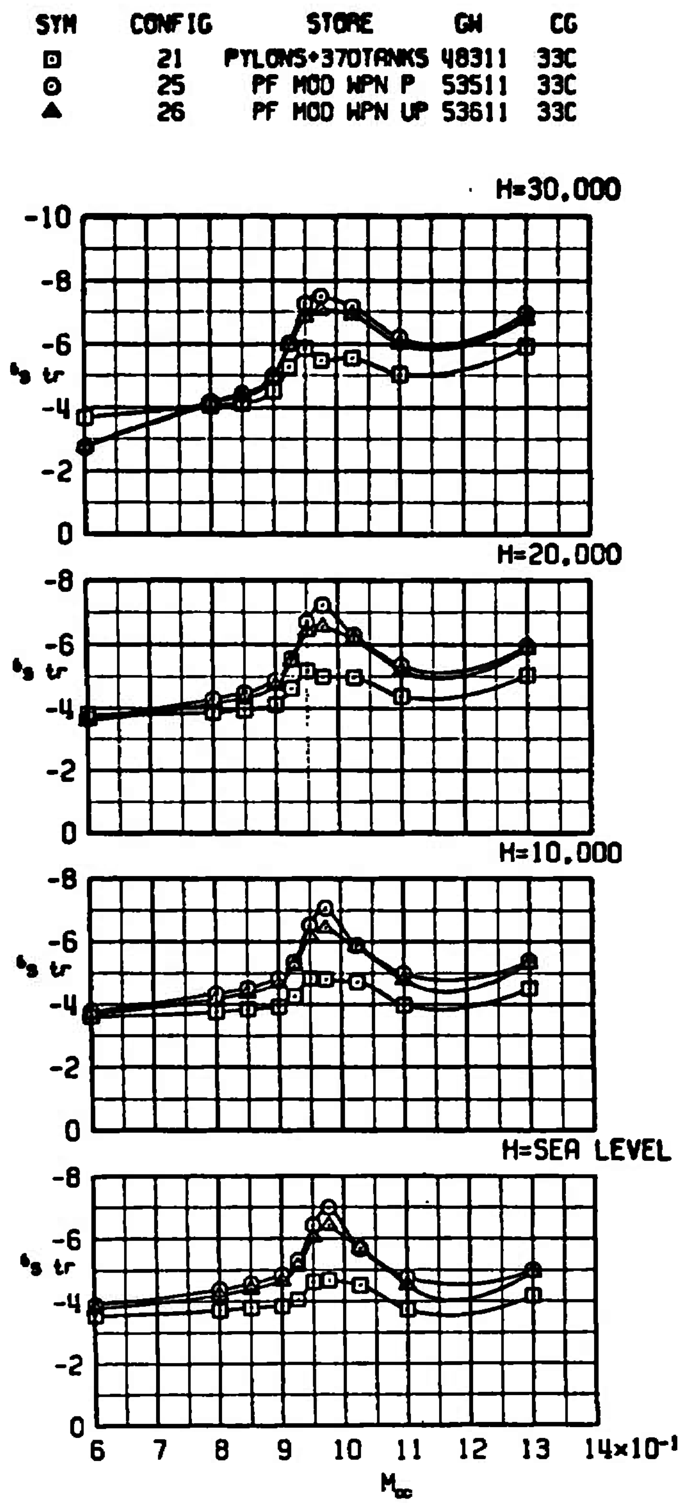

Figure 30. The effect of the PF Modular Weapons stores on trim stabilator angle.

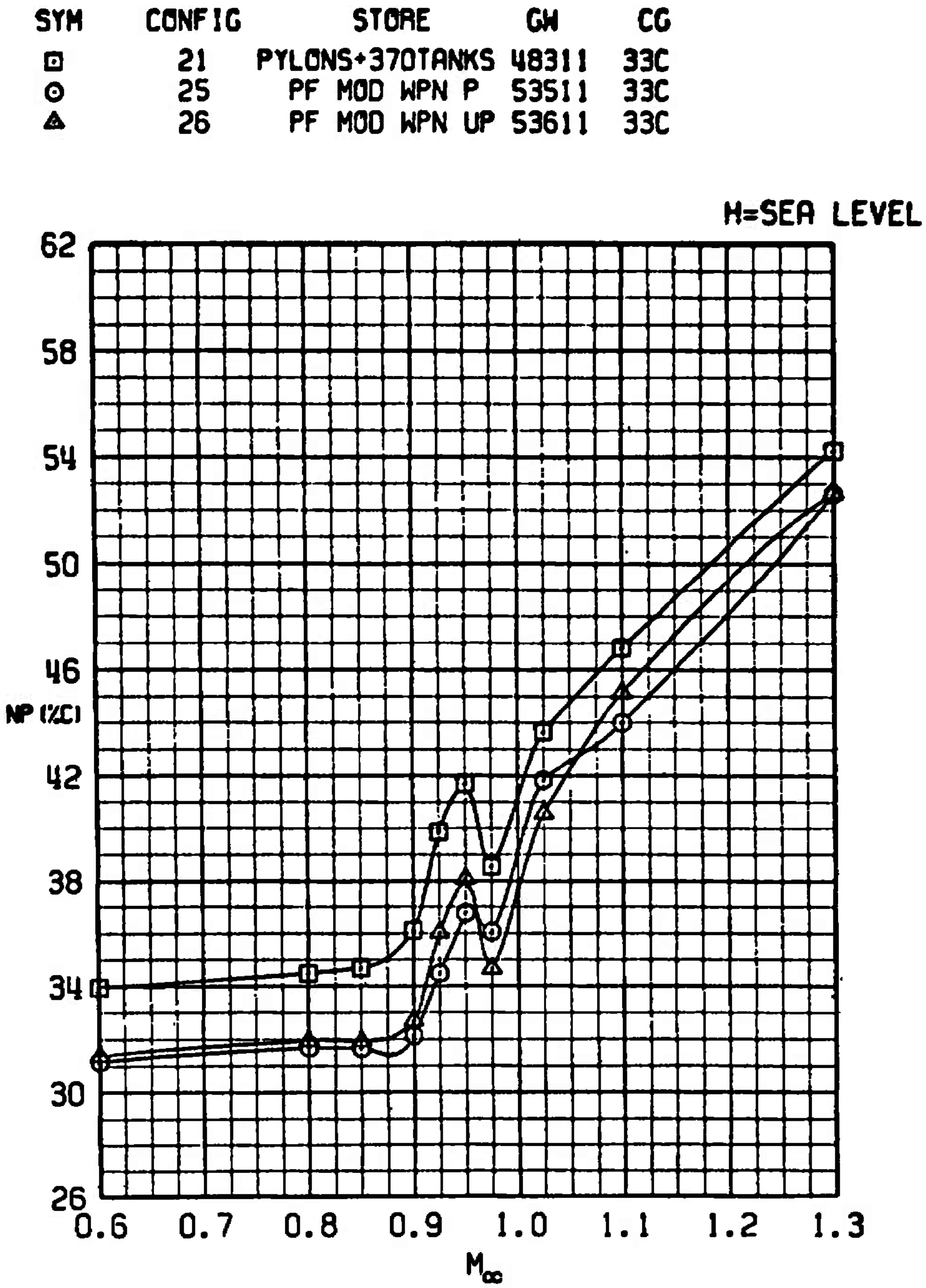

a. H = Sea level

Figure 31. The effect of the PF Modular Weapons stores on neutral-point location.

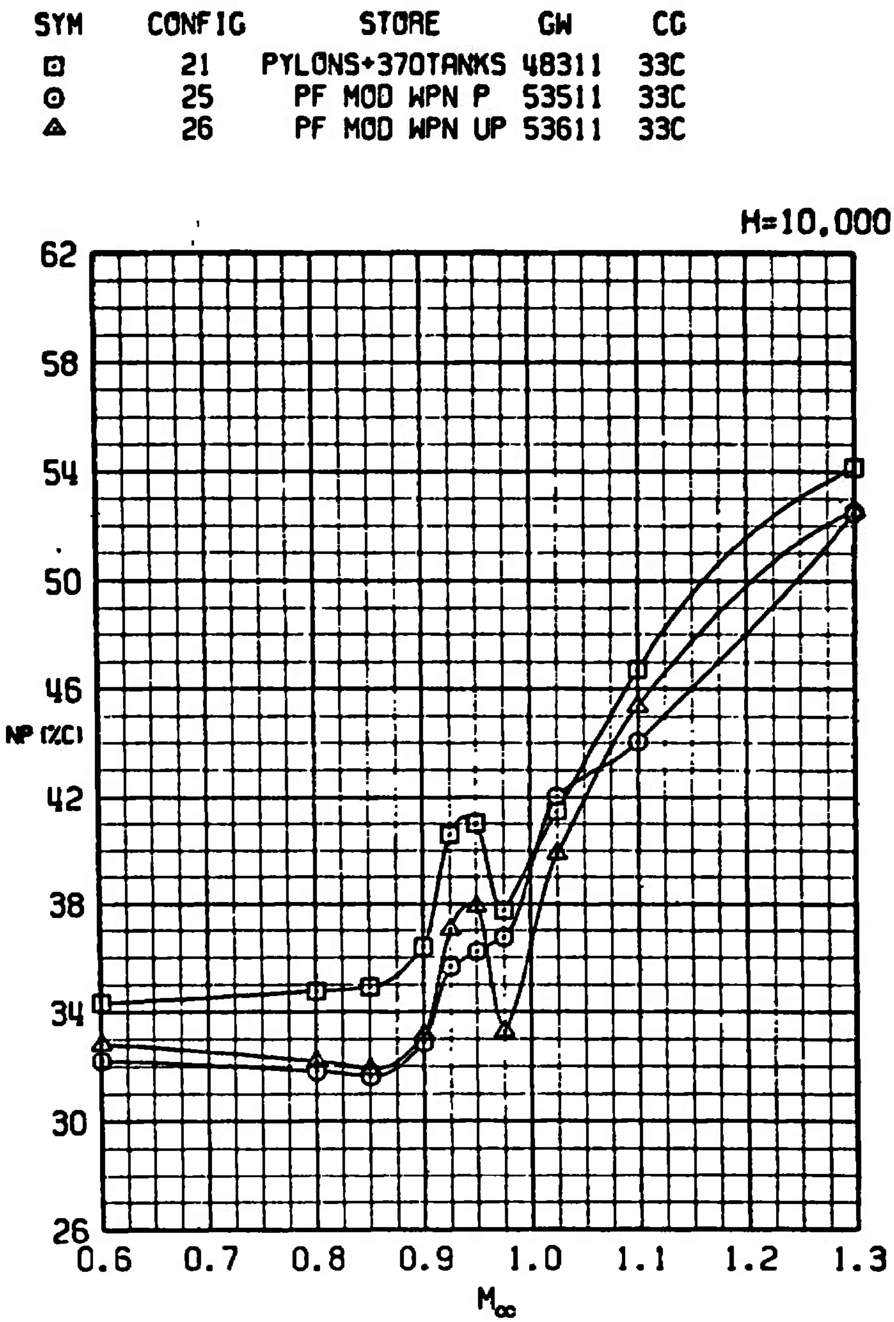

b. H = 10,000
Figure 31. Continued.

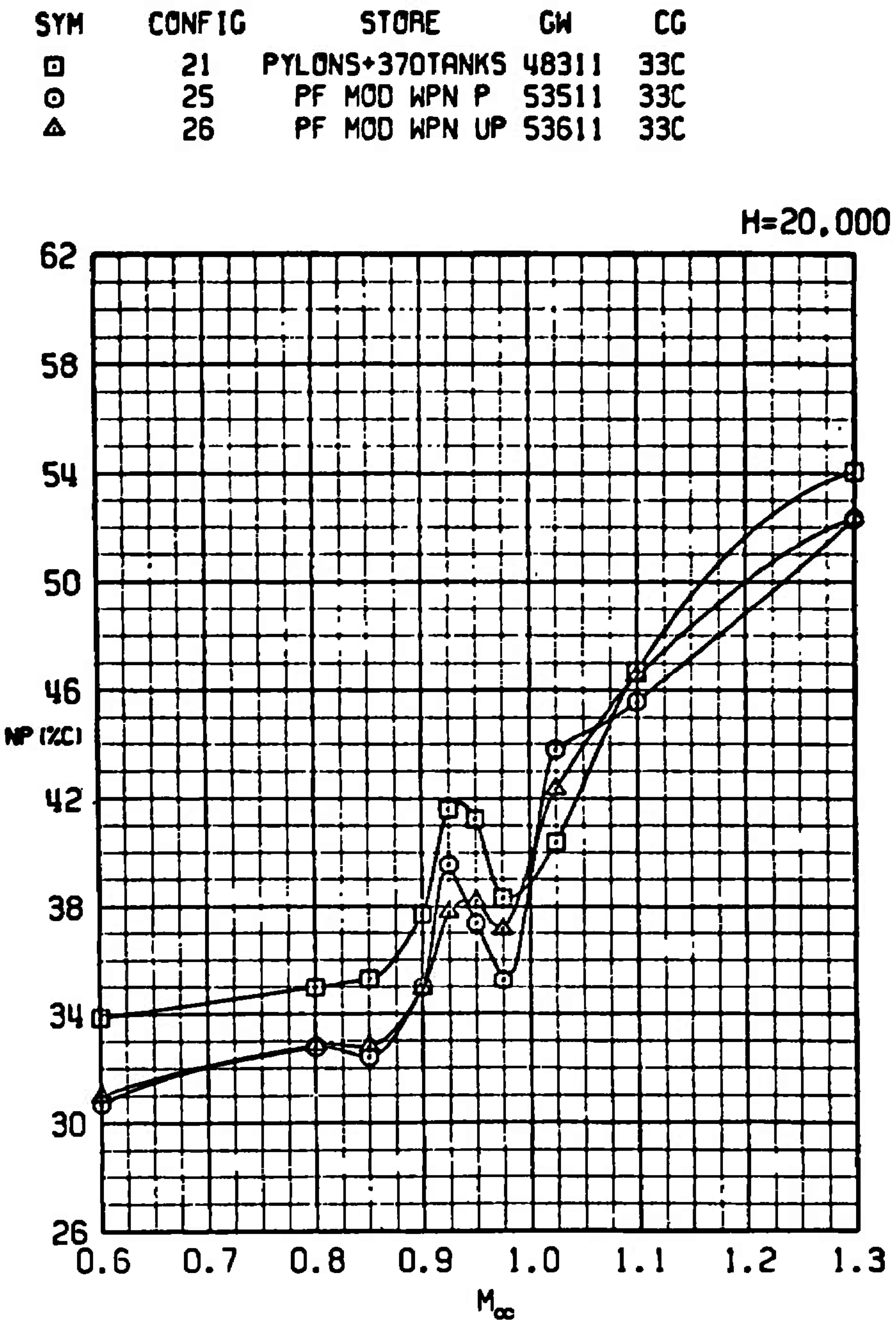

c. H = 20,000
Figure 31. Continued.

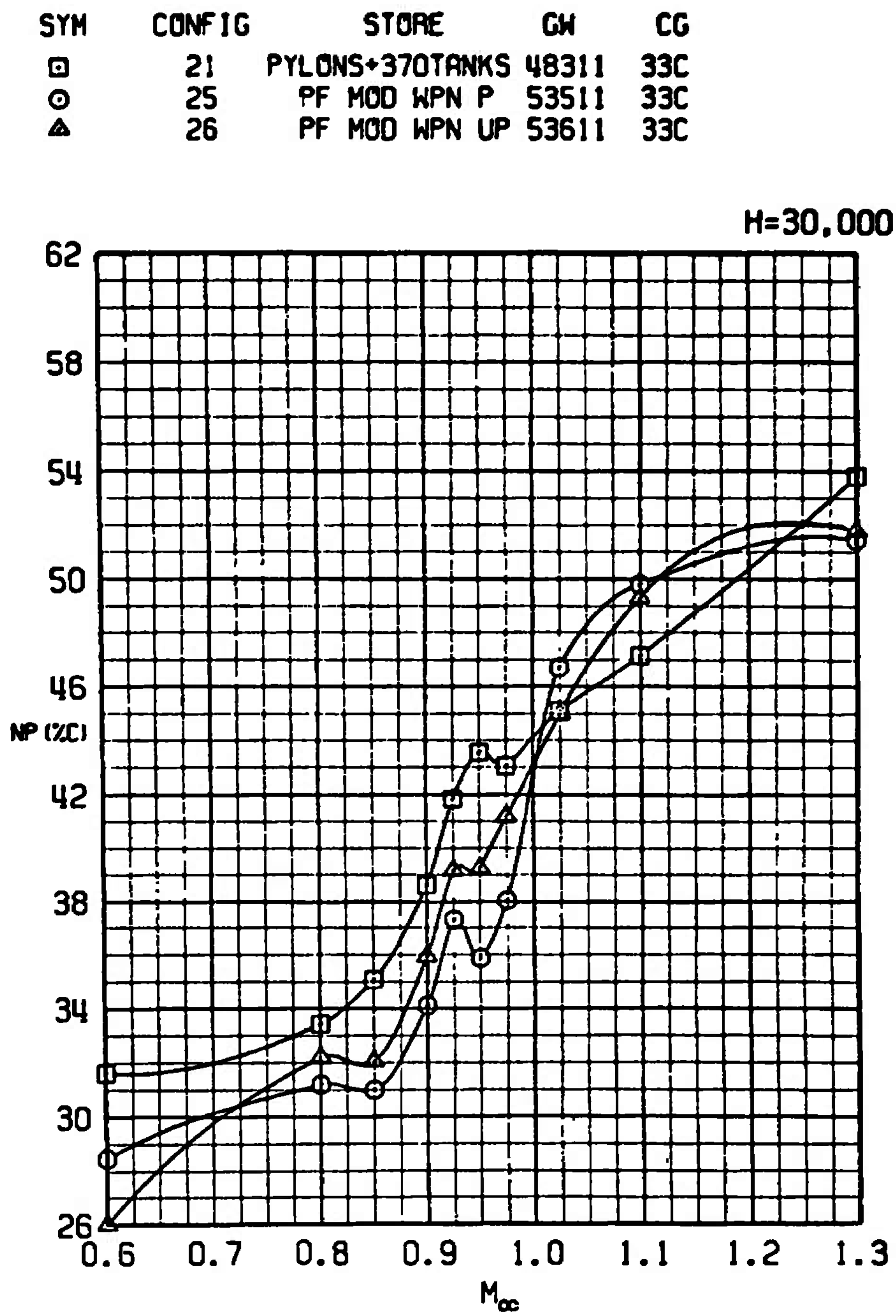

d. H = 30,000

Figure 31. Concluded.

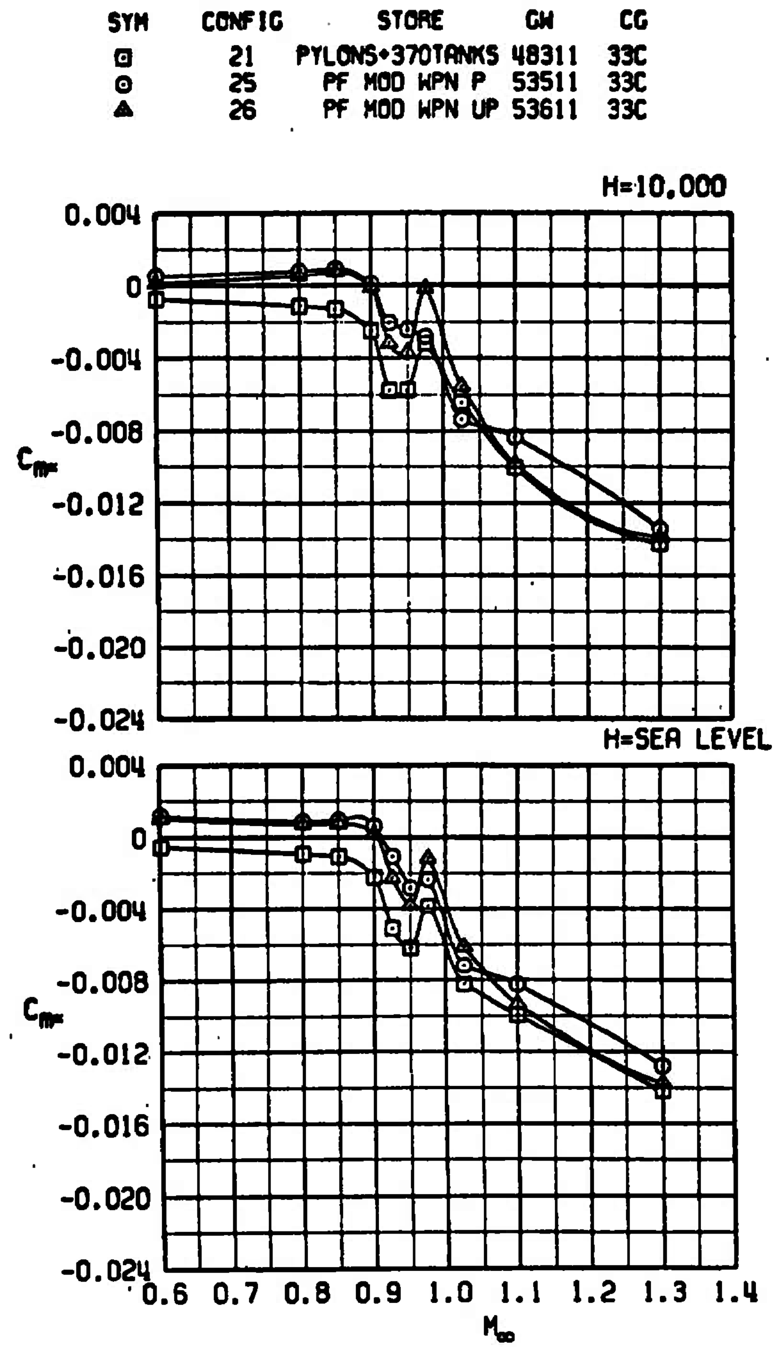

a. H = Sea level and 10,000

Figure 32. The effect of the PF Modular Weapons stores on the slope of the pitching-moment coefficient versus angle-of-attack curve at trim.

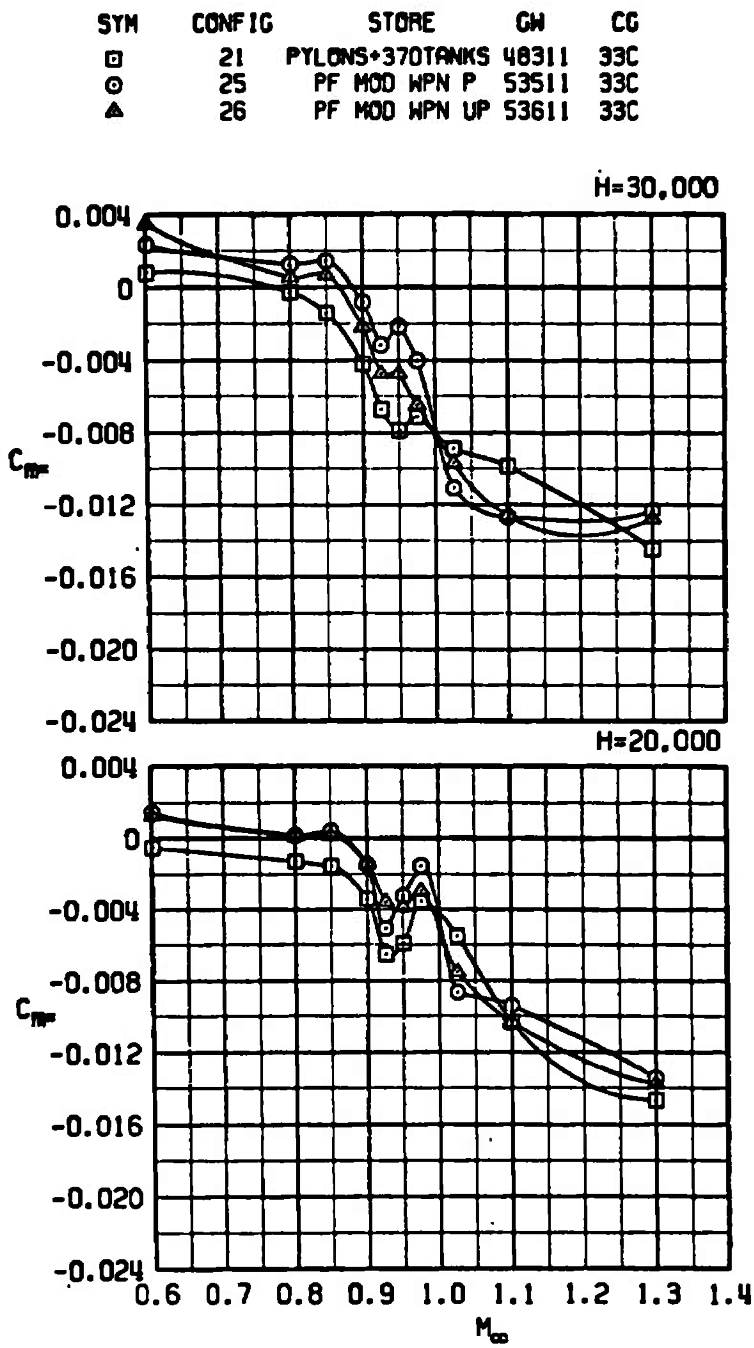

b. H = 20,000 and 30,000
Figure 32. Concluded.

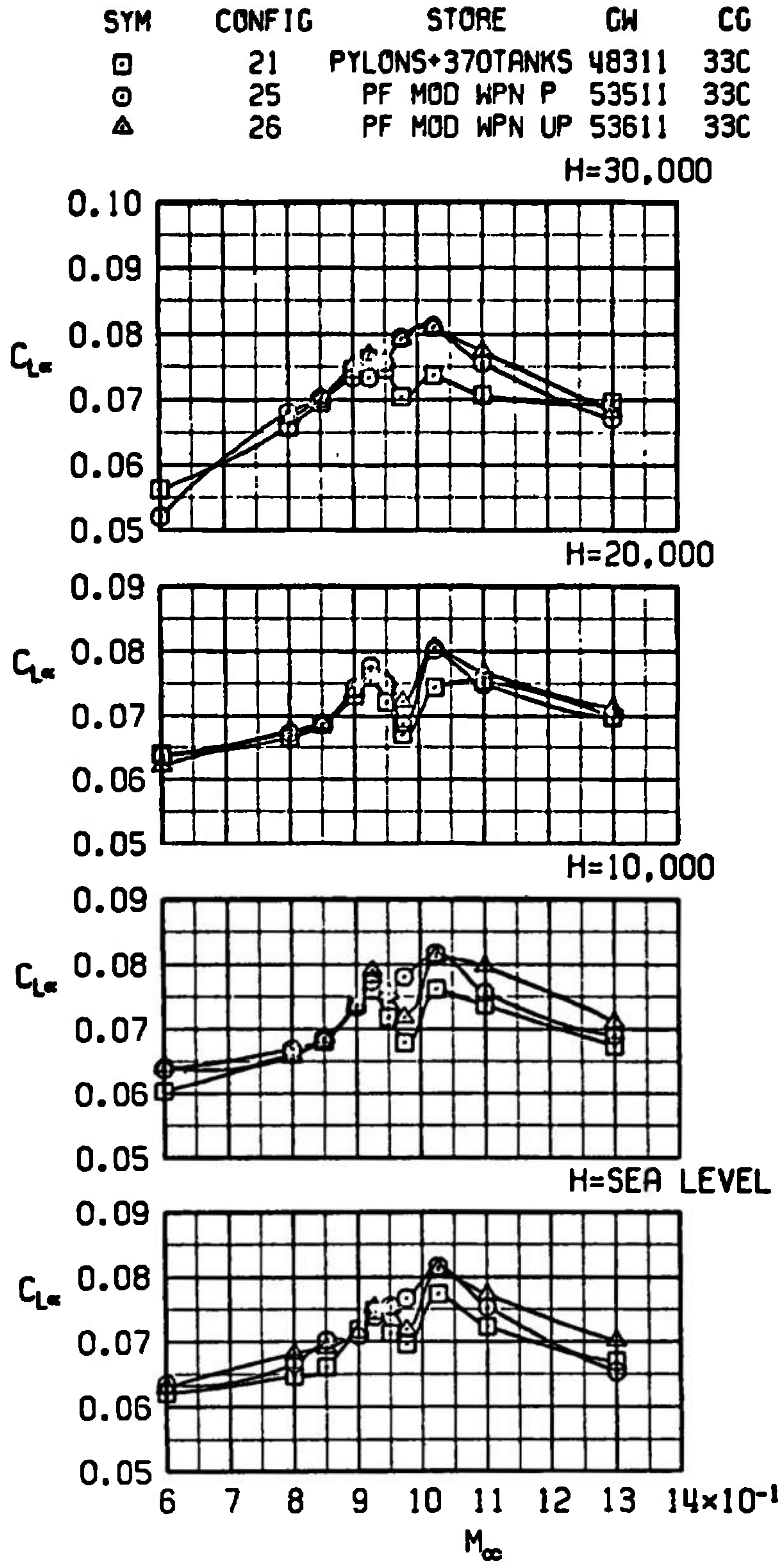

Figure 33. The effect of the PF Modular Weapons stores on the lift-curve slope at trim.

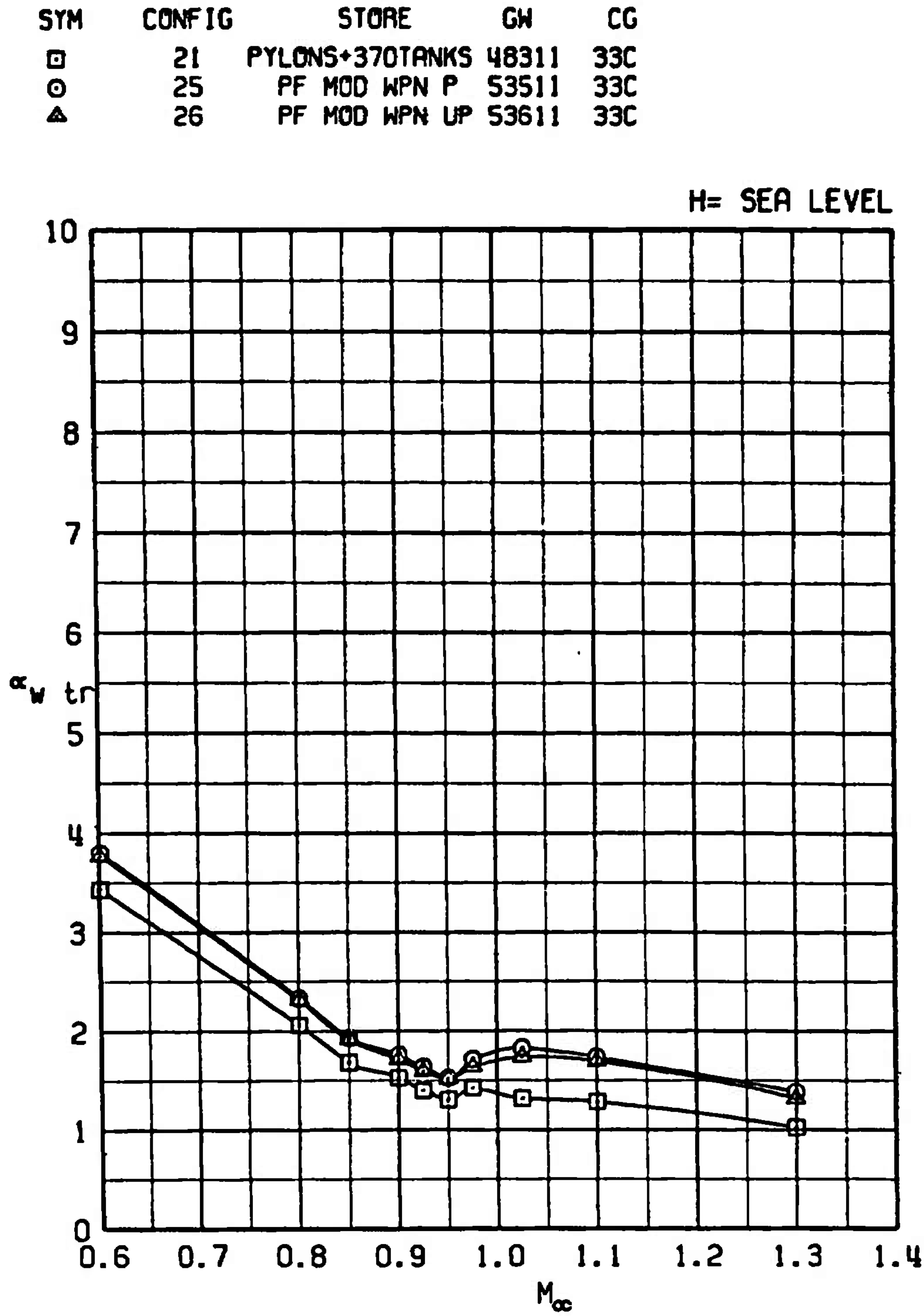

a. H = Sea level

Figure 34. The effect of the PF Modular Weapons stores on the trim wing angle of attack.

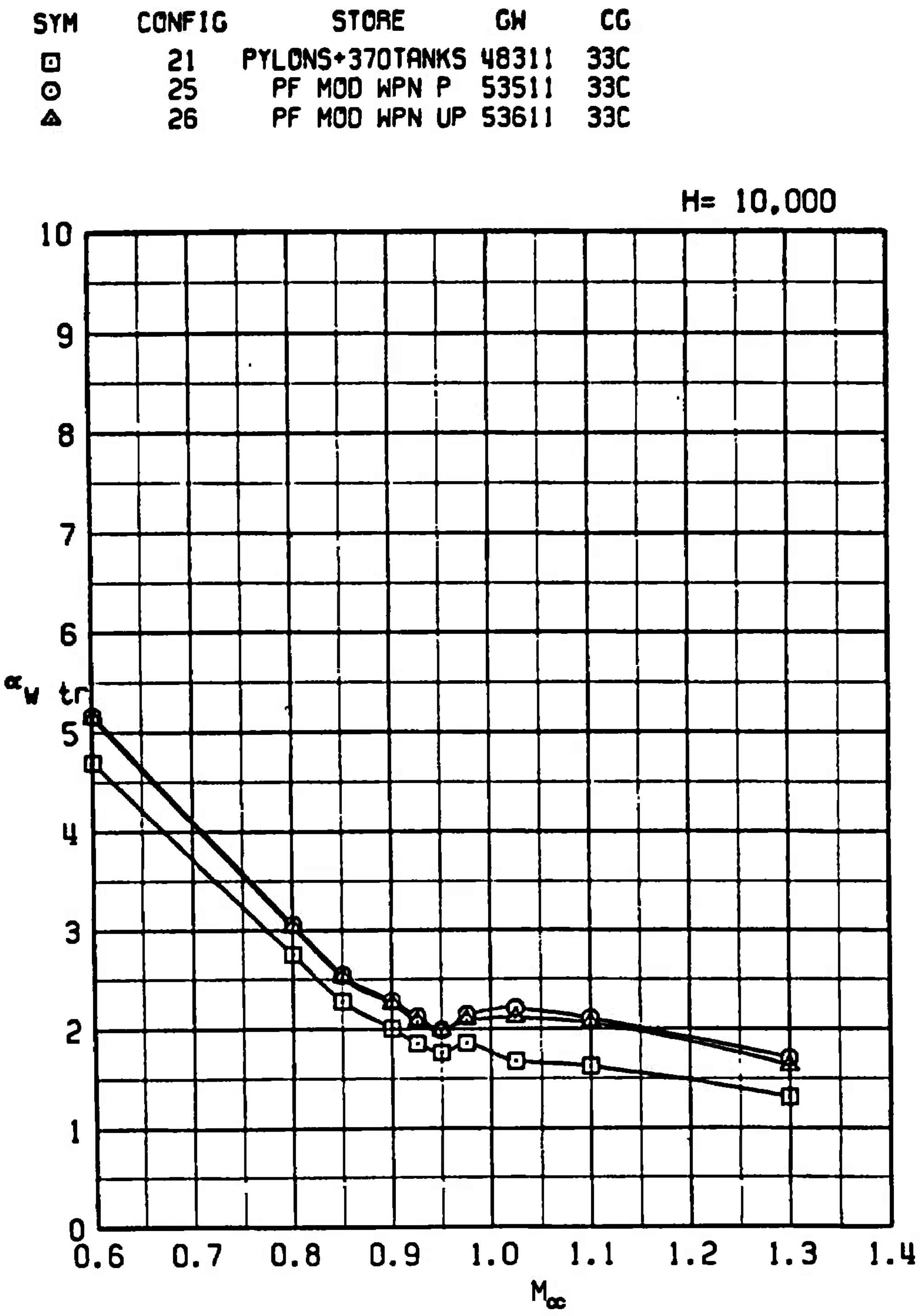

b. H = 10,000
Figure 34. Continued.

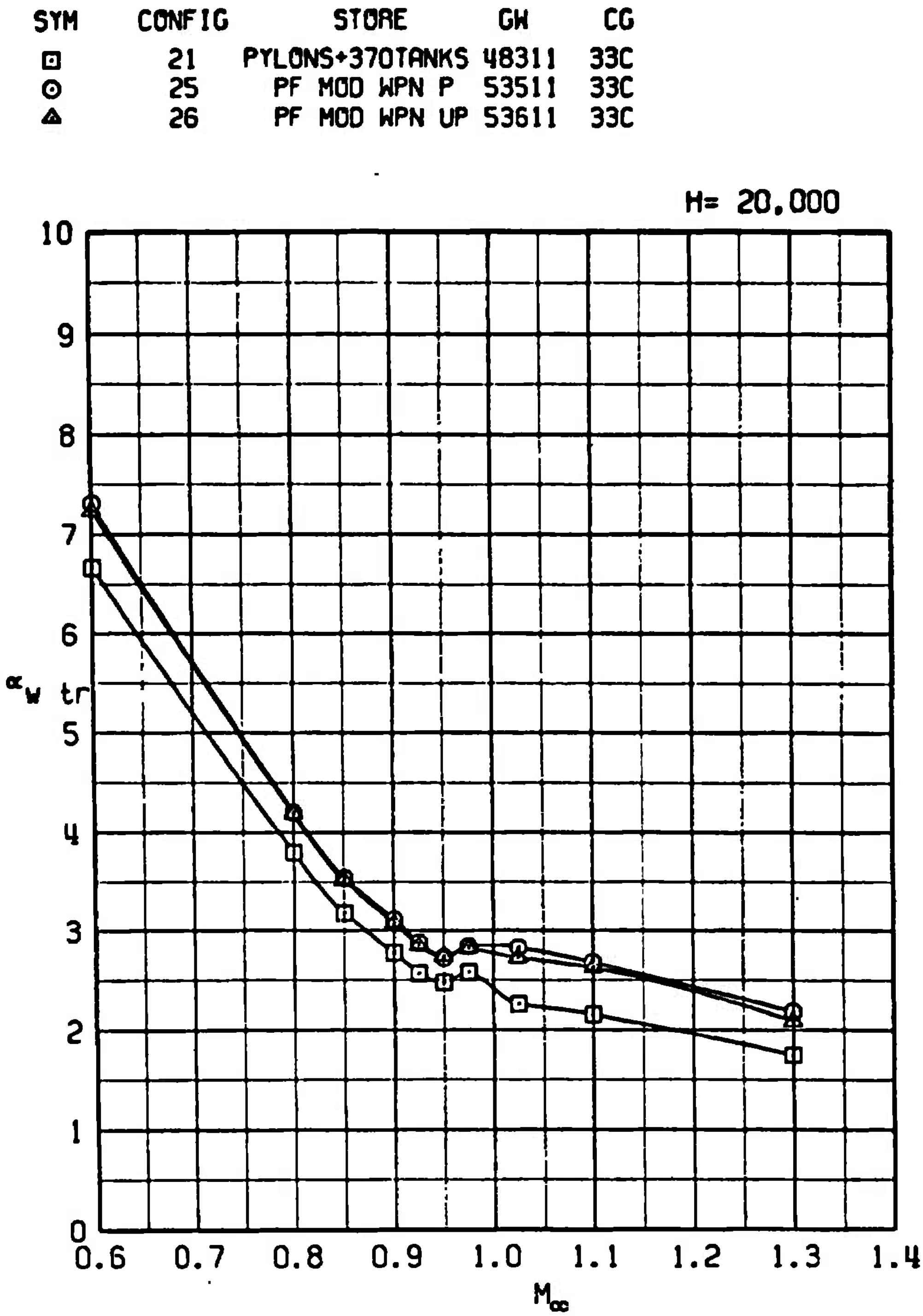

c. H = 20,000
Figure 34. Continued.

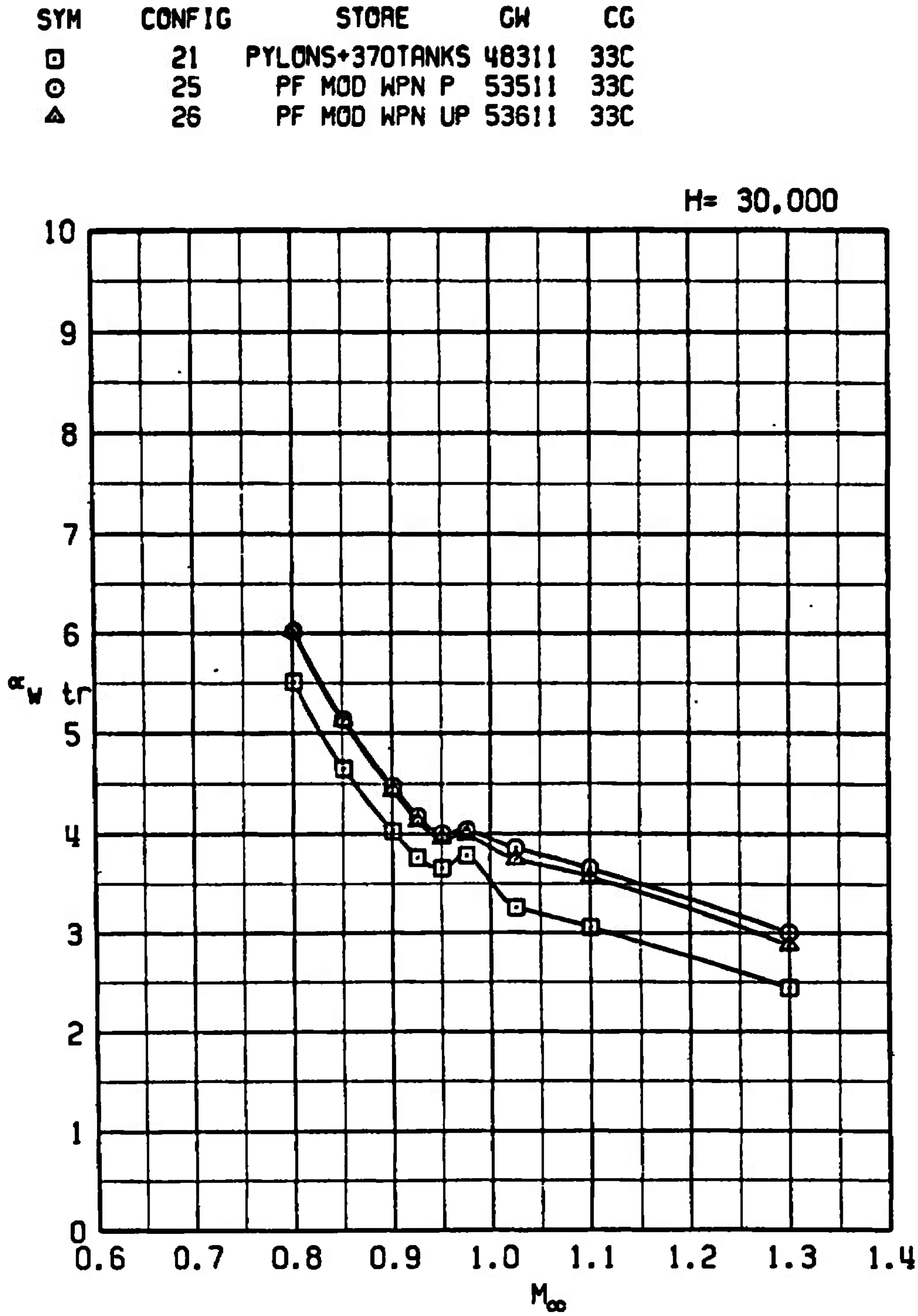

d. H = 30,000
Figure 34. Concluded.

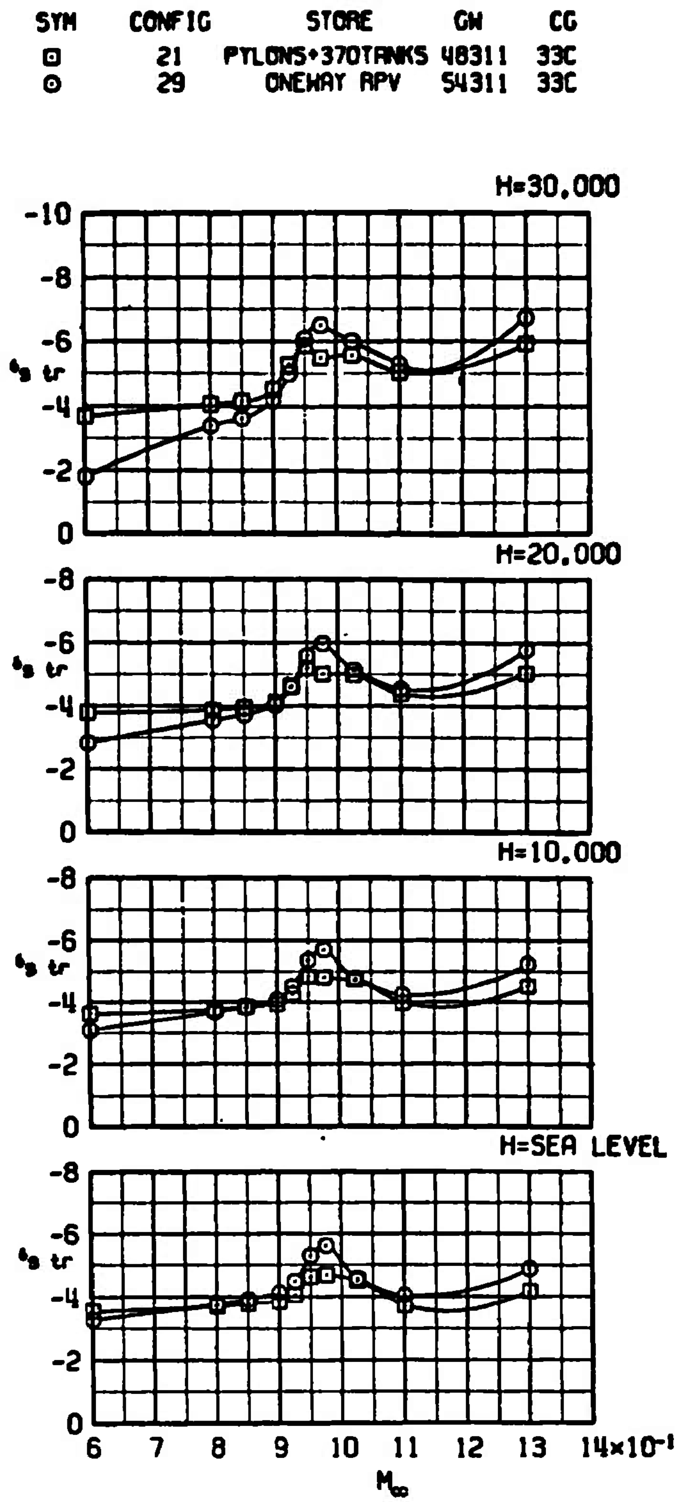

Figure 35. The effect of the Oneway RPV store on trim stabilator angle.

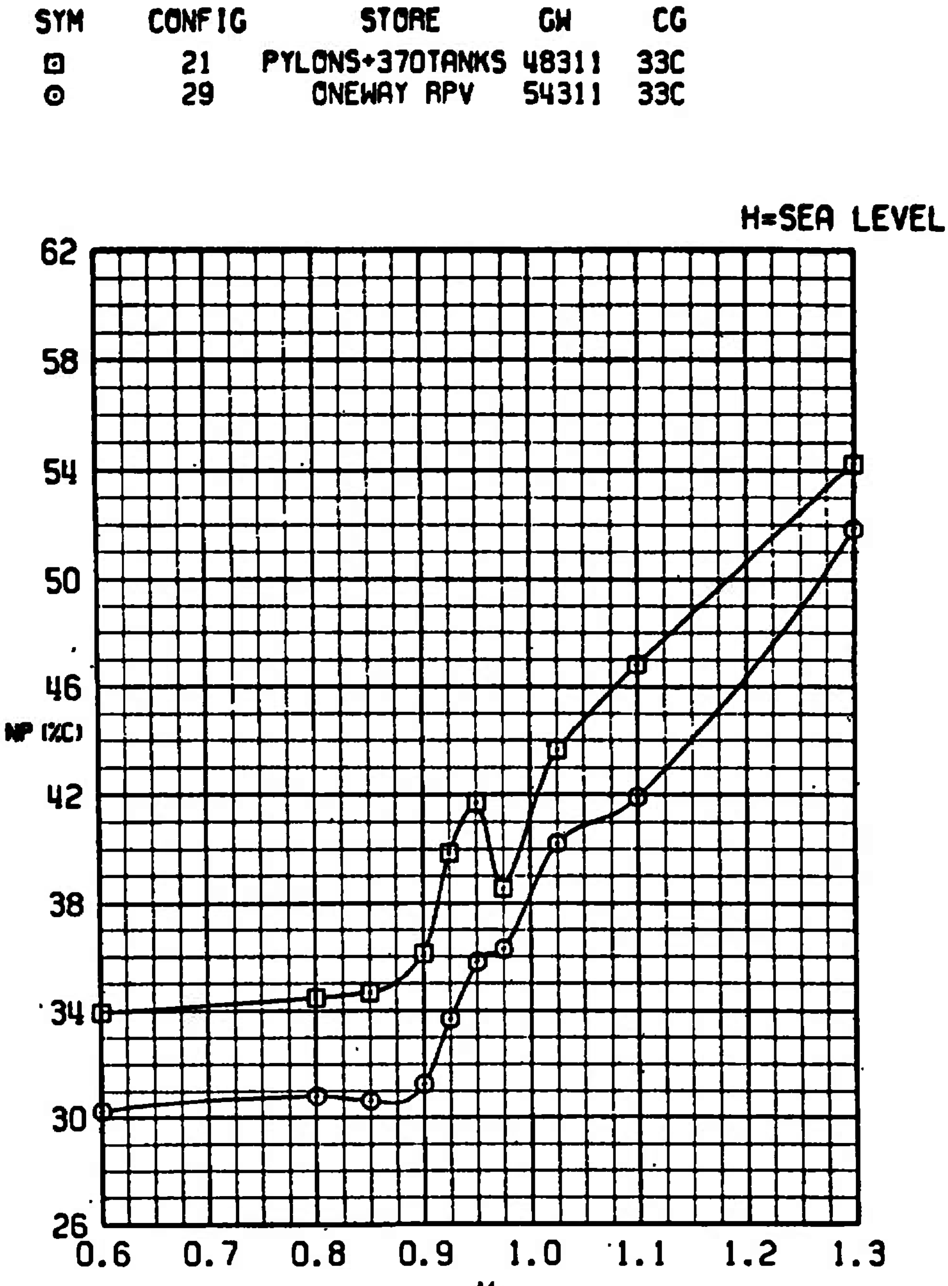

a. H = Sea level

Figure 36. The effect of the Oneway RPV store on neutral-point location.

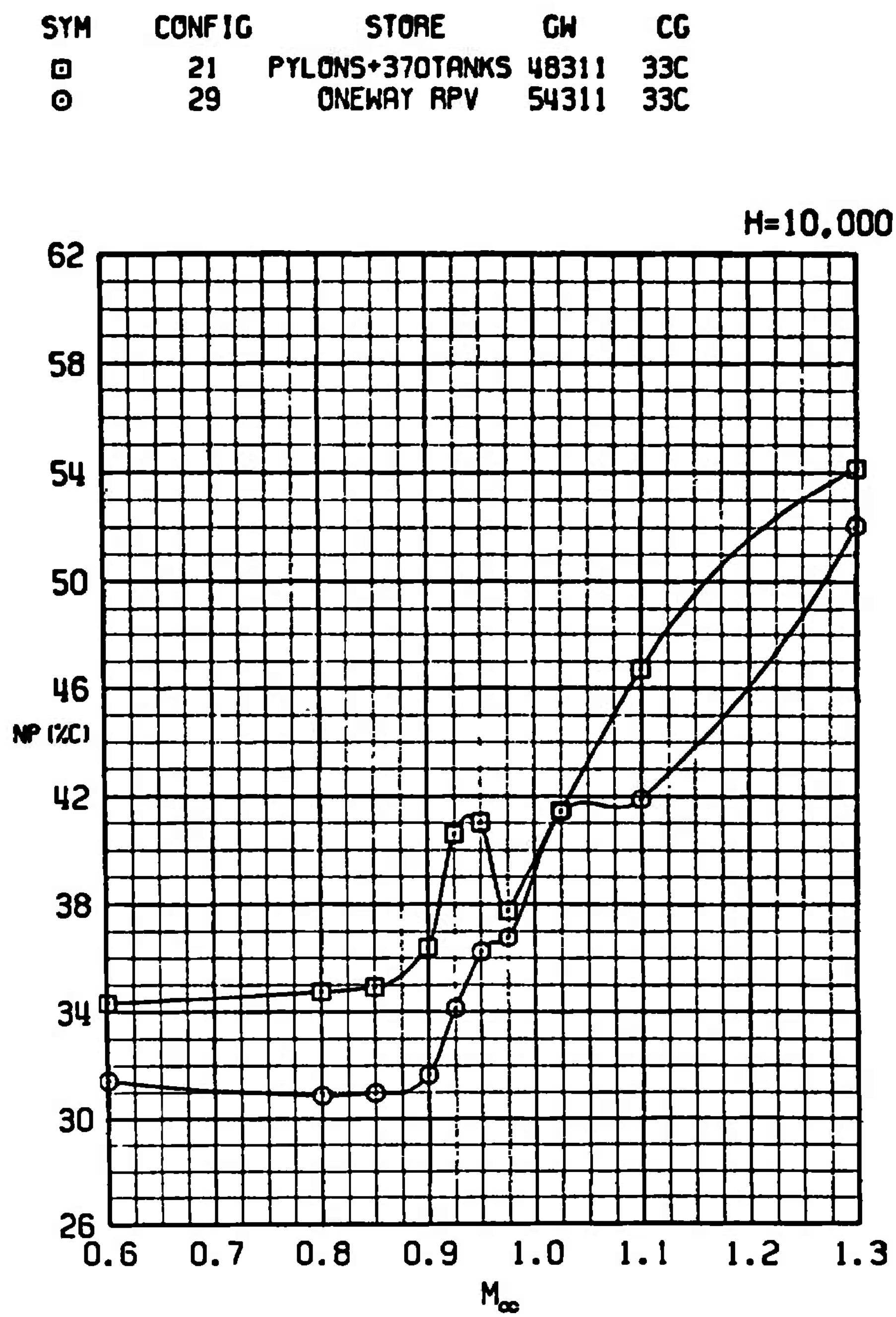

b. H = 10,000
Figure 36. Continued.

SYM	CONFIG	STORE	GW	CG
⊡	21	PYLONS+370TANKS	48311	33C
⊙	29	ONEWAY RPV	54311	33C

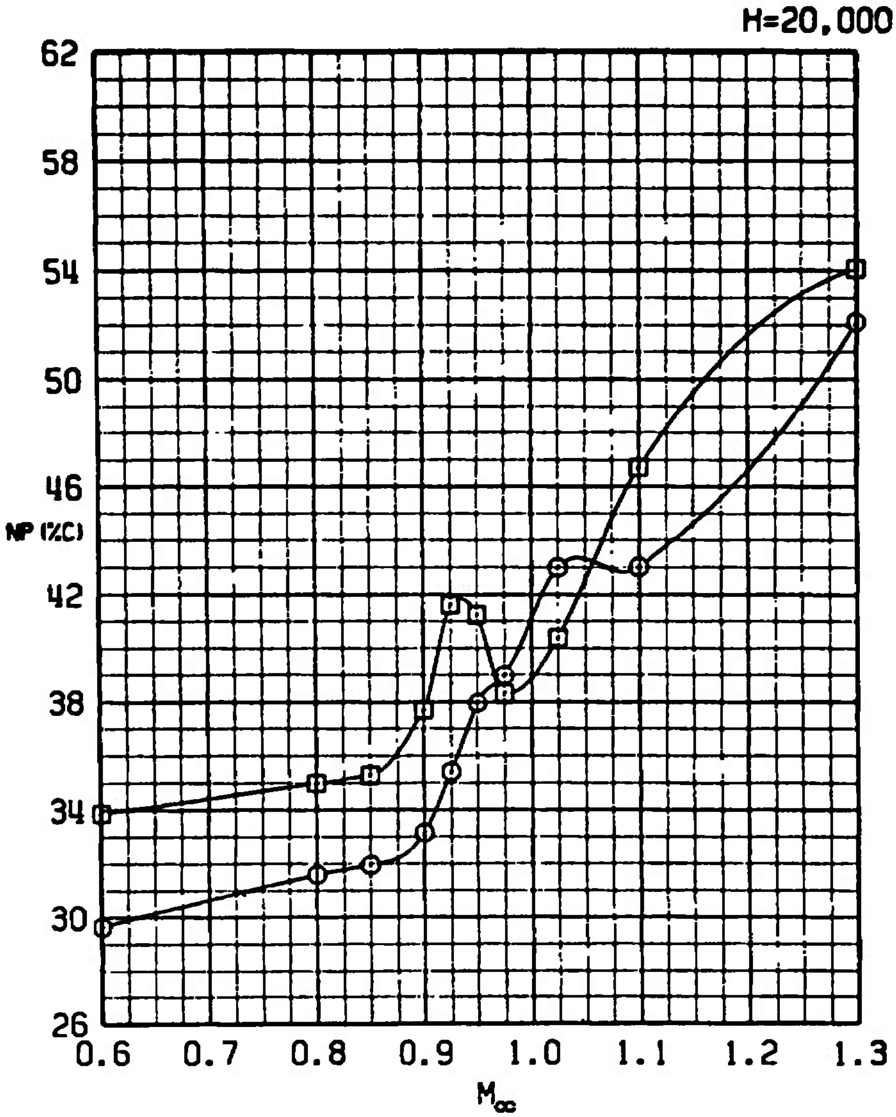

c. H = 20,000
Figure 36. Continued.

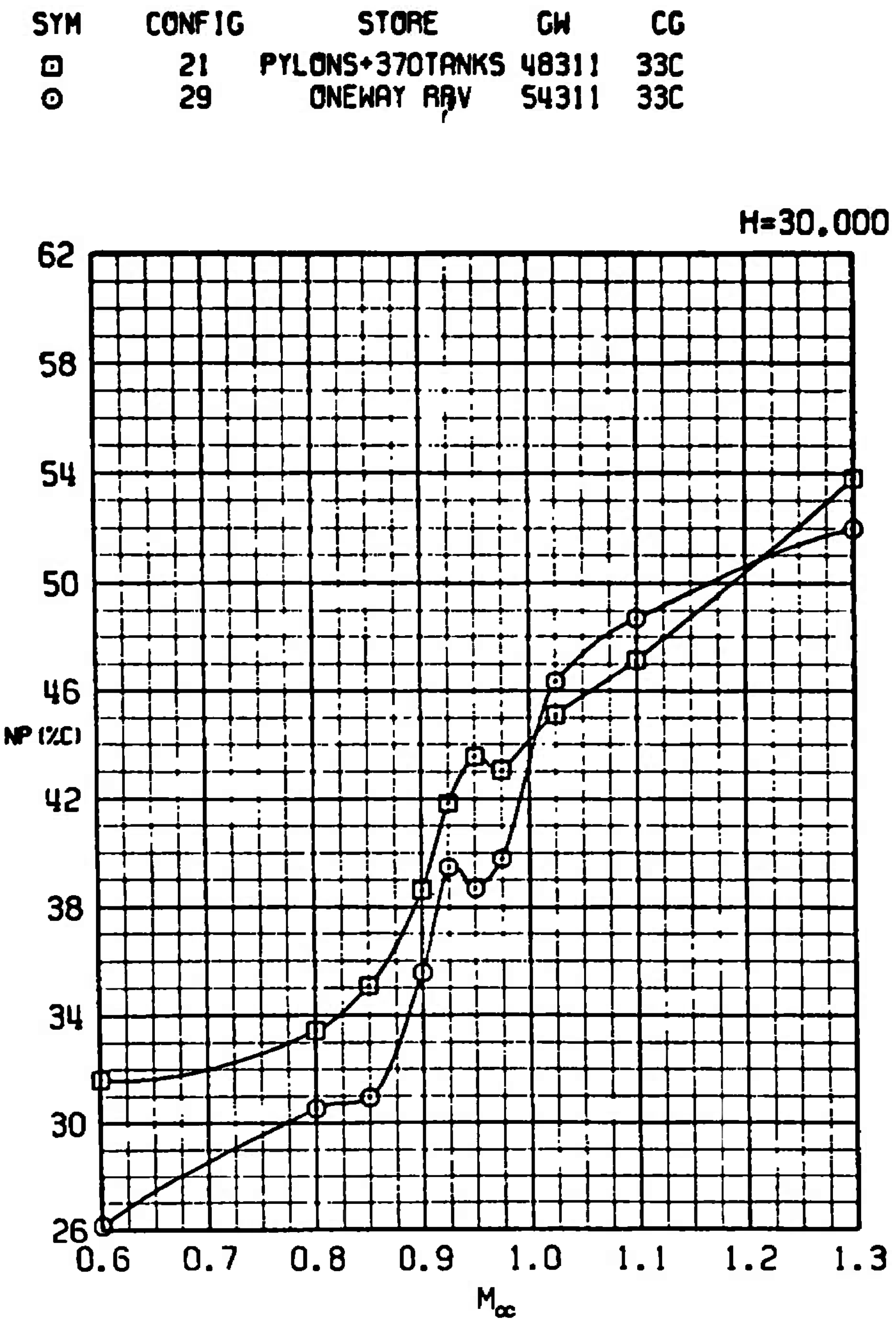

d. H = 30,000
Figure 36. Concluded.

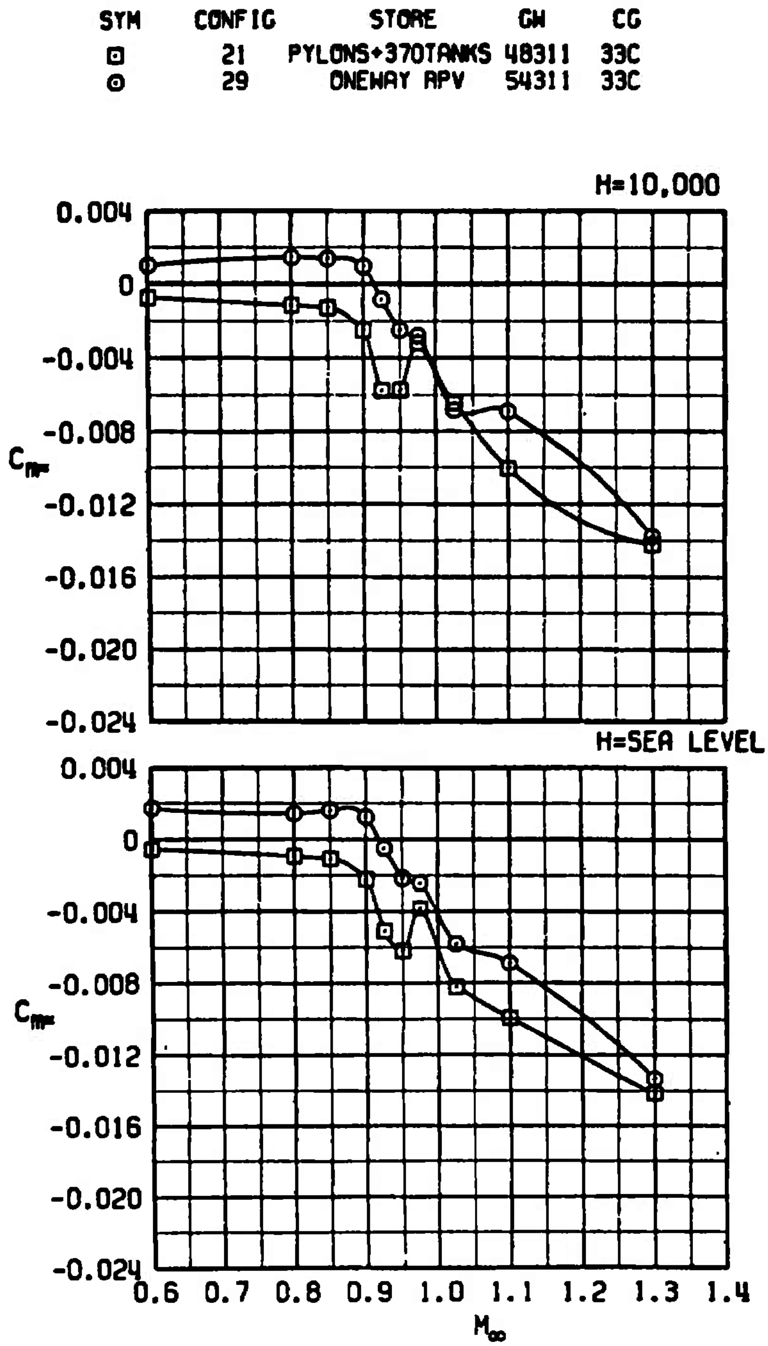

a. H = Sea level and 10,000

Figure 37. The effect of the Oneway RPV store on the slope of the pitching-moment coefficient versus angle-of-attack curve at trim.

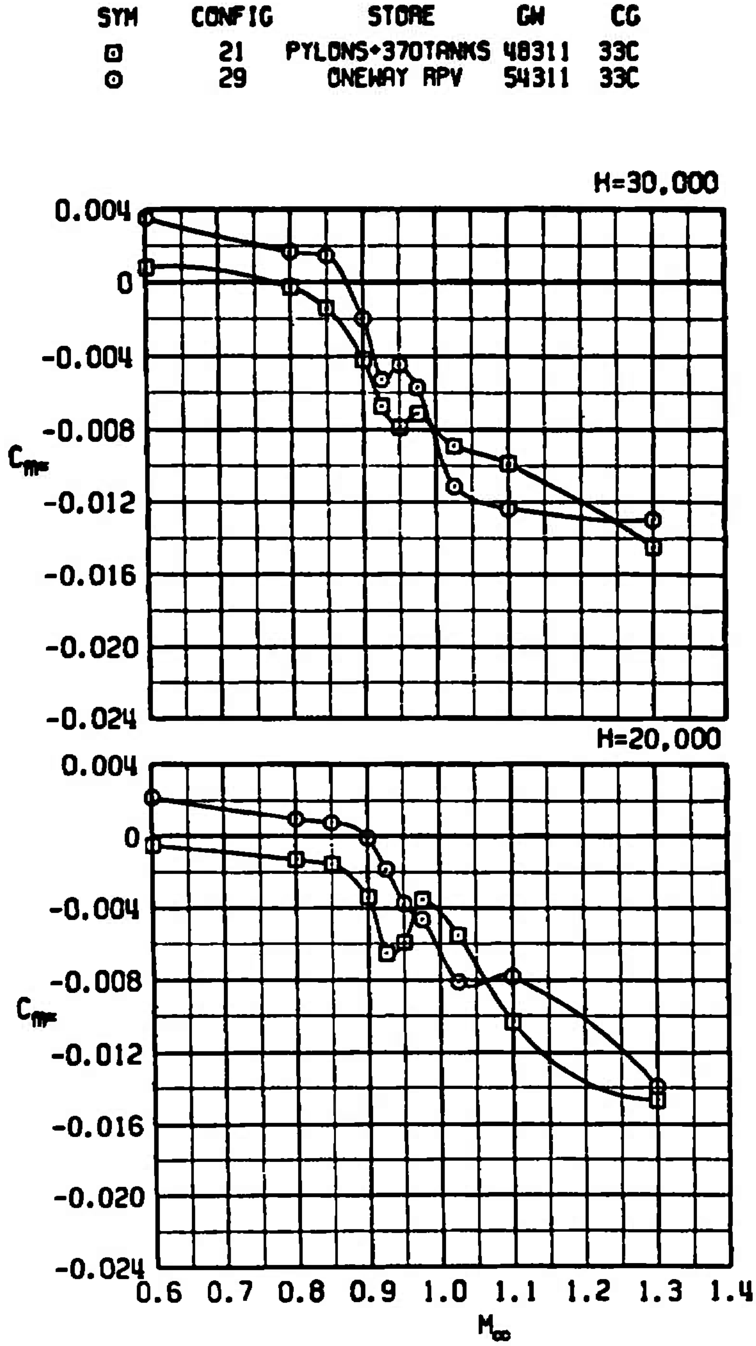

b. H = 20,000 and 30,000
Figure 37. Concluded.

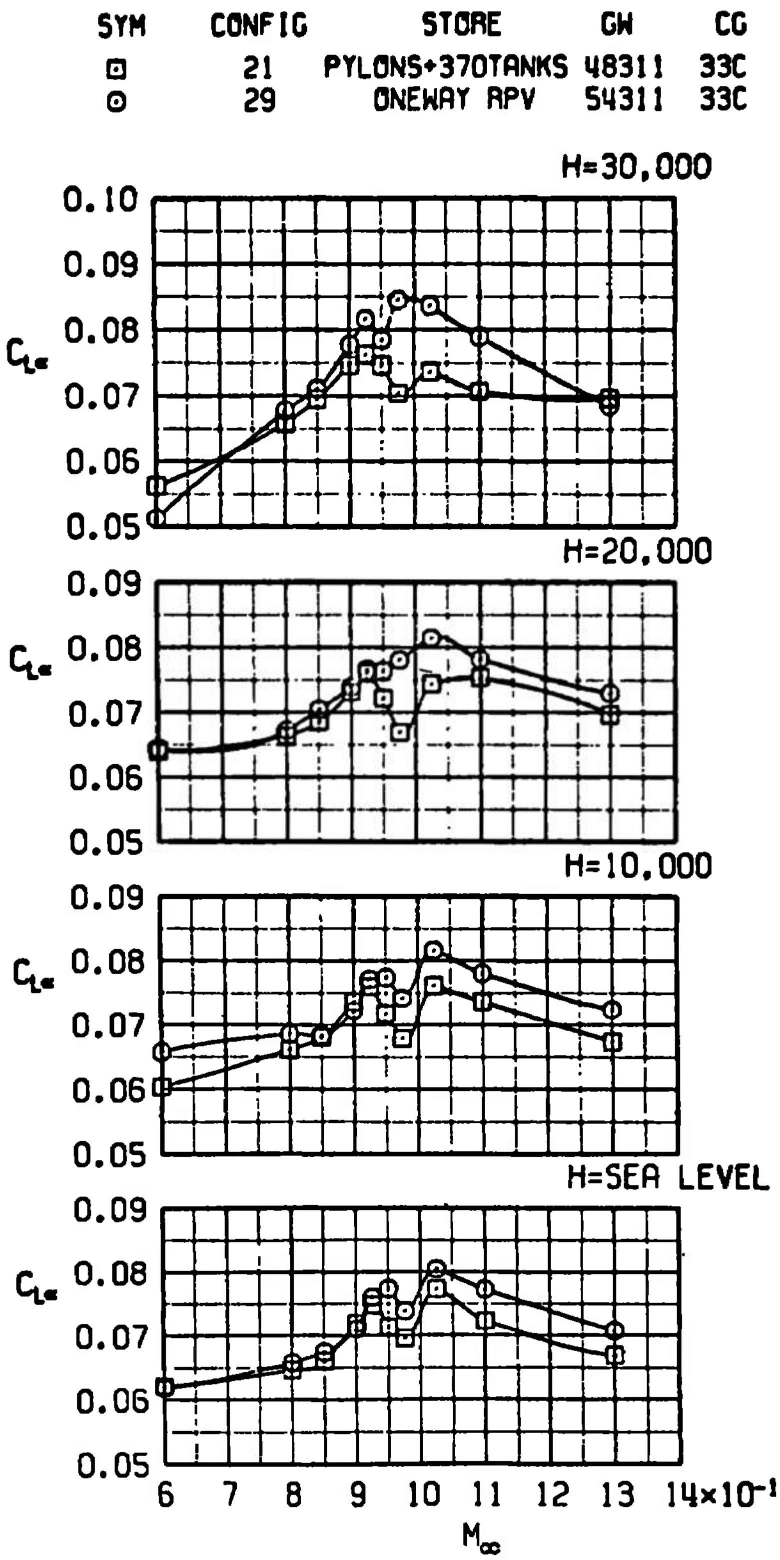

Figure 38. The effect of the Oneway RPV store on the lift-curve slope at trim.

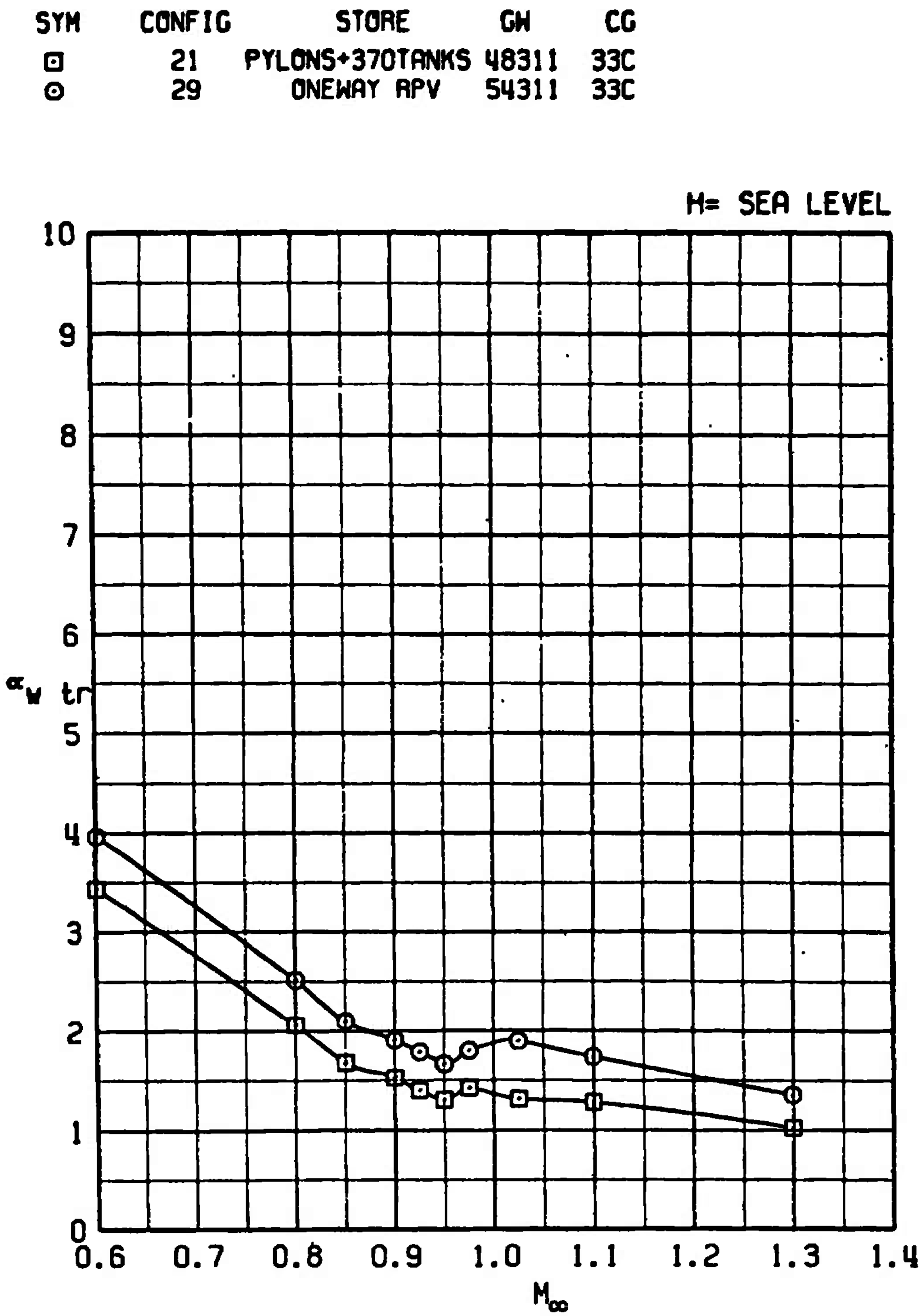

a. H = Sea level

Figure 39. The effect of the Oneway RPV store on the trim wing angle of attack.

SYM	CONFIG	STORE	GW	CG
⊡	21	PYLONS+370TANKS	48311	33C
⊙	29	ONEWAY RPV	54311	33C

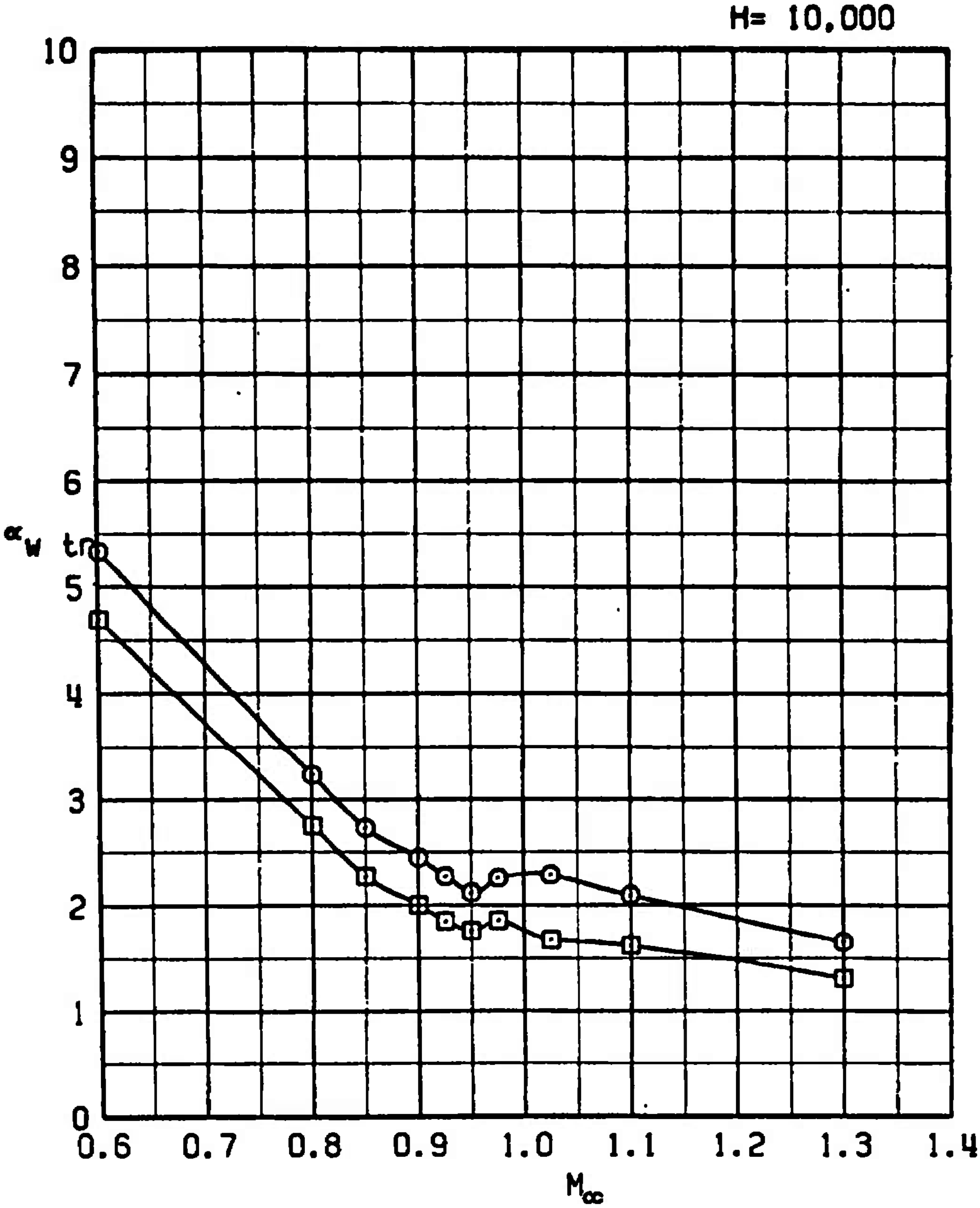

b. H = 10,000
Figure 39. Continued.

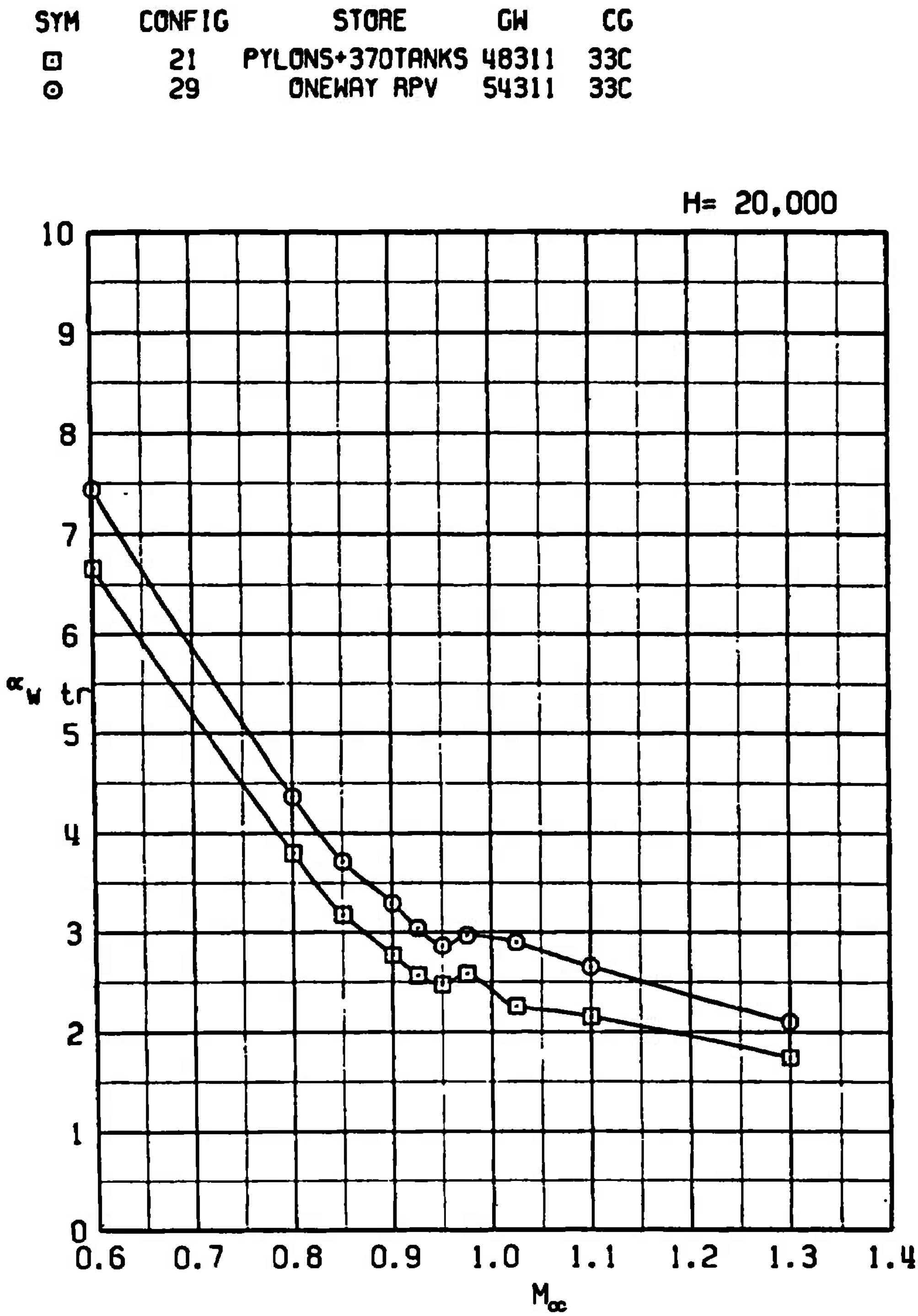

c. H = 20,000
Figure 39. Continued.

SYM	CONFIG	STORE	GW	CG
⊡	21	PYLONS+370TANKS	48311	33C
⊙	29	ONEWAY RPV	54311	33C

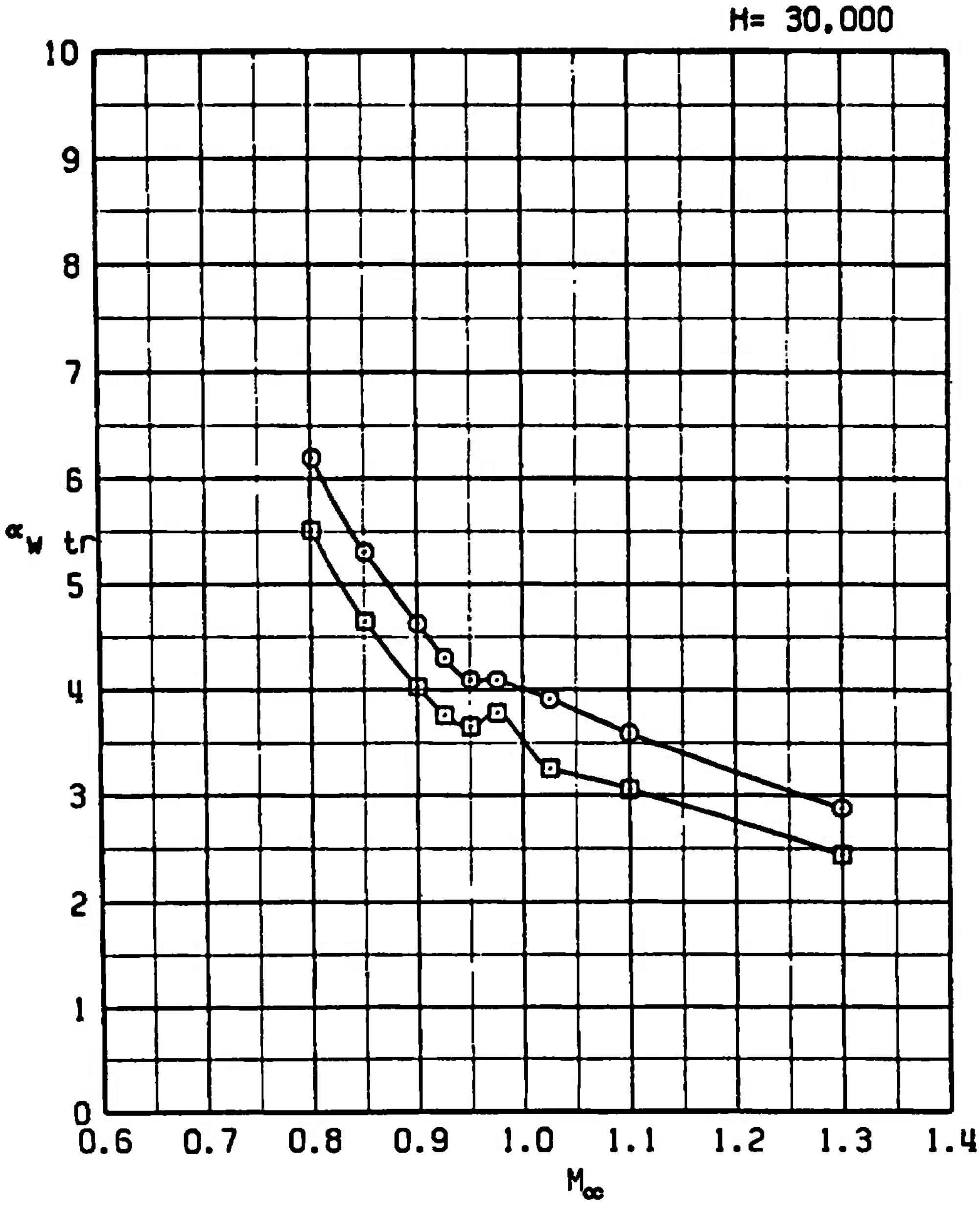

d. H = 30,000
Figure 39. Concluded.

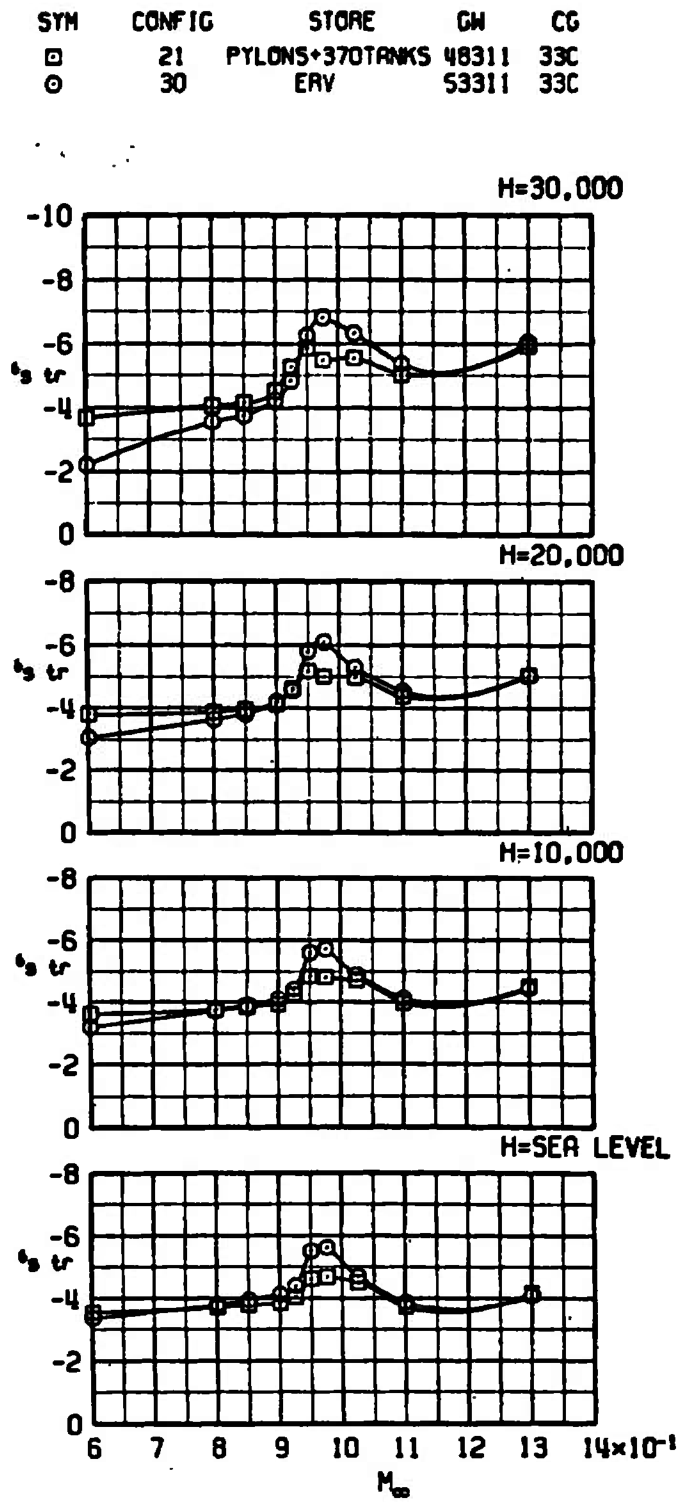

Figure 40. The effect of the ERV store on trim stabilator angle.

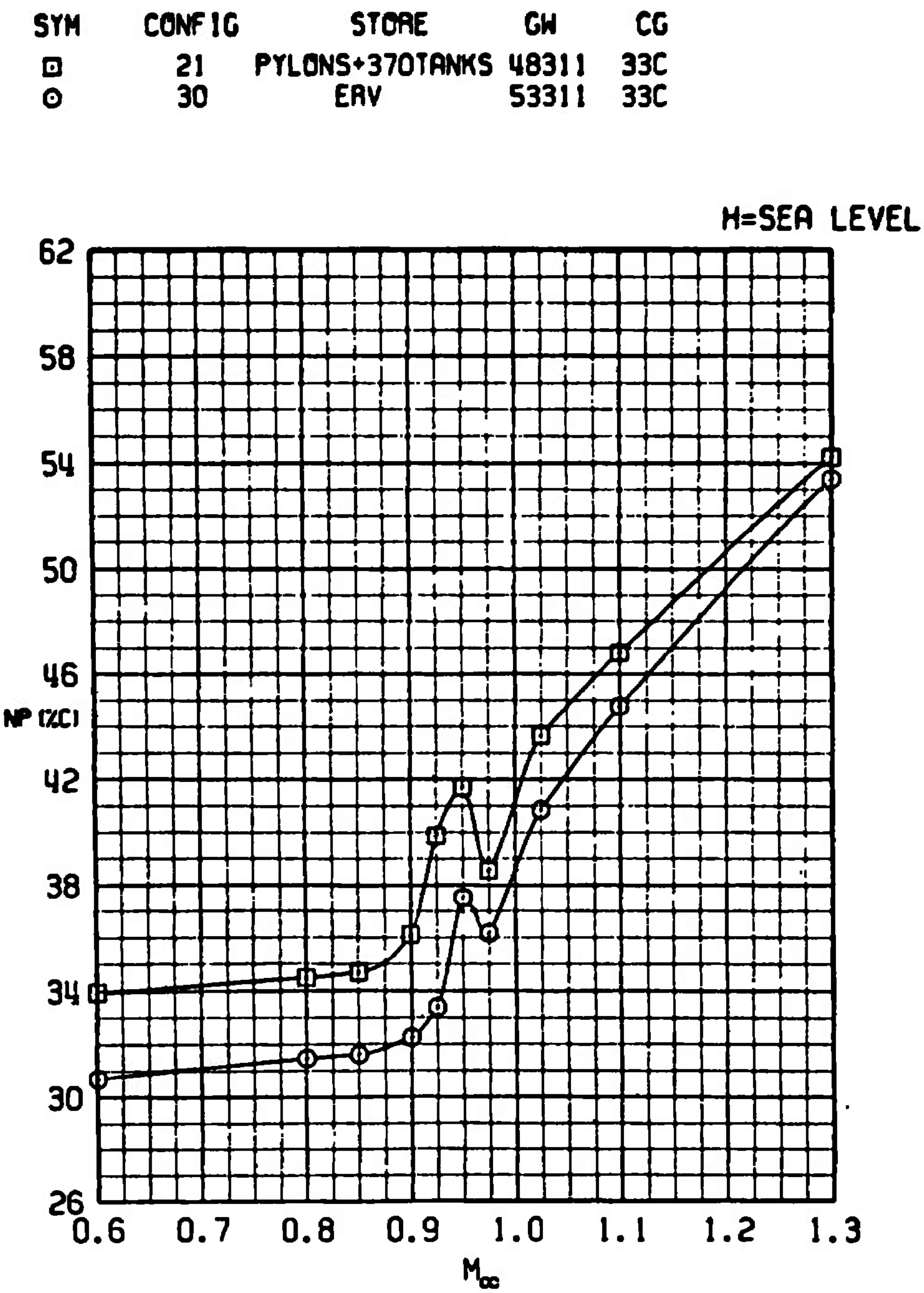

a. H = Sea level

Figure 41. The effect of the ERV store on neutral-point location.

SYM	CONFIG	STORE	GW	CG
⊡	21	PYLONS+370TANKS	48311	33C
⊙	30	ERV	53311	33C

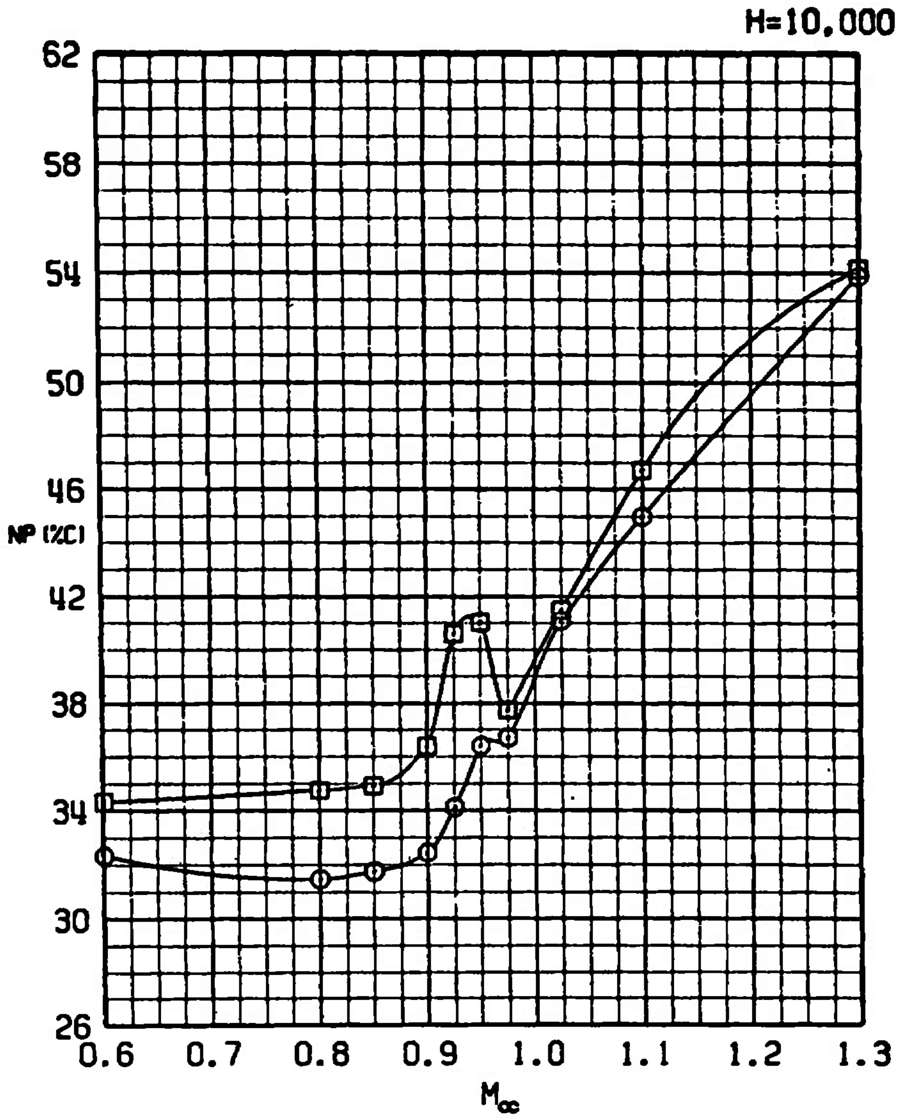

b. H = 10,000
Figure 41. Continued.

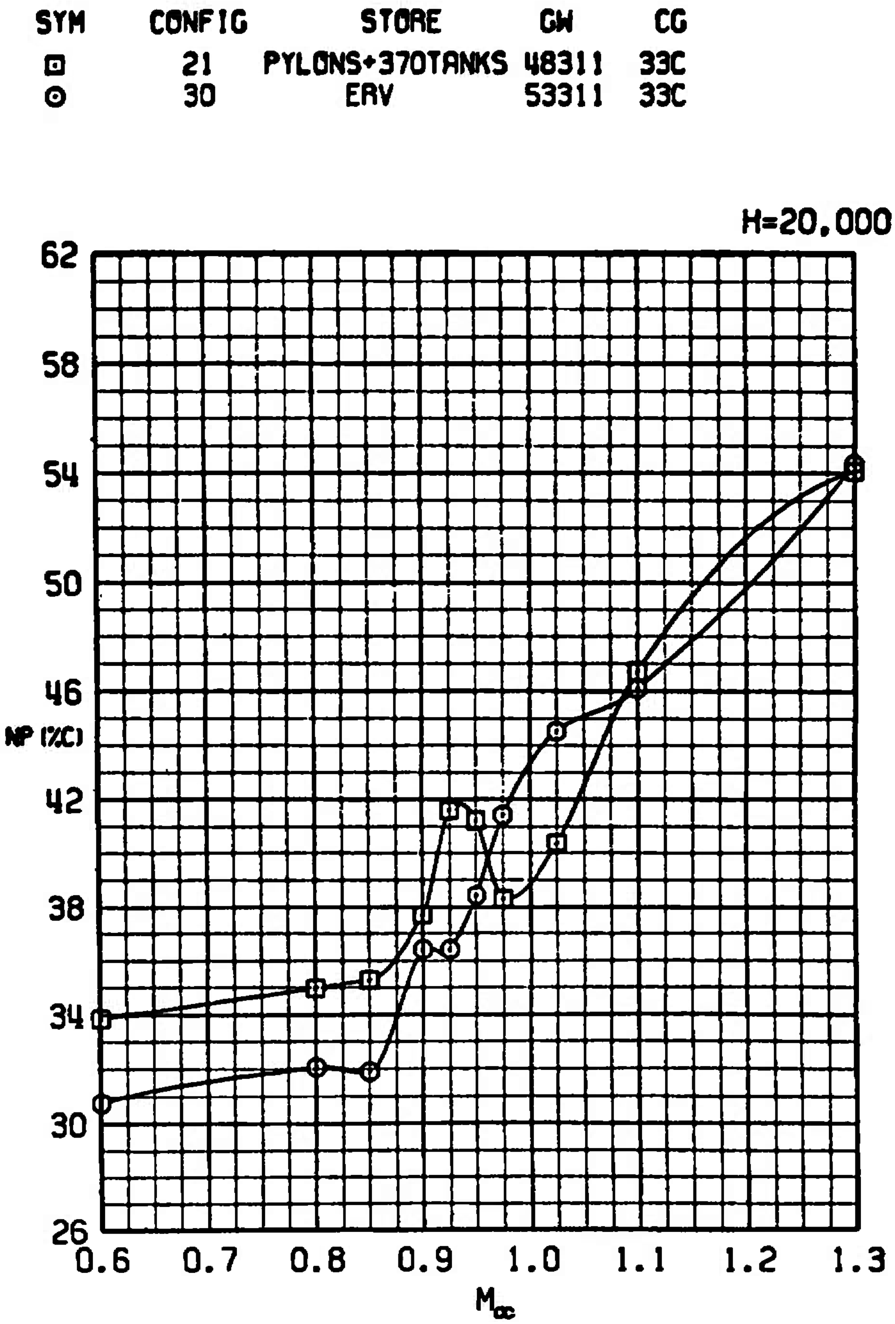

c. H = 20,000

Figure 41. Continued.

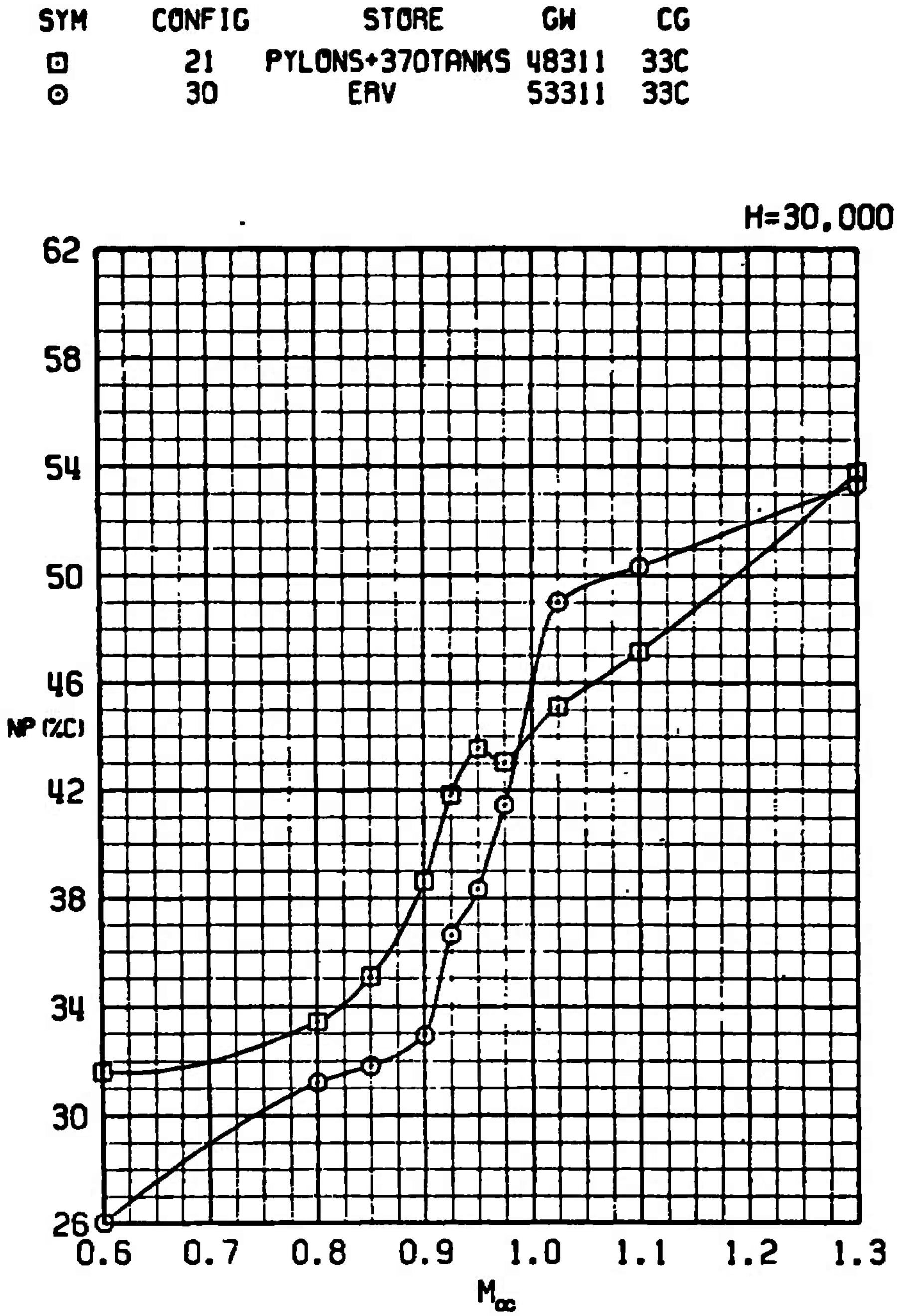

d. H = 30,000
Figure 41. Concluded.

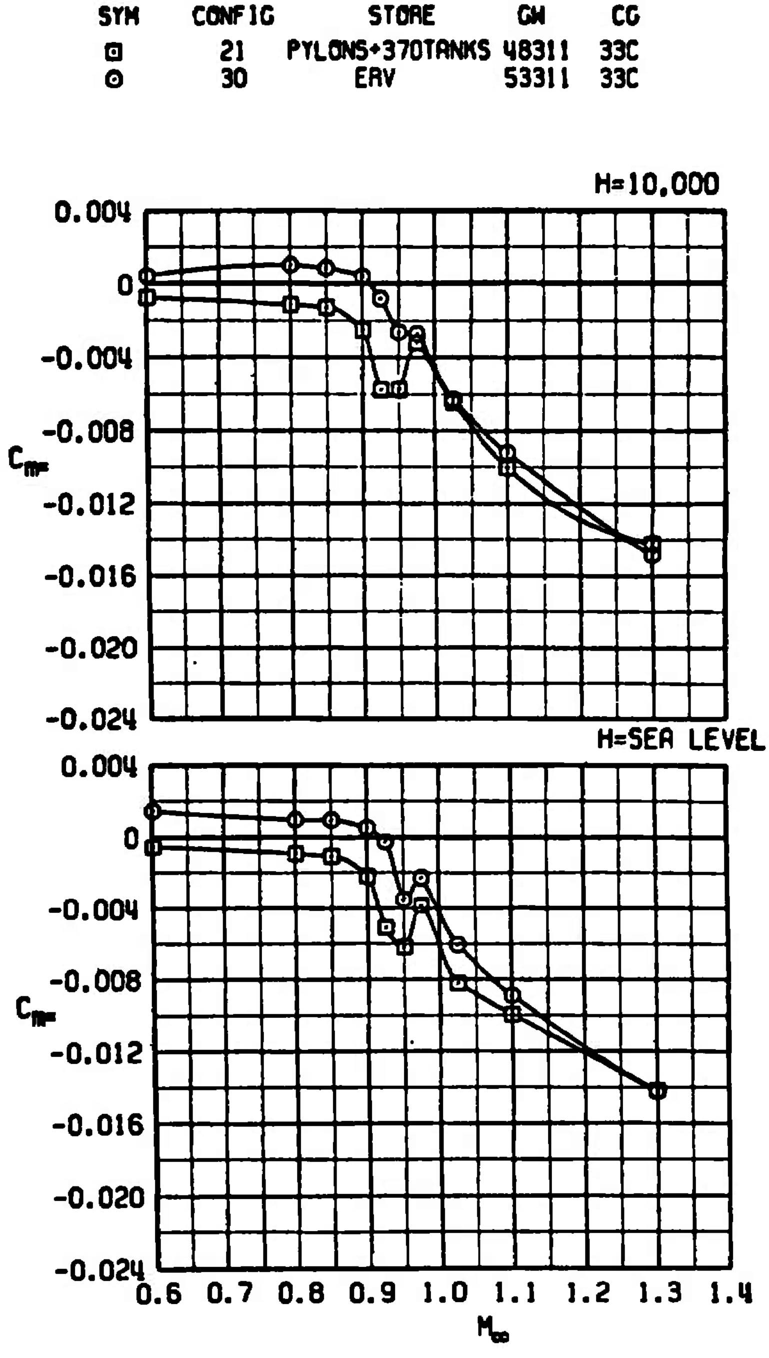

a. H = Sea level and 10,000

Figure 42. The effect of the ERV store on the slope of the pitching-moment coefficient versus angle-of-attack curve at trim.

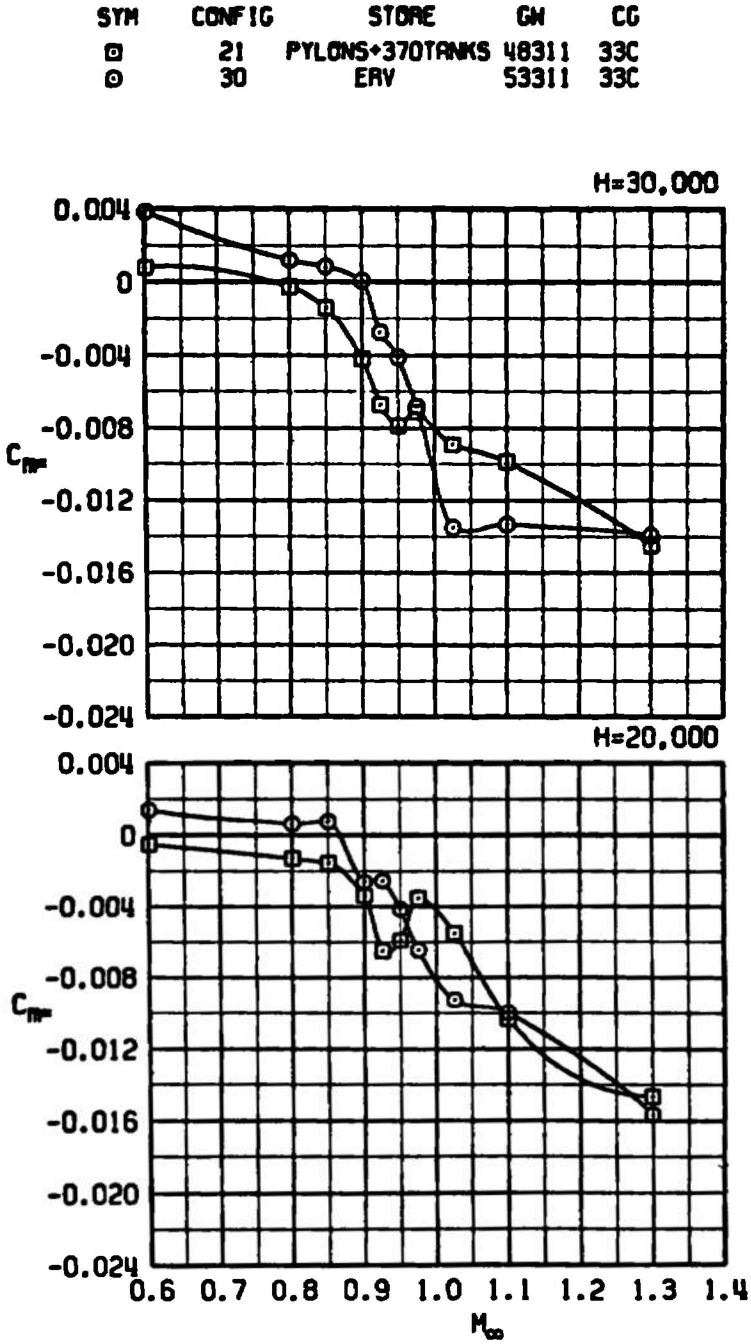

b. H = 20,000 and 30,000
Figure 42. Concluded.

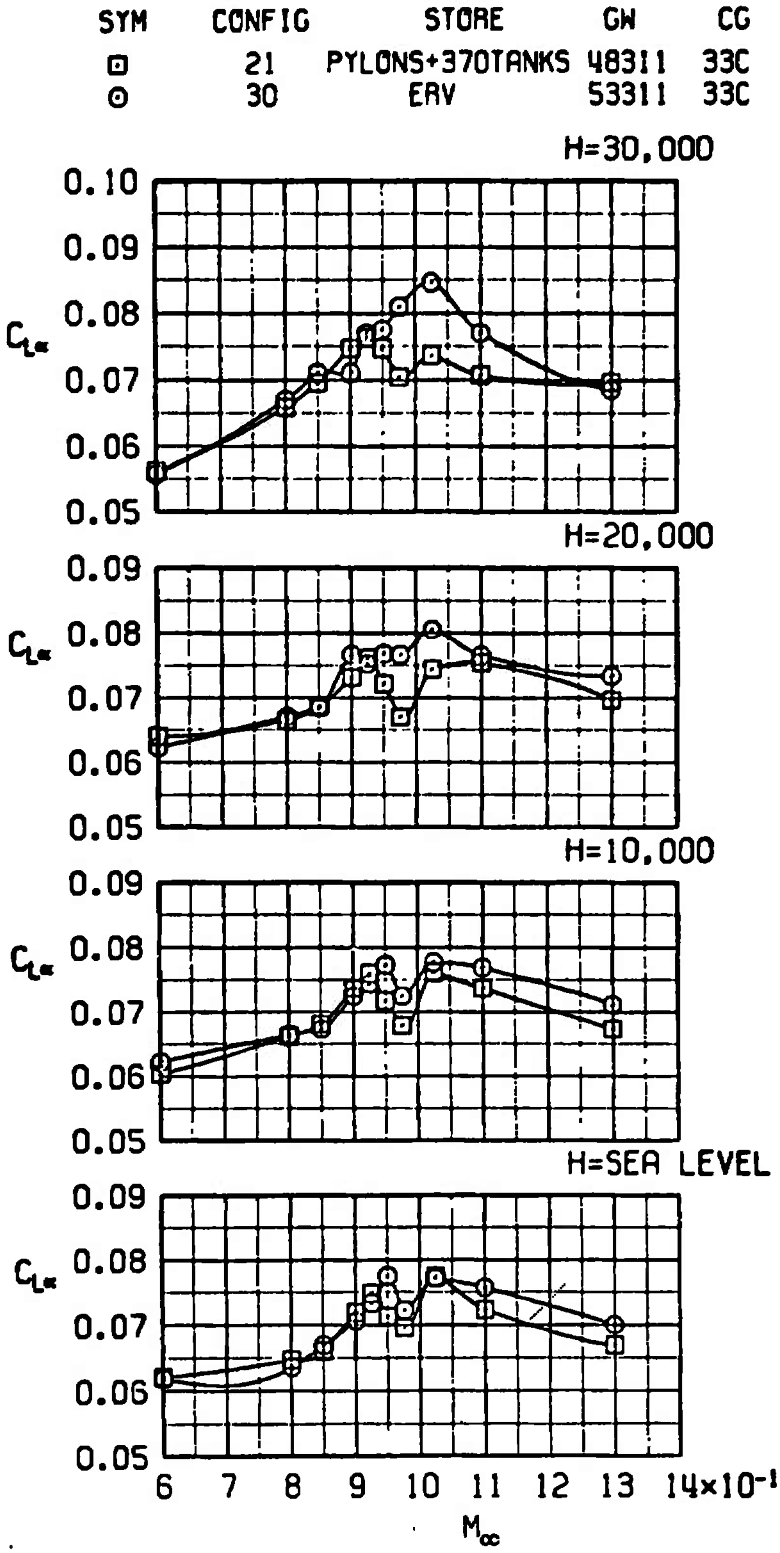

Figure 43. The effect of the ERV store on the lift-curve slope at trim.

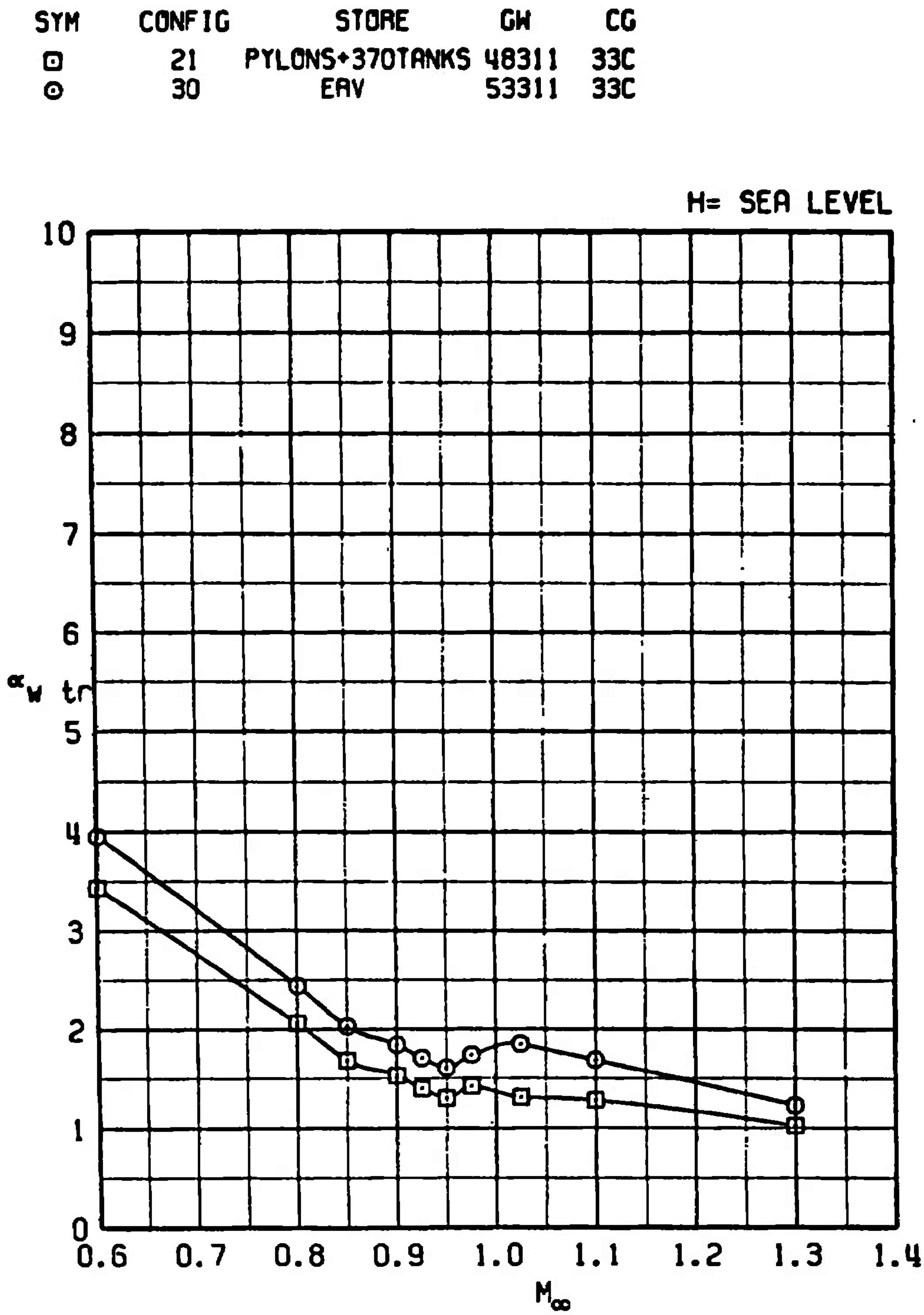

a. H = Sea level

Figure 44. The effect of the ERV store on the trim wing angle of attack.

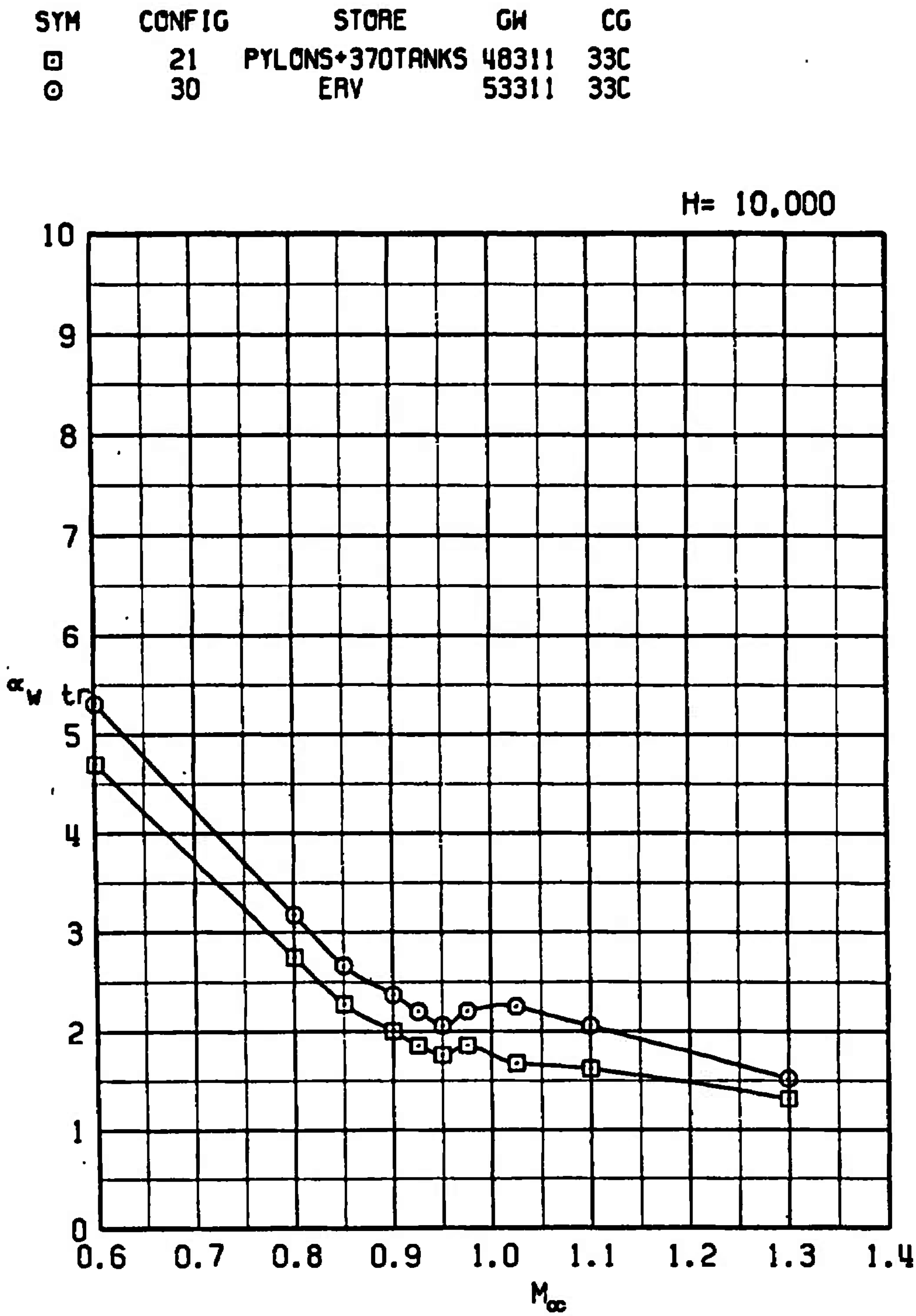

b. H = 10,000

Figure 44. Continued.

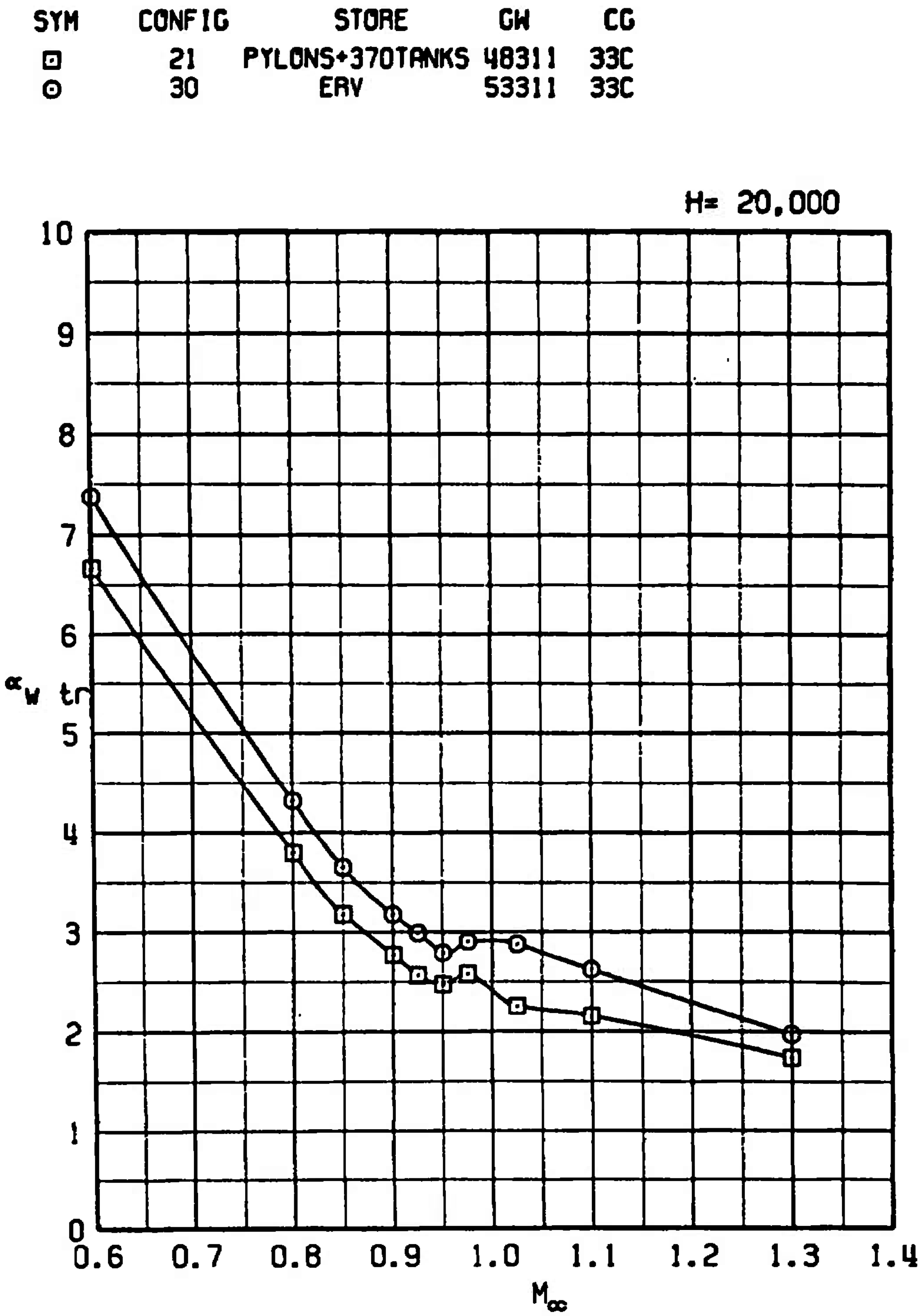

c. H = 20,000
Figure 44. Continued.

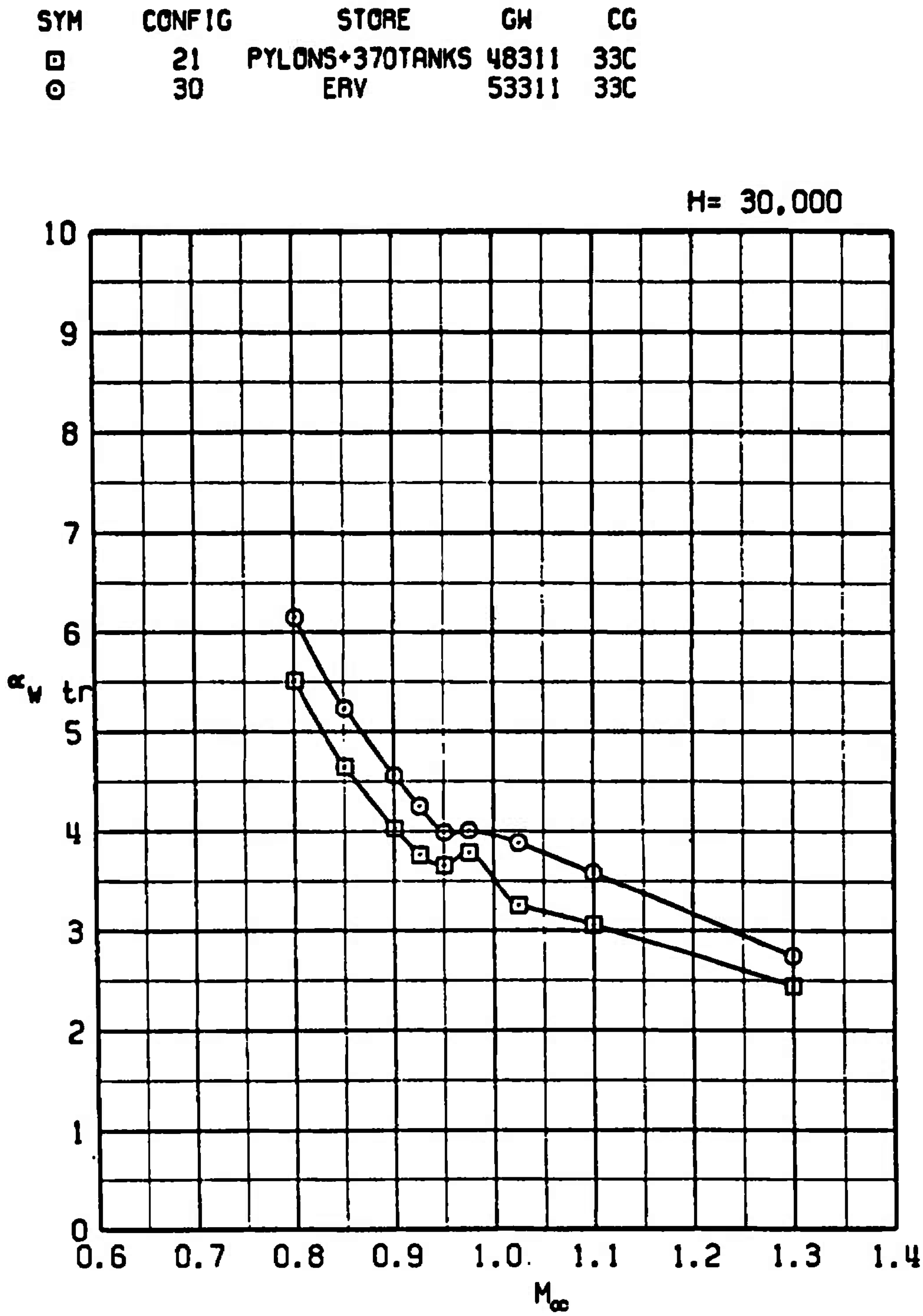

d. H = 30,000
Figure 44. Concluded.

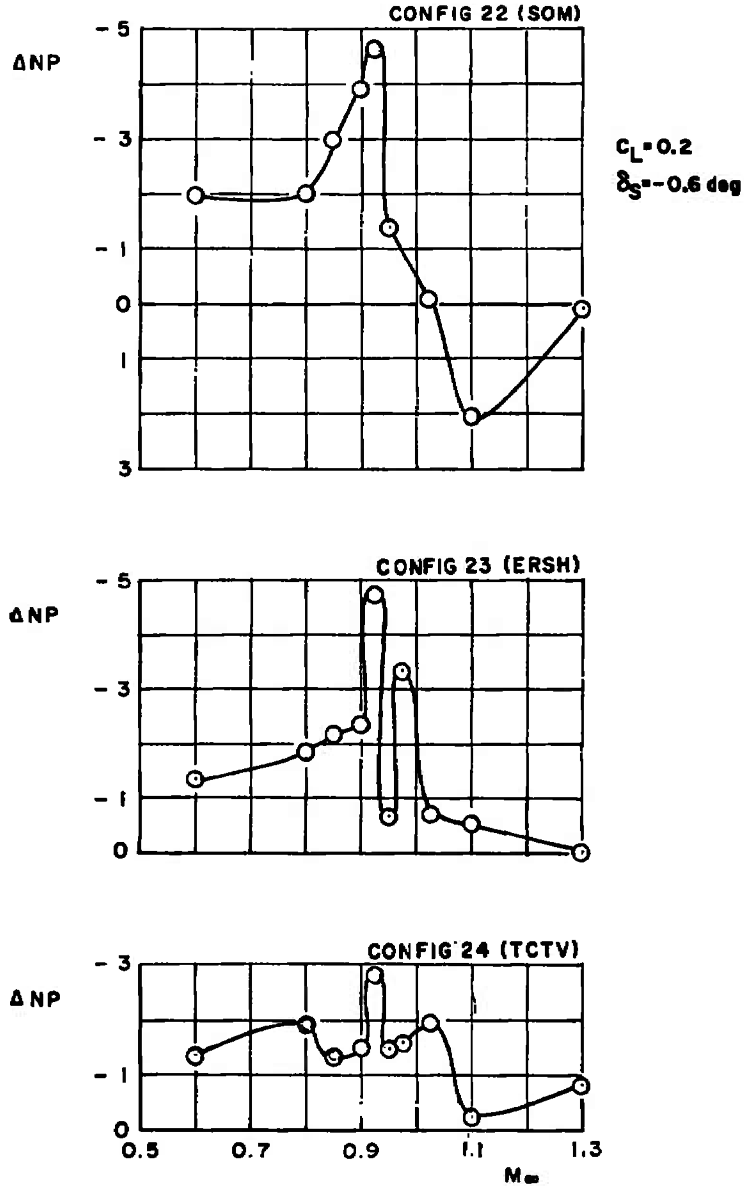

Figure 45. Incremental change in neutral-point location due to various external stores at a lift coefficient of 0.2.

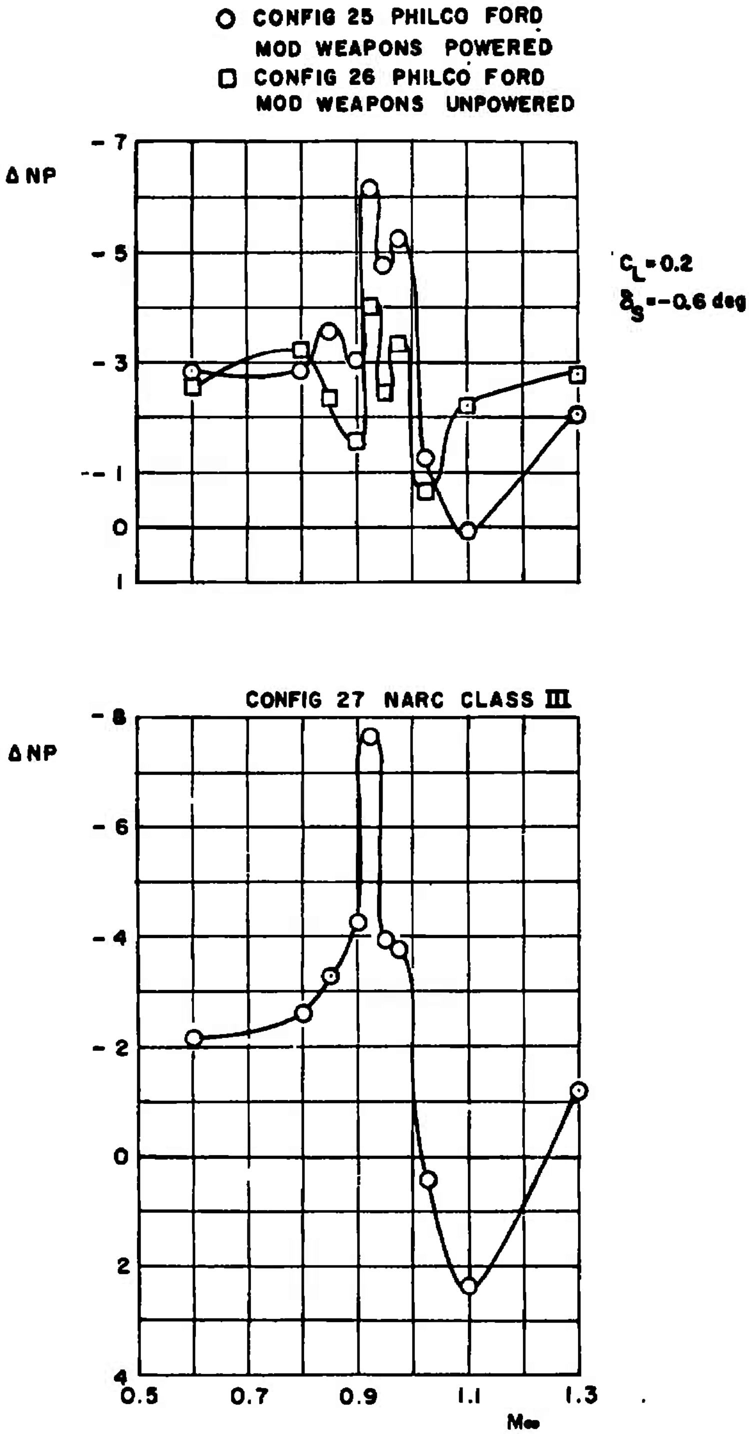

Figure 45. Continued.

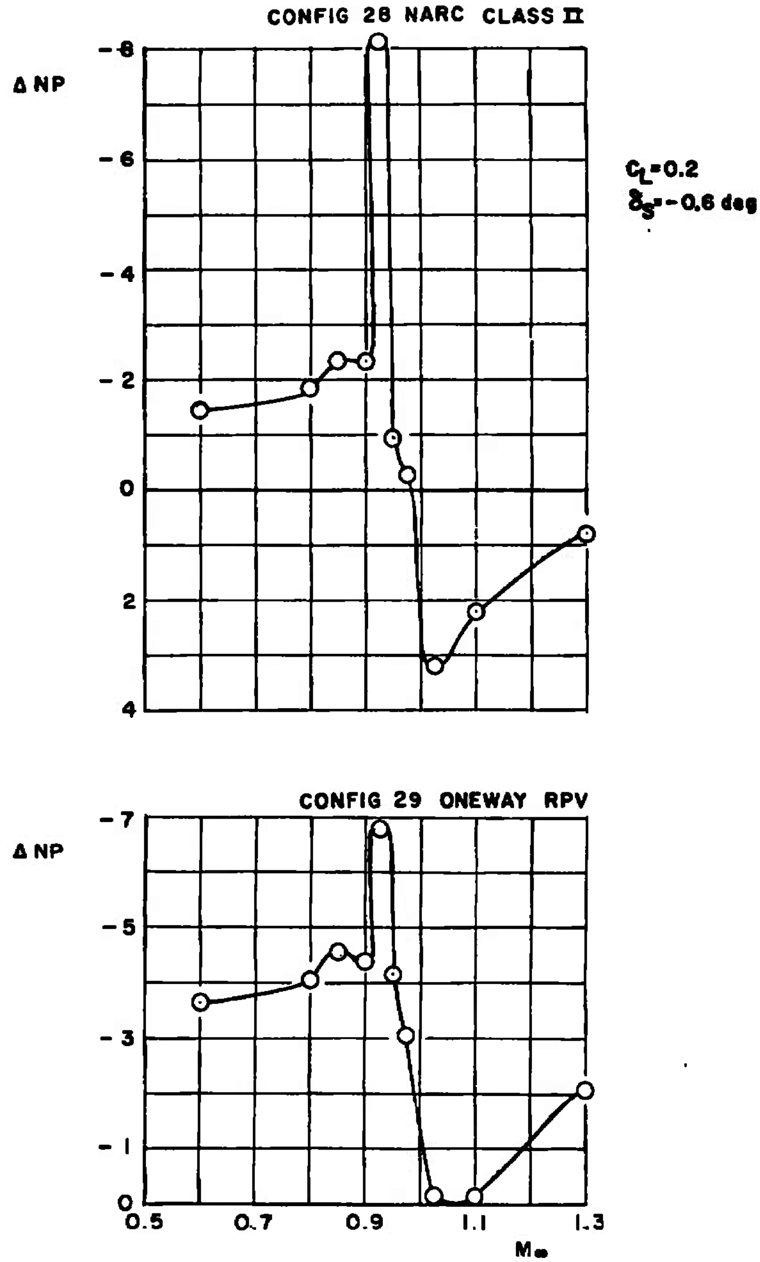

Figure 45. Continued.

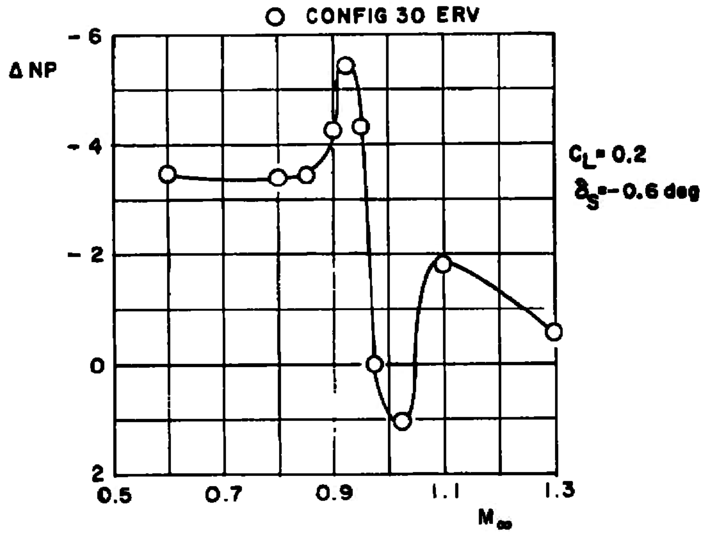

Figure 45. Concluded.

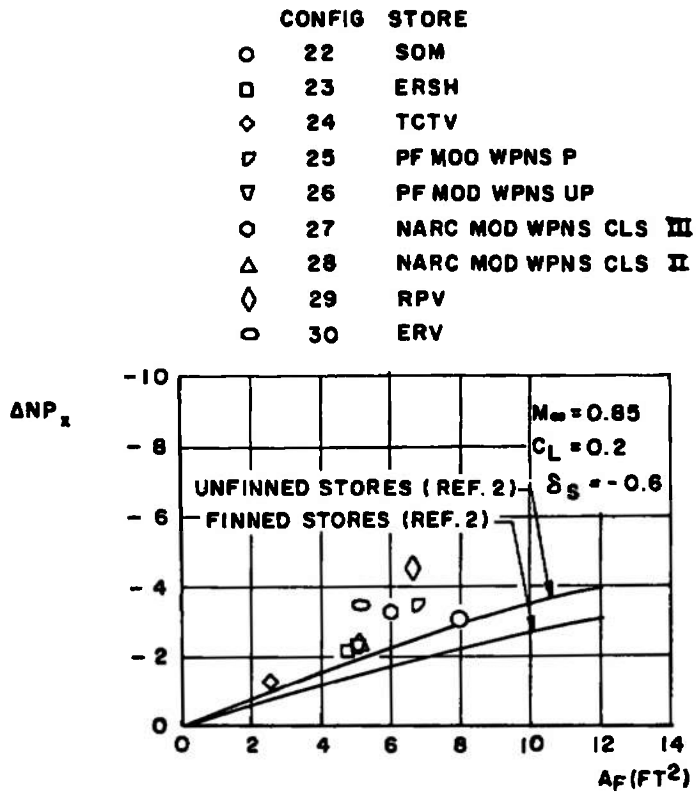

a. Wing-mounted store frontal area correlation

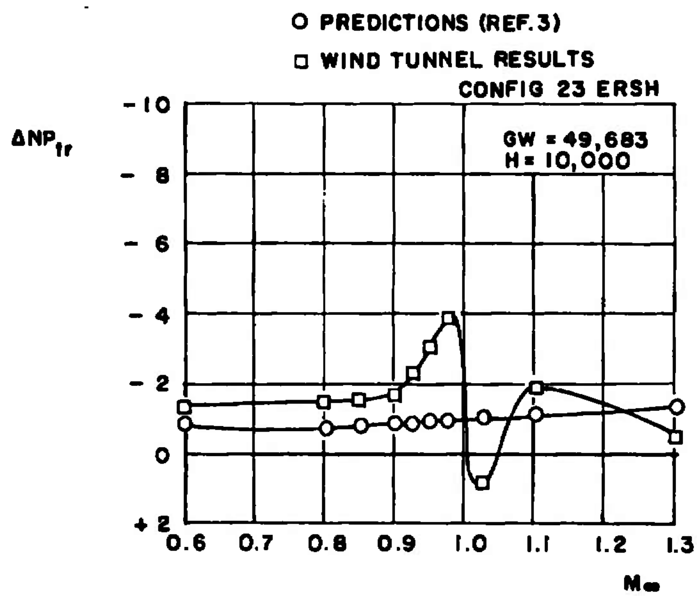

b. Generalized prediction technique of Ref. 3 (configuration 23)

Figure 46. Comparison of measured neutral-point shifts with results from existing prediction techniques.

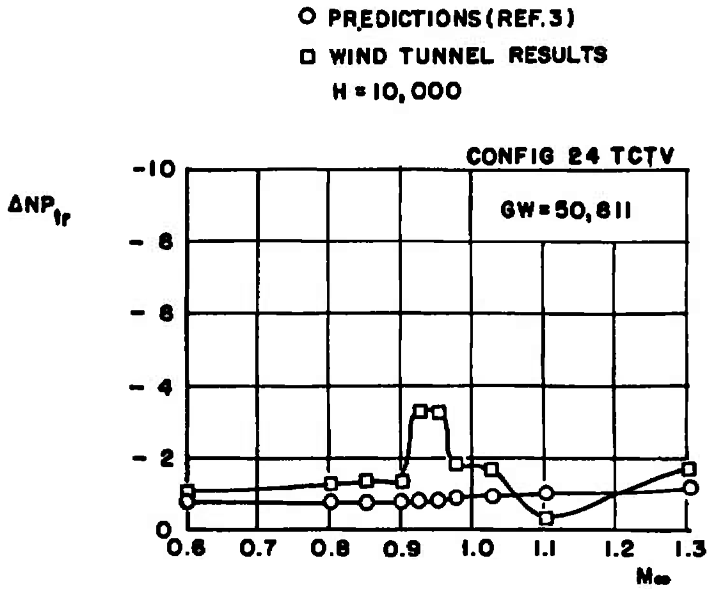

c. Generalized prediction technique of Ref. 3 (configuration 24)

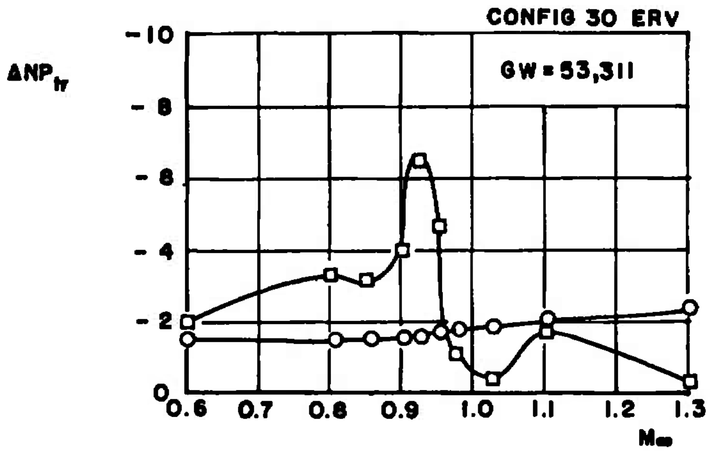

d. Generalized prediction technique of Ref. 3 (configuration 30)
Figure 46. Concluded.

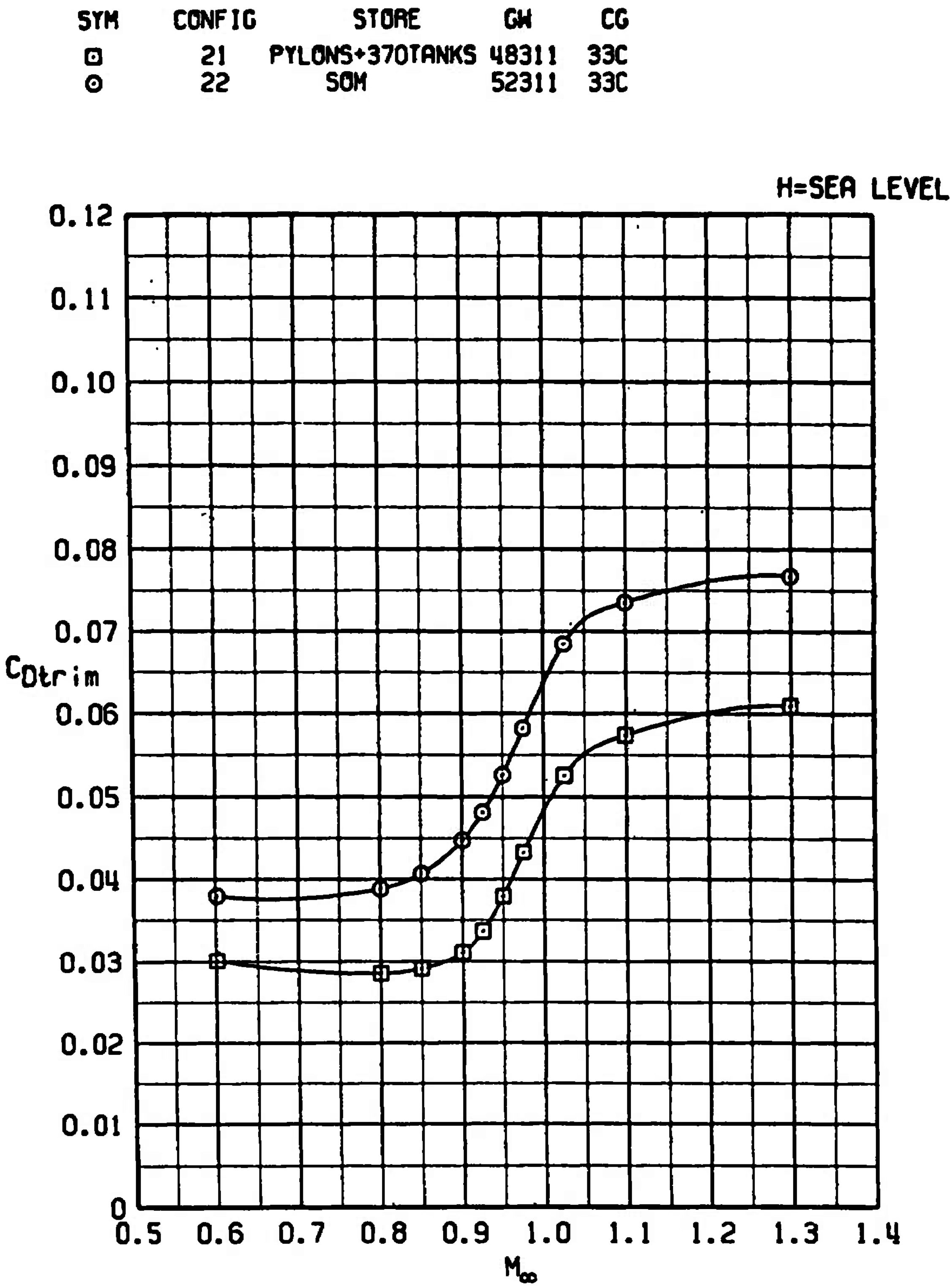

a. H = Sea level

Figure 47. The effect of the SOM store on trim drag.

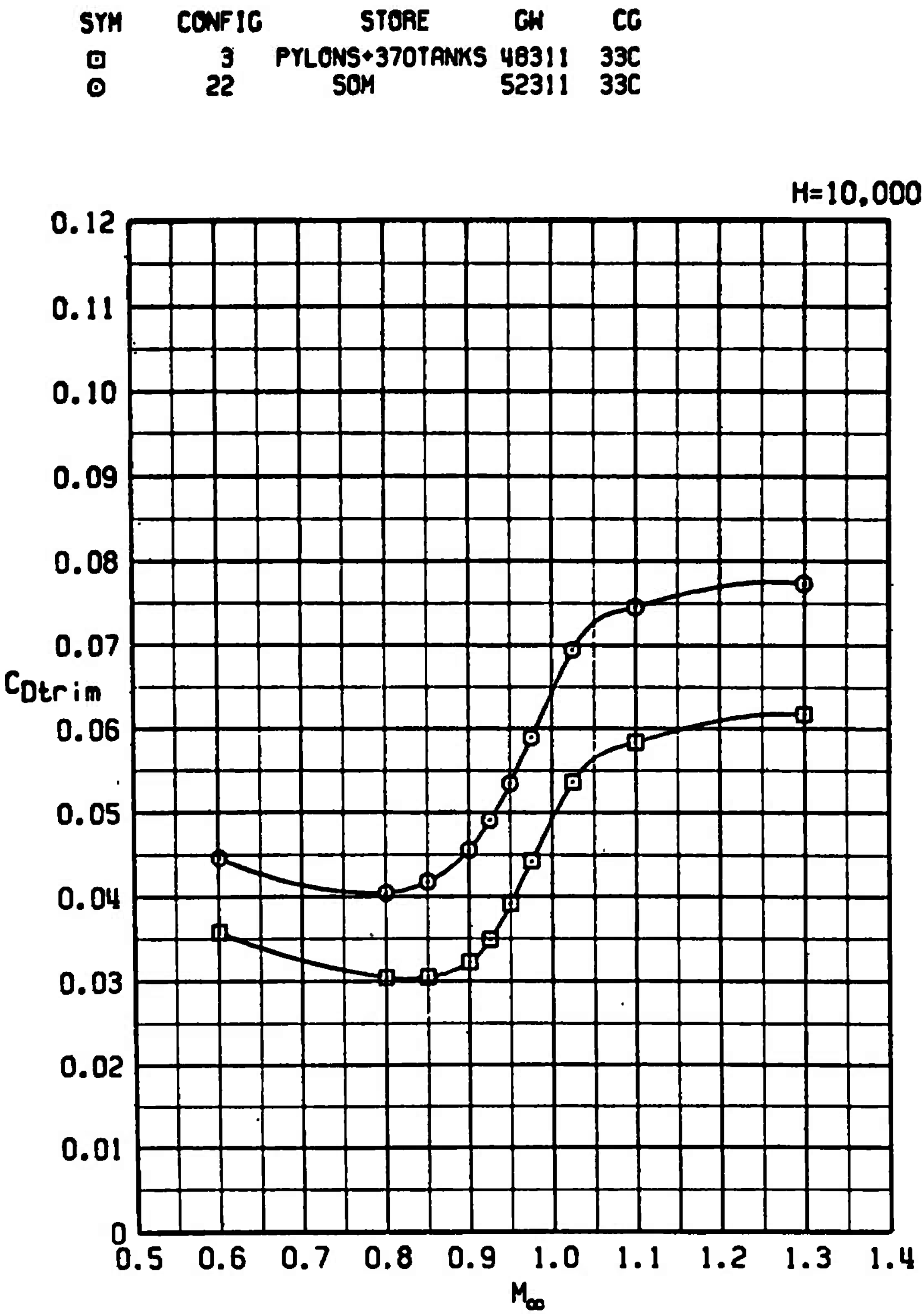

b. H = 10,000

Figure 47. Continued.

SYM	CONFIG	STORE	GW	CG
⊡	21	PYLONS+370TANKS	48311	33C
⊙	22	SOM	52311	33C

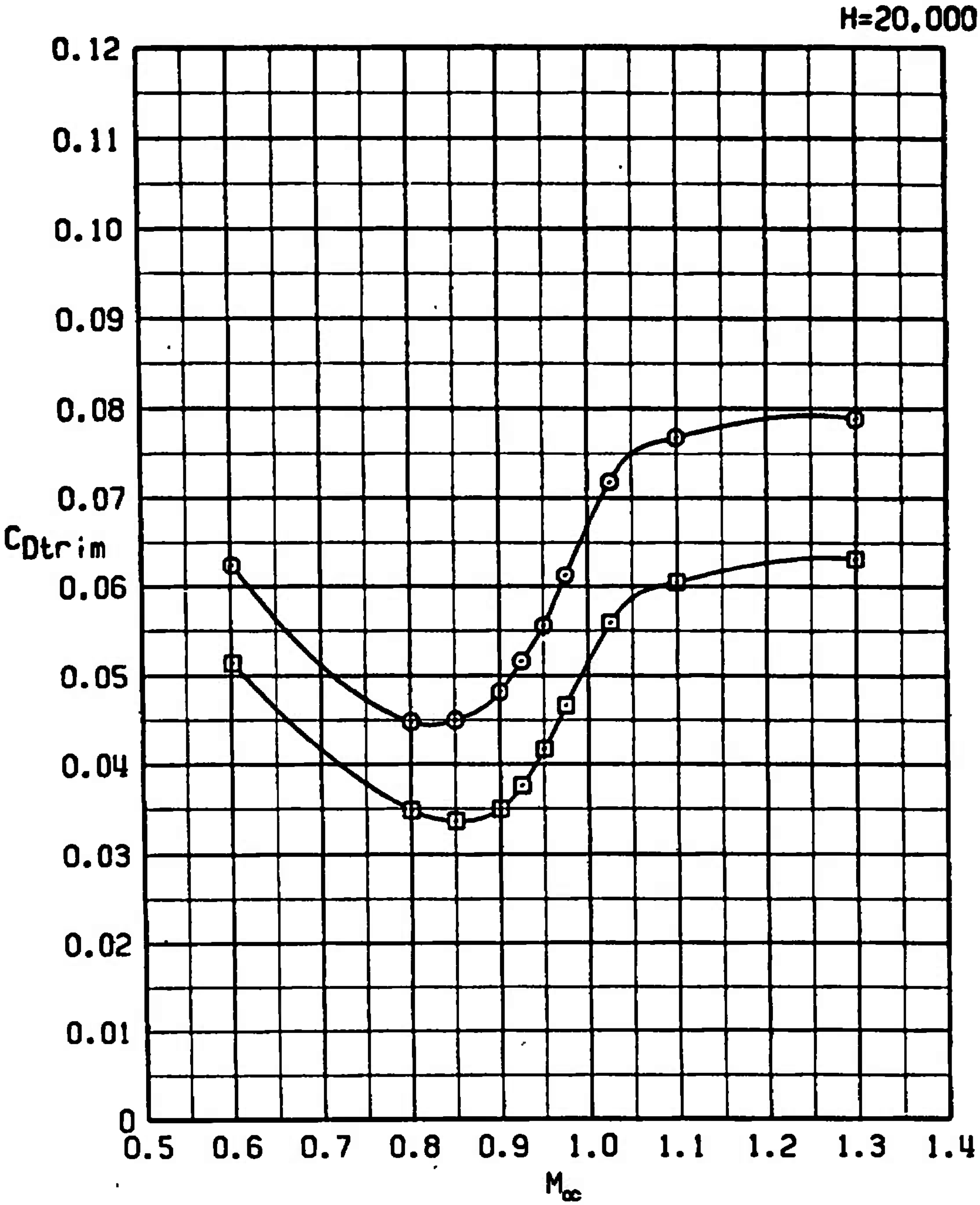

c. H = 20,000
Figure 47. Continued.

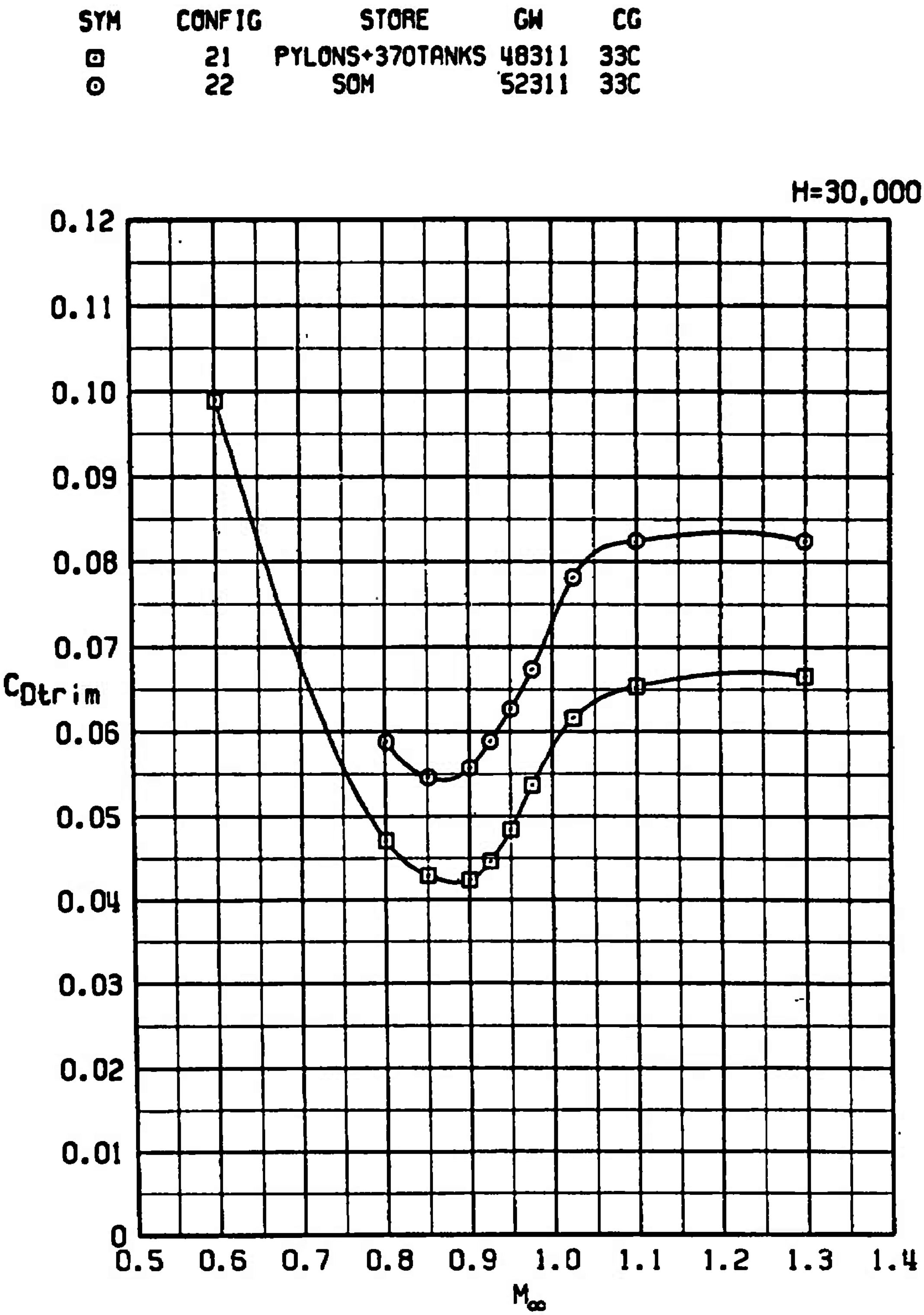

d. H = 30,000

Figure 47. Concluded.

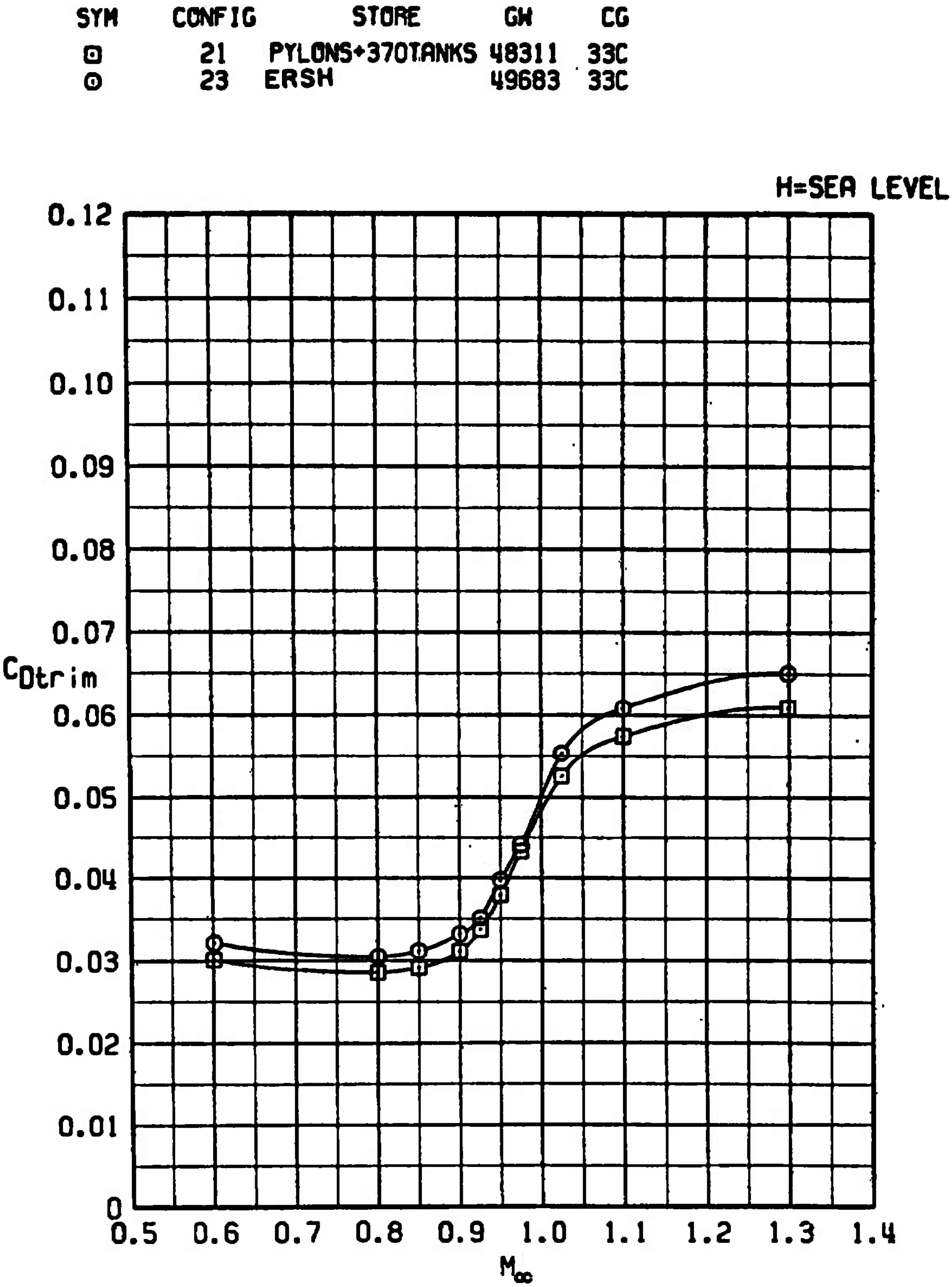

a. H = Sea level

Figure 48. The effect of the Stubby HOBOS store on trim drag.

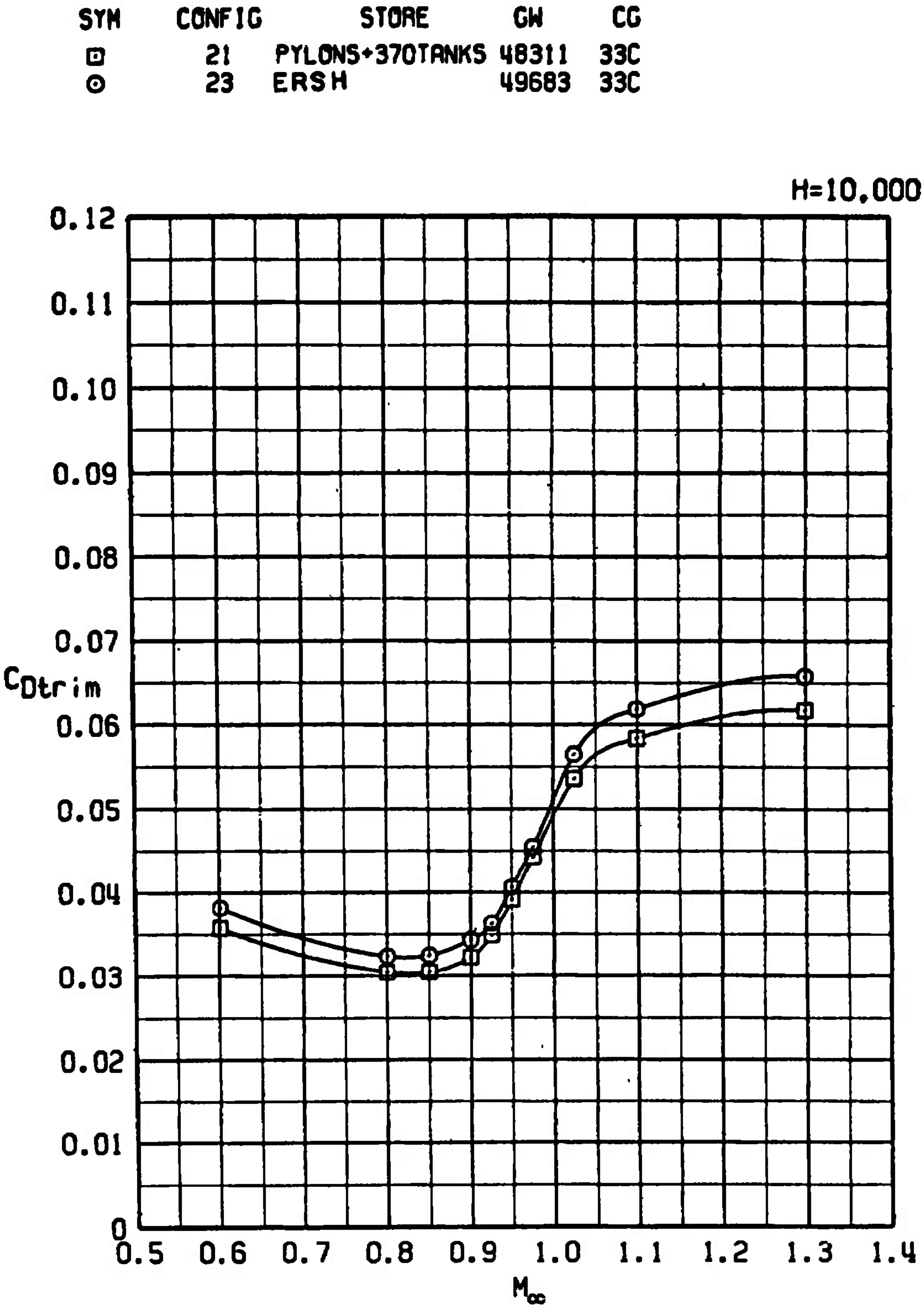

b. H = 10,000

Figure 48. Continued.

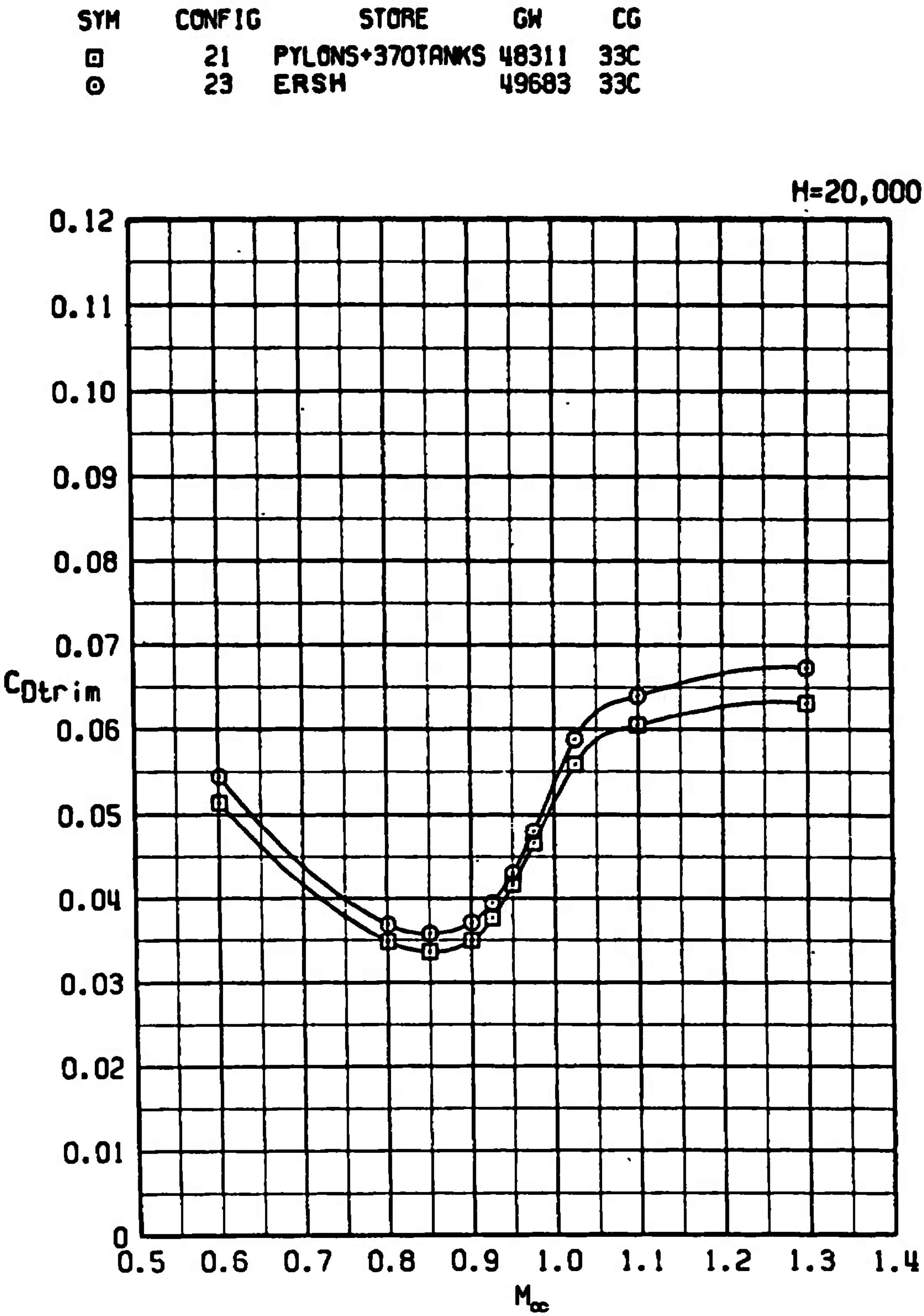

c. H = 20,000

Figure 48. Continued.

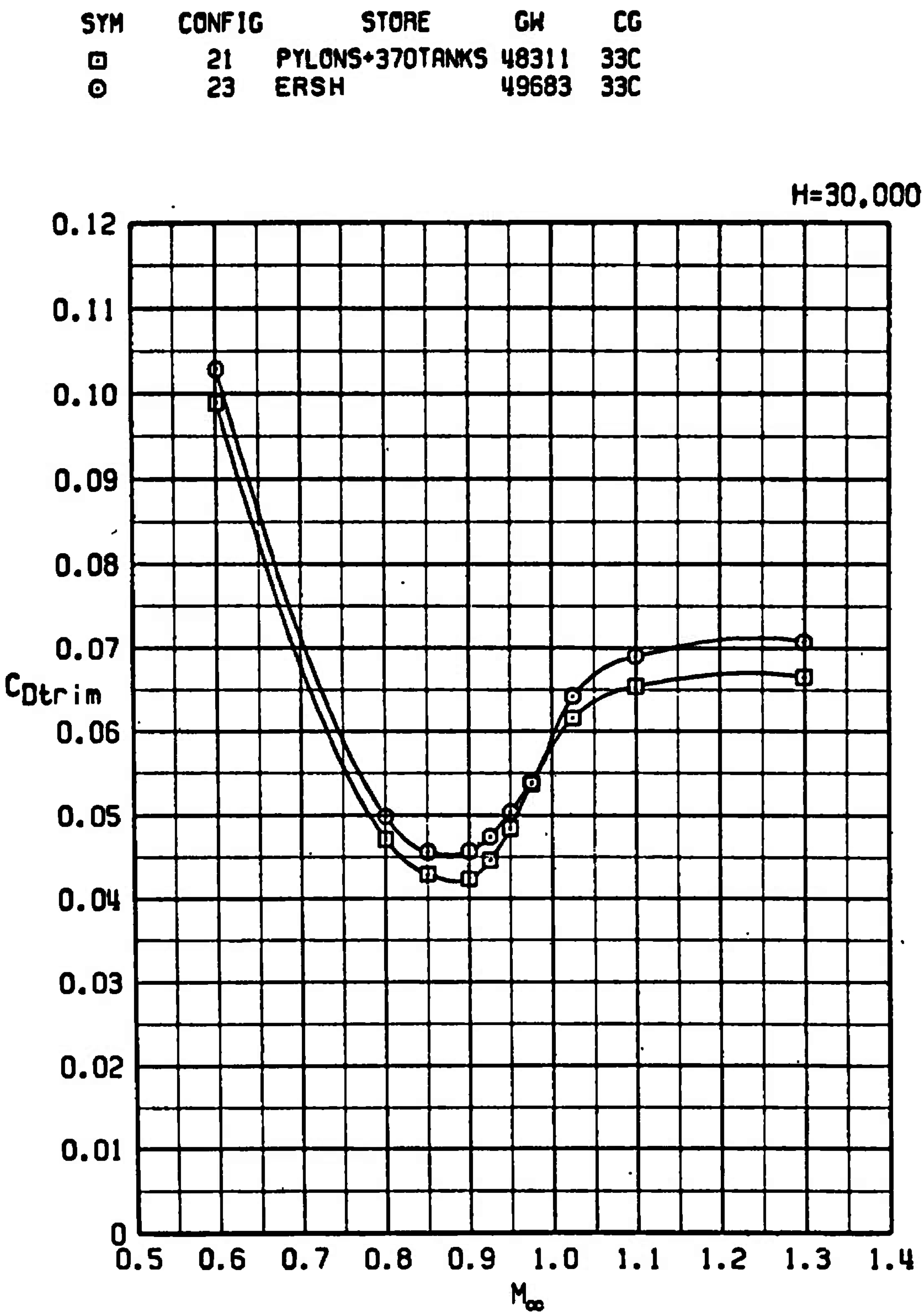

d. H = 30,000

Figure 48. Concluded.

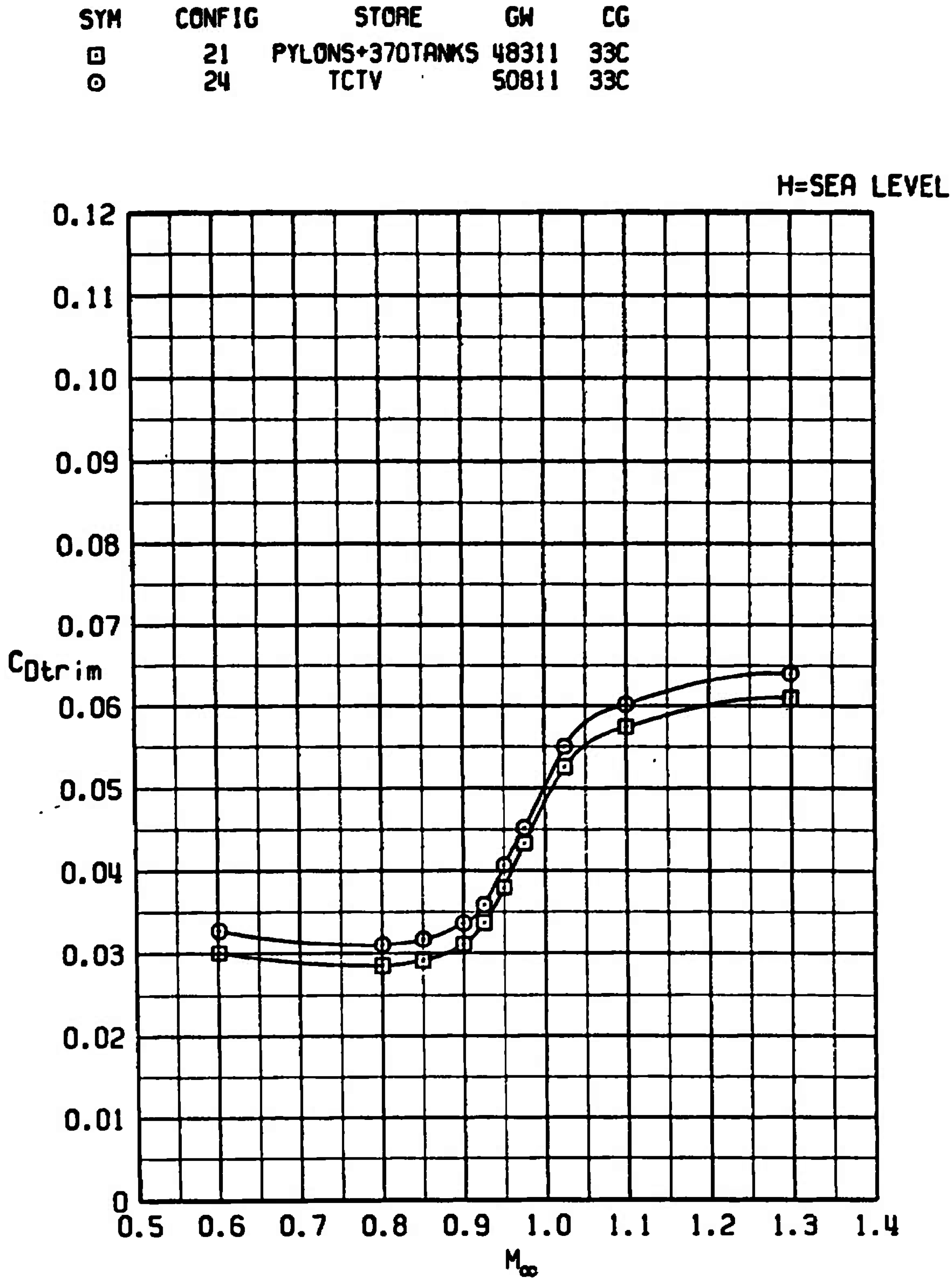

a. H = Sea level

Figure 49. The effect of the TCTV store on trim drag.

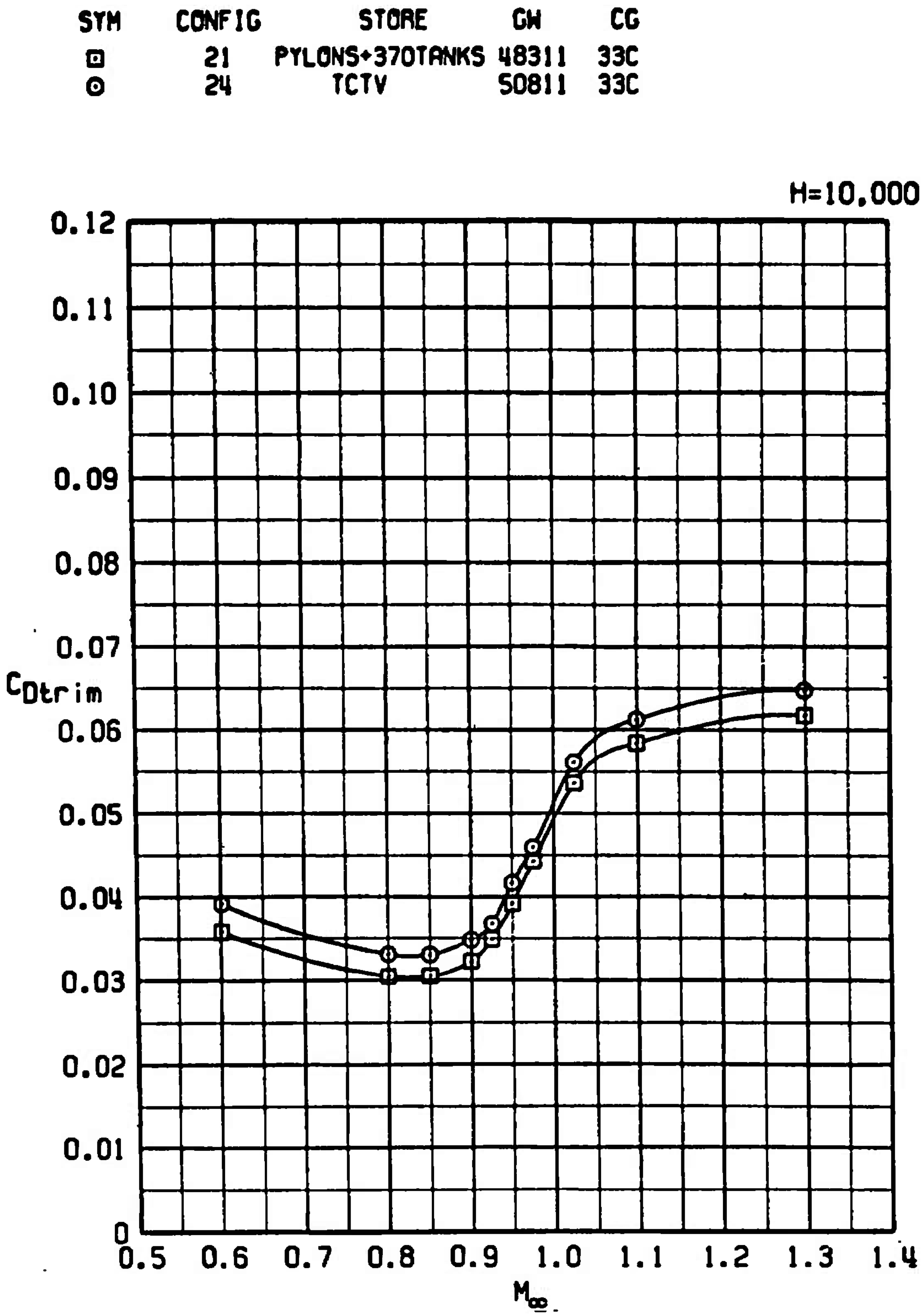

b. H = 10,000
Figure 49. Continued.

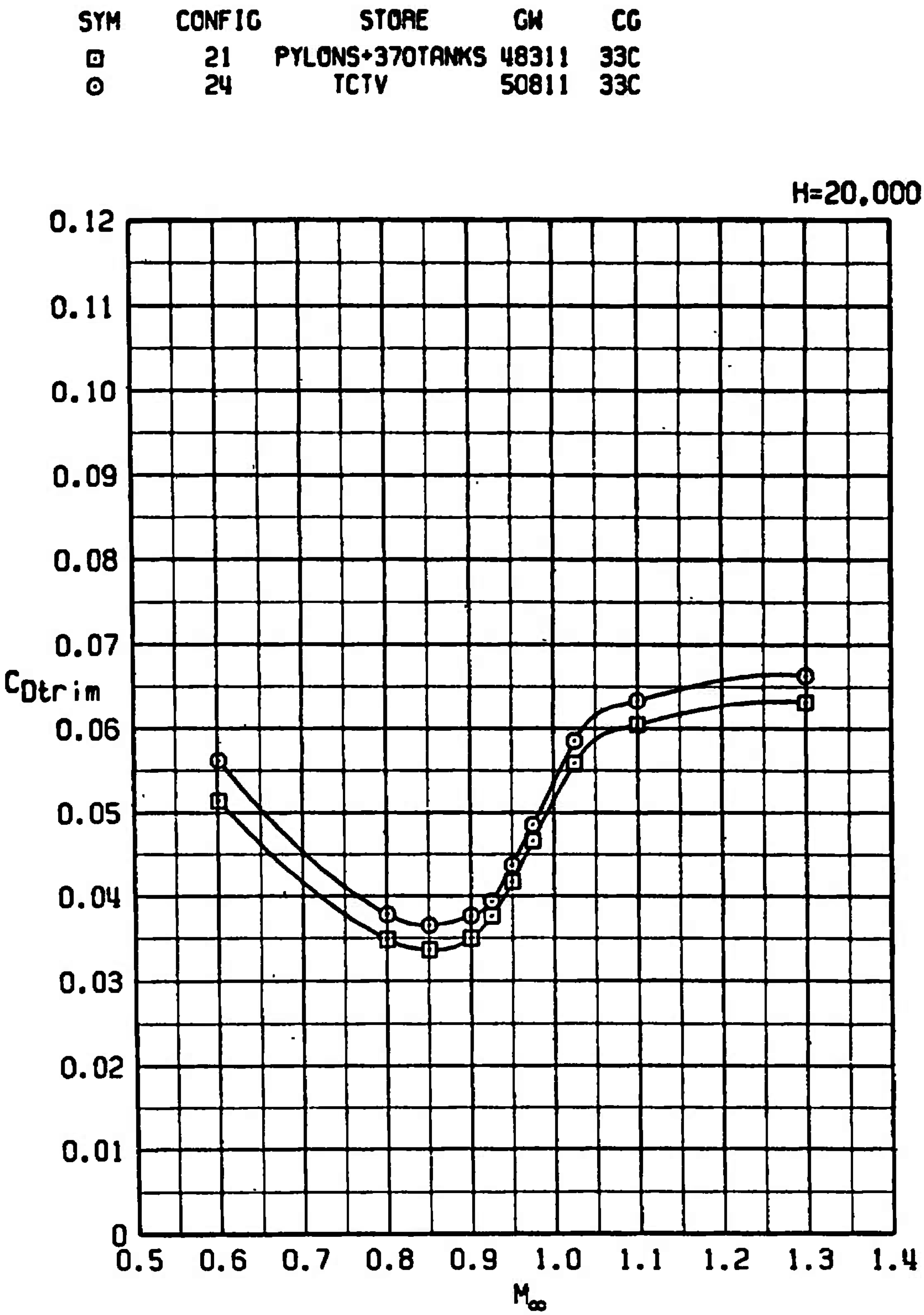

c. H = 20,000

Figure 49. Continued.

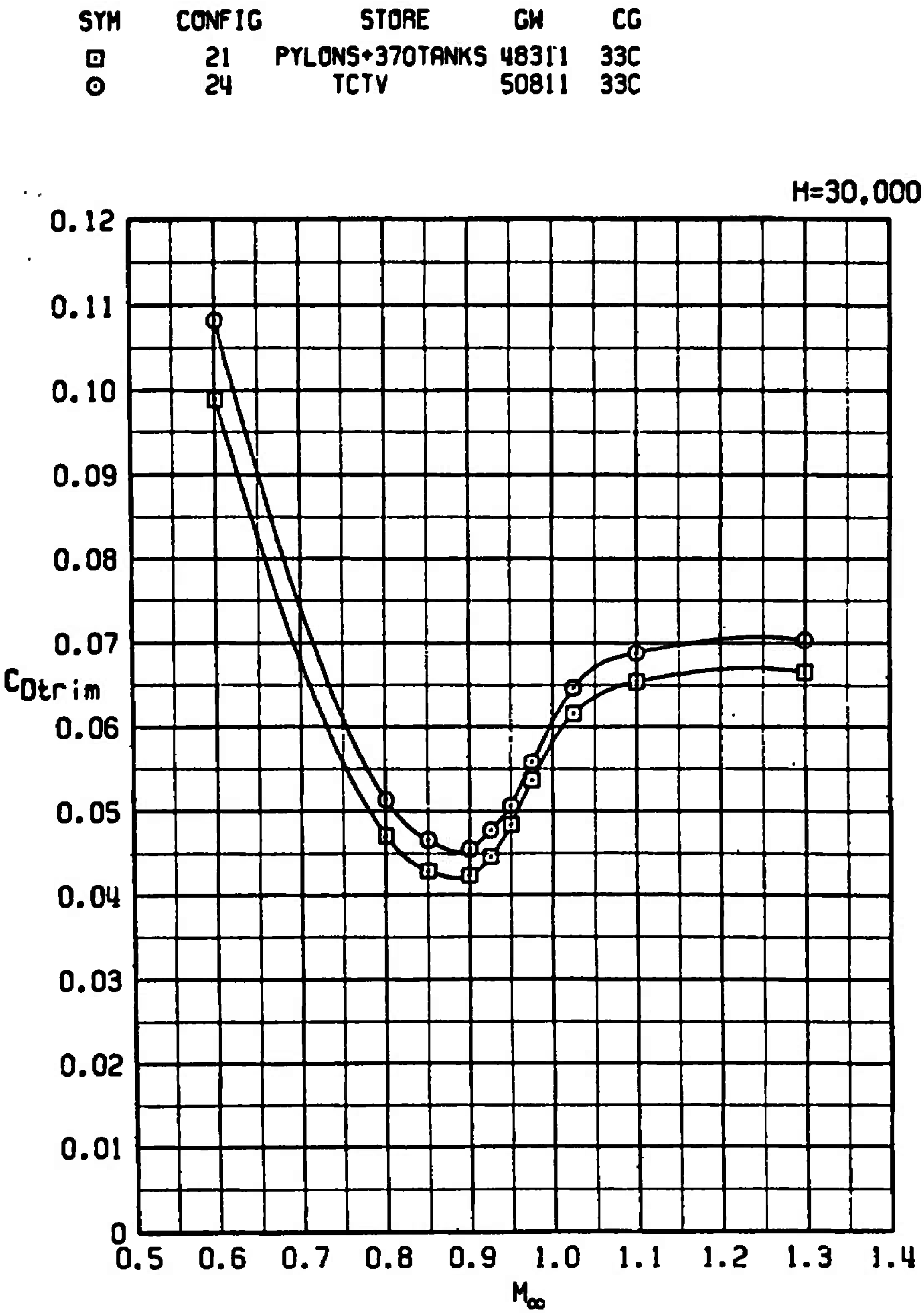

d. H = 30,000

Figure 49. Concluded.

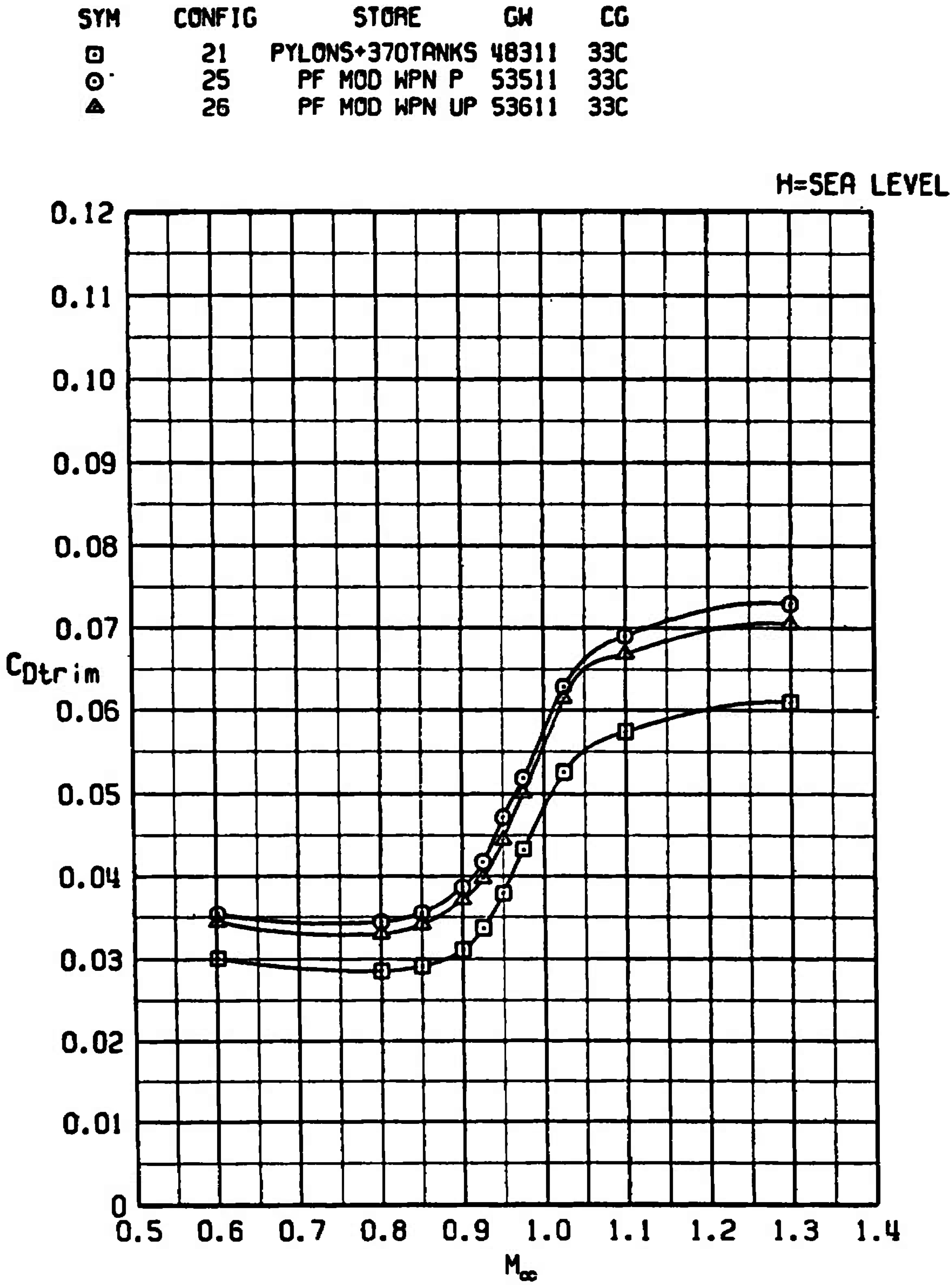

a. H = Sea level

Figure 50. The effect of the PF Modular Weapons stores on trim drag.

SYM	CONFIG	STORE	GW	CG
⊡	21	PYLONS+370TANKS	48311	33C
⊙	25	PF MOD WPN P	53511	33C
▲	26	PF MOD WPN UP	53611	33C

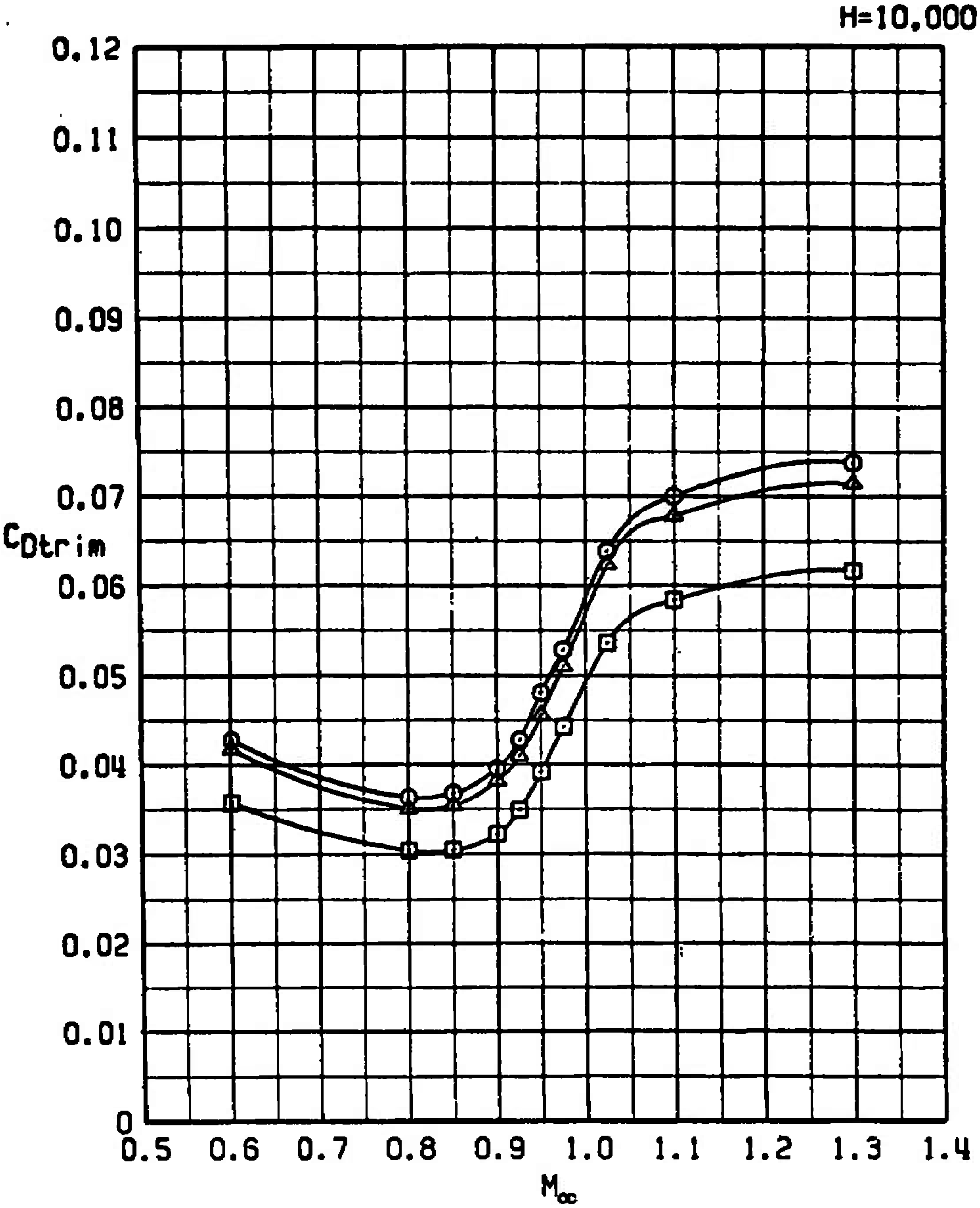

b. H = 10,000
Figure 50. Continued.

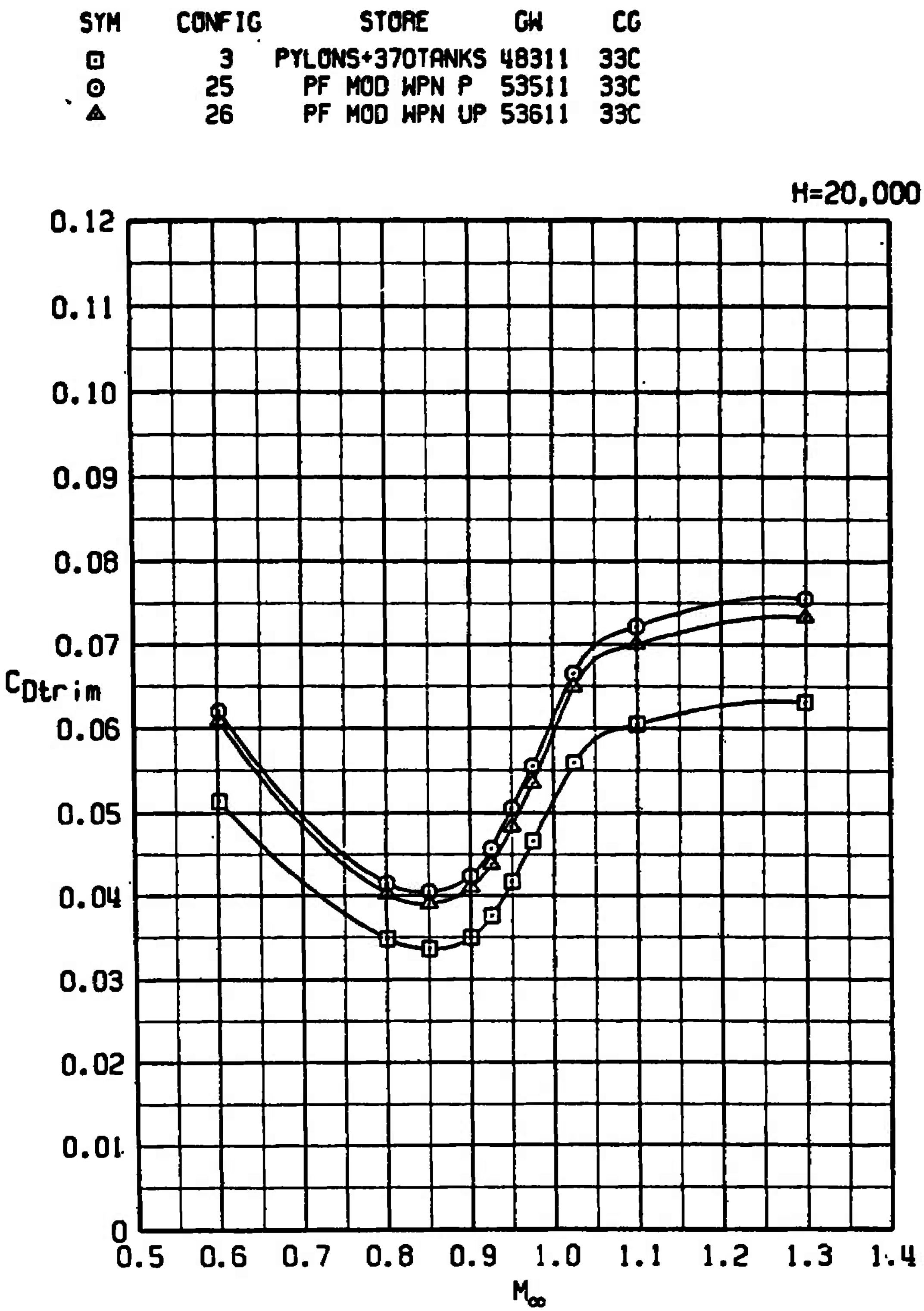

c. H = 20,000
Figure 50. Continued.

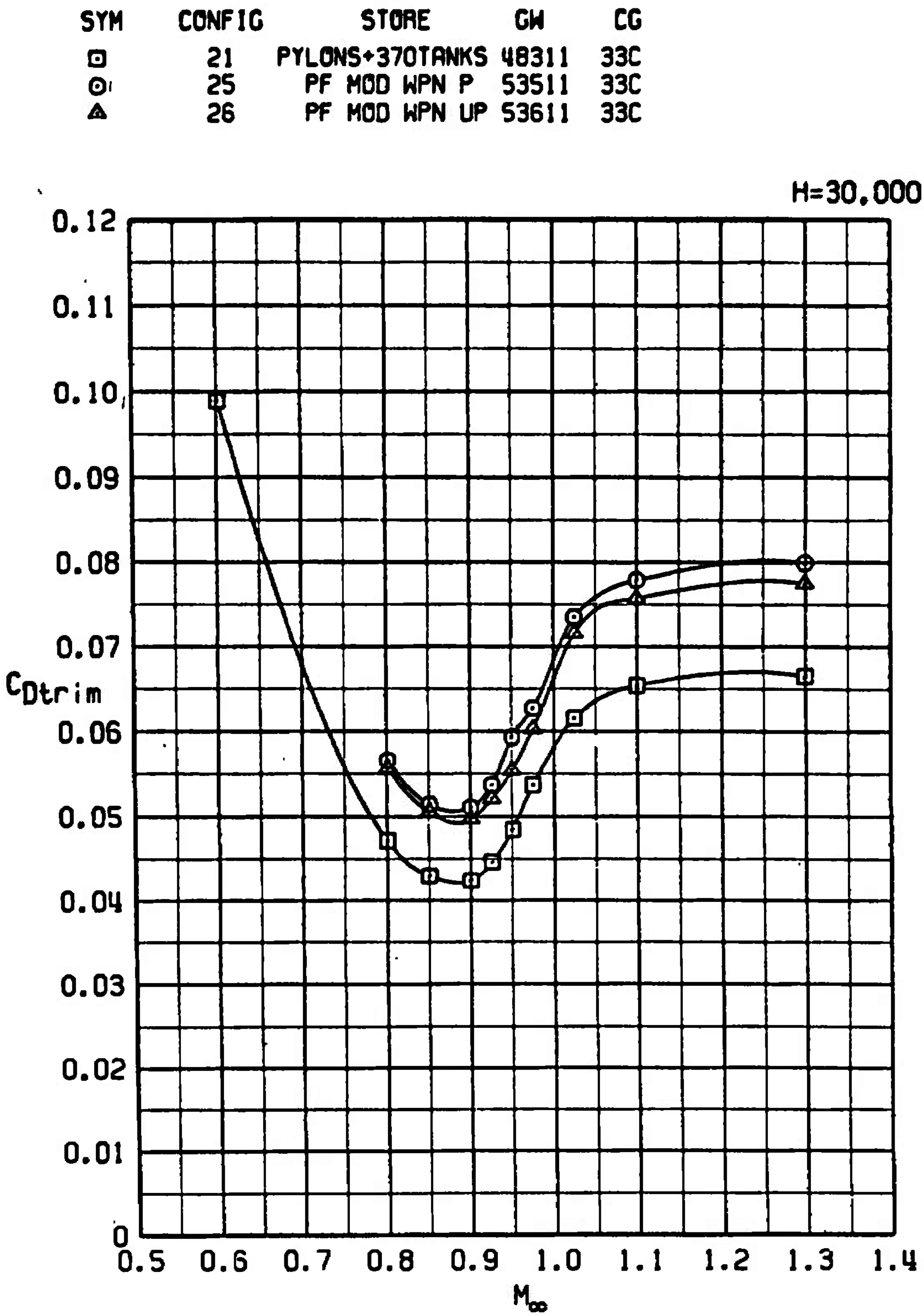

d. H = 30,000
Figure 50. Concluded.

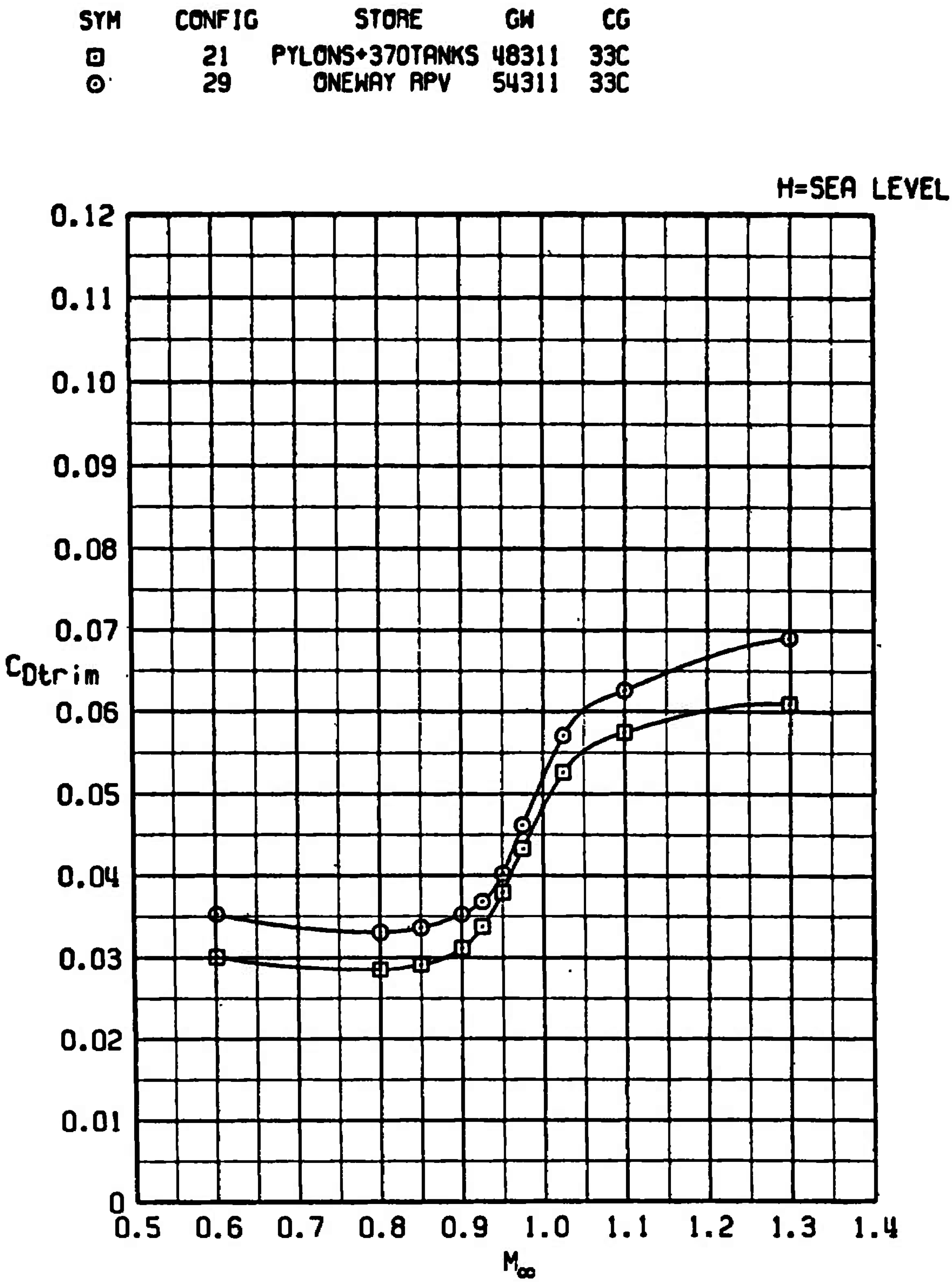

a. H = Sea level

Figure 51. The effect of the Oneway RPV store on trim drag.

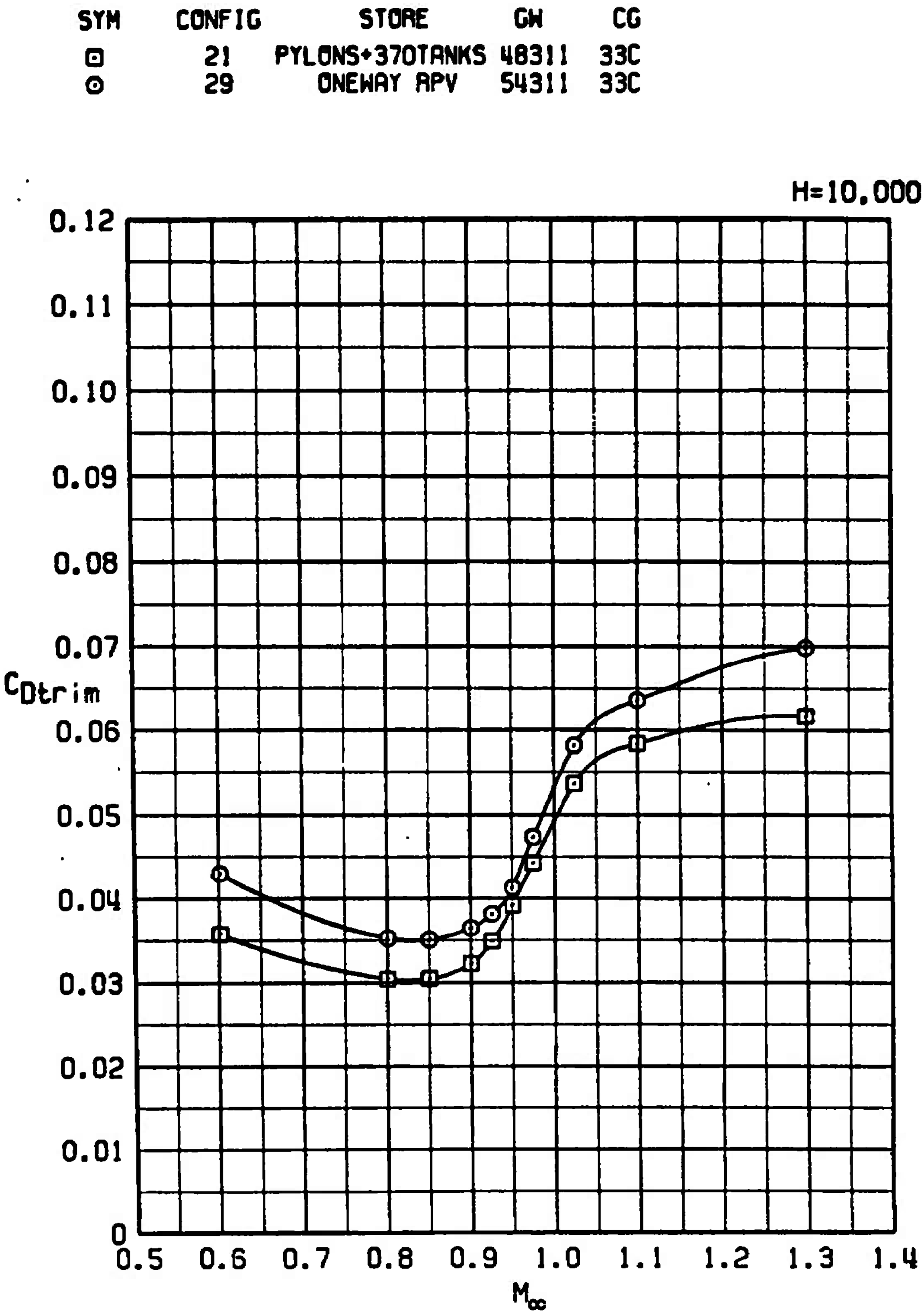

b. H = 10,000
Figure 51. Continued.

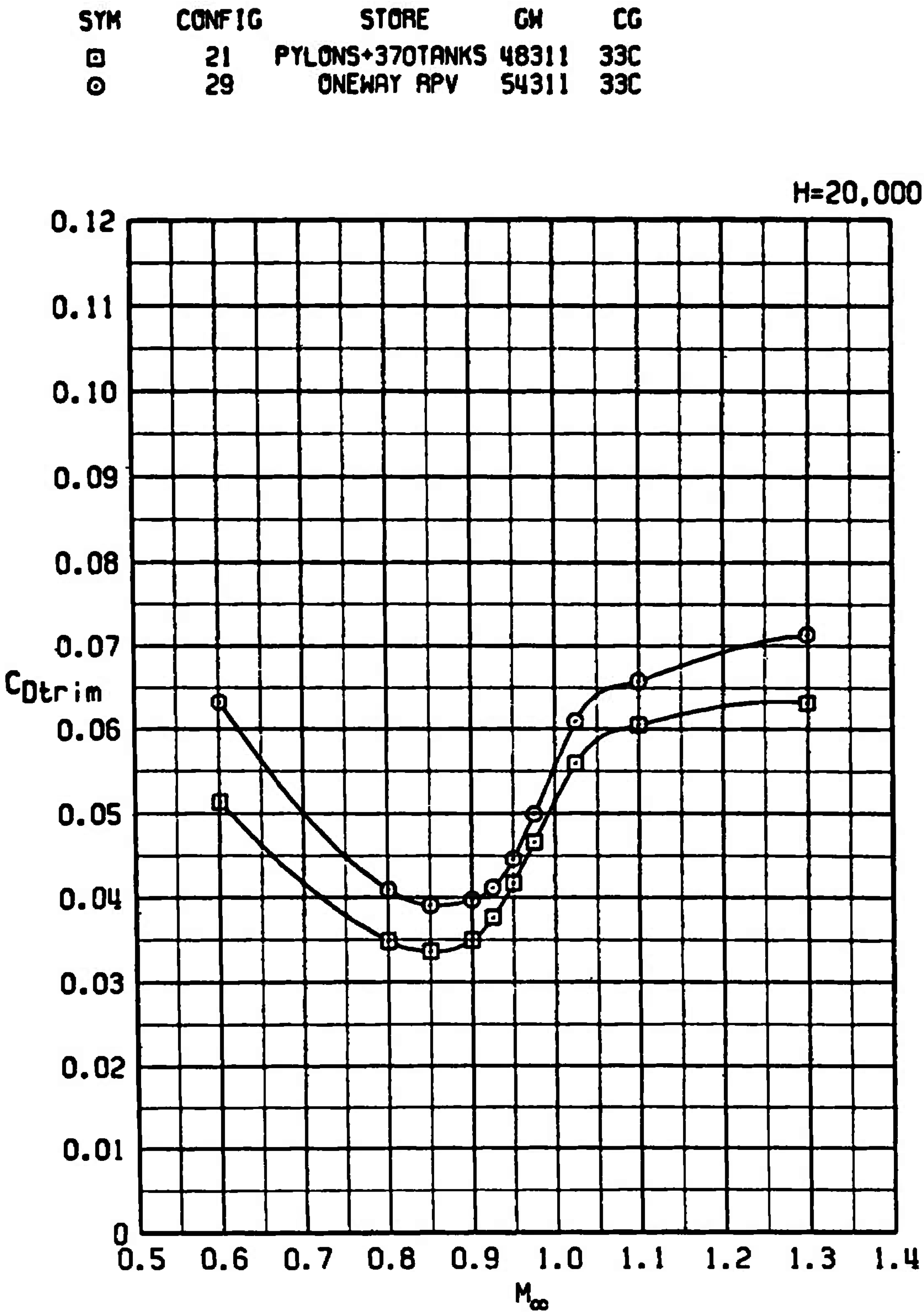

c. H = 20,000
Figure 51. Continued.

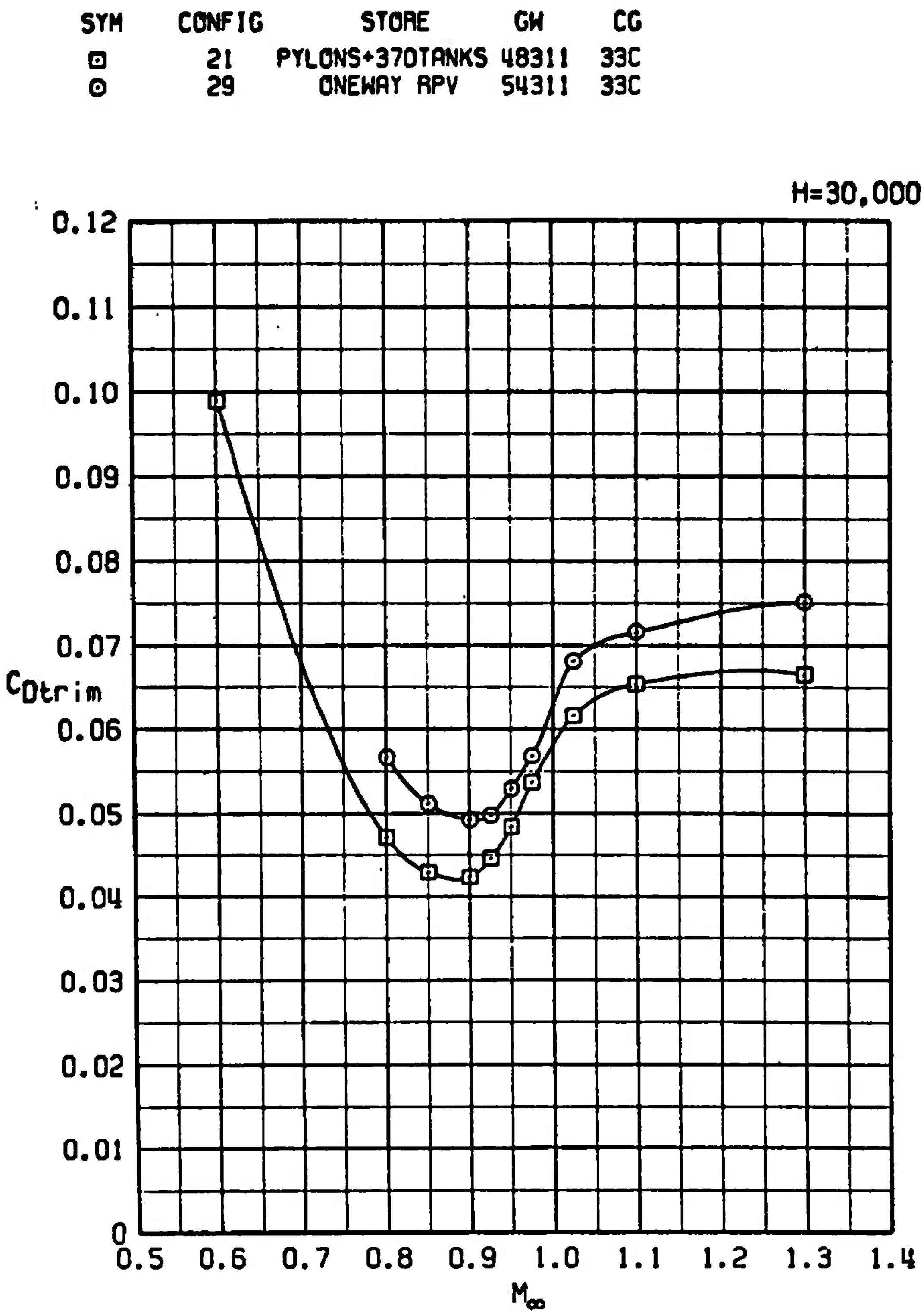

d. H = 30,000

Figure 51. Concluded.

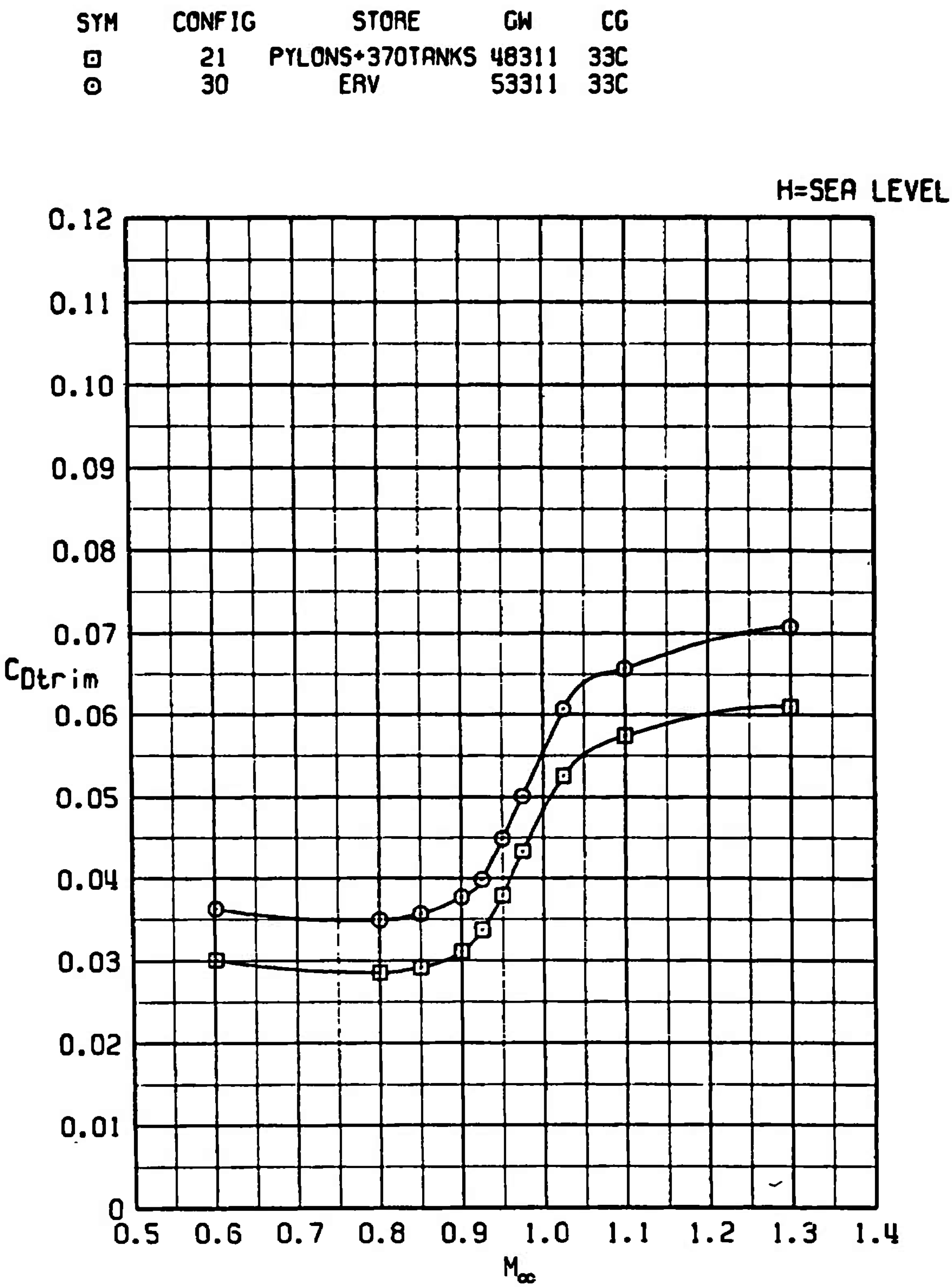

a. H = Sea level

Figure 52. The effect of the ERV store on trim drag.

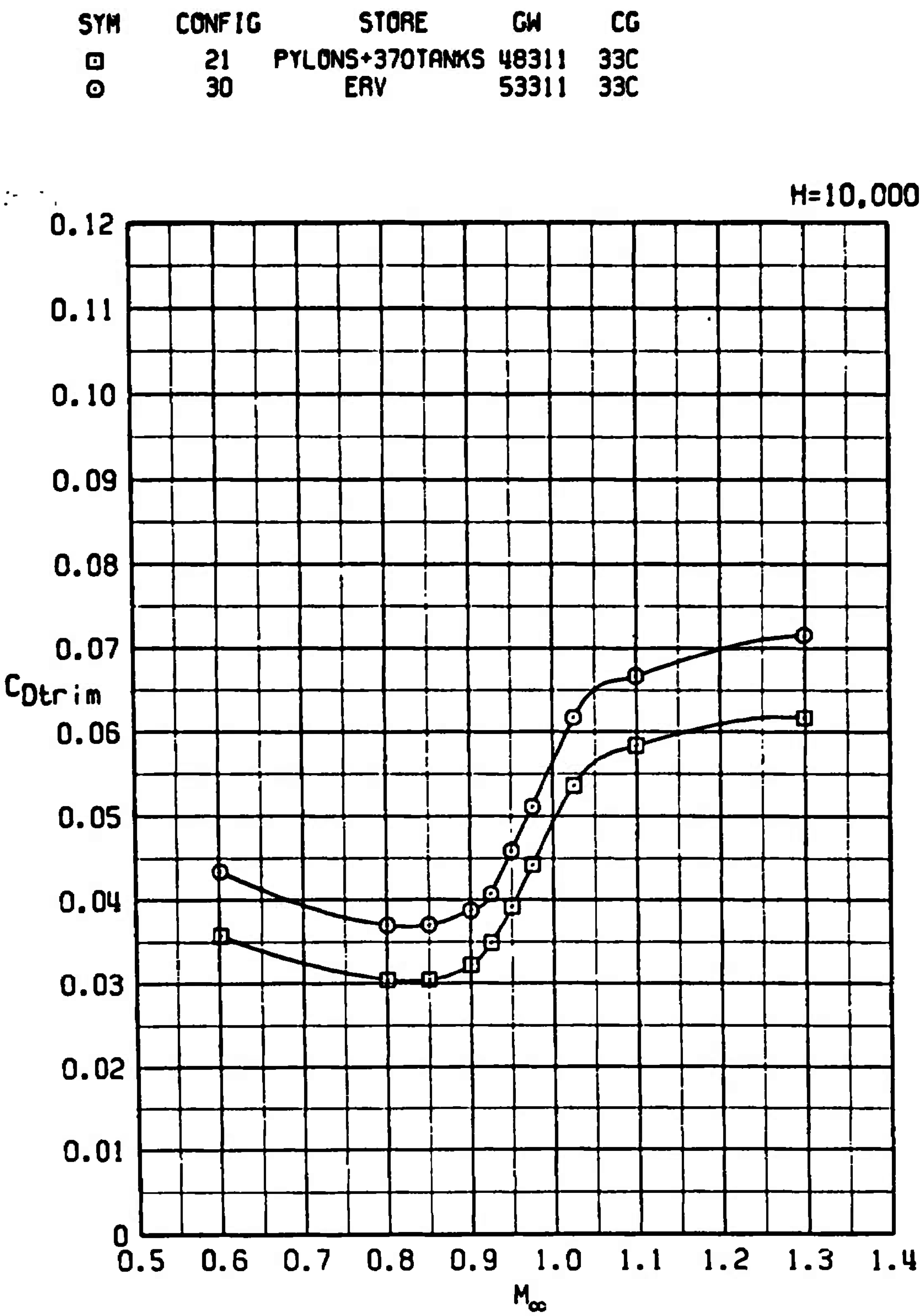

b. H = 10,000
Figure 52. Continued.

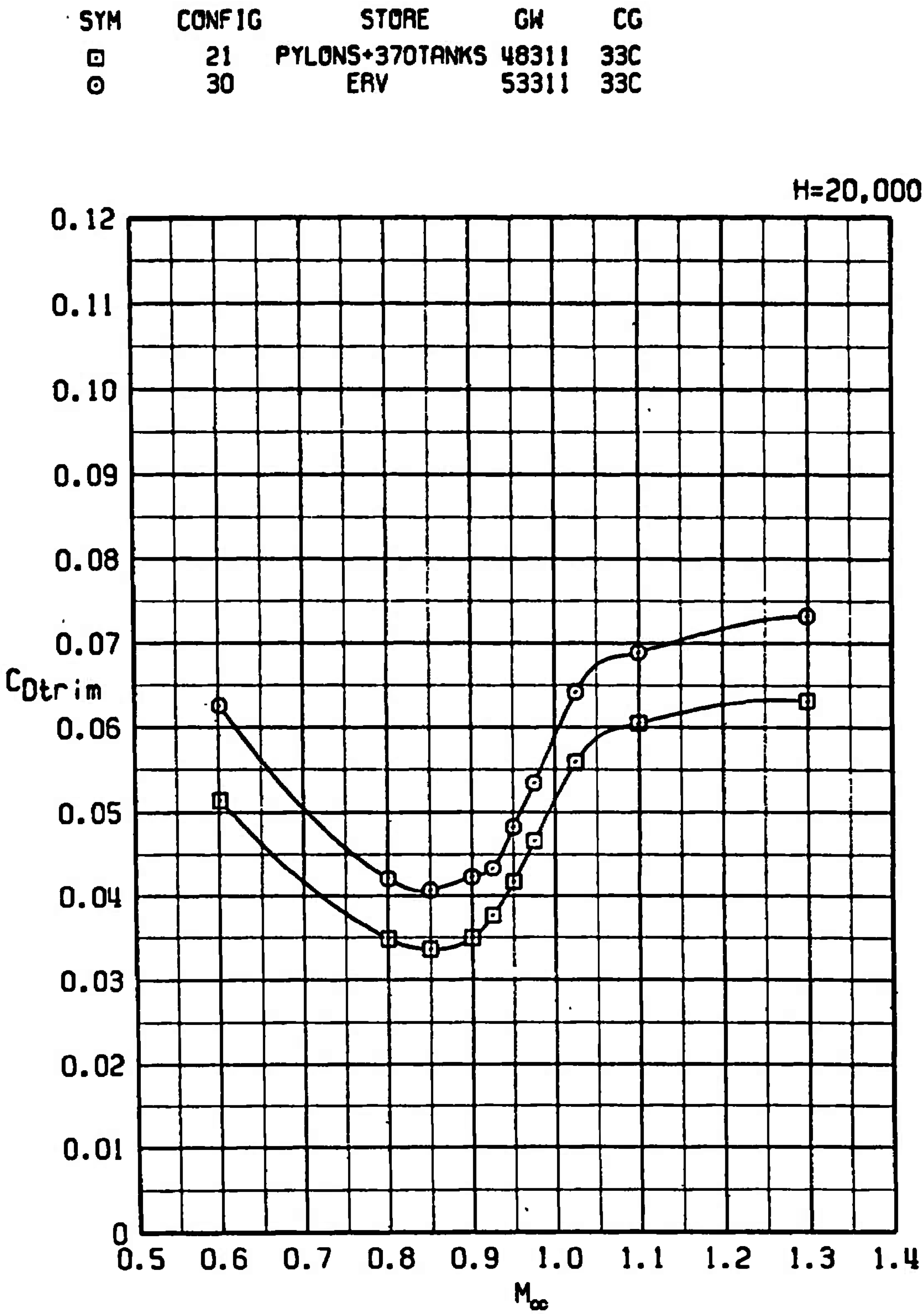

c. H = 30,000

Figure 52. Continued.

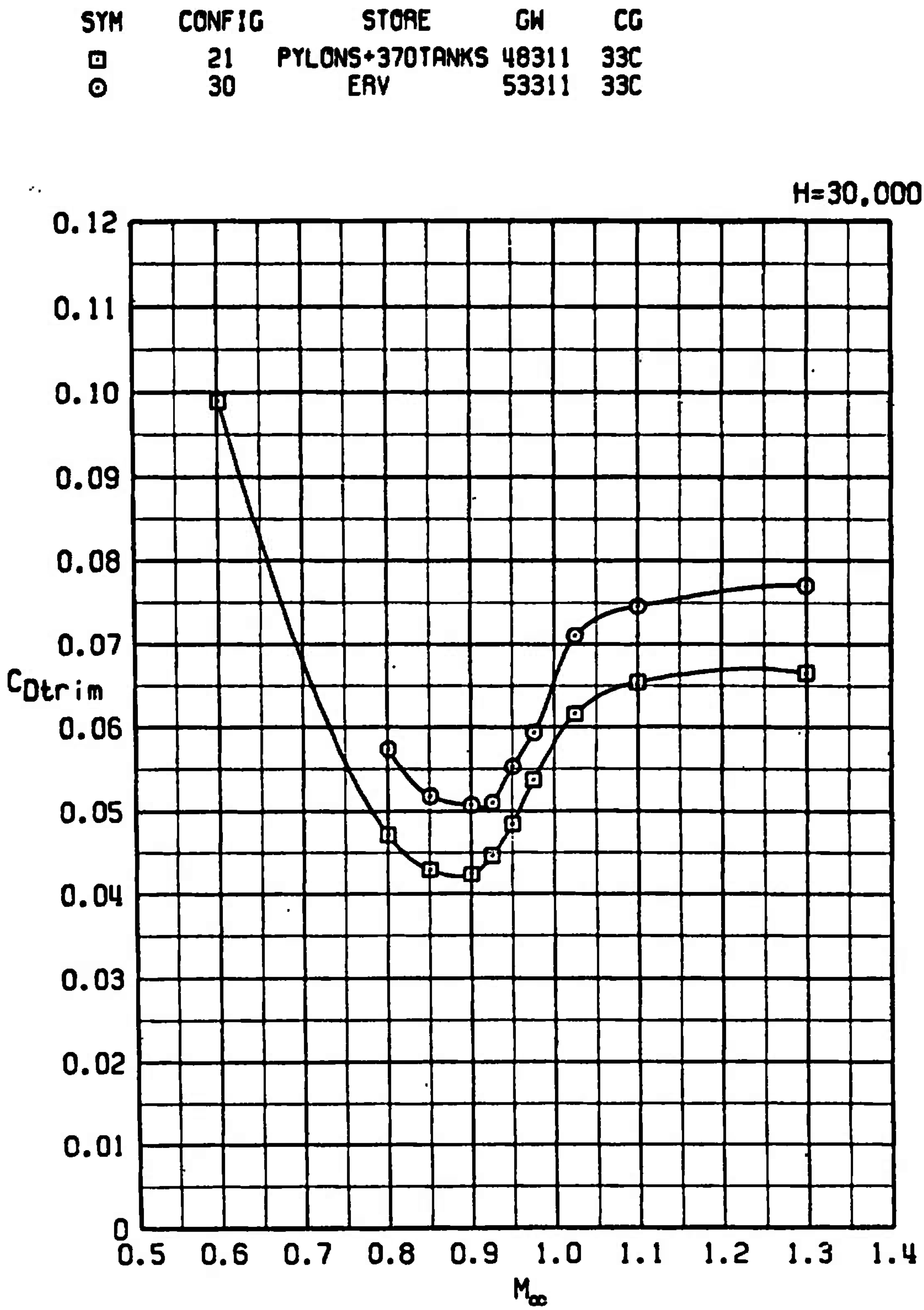

d. H = 30,000
Figure 52. Concluded.

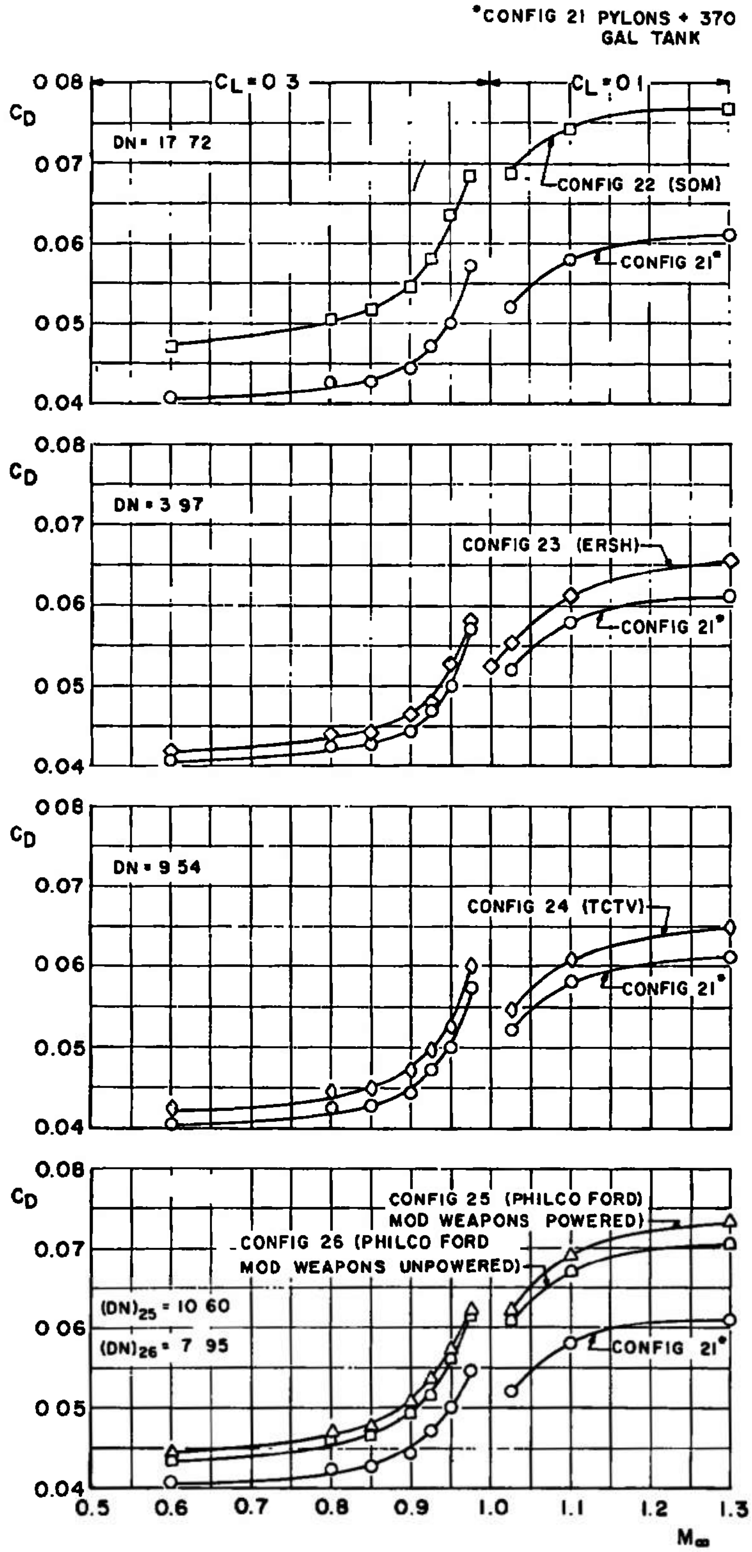

Figure 53. Drag characteristics and drag numbers for various external stores.

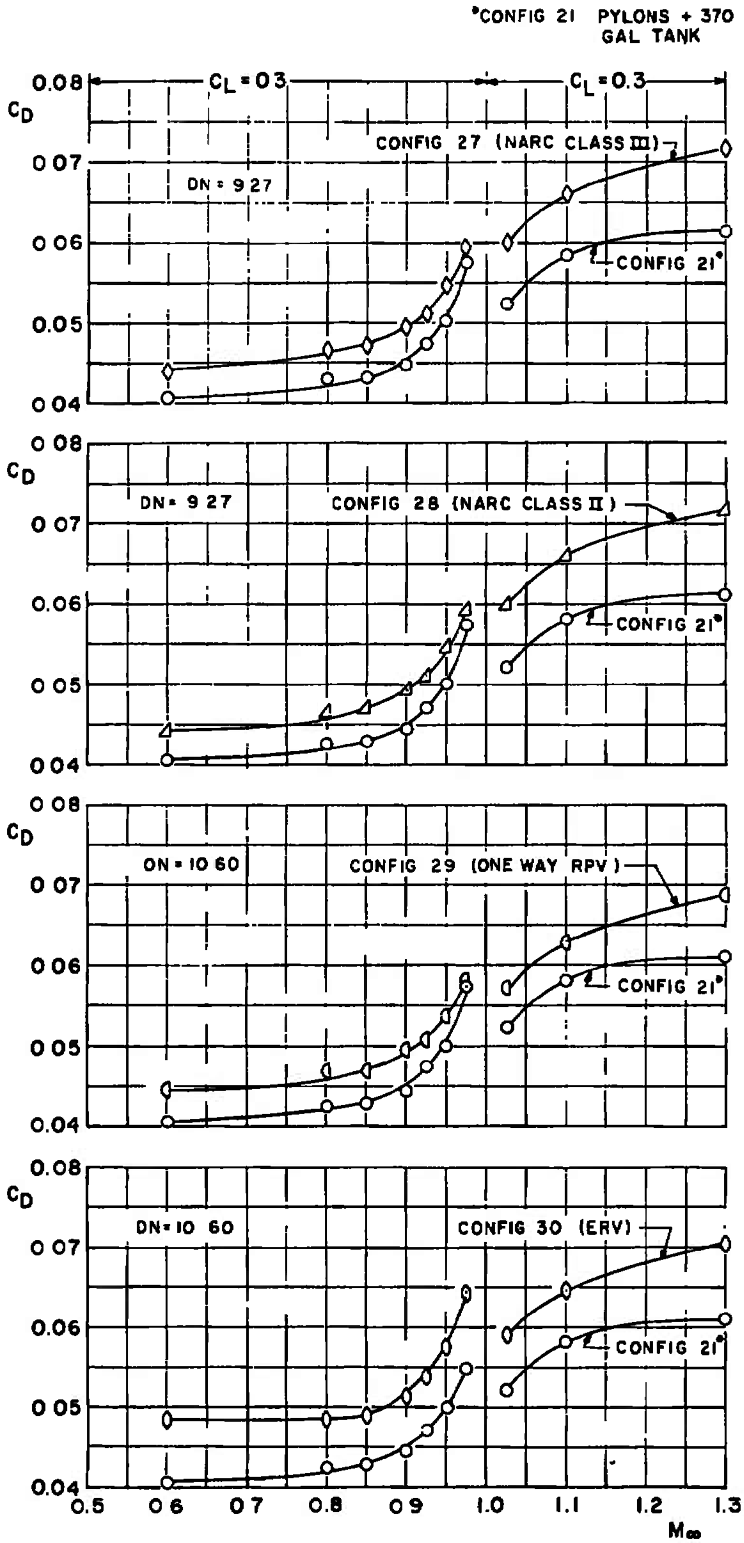

Figure 53. Concluded.

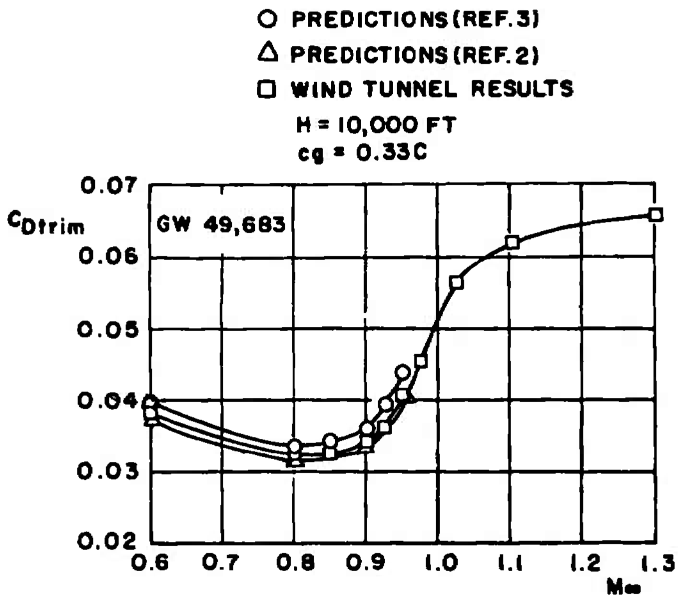

a. Configuration 23 (ERSH)

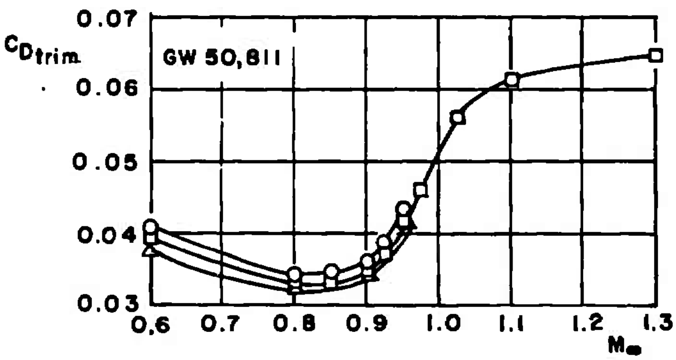

b. Configuration 24 (TCTV)

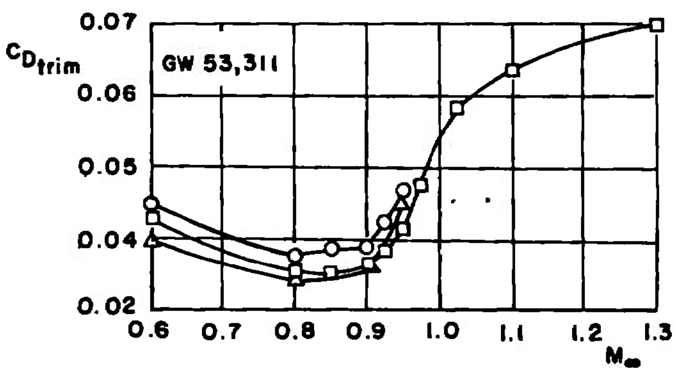

c. Configuration 30 (ERV)

Figure 54. Comparisons of measured and predicted drag.

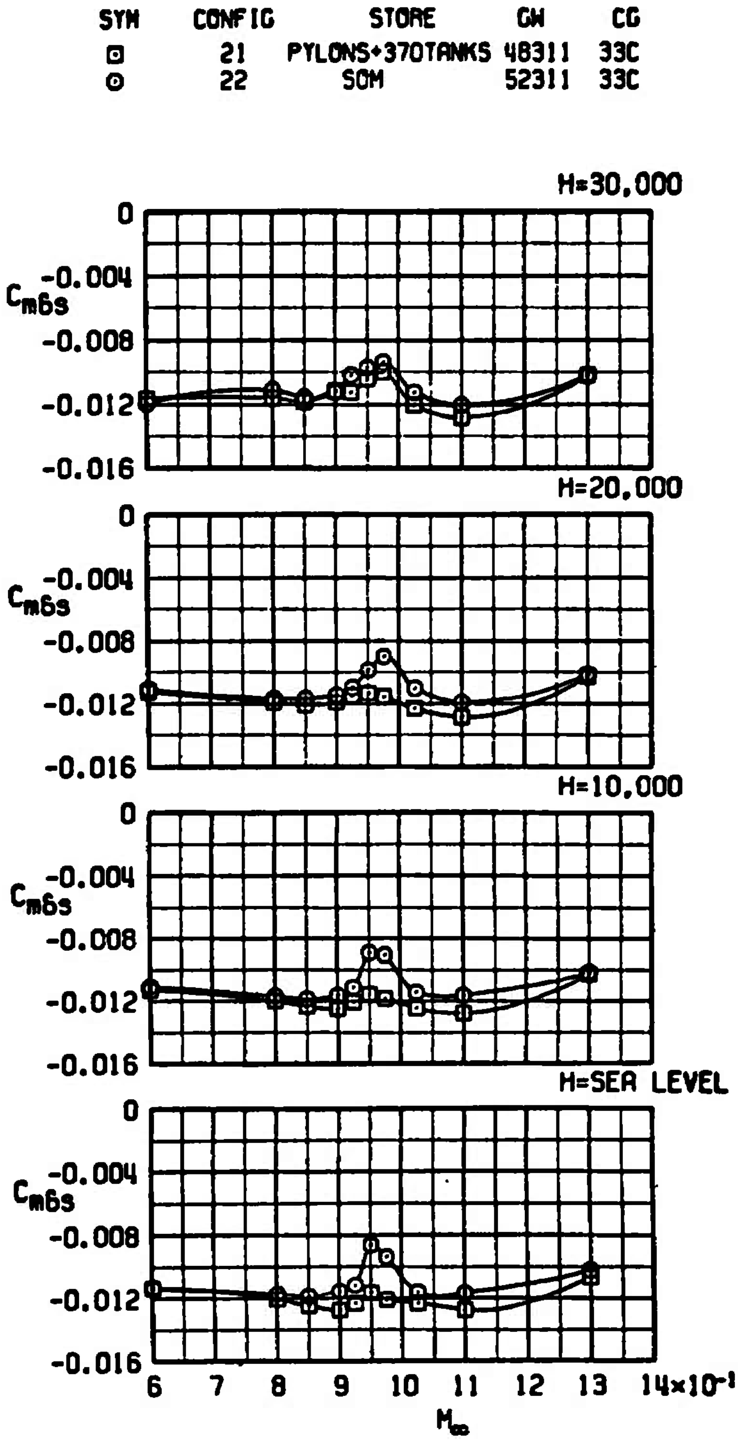

a. Stabilator power

Figure 55. The effect of the SOM store on the longitudinal control characteristics.

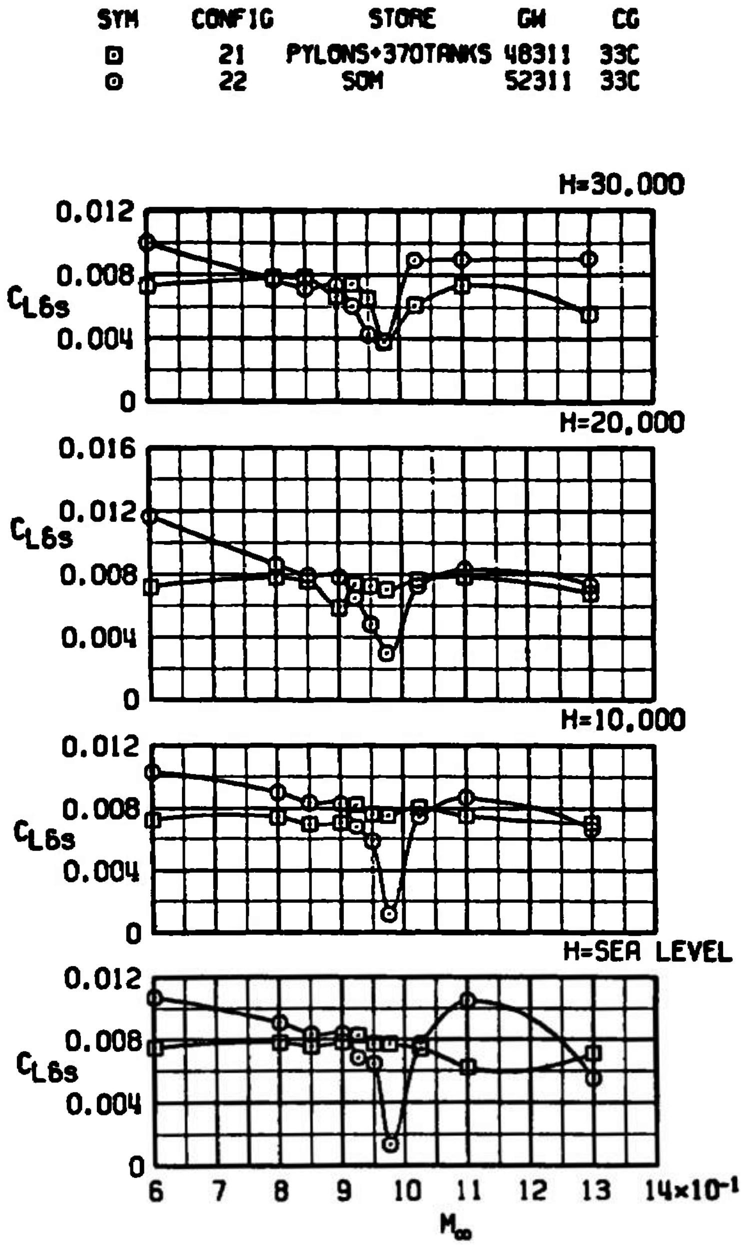

b. Stabilator lift effectiveness
Figure 55. Concluded.

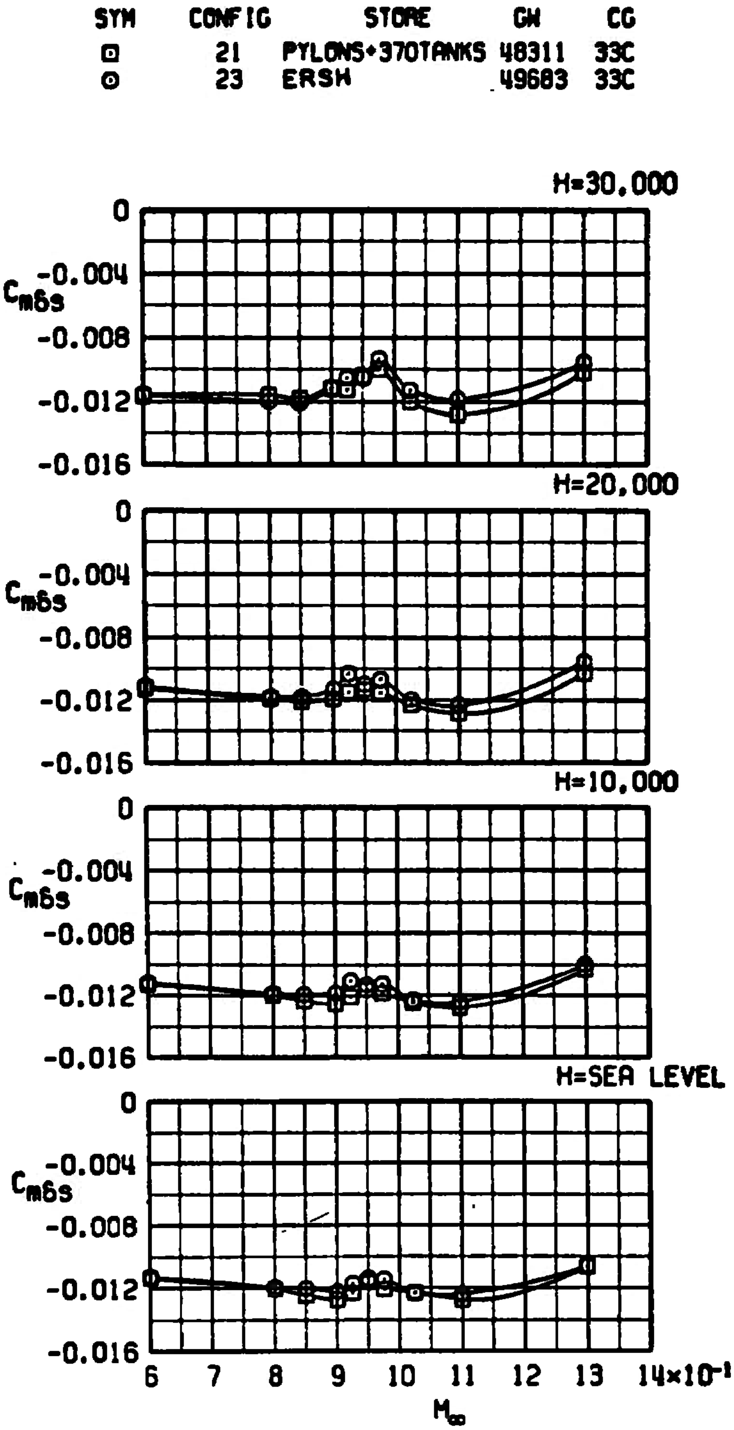

a. Stabilator power

Figure 56. The effect of the Stubby HOBOS store on the longitudinal control characteristics.

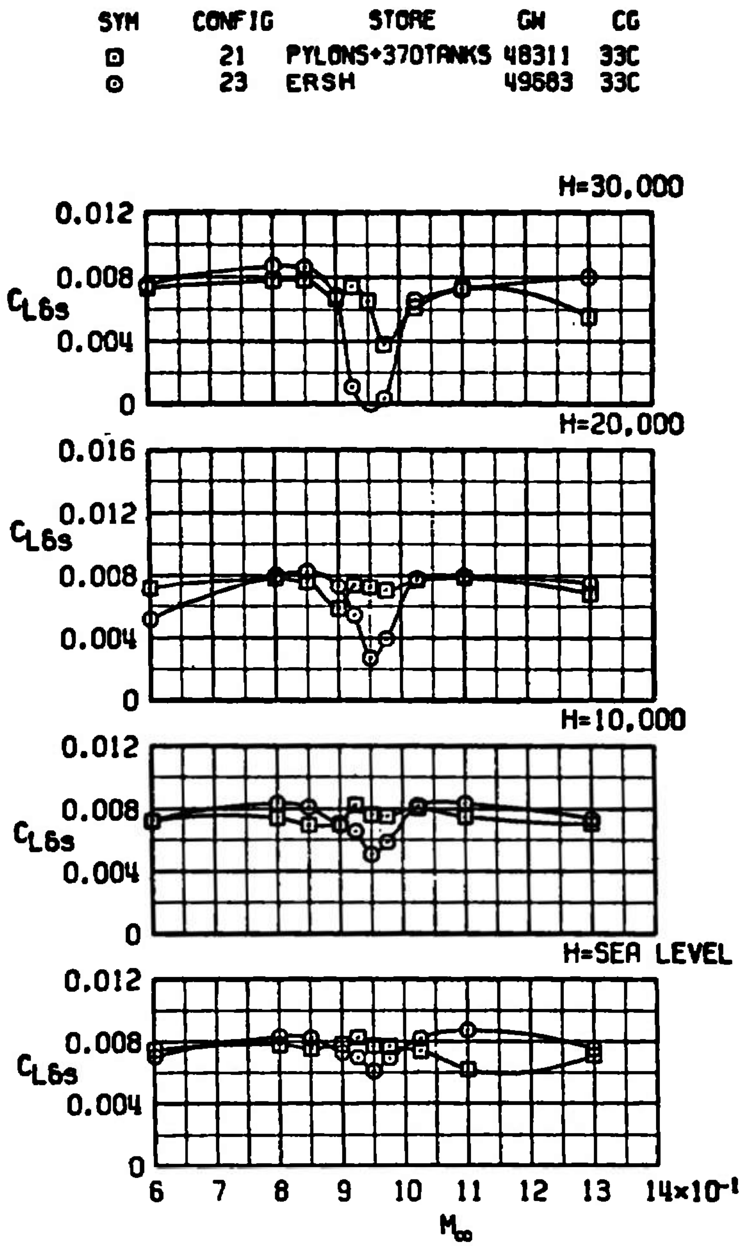

b. Stabilator lift effectiveness
Figure 56. Concluded.

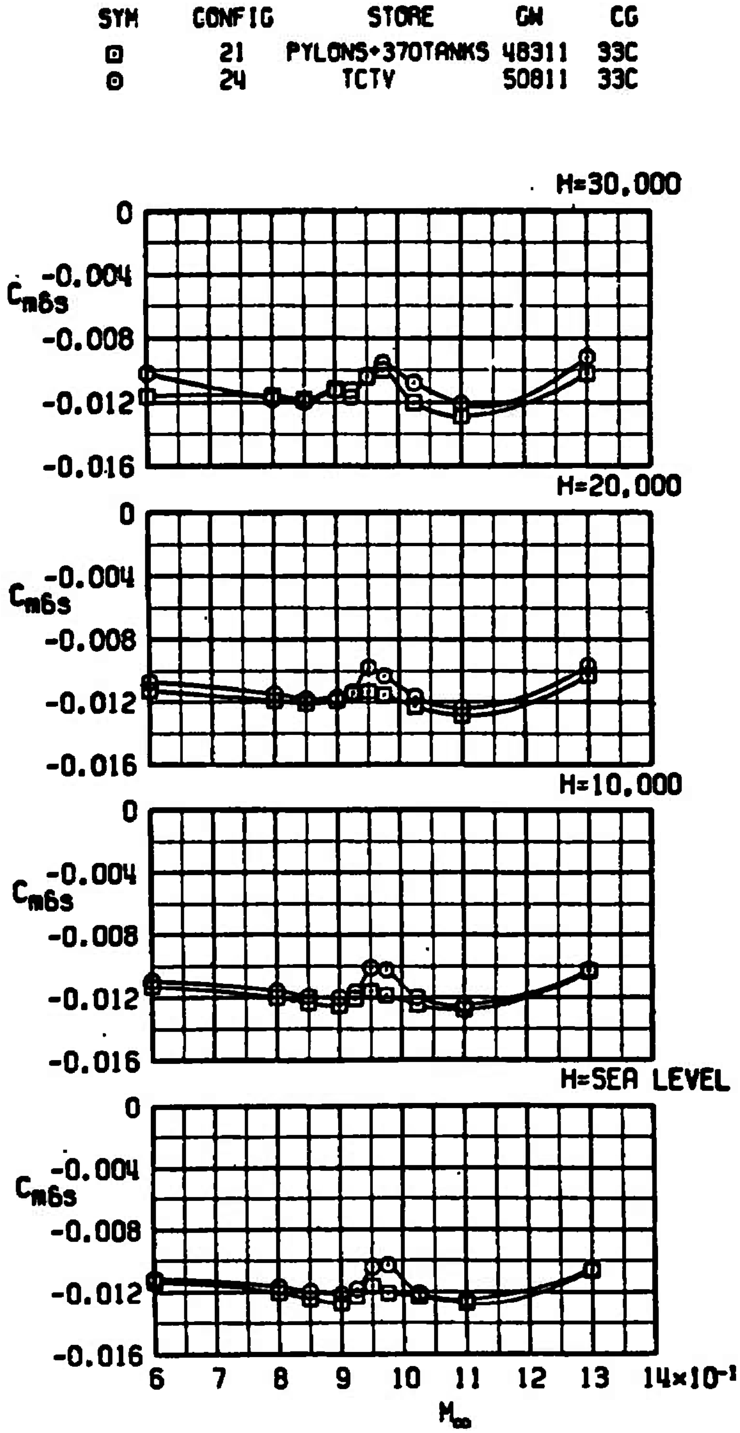

a. Stabilator power

Figure 57. The effect of the TCTV store on the longitudinal control characteristics.

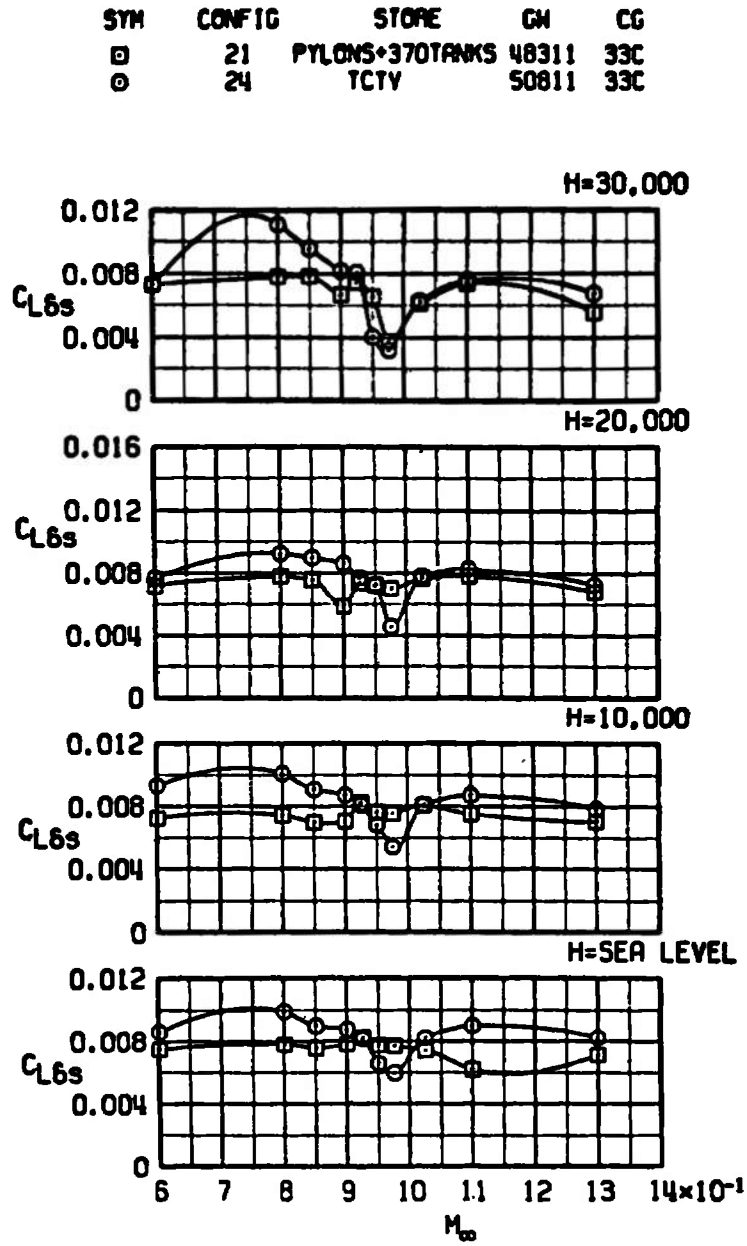

b. Stabilator lift effectiveness
Figure 57. Concluded.

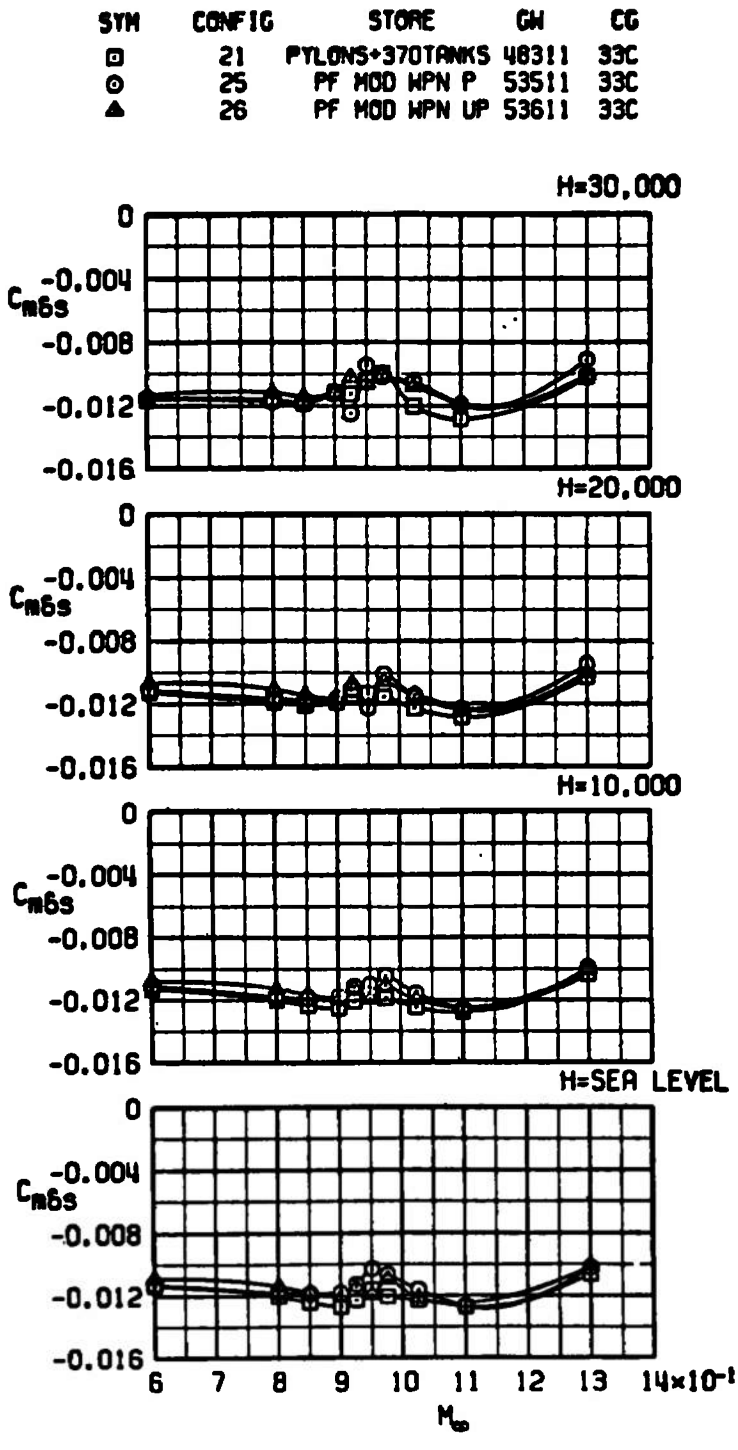

a. Stabilator power

Figure 58. The effect of the PF Modular Weapons stores on the longitudinal control characteristics.

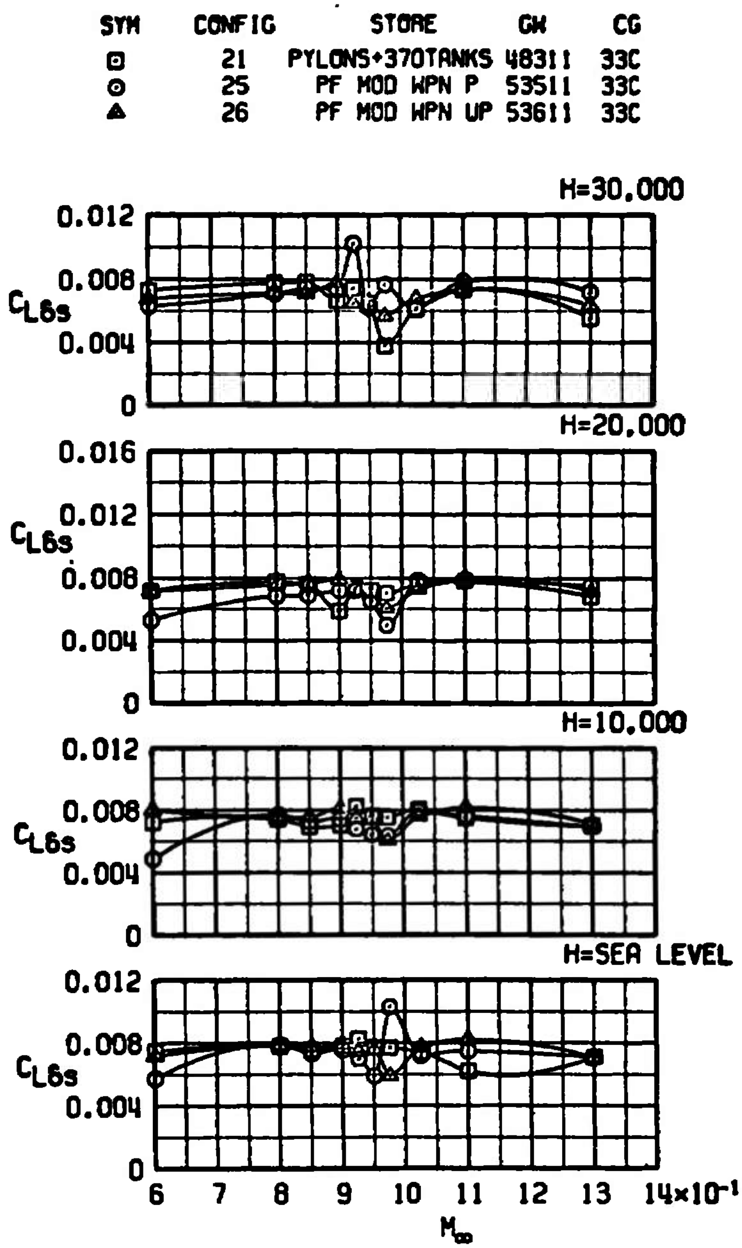

b. Stabilator lift effectiveness
Figure 58. Concluded.

SYM	CONFIG	STORE	GW	CG
⊡	21	PYLONS+370TANKS	48311	33C
⊙	29	ONEWAY RPV	54311	33C

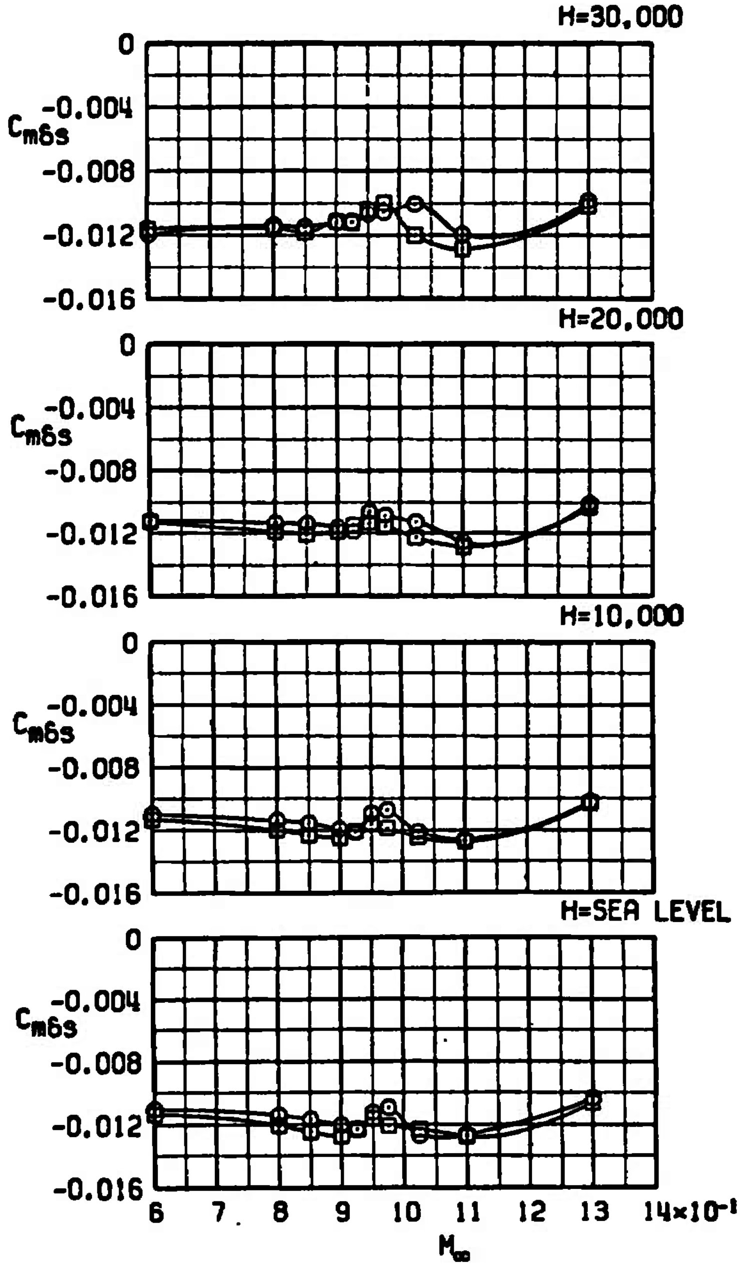

a. Stabilator power

Figure 59. The effect of the Oneway RPV store on the longitudinal control characteristics.

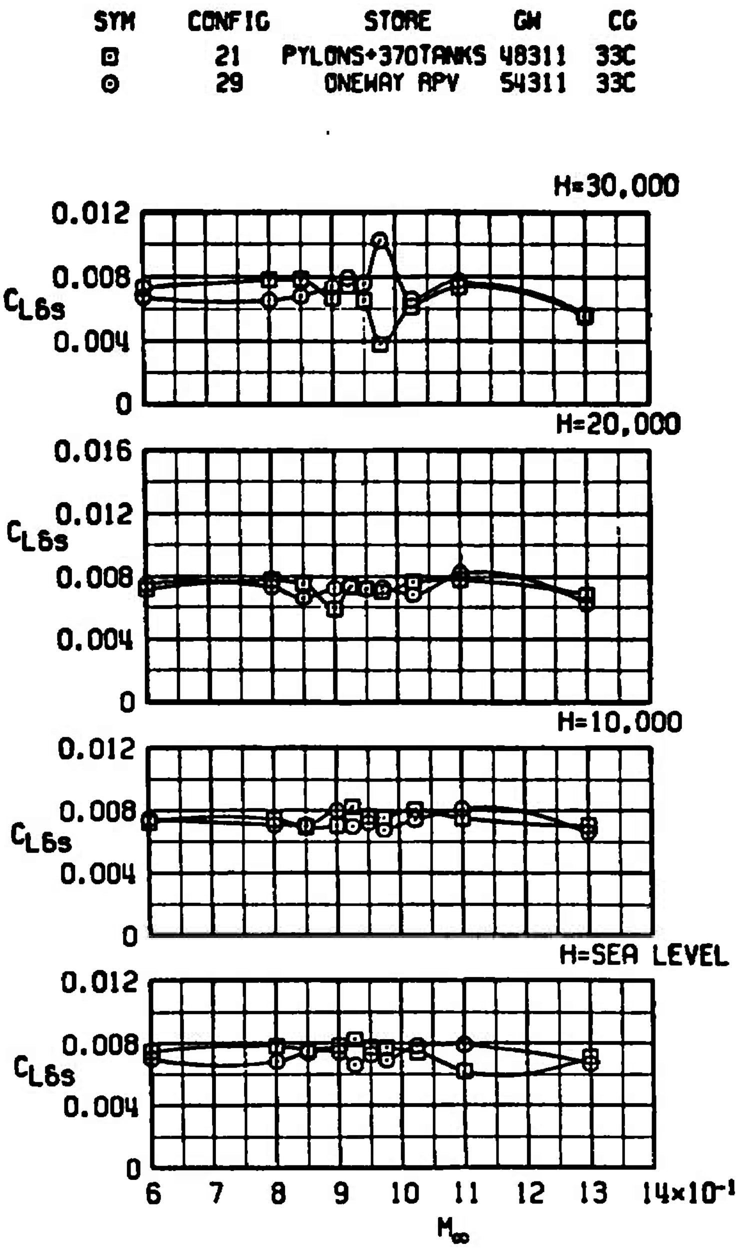

b. Stabilator lift effectiveness
Figure 59. Concluded.

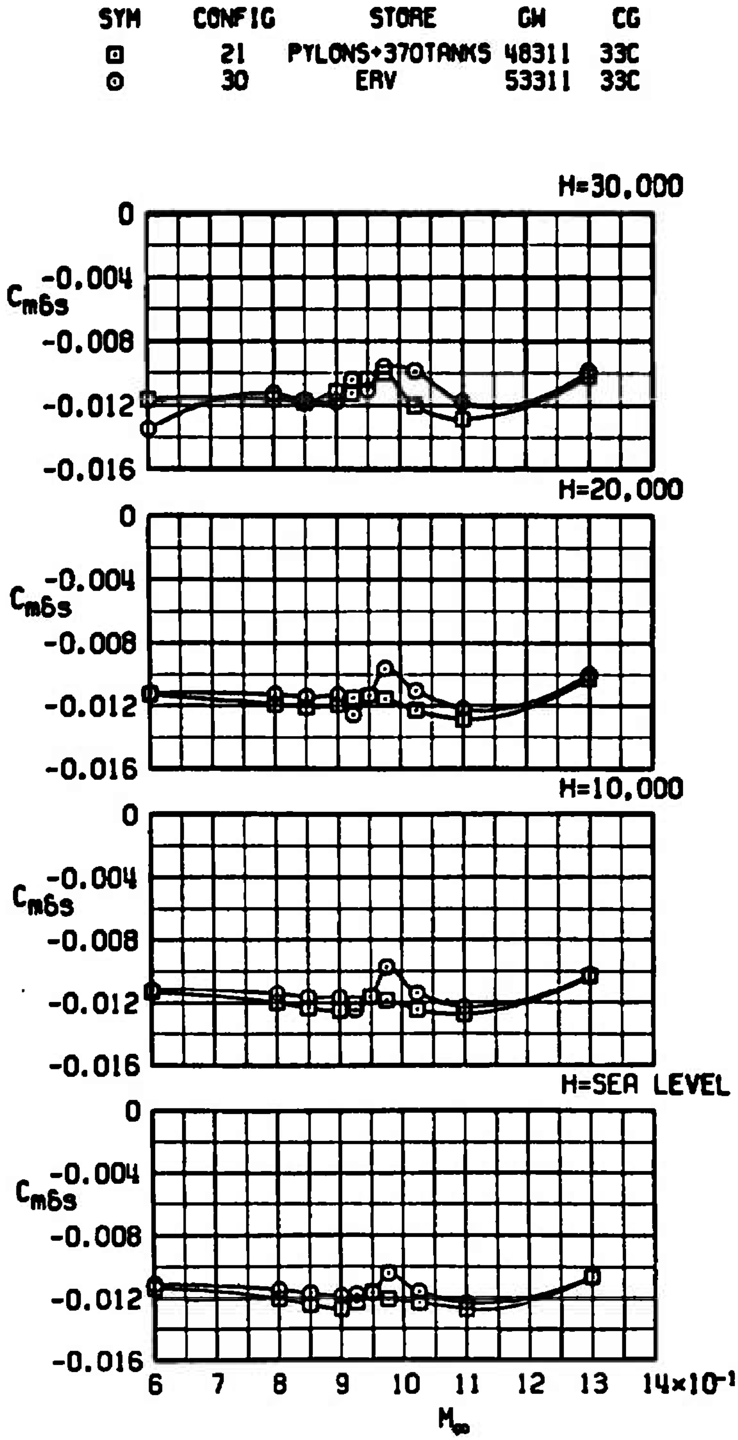

a. Stabilator power

Figure 60. The effect of the ERV store on the longitudinal control characteristics.

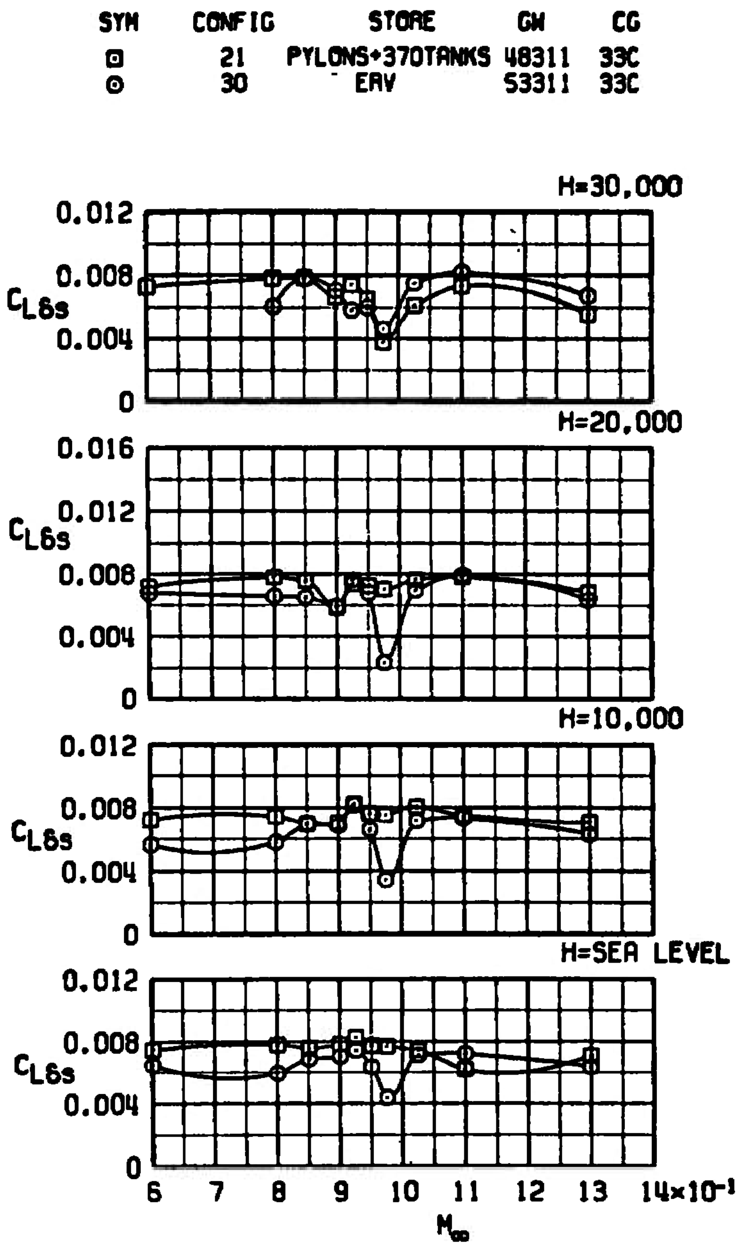

b. Stabilator lift effectiveness
Figure 60. Concluded.

Table 1. Aerodynamic Coefficient Precision

M_∞	q_∞,psf	$\pm\Delta C_m$	$\pm\Delta C_L$	$\pm\Delta C_D$
0.60	630	0.0021	0.0056	0.0012
0.80	785	0.0017	0.0038	0.0010
0.85	810	0.0016	0.0036	0.0010
0.90	860	0.0016	0.0034	0.0010
0.925	875	0.0015	0.0032	0.0010
0.975	875	0.0015	0.0031	0.0010
0.975	890	0.0015	0.0029	0.0010
1.025	920	0.0015	0.0027	0.0010
1.10	960	0.0014	0.0024	0.0009
1.30	1025	0.0013	0.0020	0.0008

NOMENCLATURE

A_F — Total wing-mounted store or store plus suspension equipment frontal area, ft^2

BL — Buttock line from plane of symmetry, in.

C_D — Drag coefficient, drag/$q_\infty S$

$C_{D_{trim}}$ — Drag coefficient at trim conditions

C_L — Lift coefficient, lift/$q_\infty S$

C_{L_α} — Slope of lift coefficient versus angle-of-attack curve at trim conditions, per degree

$C_{L_{\delta_s}}$ — Slope of lift coefficient versus stabilator angle curve at trim conditions, per degree

$C_{m\,(0.33c)}$ — Pitching-moment coefficient referenced to 33 percent of the mean aerodynamic chord and WL 1.55, pitching moment/$q_\infty Sc$

C_{m_α} — Slope of pitching-moment coefficient versus angle-of-attack curve at trim conditions, per degree

$C_{m_{\delta_s}}$ — Slope of pitching-moment coefficient versus stabilator angle curve at trim conditions, per degree

c — Theoretical mean aerodynamic chord (MAC) (see Fig. 3), 9.625 in.

cg — Center-of-gravity location, percent MAC

DN — Store or suspension equipment drag number defined as the increment in drag coefficient at $M_\infty = 0.5$ due to the total number of stores times the full-scale wing reference area (530 ft^2) times 10 divided by the total number of stores, ft^2/store

FS — Fuselage station, in.

GW — Aircraft plus stores gross weight, lb

H	Altitude, ft
M_∞	Free-stream Mach number
NP	Neutral-point location, percent MAC
ΔNP	Incremental change in neutral-point location at $C_L = 0.2$ caused by external stores (neutral-point location of configuration X at $C_L = 0.2$ minus the neutral point of the baseline configuration at $C_L = 0.2$), percent MAC
ΔNP_{tr}	Incremental change in neutral-point location due to external stores at trim conditions (neutral-point location of configuration X at trim conditions minus the neutral-point location of the clean configuration at trim conditions), percent MAC
ΔNP_X	Incremental change in neutral-point location due to the addition of external stores (neutral-point location of configuration X minus the neutral-point location of configuration Y), percent MAC
q_∞	Free-stream dynamic pressure, psf
S	Wing reference area, 1.3250 ft^2
WL	Waterline from reference horizontal plane, in.
α	Wing chord angle of attack, deg
$\alpha_{w\,tr}$	Wing chord angle of attack at trim conditions, deg
$\delta_{s_{tr}}$	Stabilator angle at trim conditions, deg